Addition of P–H Bonds to Heterocumulenes

Cameron D. Huke, MChem (Hons)

Thesis submitted to the University of Nottingham for the degree of Doctor of Philosophy

March 2023

Declaration

The work described in this thesis was carried out at the University of Nottingham between October 2018 and March 2023, under the supervision of Prof. Deborah L. Kays. All of the work is my own unless stated to the contrary and has not previously been submitted for any degrees at this or any other university.

Cameron D. Huke

Abstract

In the pursuit of synthesising novel heteroatom-rich phosphorus analogues of ubiquitous ureas, thioureas and guanidines in a sustainable manner, an atom efficient hydrofunctionalisation approach was undertaken. Either by catalysis or catalyst-free (where viable), testing the addition of different P-H bond containing substrates to multiple bond containing heterocumulenes; isocyanates (RN=C=O), isothiocyanates (RN=C=S) and carbodiimides (RN=C=NR).

A catalyst-free low solvent approach for the hydrophosphinylation of isocyanates and isothiocyanates is applicable to a range of phosphorus nucleophiles; including secondary phosphine oxides $HP(O)R_2$ (R = Ph, ^{i}Pr), phosphites $HP(O)(OR)_2$ (R = Me, Et), and methyl phenylphosphinate. The procedure tolerated isocyanates and isothiocyanates featuring a wide range of substituents in moderate to excellent yields, and by using 4 eq. of 2-MeTHF solvent, solid substrates can be utilised. Facile scale-up and simple reaction conditions make this a straightforward and practical methodology.

Low-coordinate Iron-based *m*-terphenyl precatalyst, **40** performed double hydrophosphination of isocyanates with primary phosphines, RPH_2 (R = Fc, Ad) and additionally formed novel diinsertion-cyclisation products (**52** or **55**). These are formed when less bulky aryl isocyanates are utilised with alkyl isocyanates only forming mono-insertion hydrophosphination products. Selectivity for diinsertion-cyclisation products can be achieved by decreasing solvent (C_6D_6) quantity, increasing isocyanate concentration and increasing temperature.

Additionally, **40** is an efficient precatalyst for single (with $HPPh_2$) and double (with $FcPH_2$) hydrophosphination of carbodiimides. Under moderate conditions hydrophosphination reactions undergo near quantitative ($HPPh_2$) and moderate to excellent ($FcPH_2$) conversions for a range of carbodiimides, with only 1 of 8 possible isomers selectively being formed for single hydrophosphination.

Acknowledgments

Firstly, I would like to thank Prof. Debbie Kays for giving me the opportunity to work on this project in her group and for all her support and guidance throughout my PhD. Also, thanks go to my second supervisor Prof. Jonathan McMaster.

Particular thanks go to Dr. Laurence Taylor and Dr. Amy South for initially teaching me air sensitive Schlenk line and glovebox techniques and for helpful discussions on hydrofunctionalisation catalysis. My further thanks go to Dr Yu Liu for teaching me specialised Schlenk line techniques required for the synthesis of *m*-terphenyl complexes and to Dr. Nathan Coles for helpful discussions on hydrophosphination catalysis at the end stages of my research.

A large thanks goes to all previous and current members of the Kay's lab group for welcoming me into the group and making my time very enjoyable. In particular to Olivia Churchill and Lydia Barnes for their friendship and support; with our shared enjoyment of "True Chaos Tuesdays", "Nihilistic Wednesdays" and "Throwback Thursdays". Additional thanks go to my project students Joe Snell, Kelsie Hancock, Sam Collins and Rhys Gardner for their willingness to learn and hard work.

Finally, and most importantly, I would like to thank my family for their unwavering support throughout the last four years.

Covid-19 Impact Statement

The research herein was conducted during a time period of the Covid-19 pandemic. No experimental research was undertaken during the period of March to July 2020 and October 2020 to February 2021 due to Covid-19 lockdowns; with partial returns to work in between, from July 2020 to October 2020 and March 2021 to July 2021. A full return to work commenced in July 2021, with subsequent Covid-19 research related restrictions being removed in February 2022.

Publications

Publications within the scope of this thesis

Chapter 1: Introduction:

Hydrofunctionalization reactions of heterocumulenes: Formation of C–X (X = B, N, O, P, S and Si) bonds by homogeneous metal catalysts, C. D. Huke and D. L. Kays, *Adv. Org. Chem.*, 2021, **75**, 1-54. (Doi: 10.1016/bs.adomc.2021.01.003).

Chapter 2: Catalyst-free P(O)-H addition of isocyanates and isothiocyanates

Catalyst-free Hydrophosphinylation of Isocyanates and Isothiocyanates under Low-Added-Solvent Conditions, C D. Huke, L. J. Taylor, S. P. Argent, and D. L. Kays, *ACS Sustainable Chem. Eng*. 2021, **9**, 32, 10704–10709. (Doi: 10.1021/acssuschemeng.1c02907).

Chapter 3: Hydrophosphination and Diinsertion-cyclisation of Isocyanates

Iron(II)-catalysed Double Hydrophosphination and Diinsertion-cyclisation of isocyanates, C. D. Huke, K. Hancock, L. J. Taylor, N. T. Coles and D. L. Kays*. Manuscript in preparation.

Chapter 4: Hydrophosphination of Carbodiimides

Iron(II)-catalysed Hydrophosphination of Carbodiimides, C. D. Huke, A. J. South, S. Collins, A. Insley, J. Williams, L. J. Taylor, A. M. Geer, N. T. Coles and D. L. Kays*. Manuscript in preparation.

Publications outside the scope of this thesis

Structural and Electronic Studies of Substituted m-Terphenyl Group 12 Complexes, A. J. Valentine, L. J. Taylor, A. M. Geer, C. D. Huke, K. E. Wood, W. Tovey, W. Lewis, S. P. Argent. M. Teale, J. McMaster and D. L. Kays. *Organometallics,* 2022, **41**, 11, 1426–1433. (Doi: 10.1021/acs.organomet.2c00156).

Organoruthenium Complexes Containing Hemilabile Phosphinodicarboxamide Ligands, R. Nolla-Saltiel, Ana M. Geer, H. R. Sharpe, C. D. Huke, L. J. Taylor, T. G. Linford-Wood, A. James, J. Allen, W. Lewis, A. J. Blake, J. McMaster and D. L. Kays. *ChemRxiv*, 2022. (Preprint available at 10.26434/chemrxiv-2022-37ncj).

Table of Contents

Declaration ..... **ii**

Abstract ..... **iii**

Acknowledgments ..... **iv**

Covid-19 Impact Statement ..... **v**

Publications ..... **vi**

Table of Contents ..... **viii**

List of Abbreviations xvii

Chapter 1: .....

Introduction **1**

1.1 Green chemistry 2

1.1.1 Population, environment and chemical industry 2

1.1.2 Principles in Green Chemistry 3

1.2 Heteroatom rich synthesis via hydrofunctionalisation 7

1.2.1 Hydrofunctionalisation Reactions 7

1.2.2 Heterocumulene substrates: isocyanates, isothiocyanates ..... and carbodiimides 8

1.3 Hydroamination of Heterocumulenes 11

1.4 Hydrophosphination of Heterocumulenes 16

1.5 Hydroboration of Heterocumulenes 20

1.6 Hydrosilylation of Heterocumulenes 24

1.7 Catalyst-free N-H, B-H and P-H Hydrofunctionalisations of ..... Heterocumulenes 26

1.8 Hydrofunctionalisation Catalysis with *m*-Terphenyls 31

1.9 Global Aims 36

Chapter 2: .....

Catalyst-free P(O)-H Bond Addition of Isocyanates and .....

Isothiocyanates **37**

2.1 Introduction 38

2.1.1 Hydrophosphinylation of isocyanates and isothiocyanates 38

2.1.2 Hydrophosphonylation of isocyanates and isothiocyanates 41

2.2 Aims 42

2.3 Results and Discussion 43

2.3.1 Hydrophosphinylation of isocyanates and isothiocyanates 43

2.3.1.1 Initial catalyst-free optimisation with phenyl isocyanate 43
2.3.2 Catalytic hydrophosphinylation of phenyl isocyanates with ..... *m*-terphenyl complexes. 45
2.3.2.1 Substrate scope for the hydrophosphinylation of isocyanates 45
2.3.2.2 Reaction scale-up 48
2.3.2.3 Hydrophosphinylation of isothiocyanates using $HP(O)Ph_2$ 48
2.3.2.4 Initial hydrophosphinylation of PhN=C=O using $HP(O)^iPr_2$ 49
2.3.2.5 Hydrophosphinylation of isocyanates and isothiocyanates ..... using $HP(O)^iPr_2$ 51
2.3.2.6 Proposed mechanism 51
2.3.2.7 By-product formation from hydrophosphinylation of aryl ..... isocyanates and aryl isothiocyanates 52
2.3.2.8 Detection of CO_2 from hydrophosphinylation of *p*-Tolyl ..... isocyanate 53
2.3.3 Hydrophosphonylation of isocyanates and isothiocyanates 54
2.3.3.1 Initial hydrophosphonylation of phenyl isocyanate 54
2.3.3.2 Hydrophosphonylation of phenyl isocyanate utilising ..... HP(O)Ph(OMe) $HP(O)(OEt)_2$ and $HP(O)(OMe)_2$ 56
2.3.3.3 Attempted hydrophosphonylation with PhN=C=S, $^iPrN=C=S$, ... $^iPrN=C=O$ 57
2.3.4 Crystallographic analysis 58
2.3.4.1 Diphenylphosphinyl carboxamides **44d**-**44e**, **44i**-**44j**, **44l** and **44n** . 58
2.3.4.2 Diphenylphosphinyl thiocarboxamides **45c**-**45e** and **45h** 66
2.3.4.3 Diisopropylphosphinyl (thio)carboxamides **46c**-**46d** and ..... Dimethoxylphosphonyl phenylcarboxamide **47b** 68
2.4 Conclusions 71
2.5 Future Work 73
2.6 Experimental Procedures 74
2.6.1 Hydrophosphinylation using $HP(O)Ph_2$ 74
2.6.1.1 Initial optimisation of catalyst-free hydrophosphinylation with ..... $HP(O)Ph_2$ and Ph-N=C=O 74
2.6.1.2 Variation of phenyl isocyanate concentration 74
2.6.1.3 Variation of diphenylphosphine oxide concentration 74
2.6.1.4 Neat reaction under an inert atmosphere 75
2.6.1.5 Neat reaction in air 75
2.6.1.6 Variation of solvent type and volume 75
2.6.1.7 General procedure for hydrophosphinylation of isocyanates and ..... isothiocyanates with $HP(O)Ph_2$, 44a – 45h (for NMR yields) 76

2.6.1.8 General procedure for hydrophosphinylation of isocyanates and isothiocyanates with $HP(O)Ph_2$, 44a – 45h (for isolated yields) 76
2.6.1.9 Procedure for the gram scale hydrophosphinylation of phenyl isocyanate 77
2.6.2 Hydrophosphinylation with $HP(O)^iPr_2$ 77
2.6.2.1 Initial optimisation of catalyst-free hydrophosphinylation using $HP(O)^iPr_2$ 77
2.6.2.2 General procedure for hydrophosphinylation of isocyanates and isothiocyanates with $HP(O)^iPr_2$, **46a** – **46**c (for NMR yields) 78
2.6.2.3 General procedure for hydrophosphinylation of isocyanates and isothiocyanates with $HP(O)^iPr_2$, **46a** – **46c** (for isolated yields) 78
2.6.3 Hydrophosphinylation with HP(O)Ph(OMe) and Hydrophosphonylation with $HP(O)(OEt)_2$ and $HP(O)(OMe)_2$ 79
2.6.3.1 Initial optimisation 79
2.6.3.2 Hydrophosphinylation with HP(O)Ph(OMe) and Hydrophosphonylation with $HP(O)(OEt)_2$ with other electrophiles 79
2.6.3.3 General procedure for hydrophosphinylation of phenyl isocyanate with HP(O)(Ph)(OMe), $HP(O)(OEt)_2$ and $HP(O)(OMe)_2$ (for NMR yields) 80
2.6.3.4 Procedure for the hydrophosphinylation of phenyl isocyanate with HP(O)(Ph)(OMe), $HP(O)(OEt)_2$ and $HP(O)(OMe)_2$ 80
2.6.4 Synthesis of $Fe(C_6H_3\text{-}2,6\text{-}Mes_2)_2$ (**40**) 82
2.6.5 Yields and characterisation data for **44a**–**44n** 83
2.6.5.1 $Ph_2P(O)C(O)NH(Ph)$ (**44a**) 83
2.6.5.2 $Ph_2P(O)C(O)NH(4\text{-}MeC_6H_4)$ (**44b**) 84
2.6.5.3 $Ph_2P(O)C(O)NH(4\text{-}BrC_6H_4)$ (**44c**) 84
2.6.5.4 $Ph_2P(O)C(O)NH(2\text{-}FC_6H_4)$ (**44d**) 85
2.6.5.5 $Ph_2P(O)C(O)NH(3,5\text{-}(OMe)_2C_6H_3)$ (**44e**) 85
2.6.5.6 $Ph_2P(O)C(O)NH(4\text{-}NO_2C_6H_4)$ (**44f**) 86
2.6.5.7 $Ph_2P(O)C(O)NH(^iPr)$ (**44g**) 86
2.6.5.8 $Ph_2P(O)C(O)NH(^tBu)$ (**44h**) 87
2.6.5.9 2.4.4.9 – $Ph_2P(O)C(O)NH(Et)$ (**44i**) 88
2.6.5.10 $Ph_2P(O)C(O)NH(^nPr)$ (**44j**) 88
2.6.5.11 $Ph_2P(O)C(O)NH(^nHex)$ (**44k**) 89
2.6.5.12 $Ph_2P(O)C(O)NH(CH_2)Ph$ (**44l**) 90
2.6.5.13 $Ph_2P(O)C(O)NH(Cy)$ (**44m**) 90
2.6.5.14 $Ph_2P(O)C(O)NH(CH_2)(C_4H_3O)$ (**44n**) 91
2.6.6 Yields and characterisation data for **45a**–**45h** 92

2.6.6.1 $Ph_2P(O)C(S)NH(Ph)$ (**45a**) 92
2.6.6.2 $Ph_2P(O)C(S)NH(4\text{-}MeC_6H_4)$ (**45b**) 92
2.6.6.3 $Ph_2P(O)C(S)NH(4\text{-}ClC_6H_4)$ (**45c**) 93
2.6.6.4 $Ph_2P(O)C(S)NH(4\text{-}MeOC_6H_4)$ (**45d**) 94
2.6.6.5 $Ph_2P(O)C(S)NH(4\text{-}NO_2C_6H_4)$ (**45e**) 94
2.6.6.6 $Ph_2P(O)C(S)NH(Cy)$ (**45f**) 95
2.6.6.7 $Ph_2P(O)C(S)NH(^iPr)$ (**45g**) 96
2.6.6.8 $Ph_2P(O)C(S)NH(CH_2CH{=}CH_2)$ (**45h**) 96
2.6.7 Yields and characterisation data for $HP(O)(^iPr)_2$ ..... and **46a**–**46c** 97
2.6.7.1 $HP(O)(^iPr)_2$ 97
2.6.7.2 $(^iPr)_2P(O)C(O)NH(Ph)$ (**46a**) 97
2.6.7.3 $(^iPr)_2P(O)C(S)NH(Ph)$ (**46b**) 98
2.6.7.4 $(^iPr)_2P(O)C(S)NH(^iPr)$ (**46c**) 99
2.6.8 Crude yields and characterisation data for **47a**–**47c** 99
2.6.8.1 $(EtO)_2P(O)C(O)NH(Ph)$ (**47a**) 99
2.6.8.2 $(MeO)_2P(O)C(O)NH(Ph)$ (**47b**) 100
2.6.8.3 $(MeO)PhP(O)C(O)NH(Ph)$ (**47c**) 100
2.6.9 Mechanistic Experiments 101
2.6.9.1 Hydrophosphinylation of isocyanates in the presence of ..... cumene 101
2.6.9.2 Hydrophosphinylation of isocyanates in the presence of 1,4-cyclohexadiene 101
2.6.9.3 Detection of CO_2 from hydrophosphinylation of *p*-TolN=C=O 102
2.6.10 Summary of spectroscopic data 103
Chapter 3: .....
Hydrophosphination and Diinsertion-cyclisation of Isocyanates **104**
3.1 Introduction 105
3.2 Aims 108
3.3 Results and Discussion 109
3.3.1 Hydrophosphination of isocyanates with ..... ferrocenylphosphine 109
3.3.1.1 Initial catalyst-free hydrophosphination of PhN=C=O. 109
3.3.1.2 Initial catalytic hydrophosphination of PhN=C=O with $FcPH_2$ 111
3.3.1.3 Catalytic double hydrophosphination of aryl isocyanates 114
3.3.1.4 Catalytic double hydrophosphination of alkyl isocyanates 116
3.3.2 Solvent variation to THF 117

3.3.3 Diinsertion-cyclisation of aryl isocyanates with $FcPH_2$ 119
3.3.3.1 Introduction 119
3.3.3.2 Initial diinsertion-cyclisation optimisation 122
3.3.3.3 Diinsertion-cyclisation of aryl isocyanates 124
3.3.4 Hydrophosphination of isocyanates with $AdPH_2$ 125
3.3.4.1 Initial catalyst-free hydrophosphination with $AdPH_2$ 125
3.3.4.2 Initial Catalytic Hydrophosphination with $AdPH_2$ and PhN=C=O ... 128
3.3.4.3 Diinsertion-cyclisation of aryl isocyanates and double ..... hydrophosphination of alkyl isocyanates with $AdPH_2$ 132
3.3.5 Mechanistic studies 134
3.3.5.1 Poisoning experiments 134
3.3.5.2 Stoichiometric studies 135
3.3.5.3 Potential mechanism for double hydrophosphination 137
3.3.5.4 Potential mechanisms for diinsertion or diinsertion-cyclisation ... 138
3.3.6 Crystallographic studies 141
3.3.6.1 Ferrocenyl diarylphosphinocarboaxmides **49a**-**49d** 141
3.3.6.2 Ferrocenyl dialkylcarboxamides **51a**-**51b** 144
3.3.6.3 Mixed addition product: 1-(4,6-dioxo-1,3,5-triphenyl-1,3,5- ..... triazinan-2-yl)-1-ferrocenyl-*N*- ..... phenylphosphinocarboxamide, **56** 146
3.4 Conclusions 151
3.5 Future Work 154
3.6 Experimental Procedures 157
3.6.1 Double hydrophosphination with $FcPH_2$ 157
3.6.1.1 Initial catalyst-free Variation of solvent type and concentration .. 157
3.6.1.2 Initial neat catalyst-free variation of temperature 157
3.6.1.3 Initial neat catalyst-free variation of phenyl isocyanate ..... concentration 157
3.6.1.4 Initial catalytic variation of temperature and phenyl isocyanate ..... concentration 158
3.6.1.5 General procedure for the double hydrophosphination of ..... isocyanates with $FcPH_2$ (NMR yields) 158
3.6.1.6 Double hydrophosphination of aryl isocyanates with $FcPH_2$ ..... (isolated yields) **49a**-**49d** 159
3.6.1.7 Double hydrophosphination of alkyl isocyanates with $FcPH_2$ ..... (isolated yields) **51a**-**51c** 159
3.6.1.8 *In situ* single hydrophosphination of PhN=C=O in THF 160
3.6.2 Diinsertion-cyclisation with $FcPH_2$ 160

3.6.2.1 Catalytic diinsertion-cyclisation optimisation variation of isocyanate concentration, catalyst loading, solvent concentration or temperature ... 160
3.6.2.2 General procedure for the diinsertion-cyclisation of aryl isocyanates with $FcPH_2$ (NMR yields) ... 161
3.6.2.3 Diinsertion-cyclisation of phenyl isocyanate with $FcPH_2$ (isolated yield) ... 161
3.6.3 Double hydrophosphination and diinsertion-cyclisation with $AdPH_2$ ... 162
3.6.3.1 Initial catalyst-free optimisation variation of temperature and of solvent ... 162
3.6.3.2 Initial catalytic optimisation reactions for double hydrophosphination with $AdPH_2$ and PhN=C=O variation catalyst loading, temperature or time ... 162
3.6.3.3 General procedure for the double hydrophosphination or diinsertion- cyclisation of isocyanates with $AdPH_2$ (NMR yields) ... 163
3.6.4 Stoichiometric NMR reactions ... 163
3.6.4.1 Stoichiometric reaction of $FcPH_2$ and $Fe(C_6H_3\text{-}2,6\text{-}Mes_2)_2$ ... 163
3.6.4.2 Stoichiometric reaction of PhN=C=O and $Fe(C_6H_3\text{-}2,6\text{-}Mes_2)_2$ ... 163
3.6.4.3 Stoichiometric reaction of PhN=C=O, $FcPH_2$ and $Fe(C_6H_3\text{-}2,6\text{-}Mes_2)_2$ ... 164
3.6.5 Catalytic hydrophosphination with additives ... 164
3.6.5.1 Catalytic hydrophosphination of isocyanates in the presence of Hg(0) ... 164
3.6.5.2 Catalytic hydrophosphination of isocyanates in the presence of CS_2 ... 164
3.6.5.3 Catalytic hydrophosphination of isocyanates in the presence of $PhPMe_2$ ... 165
3.6.5.4 Catalytic hydrophosphination of isocyanates in the presence of cumene ... 165
3.6.5.5 Catalytic hydrophosphination of Carbodiimides in the presence of 1,4-cyclohexadiene ... 165
3.6.6 Yields and characterisation for **49a**-**49d** ... 166
3.6.6.1 $FcP(C(O)N(H)Ph)_2$ (**49a**) ... 166
3.6.6.2 $FcP(C(O)N(H)p\text{-}Tol)_2$ (**49b**) ... 166
3.6.6.3 $FcP(C(O)N(H)(4\text{-}OMeC_6H_4))_2$ (**49c**) ... 167
3.6.6.4 $FcP(C(O)N(H)3\text{-}ClC_6H_4)_2$ (**49d**) ... 168
3.6.7 Yields and characterisation for **51a**-**51c** ... 168
3.6.7.1 $FcP(C(O)N(H)Cy)_2$ (**51a**) ... 168
3.6.7.2 $FcP(C(O)N(H)^iPr)_2$ (**51b**) ... 169

3.6.7.3 FcP(C(O)N(H)^{t}Bu)$_2$ (**51c**) 170
3.6.8 Yields and characterisation for **52a**-**52d** 170
3.6.8.1 FcP-(C(O)N(Ph)C(O)N(Ph)- (**52a**) 170
3.6.8.2 FcP-(C(O)N(*p*-Tol)C(O)N(*p*-Tol)- (**52b**) 171
3.6.8.3 FcP-(C(O)N(4-OMeC$_6$H$_4$)C(O)N(4-OMeC$_6$H$_4$)- (**52c**) 171
3.6.8.4 FcP-(C(O)N(3-ClC$_6$H$_4$)C(O)N(3-ClC$_6$H$_4$)- (**52d**) 171
3.6.9 Yields and characterisation for **53a** and **54a-54c** 172
3.6.9.1 AdP(H)(C(O)N(Ph)C(O)NH(Ph) (**53a**) 172
3.6.9.2 AdP(C(O)NH(Ph)$_2$ (**54a/54a'/54a''**) 172
3.6.9.3 AdP(C(O)N(H)Cy)$_2$ (**54b**) 173
3.6.9.4 AdP(C(O)N(H)^{t}Bu)$_2$ (**54c**) 173
3.6.10 Yields and characterisation for **55b**-**55d** 174
3.6.10.1 AdP-(C(O)N(*p*-Tol)C(O)N(*p*-Tol)- (**55b**) 174
3.6.10.2 AdP-(C(O)N(4-OMeC$_6$H$_4$)C(O)N(4-OMeC$_6$H$_4$)- (**55c**) 174
3.6.10.3 AdP-(C(O)N(3-ClC$_6$H$_4$)C(O)N(3-ClC$_6$H$_4$)- (**55d**) 174
3.6.11 Summary of spectroscopic data 175

Chapter 4: .....

Hydrophosphination of Carbodiimides **176**

4.1 Introduction 177
4.1.1 Hydrophosphination of carbodiimides with secondary phosphines 177
4.1.2 Hydrophosphination of carbodiimides with primary phosphines 179
4.2 Aims 181
4.3 Results and Discussion 182
4.3.1 Single hydrophosphination of carbodiimides with HPPh$_2$ 182
4.3.1.1 Attempted catalyst-free hydrophosphination of ^{i}PrN=C=N^{i}Pr with HPPh$_2$ 182
4.3.1.2 Initial catalytic hydrophosphination of ^{i}PrN=C=N^{i}Pr with HPPh$_2$ ... 182
4.3.1.3 Catalytic single hydrophosphination of carbodiimides with HPPh$_2$ 185
4.3.1.4 Scaled up isolation catalytic hydrophosphination of CyN=C=NCy ..... with HPPh$_2$ 186
4.3.2 Catalytic hydrophosphination of carbodiimides with HP^{i}Pr$_2$ 187
4.3.2.1 Initial attempted hydrophosphination of ^{i}PrN=C=N^{i}Pr with ..... HP^{i}Pr$_2$ 187
4.3.2.2 Single hydrophosphination of CyN=C=NCy and ^{t}BuN=C=NEt with ..... HP^{i}Pr$_2$ 188

4.3.3 Double hydrophosphination of carbodiimides with $FcPH_2$ 190
4.3.3.1 Initial catalyst-free control reaction 190
4.3.3.2 Initial catalytic hydrophosphination of CyN=C=NCy with $FcPH_2$ ... 191
4.3.3.3 Double hydrophosphination of carbodiimides with $FcPH_2$ 195
4.4 Conclusions 200
4.5 Future Work 202
4.6 Experimental Procedures 203
4.6.1 Hydrophosphination of carbodiimides with $HPPh_2$ 203
4.6.1.1 initial catalyst-free control reaction in solution and neat 203
4.6.1.2 Initial catalytic optimisation reactions hydrophosphination with ..... $HPPh_2$ 203
4.6.1.3 General procedure for the hydrophosphination of carbodiimides ..... with $HPPh_2$ (NMR yields) 203
4.6.1.4 Scaled up reaction of CyN=C=NCy and $HPPh_2$ 204
4.6.2 Hydrophosphination of carbodiimides with HP^iPr_2 204
4.6.2.1 initial catalyst-free control reaction 204
4.6.2.2 Initial catalytic hydrophosphination of ^{i}PrN=C=N^{i}Pr with HP^iPr_2 ... 205
4.6.2.3 General procedure for the hydrophosphination of CyN=C=NCy ..... and ^{t}BuN=C=NEt with HP^iPr_2 (NMR yields) 205
4.6.3 Hydrophosphination of carbodiimides with $FcPH_2$ 205
4.6.3.1 initial catalyst-free control reaction 205
4.6.3.2 Initial catalytic hydrophosphination of CyN=C=NCy with $FcPH_2$ ... 206
4.6.3.3 General procedure for the hydrophosphination of carbodiimides ..... with $FcPH_2$ (NMR yields) 206
4.6.3.4 Scaled up hydrophosphination of cyclohexyl isocyanate with ..... $FcPH_2$ (isolated yields) 207
4.6.4 Yields and characterisation for **60a**-**60d** 207
4.6.4.1 $Ph_2PC(=NCy)NH(Cy)$ (**60a**) 207
4.6.4.2 $Ph_2PC(=N^iPr)NH(^iPr)$ (**60b**) 208
4.6.4.3 $Ph_2PC(=NEt)NH(^tBu)$ (**60c**) 208
4.6.4.4 $Ph_2PC(=NPh)NH(Ph)$ (**60d**) 209
4.6.5 Yields and characterisation for **62c**-**62e** 210
4.6.5.1 $FcPH(C(=NEt)NH(^tBu)$ (**62c**) 210
4.6.5.2 FcPH(C(=NPh)NH(Ph)) (**62d**) 210
4.6.5.3 FcPH(C(=NMes)NH(Mes)) (**62e**/**62e'**) 210
4.6.6 Yields and characterisation for **63a**-**63e** 211
4.6.6.1 $FcP(C(=NCy)NH(Cy))_2$ (**63a**) 211
4.6.6.2 $FcP(C(=N^iPr)NH(^iPr))_2$ (**63b**) 212

4.6.6.3 FcP(C(=NEt)NH(^{t}Bu))$_2$ (**63c**) 212
4.6.6.4 FcP(C(=NPh)NH(Ph))$_2$ (**63d**) 213
4.6.6.5 FcP(C(=NMes)NH(Mes))$_2$ (**63e**) 213
Chapter 5: .....
Concluding Remarks **214**
Chapter 6: .....
General Experimental **220**
6.1 General Experimental 221
6.1.1 Manipulation of air sensitive compounds 221
6.1.2 Preparation of solvents 221
6.1.3 Preparation of reagents 221
6.1.3.1 P(O)-H and P-H reagents 221
6.1.3.2 Heterocumulene reagents 222
6.1.3.3 General use and handling considerations 223
6.2 Physical Measurements 224
6.2.1 NMR spectroscopy 224
6.2.2 Mass spectrometry 224
6.2.3 Elemental analysis 224
6.2.4 Infrared spectroscopy 224
6.2.5 X-ray crystallography 225
References **228**
Appendices **238**
8.1 Crystallographic Data 239
8.2 List of Compounds 243

List of Abbreviations

Å	Angstrom, 10^{-10} m	*J*	Coupling constant (NMR)
Ad	1-adamantyl	*m*	*meta*
Alk	Alkyl	m	Multiplet (NMR)
Ar	Aryl	Me	Methyl, CH_3^-
ATR	Attenuated total reflectance	Mes	Mesityl, 2,4,6-$Me_3C_6H_2$–
		^{n}Hx	*n*-Hexyl, $CH_3(CH_2)_5^-$
Bn	Benzyl, $C_6H_5CH_2$-	Naph	1-Naphthyl, $C_{10}H_7^-$
br	broad	NMR	Nuclear magnetic resonance
COD	1,5-Cyclooctadiene, $[-(CH_2)_2-CH=CH-]_2$	^{n}Pr	*n*-propyl, $MeCH_2CH_2$−
		o	*ortho*
Cy	Cyclohexyl, C_6H_{11}–	*p*	*para*
d_1	NMR relaxation delay	Ph	Phenyl
d	Doublet (NMR)	ppm	Parts per million
Et	Ethyl, CH_3CH_2–	^{p}*tol*	*para*-tolyl, 4-MeC_6H_4
Fc	Ferrocene, $Fe(\eta^5-C_5H_5)_2$	R	Alkyl, aryl, organic group
HBBN	9-Borabicyclo[3.3.1] nonane. $[H-B(CH)_2((CH_2)_3)_2]_2$	s	Singlet (NMR); second(s)
		t	Triplet (NMR)
		^{t}Bu	*tert*-Butyl, Me^3C-
HBpin	Pinacolborane, $HB(O_2C_2(CH_3)4)$	THF	Tetrahydrofuran
		Tosyl	$SO_2C_6H_4$-4-CH_3
hr	hour	Xyl	Xylyl, 2,6-$Me_2C_6H_3$−
i	*ipso*	δ	Chemical shift (NMR)
^{i}Pr	*iso*-Propyl, Me_2CH^-		
IR	Infrared		

Chapter 1:

Introduction

1.1 Green chemistry

1.1.1 Population, environment and chemical industry

The world's population is undergoing exponential growth, with the population reaching 1 billion by 1800, 2 billion by 1930, 6 billion by 1999 and currently sits at 7.9 billion in 2023 with the United Nations (UN) predicting by 2050 the global population will surpass 10 billion.[1,2] This increasingly rapid population growth is generating economic and social problems of similarly increasing magnitude, with economic output increasing twentyfold and material consumption increasing eightfold over the last century.[3]

One of the greatest consequences of this meteoric population growth and subsequent anthropogenic activity has been on the environment.[4] With consequences not limited to deforestation, ozone layer depletion from CFCs, ocean acidification and ocean levels rising. All of these can be directly linked to emissions from the burning of fossil fuels leading to climate change and global warming.[4] Worryingly, the already large demand and strain placed on the environment is expected to increase alongside population growth. In an attempt to provide frameworks for beginning to tackle such a mountainous problem, the UN has put forward its 17 sustainable development goals from the 2030 Agenda for Sustainable Development.[5]

For a wider societal change, all sectors will need to evolve to these current problems. One of the largest industries playing a particular role is the chemical industry with a wide-ranging reach from bulk commodity chemicals (e.g. plastics and fertilisers), speciality chemicals (e.g. agrochemicals, and adhesives), and fine chemicals (e.g. pharmaceuticals). A perhaps understated fact about the chemical industry is that 90% of the materials used a derived from crude oil feedstocks.[6] it is clear that to align itself with Sustainable Development modern

chemical industry needs to adapt by either using the current petrochemical resources more efficiently or perhaps alternative resources altogether.

1.1.2 Principles in Green Chemistry

In recent times Green Chemistry has emerged as a multi-disciplinary field which can be implemented into pre-existing classical chemical fields of organic and inorganic chemistry, allowing for a wider potential to meet sustainability goals. The definition of Green Chemistry was first formulated in the 1990s as "design of chemical products and processes to reduce or eliminate the use and generation of hazardous substances" by P. Anastas and J.C. Warner.[7] With this definition 12 key principles of Green Chemistry were defined, allowing for deeper integration of Green Chemistry in all areas of chemistry (**Table 1**). Alongside these definitions, it is useful to use the CHEM 21 (Chemical Manufacturing Methods for 21st Century Pharmaceuticals) which can be utilised as a scoring system for each principle with green, yellow or red "flags".[8] Green denotes "preferred", amber denotes "acceptable-some issues" and red "undesirable". Below this introduction will discuss how some of these core principles are applied to this thesis.

Atom economy (**Table 1**, 2) is a measure of reaction efficiency, simply defined as: $\frac{molecular\ weight\ of\ desired\ products}{total\ molecular\ weight\ of\ reactants}$ x 100. Atom economy is at the core of the work of this thesis, with the hydrofunctionalization methodology (Chapters 1.2-1.9) designed in principle to be 100% atom efficient. In reality, it is difficult for a reaction to be 100% atom-efficient with no side products forming whatsoever, as well as 100% yield being needed in addition to be truly 100% atom-efficient. However, throughout this thesis these conditions are balanced through changing conditions of catalyst loading, solvent volume and reactant ratios for a more accurate representation of reaction sustainability.

Table 1. 12 Principles of Green Chemistry.[7]

Principle	Meaning
1) Prevention	"It is better to prevent waste than to treat or clean up waste after it has been created."
2) Atom economy	"Synthetic methods should be designed to maximize the incorporation of all materials used in the process into the final product."
3) Less hazardous Chemical Synthesis	"Wherever practicable, synthetic methods should be designed to use and generate substances that possess little or no toxicity to human health and the environment."
4) Designing Safer Chemicals	"Chemical products should be designed to affect their desired function while minimizing their toxicity."
5) Safer Solvents and Auxiliaries	"The use of auxiliary substances (e.g., solvents, separation agents, etc.) should be made unnecessary wherever possible and innocuous when used."
6) Design for Energy Efficiency	"Energy requirements of chemical processes should be recognized for their environmental and economic impacts and should be minimized. If possible, synthetic methods should be conducted at ambient temperature and pressure."
7) Use of renewable feedstocks	"A raw material or feedstock should be renewable rather than depleting whenever technically and economically practicable."
8) Reduce Derivatives	"Unnecessary derivatization (use of blocking groups, protection/ deprotection, temporary modification of physical/chemical processes) should be minimized or avoided if possible, because such steps require additional reagents and can generate waste."
9) Catalysis	"Catalytic reagents (as selective as possible) are superior to stoichiometric reagents."
10) Design for degradation	"Chemical products should be designed so that at the end of their function they break down into innocuous degradation products and do not persist in the environment."
11) Real-time Analysis for Pollution Prevention	"Analytical methodologies need to be further developed to allow for real-time, in-process monitoring and control prior to the formation of hazardous substances."
12) Inherently Safer Chemistry for Accident Prevention	"Substances and the form of a substance used in a chemical process should be chosen to minimize the potential for chemical accidents, including releases, explosions, and fires."

Perhaps the second core tenet of this work is the use of catalysts over stoichiometric reagents (**Table 1**, 9). However wherever possible and comparable in terms of yields and selectivity a catalyst-free approach is untaken. Over factors considered in assessing a catalyst-free versus catalytic methodology, include the use of excess equivalents (often described in literature unrecovered "solvent") of starting materials to obtain comparable to catalytic yields or excessively high temperatures (e.g. >80 °C).

The type of catalyst employed is also significant, most chemo-catalytic systems employ a metal centre and the sustainability and reserves of the particular metal need to be considered. The European Union (EU) labels an element as a red flag if is at risk of depletion in the next 5-50 years (and/or a geopolitical supply risk).[9] If the element is a risk of depletion in the next 50-500 years it is then an orange flag risk and if widely available a green flag.[10] Importantly from this many pharmaceuticals and agrochemicals involve steps using these "red flag" elements as part of metals catalysts, for example, "platinum group metals" Ruthenium, rhenium, palladium, osmium, iridium and platinum. Thus, this work attempts to utilise a more sustainable approach of limiting use to only first-row transition metals, with iron being the first metal employed as this is defined as a "green flag" and other commonly used first-row transition metals such as cobalt, nickel and copper used in hydrofunctionalisation are "orange flag".[10]

Typically, within organometallic catalytic chemistry, the vast majority of solvents used are derived from petrochemicals with common solvents used in organometallic chemistry being dichloromethane, benzene, hexane and tetrahydrofuran (THF). Where possible bioderived solvents are used such as 2-MeTHF instead of THF (**Table 1,** 7). However, in many cases this is not possible due to limitations of the air-sensitive oxophilic nature of the catalyst class used (Chapter 1.9). Further to this solvent focus, several initial NMR reactions are

performed in deuterated benzene (red flag classified) out of necessity for catalyst compatibility, however, the use is minimised quantity-wise by only from initial small NMR reactions (~0.5 mL). For scale-up reactions however deuterated benzene is replaced by the less problematic “orange flag” toluene (~5.0-30 mL) (**Table 1**, 5). Further to this solvent focus wherever possible without diminishing the yields or chemoselectivity of the reaction, all reactions are performed with the minimum amount of solvent (reaction solvent and work-up solvent) in some cases being performed neat without any solvent. Allowing for a more sustainable reaction overall when considering total reaction mass and not just efficiency.

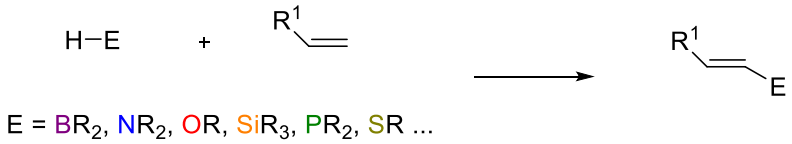
The compounds synthesised herein are organophosphorus-based, a concern regarding some organophosphorus compounds, particularly primary phosphines is their hazardous, malodorous and pyrophoric nature (**Table 1**, 3). Typically, the prototypical primary phosphine used is phenylphosphine (H_2PPh) however this is extremely malodorous and pyrophoric. To circumvent this issue the much less malodorous and pyrophoric (only >40 °C) primary phosphine ferrocenyl phosphine, $FcPH_2$ is utilised. Additionally, initial reactions were monitored in sealed J Young NMR tubes by ^{31}P NMR spectroscopy allowing for real-time analysis if any potentially pyrophoric primary phosphines form and if they persist until the end of the reaction (**Table 1,** 11).

Ideally, all reactions should be performed in as ambient conditions as possible, CHEM 21 defines 0 to 70 °C as green flag, -20 to 140 °C as orange flag and red flag >140 °C.[8] Green flag is utilised first attempting the reaction at ambient temperatures and pressures, increasing temperature to 60 °C only if needed (**Table 1**, 6) and potentially only past this point if the product being formed is novel but with other conditions (e.g. time or catalyst loading) modified first to avoid this if possible.

1.2 Heteroatom rich synthesis via hydrofunctionalisation

1.2.1 Hydrofunctionalisation Reactions

Heteroatom containing organic molecules have found widespread success and applications in both industry and academia in areas such as pharmaceuticals,[11–13] fine and bulk chemicals, agrochemicals,[14] coordination chemistry,[15–17] and catalysis.[18–20] The resulting demand and growing need for more sustainable chemical processes has led the chemical community to develop more efficient and selective processes for the design of these molecules. Hydrofunctionalisation, also known as heterofunctionalisation or hydroelementation is a popular route to synthesise heteroatom rich compounds. Hydrofunctionalisation involves the addition of an E–H bond (E = OR, SR, NR_2, PR_2, BR_2 etc.) to an unsaturated organic molecule such as an alkene or alkyne (**Scheme 1**).



Scheme 1. *General scheme for hydrofunctionalisation of alkenes.*

These reactions are highly desirable as they have the potential to be 100% atom efficient and utilise easily accessible low-cost starting materials. Additionally, the use of catalysts in these reactions can further improve the worth of this methodology by controlling selectivity and improving yields.

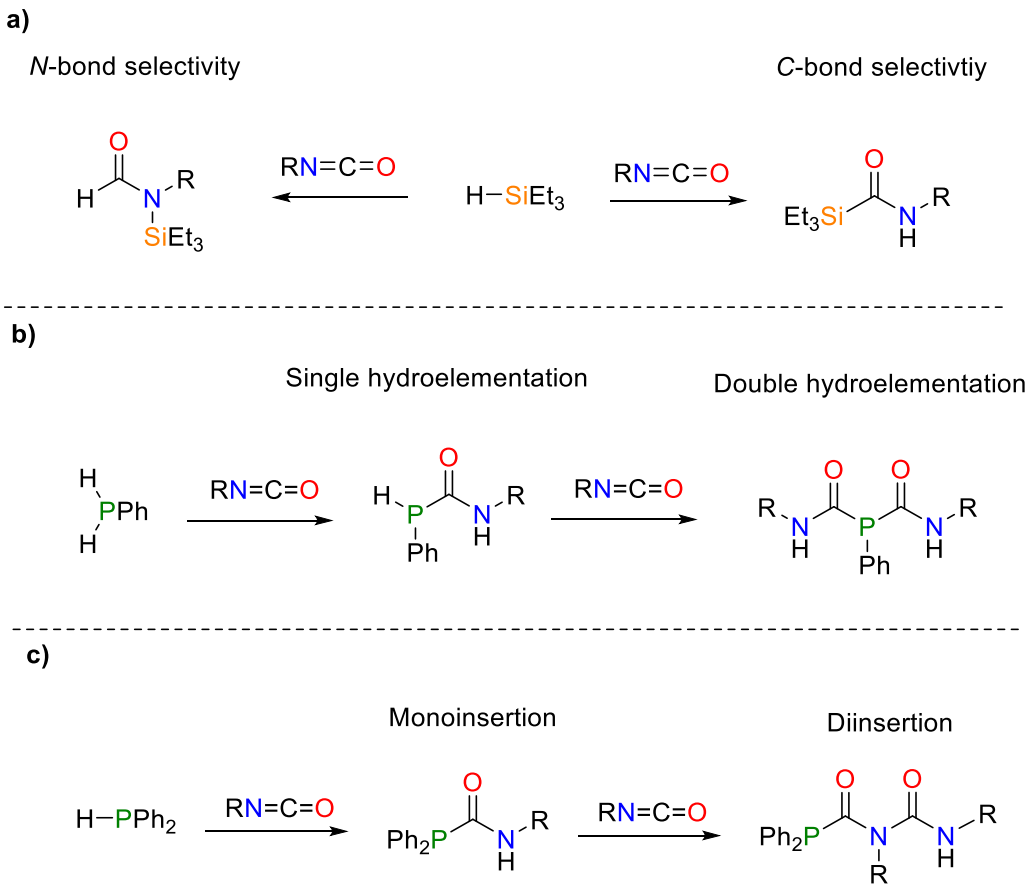
1.2.2 Heterocumulene substrates: isocyanates, isothiocyanates and carbodiimides

In the last decade, hydrofunctionalisation has witnessed intensive research, mainly using alkene,[21–25] alkyne[26–30] and allene[31–36] substrates (with some additional examples using carbonyls[37,38] and nitriles[39–42]). In more recent times, the desire of chemists to synthesise more heteroatom-rich moieties has resulted in the hydrofunctionalisation of heterocumulene substrates mainly isocyanates (R-N=C=O), isothiocyanates (R-N=C=S) and carbodiimides (R-N=C=N-R). The products of these reactions are heteroatom-rich urea, thiourea and guanidine derivatives that have uses as pharmaceutical analogues,[43,44] organic synthons[45,46] and multidentate ligands.[47–50]

Compared to their single-bonded counterparts, heterocumulenes have more synthetic possibilities with potential reactions spreading across, unsaturated bond selectivity (**Scheme 2** (a)), double hydrofunctionalisations of a heterocumulene substrate (**Scheme 2** (b)) and multiple heterocumulene insertions into a single E-H moiety (**Scheme 2** (c)), and reactions involving combinations of these different reaction classes.

In general, the reactivity of these heterocumulene substrates can be explained through the electrophilicity of major and minor resonance structures. With isocyanates being the most electrophilic and carbodiimides being the least and isothiocyanates being somewhere between both (**Scheme 3**, above). This theoretically allows all heterocumulenes to be involved in the more complex reactions such as double hydroelementation or diinsertion reactions, however in reality as electrophilicity drops off from the level of isocyanates these more complex

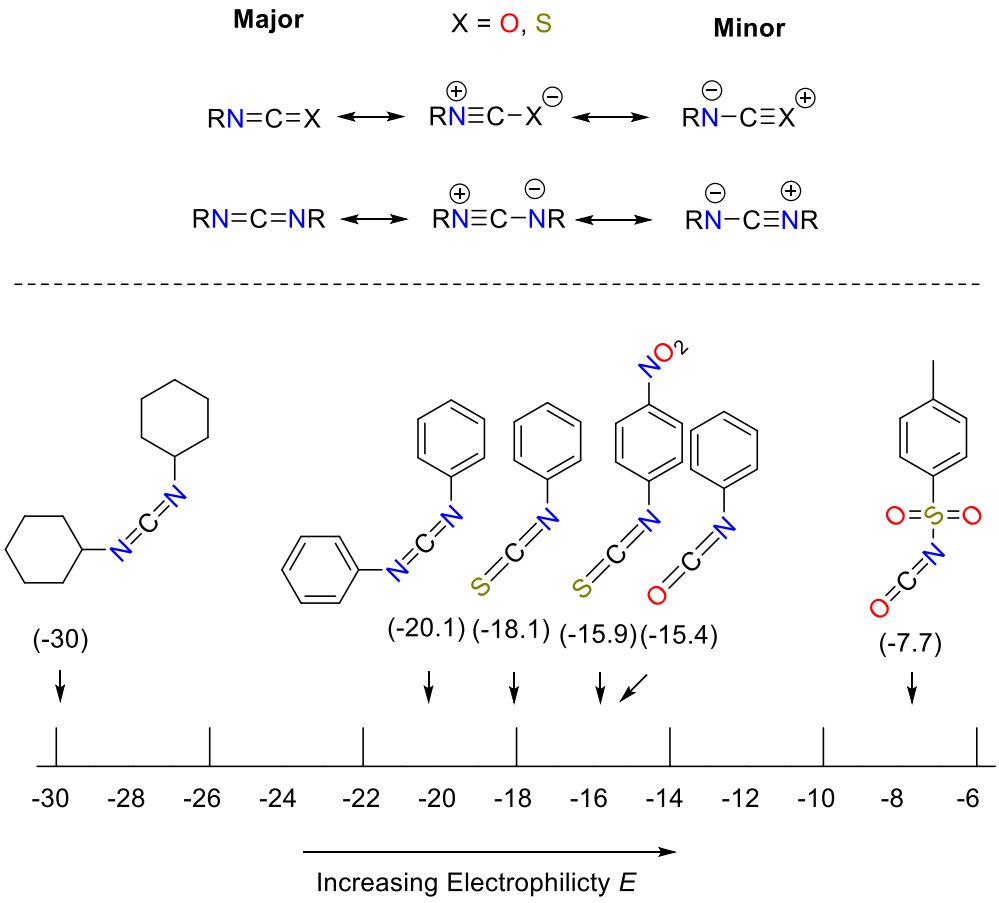
reactions become much harder and is reflected in a comparative lack of examples with isothiocyanates and carbodiimides undergoing these more complex reactions in literature.[51]



Scheme 2. *a) General scheme for hydrosilylation of isocyanates highlighting C- or N-bond chemoselectivity. b) General scheme for single or double hydrophosphination into one or two P-H bonds. c) (single) Hydrophosphination with monoinsertion or diinsertion of isocyanates into a single P-H bond.*

Recently Mayr *et al.* have quantified the electrophilicity of various heterocumulenes through experimental reactions with reference nucleophiles and computational analysis, using the linear free-energy relationship, $\log k_2(20\ °C) = S_N(N + E)$ (where N = nucleophilicity, E = electrophilicity, S_N = nucleophile specific slope parameter, k_2 = 2nd order rate constant for reaction of the heterocumulene with the reference

nucleophile) (**Scheme 3**, below).[52–56] This showed as expected PhN=C=O was more electrophilic (-15.38) than Ph-N=C=S (-18.15) but the addition of an electron withdrawing tosyl group made TsN=C=O much more electrophilic (-7.69). Conversely, the addition of an electron withdrawing 4-NO_2 group to PhN=C=S makes 4-$NO_2C_6H_4$N=C=S vastly increases electrophilicity to (-15.9) to a point where PhN=C=O and 4-$NO_2C_6H_4$N=C=O have very similar electrophilicity values. PhN=C=NPh (-20.1) is much less electrophilic than both isocyanate and isothiocyanates. CyN=C=NCy (-30.0) is the least electrophilic heterocumulene to the point that reactions with the reference nucleophiles take place so slowly the electrophilicity value can only be determined computationally.[56]

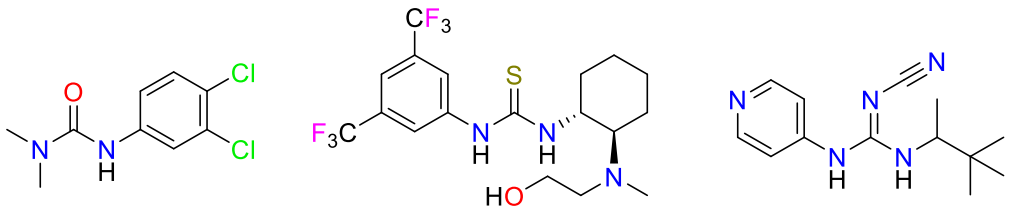


***Scheme 3**. (Above) isocyanate (X=O), isothiocyanate (X=S) and carbodiimide resonance structures. (Below) Electrophilicity (logarithmic) of various isocyanates, isothiocyanates and carbodiimides.*[56]

The following sub-chapters of this introduction will outline advances in the hydroboration, hydrosilylation, hydroamination and hydrophosphination of heterocumulenes by homogeneous catalysts and additionally, catalyst-free methodologies where comparable to catalytic processes, paying particular attention to highlighting the more novel successes where possible. This introduction will conclude with a discussion of hydrofunctionalisations using *m*-terphenyl catalysts to introduce the reader to the catalyst class used throughout this thesis.

1.3 Hydroamination of Heterocumulenes

The hydroamination of isocyanates, isothiocyanates and carbodiimides leads to the synthesis of urea, thiourea and guanidine derivatives. These compounds are essential for pharmaceuticals,[43,44,57,58] agrochemicals,[45,59–62] materials,[63,64] biological systems,[65,66] supramolecular chemistry[67,68] and synthetic chemistry (**Scheme 4**).[45,46] Common synthetic methodologies for the synthesis of ureas typically utilise rare noble metals; for example in the reduction of nitro compounds with carbon monoxide,[69] oxidative carbonylation of amines,[70,71] and cross-coupling of aryl chlorides with sodium cyanate,[72] additionally stoichiometric reagents are sometimes used.[73] The most widely used syntheses for thioureas are the condensation of primary and secondary amines with isothiocyanate,[74] thiophosgene[75] or its derivatives.[76] More examples include, the reaction between primary amines and carbon disulfide in the presence of mercury acetate, and the reaction of unsubstituted thioureas with primary alkyl amines is also used.[77,78] Contrary to these reactions hydroamination can be a simple alternative route that avoids the use of these excess stoichiometric reagents and harsh conditions.



Scheme 4. *Urea, thiourea and guanidine motifs in agrochemicals, catalysis and pharmaceuticals.*[79–81]

The first catalytic hydroamination of carbodiimides with aryl amines was reported by Richeson *et al.* in 2003.[82] Utilising 1.0 mol% of titanium(IV) imido precatalyst **1** (**Figure 1**) at an elevated temperature of 105 °C a range of substituted primary aryl amines, H_2NR (R = Mes, C_6F_5 or C_6H_4R'; R' = 4-MeO, 2-MeO, 4-Cl, 4-$NCCH_2$) in good to excellent yields (82-97%) (**Scheme 5**). Additionally, precatalyst **1** can perform a transamination reaction on the subsequent guanidine hydroamination product if a more nucleophilic alkyl primary amine such as $^{i}PrNH_2$ is introduced.

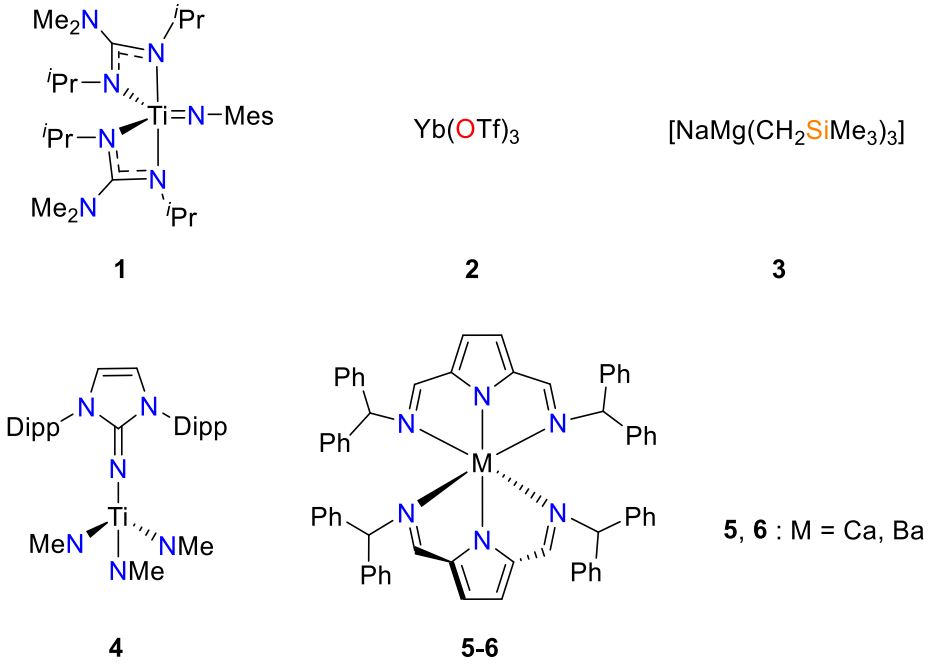
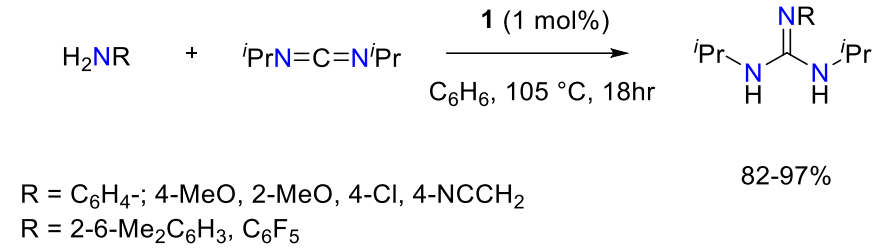
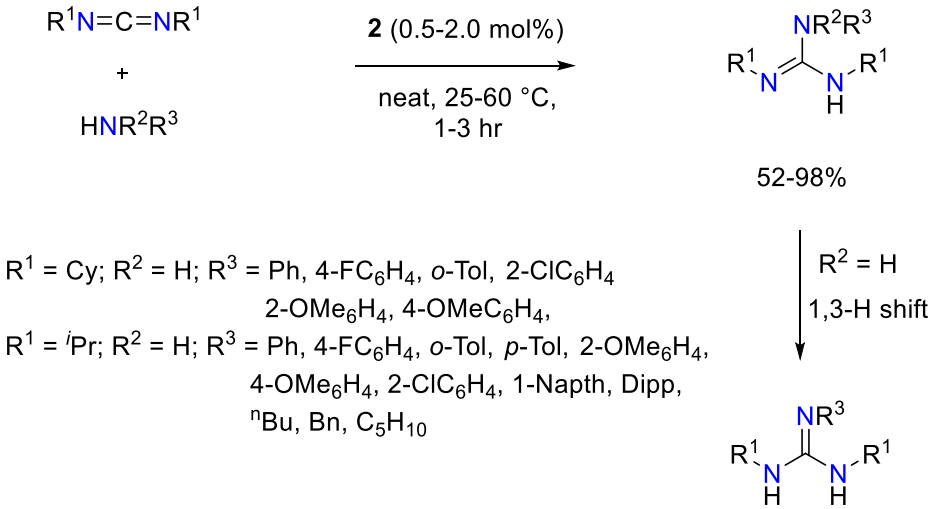


Figure 1. *Hydroamination precatalysts **1** by Richeson et al.*[82]*, **2** by Shen et al.,*[83] ***3*** *by Hevia et al.,*[84] ***4*** *and **5**-**6** by Panda et al.*[85,86]



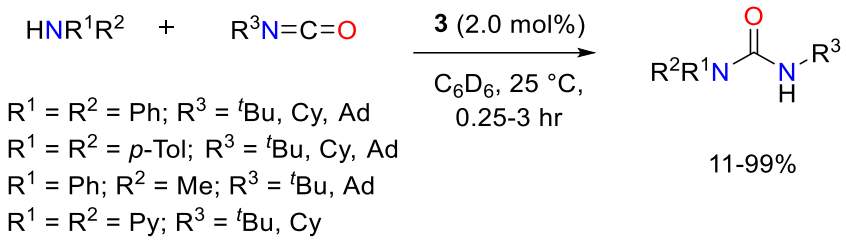
***Scheme 5**. Hydroamination of ^{i}PrN=C=N^{i}Pr by precatalyst **1** utilising aryl amines.*[82]

The use of a simpler precatalyst **2**, Yb(OTf)$_3$ (**Figure 1**) in 0.5-2.0 mol% catalyst loading has been shown to be effective for the hydroamination of CyN=C=NCy with aromatic, aliphatic and heterocyclic secondary amines in neat conditions (**Scheme 6**).[83] The use of primary amines requires only 0.5 mol% of **2** and temperatures of 25 °C for moderate to excellent yields (52-98%) however in order to use secondary amines the precatalyst loading of **2** has to be increased to 2.0 mol% and the temperature to 60 °C giving moderate to excellent yields (76-95%). It should also be noted when primary amines are used the expected products undergo a 1,3-H-shift to give the observed products (**Scheme 6**).



***Scheme 6.** Hydroamination of carbodiimides by precatalyst **2** utilising primary and secondary amines.*[83]

Catalyst loadings of 2 mol% of **3** catalyse the hydroamination of a variety of alkyl isocyanates and aryl secondary amines (**Scheme 7**). More sterically encumbered $HN(SiMe_3)_2$ was not tolerated, and $HNPy_2$ was also poorly tolerated, potentially due to the pyridyl donors forming a contact ion pair of sodium magnesiates reducing the coordination flexibility.



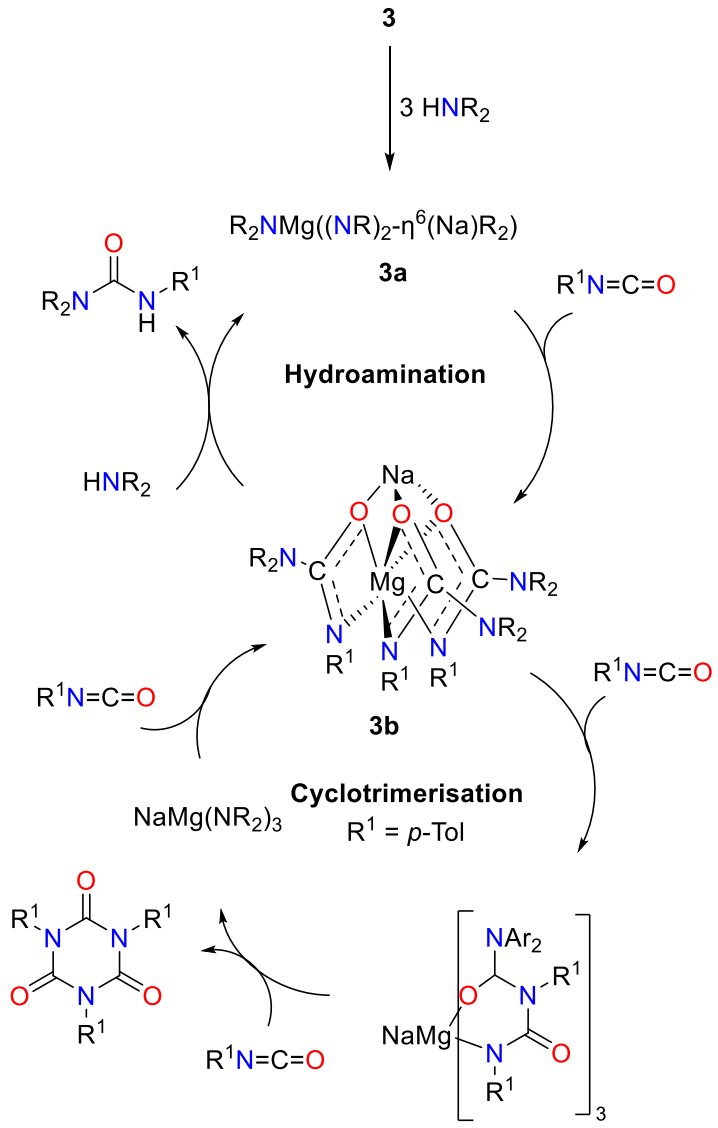
***Scheme 7**. Hydroamination of alkyl isocyanates by precatalyst **3**.*[84]

The hydroamination mechanism proceeds *via* protonation by three equivalents of $HNAr_2$ to yield **3a** followed by three isocyanate insertions to yield **3b** and completion of the catalytic cycle by protonation by $HNAr_2$ (**Scheme 8**). When the more electrophilic and bulkier *p*-TolN=C=O is used instead of PhN=C=O, the cyclotrimerisation product, $[p\text{-TolN-C=O}]_3$ is formed by sequential isocyanate insertions until **3b** is reformed.

In the presence of 5.0 mol% of imidazolin-2-iminato titanium-based precatalyst **4**, phenyl isocyanate undergoes hydroamination by a variety of aryl amines, HNR^1R^2 (R^1 = H; R^2 = ^{t}Bu, Et, Mes, Dipp, 2-FC_6H_4 and $R^1 = R^2 = {}^i$Pr = pyrrolidine with isocyanates, RN=C=O (R = Ph, *p*-Tol and 4-ClC_6H_4.[85]

Initially using precatalysts **5**-**6** no hydroamination product was observed from the reaction between aryl isocyanates and primary aryl amines, with heating to 60 °C required to initiate the reaction. Further optimisation found the use of the solvents benzene, toluene and THF were inferior to performing the reaction without solvent. The reaction between *p*-TolN=C=O with H_2NPh and substituted secondary amines HNR_2 bearing electron-donating groups (R = 4-$OMeC_6H_4$, 2-MeC_6H_4, 2,6-$Me_2C_6H_3$, Bn), proceeded with excellent yields but

arylamines with electron withdrawing groups (R = 2-$NO_2C_6H_4$, 2-FC_6H_4, 2-BrC_6H_4) showed slightly lower conversions.[85] The same functional group scope of arylamines is also applicable to phenyl isothiocyanate.



Scheme 8. *Hydroamination mechanism for PhN=C=O and cyclotrimerisation mechanism for p-TolN=C=O .*[84]

1.4 Hydrophosphination of Heterocumulenes

In 1980 the first synthesis of neutral phosphaguanidines was reported by the addition of $HPPh_2$ to *p*-TolN=C=N*p*-Tol at elevated temperatures,[87,88] and additionally in 1980 silylated phosphaguanidines by utilising *bis*-silyated phosphines.[89] However the first catalytic synthesis of phosphaguanines was not reported until 2006 by Hou *et al*.[90] by utilising commercially available alkali metal compounds **7-11** (**Figure 2**) as precatalysts for the hydrophosphination of carbodiimides. In this work the activity increased as the metal size became larger (K > Na > Li), with 1.0 mol% of **9** reacting with ^{i}PrN=C=N^{i}Pr and wide range of secondary aryl phosphines (2/3/4-Me-, 4-OMe-, 4-Cl-, 4-Br-, 3,5-Me_2- and 3,5-$(OMe)_2$-substituted) in near quantitative yields (**Scheme 9**)

Additionally, a range of symmetric and asymmetric carbodiimides could be utilised (R^1, R^2 = Cy, *p*-Tol; ^{t}Bu, Et; Ph, Cy) (**Scheme 9**). For the more challenging mixed alkyl/aryl phosphine HPPhEt and dialkyl phosphine HP$^{i}Bu_2$, a higher (3.0 mol%) loading of **9** was required for the hydrophosphination of ^{i}PrN=C=N^{i}Pr. Primary phosphines (H_2PPh and H_2PCy) were also well-tolerated and the use of H_2PCy afforded the double hydrophosphination product (^{i}PrN=CNH^{i}Pr)$_2$(PCy) as a minor product of the reaction.

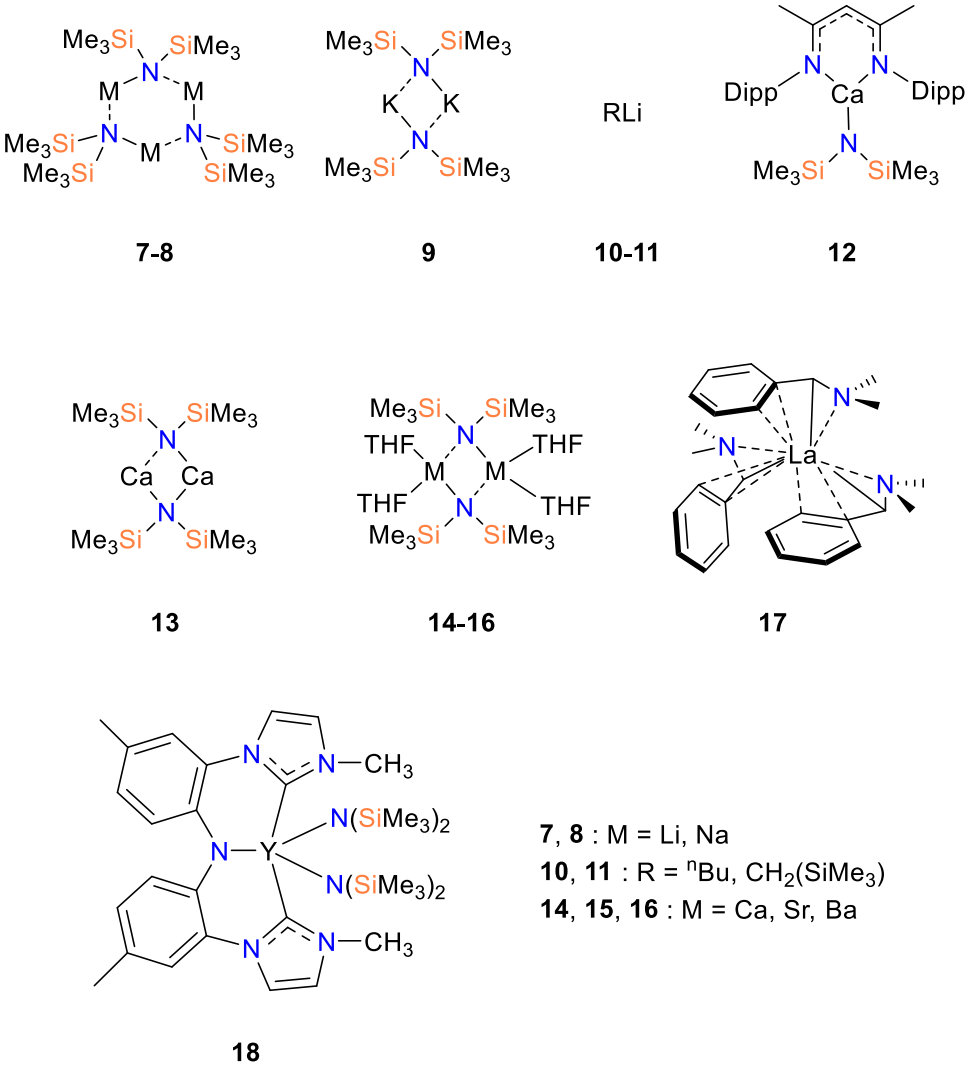
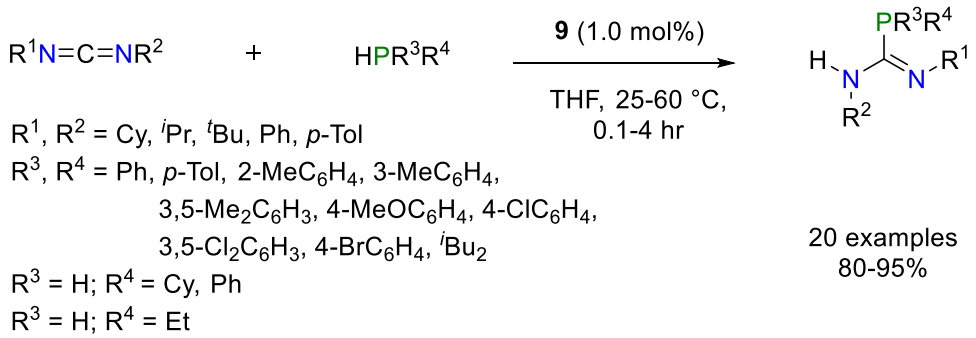


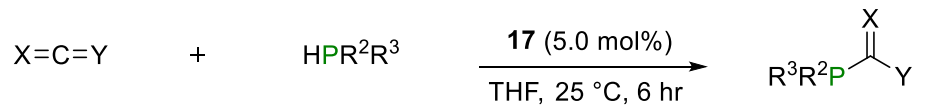
Figure 2. *Heterocumulene hydrophosphination precatalysts,* ***7-12*** *by Hou et al.,*[90] ***13-16*** *by Procopiou et al.,*[91] ***17*** *by Schmidt et al.,*[92] *and* ***18*** *by Wang et al.*[93]



Scheme 9*. Hydrophosphination of carbodiimides by precatalyst* ***9.***[90]

Proceeding this work, analogous homoleptic and heteroleptic group 2 amide complexes **13-16** (**Figure 2**) were investigated for the hydrophosphination of carbodiimides.[91] Strontium precatalyst **15** was found to be the most active and by utilising 2.0 mol% with $HPPh_2$, hydrophosphination of alkyl carbodiimides $R^1N=C=NR^2$ ($R^1 = R^2 = {}^i$Pr, Cy and $R^1 = {}^t$Bu, R^2 = Et; 95-99% as determined by ^{1}H NMR spectroscopy) was successful, but the use of more sterically demanding ^{t}BuN=C=N^{t}Bu and the more electron rich phosphine $HPCy_2$ were unsuccessful. The more electron-donating $HP(p\text{-Tol})_2$ substrate could be utilised; however, this required the use of increased catalyst loadings.

Homoleptic α-metalated dimethylbenzylamine precatalyst **17** is an efficient catalyst for the hydrophosphination of a range of isocyanates, isothiocyanates and carbodiimides. Conversions for all substrates are near quantitative as determined by NMR spectroscopy, but the isolated yields were significantly lower (**Scheme 10**). Steric bulk was a limiting factor in hydrophosphination as shown with the use of ^{t}BuN=C=O and AdN=C=O, with low conversions as determined by ^{31}P NMR spectroscopy of 20% and 38% respectively. The use of more acidic $HP(^t\text{Bu})_2$ gave no products at all with ^{i}PrN=C=N^{i}Pr; even with further heating to 80 °C for 36 hours. Little effect of electronics on the phosphine was seen with $HP(4\text{-OMeC}_6H_4)_2$ and $HP(4\text{-MeC}_6H_4)_2$, which afforded hydrophosphination products in similar yields to $HPPh_2$.

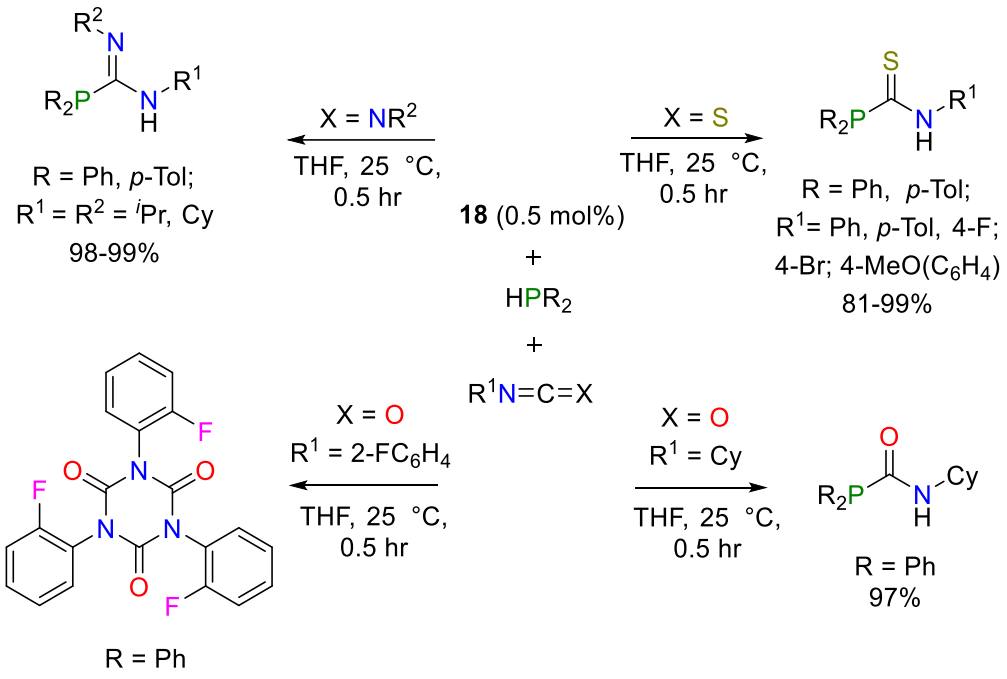


X = Y = NR^1= ^{i}Pr, Cy; $R^2 = R^3$ = Ph
X = O; Y = NR^1 = Ph, Cy, Ad, Napthyl, 4-FC_6H_4;
4-ClC_6H_4, 4-BrC_6H_4, 4-$MeOC_6H_4$,
4-$CF_3C_6H_4$; $R^2 = R^3$ = Ph
X = O; Y = NR^1 = 4-$CF_3C_6H_4$, 4-BrC_6H_4;
$R^2 = R^3$ = *p*-Tol, 4-$MeOC_6H_4$
X = S; Y = NR^1 = Ph; $R^2 = R^3$ = Ph

14 examples
38-93%

***Scheme 10**. Hydrophosphination of heterocumulenes by **17**.*[92]

The N-heterocyclic carbene complex **18** catalyses hydrophosphination reactions using $HPPh_2$ or $HP(4\text{-}MeC_6H_4)_2$ with CyN=C=NCy or ^{i}PrN=C=N^{i}Pr in near-quantitative yields with only 0.5 mol% catalyst loadings at ambient temperature (**Scheme 11**). However, as with previous examples, the elusive ^{t}BuN=C=N^{t}Bu hydrophosphination product could not be obtained (**Scheme 10**).[91]

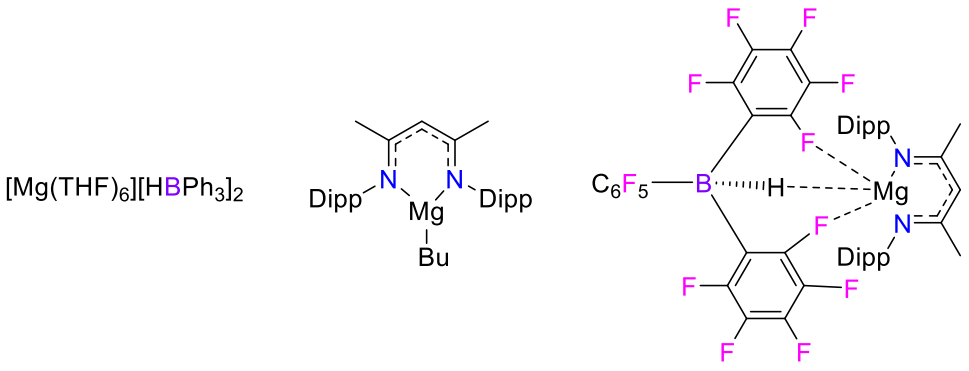


Scheme 11. *Hydrophosphination of carbodiimides, isocyanates and isothiocyanates by* ***18****.*[93]

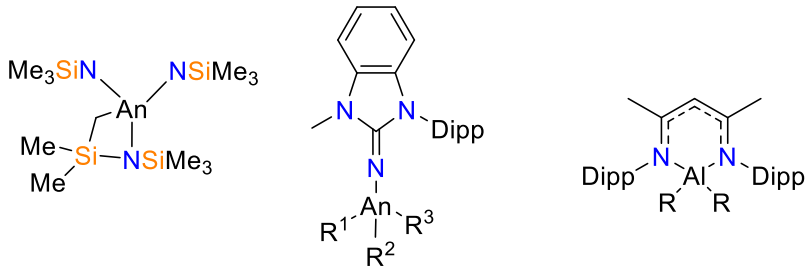
In addition, utilising precatalyst **18** excellent yields were obtained for a variety of functionalised aryl isothiocyanates ($4\text{-}FC_6H_4$, $4\text{-}BrC_6H_4$, $4\text{-}MeC_6H_4$, $4\text{-}MeOC_6H_4$-substituted substrates in 94-99% yields); slightly lower yields were obtained for $HP(4\text{-}MeC_6H_4)_2$ compared to $HPPh_2$ (**Scheme 11**). Interestingly, the use of the alkyl isocyanate CyN=C=O afforded the hydrophosphination product, but the aromatic isocyanate $4\text{-}FC_6H_4N$=C=O produced the isocyanurate, a product of isocyanate cyclotrimerisation (**Scheme 10**).

1.5 Hydroboration of Heterocumulenes

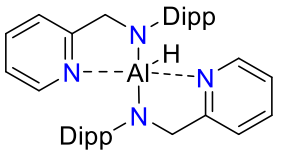
Complex **19** (**Figure 3**) catalyses the double hydroboration of ^{i}PrN=C=N^{i}Pr and ^{t}BuN=C=O, whereby 2 equivalents of HBpin insert across the unsaturated bonds, reaching 100% conversion by ^{1}H NMR spectroscopy (**Scheme 12**).[94] The hydridicity of the $[HBPh_3]^-$ ion is critical for catalysis, with the perfluorinated analogue $[Mg(THF)_6][HB(C_6F_5)_3]_2$ exhibiting inferior catalytic performance in optimisation reactions for the hydroboration for other C=O bond substrates.[94]



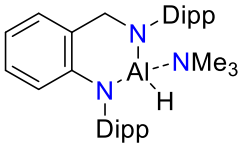
19 **20** **21**



22-23 **24-27** **28-29**



30

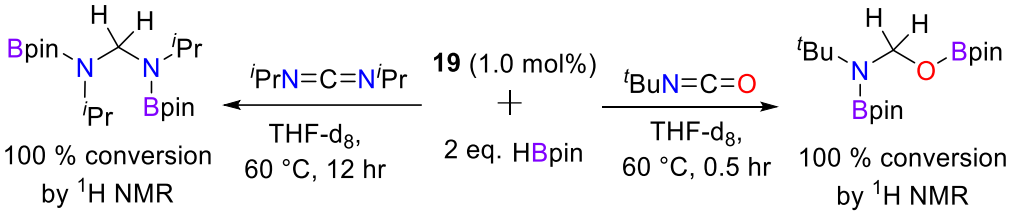


31

22-23: An = U, Th
24-25: $R^1 = R^2 = R^3 =$ $N(SiMe_3)_2$: An = U, Th
26-27: $R^1 = R^2 = Cp^*$, R^3 = Me : An = U, Th
28-29: R = H, Me

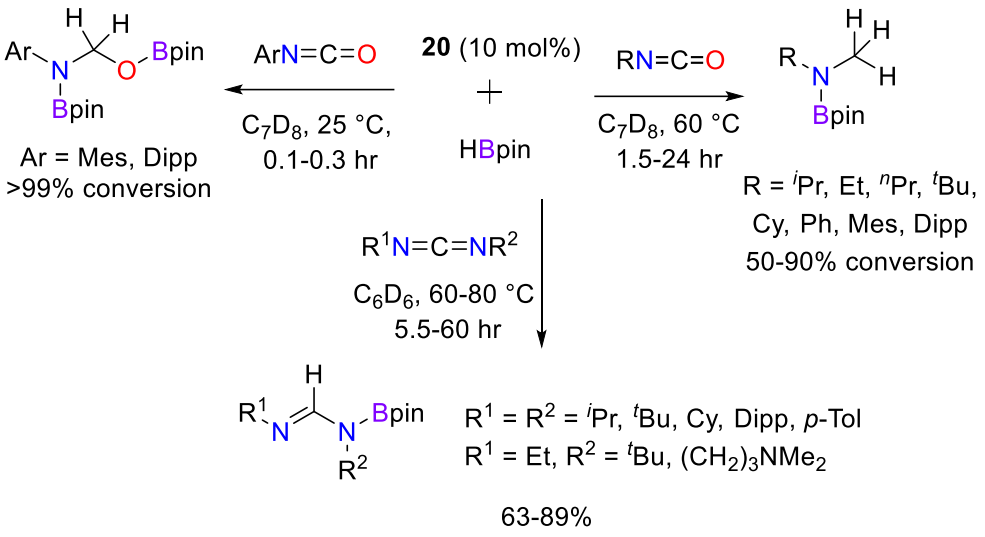
Figure 3. *Precatalysts for the hydroboration of heterocumulenes:* ***19*** *by Okuda et al.,*[94] ***20*** *and* ***21*** *by Hill et al.,*[95,96]*,* ***22-27*** *by Eisen et al.,*[97] *and* ***28-31*** *by Roesky et al.*[98,99]

The *β*-diketiminato precatalyst **20** (**Figure 3**) has been used in the hydroboration of various alkyl and aryl carbodiimides (**Scheme 13**, below).[95] Increasing the steric bulk (to *tert*-butyl) necessitated longer reaction times, from 15 hours (for R = Cy, ^{i}Pr) to 60 hours, along with elevated temperature (80 °C). Aryl-substituted carbodiimides also required the use of elevated temperatures to reach high conversions, albeit with similar reaction times to secondary alkyl carbodiimides.



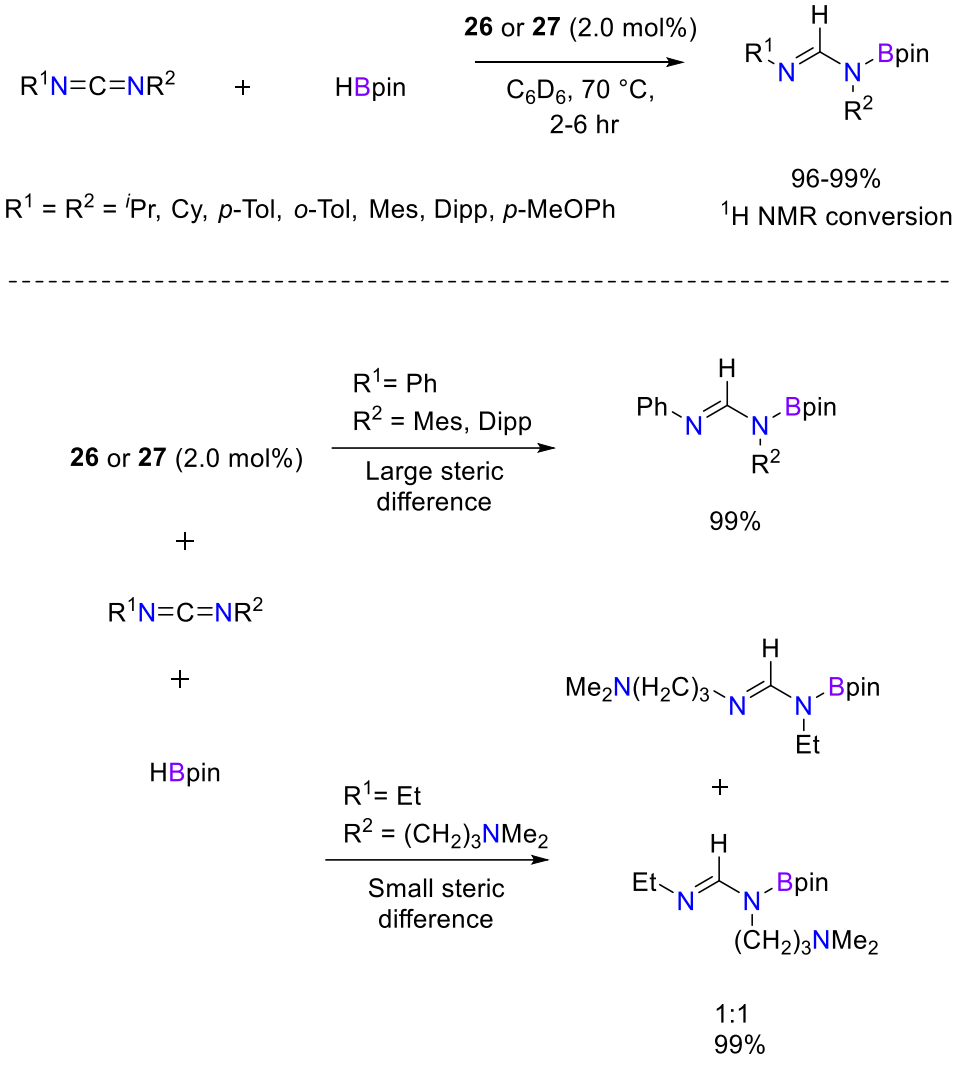
***Scheme 12**. (Left) Double hydroboration of diisopropyl carbodiimide and (right) double hydroboration of tert-butyl isocyanate.*[94]

The use of two equivalents of HBpin with **20** at temperatures of 80-100 °C failed to afford double hydroboration products, instead leading to the decomposition of HBpin, as signified by B_2pin_3 formation. In a subsequent report, Hill and co-workers demonstrated that under similar conditions the hydroboration of alkyl and sterically-encumbered aryl isocyanates catalysed by **20**, did not afford the expected products, but instead underwent hydrodeoxygenation yielding methylamines, RN(Bpin)CH_3 (R = ^{i}Pr, ^{t}Bu, Cy, Et, ^{n}Pr, Ph, Mes and Dipp, where Mes = 2,4,6-$Me_3C_6H_2$ and Dipp = 2,6-$^{i}Pr_2C_6H_3$) and $O(Bpin)_2$ (**Scheme 13**, right).[100] Under less forcing conditions, bulky MesN=C=O and DippN=C=O rapidly form double hydroboration products *in situ* (**Scheme 13**, left). In an extension of this work, Hill and co-workers have pursued magnesium β-diketiminato precatalysts further, synthesising complex **21** (**Figure 3**) bonded by two *ortho* fluorides to the Mg centre along with one Mg–H bond. **21** is capable of the double hydroboration of ^{i}PrN=C=N^{i}Pr at lower temperatures of 60 °C yielding the respective bis(*N*-boryl)aminal in 70% yield.[96]



***Scheme 13**. (Left) Dihydroboration of bulky aryl isocyanates (Mes = 2,4,6-$Me_3C_6H_3$, Dipp = 2,6-$^iPr_2C_6H_3$), (right) hydrodeoxygenation of isocyanates and (below) Monohydroboration of symmetrical and unsymmetrical carbodiimides by **20**.*[95,100]

Eisen *et al*. have prepared a series of actinide complexes **22**-**27** for the hydroboration of carbodiimides (**Figure 3**).[97] Initial optimisation reactions showed that the steric demand of the ancillary ligands demonstrated little influence on the catalytic behaviour, and that thorium-containing precatalysts **22**-**27** gave higher yields than the uranium analogues.[97] The best-performing precatalysts were **24**-**27** all giving rise to the monohydroboration product in a selective and almost quantitative fashion in a lesser time of 3 hours (**Scheme 14**, above). Using precatalysts **26**-**27** a range of alkyl and aryl carbodiimides were tolerated in almost quantitative yields with monohydroboration selectivity, even with two equivalents of HBpin. For unsymmetrical carbodiimides with similar-sized substituents little selectivity was observed, but the selectivity improved for substituents with a larger steric discrepancy. For both products, the Bpin group is bound to the nitrogen atom bearing the bulkier substituent (**Scheme 14**, below).

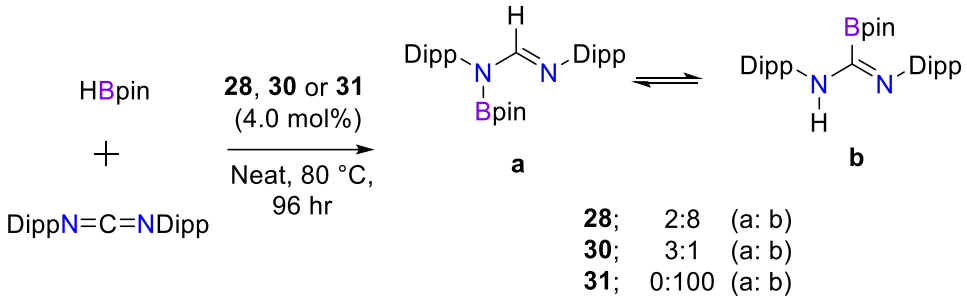


Scheme 14. *(Above) Monohydroboration of carbodiimides by **26** or **27** and (below) hydroboration of unsymmetrical carbodiimides by **26** or **27**.*[97]

Roesky *et al*. have investigated β-diketiminato (**28** and **29**) and hydridic aluminium (**30** and **31**) precatalysts (**Figure 3**).[98,99] Precatalyst **28** catalyses the hydroboration of alkyl carbodiimides (cyclohexyl and *iso*-propyl) with near quantitative conversion in 12 hours at 80 °C; a reduction in temperature (70 °C) leads to a reduction in yields to *ca.* 80%. The bulkier ^{t}BuN=C=N^{t}Bu required a significantly longer reaction time, but the even bulkier DippN=C=NDipp substrate reacted in quantitative conversions in under two hours.

When sterically demanding DippN=C=NDipp is used with precatalysts **28**, **30**, **31**. The monohydroboration product undergoes a shift to form the first-ever

reported example of a *C*-borylformamidine, identified in the ^{1}H NMR spectrum by a shift from 8.05 ppm of NC*H*N to 9.73 ppm of Ar-N*H*C (**Scheme 15**). Utilising precatalyst **31** the *C*-borylformamidine can be selectively synthesised in 60% yield. The rearrangement can be explained by potential intermolecular hydrogen bonding forces formed by *H*N=C increasing stability compared to the *N*-borylformamidine. Additionally, the electrophilicity of the boron atom of Bpin could allow for a shift from the C-N bond to the more electron rich C=N bond.



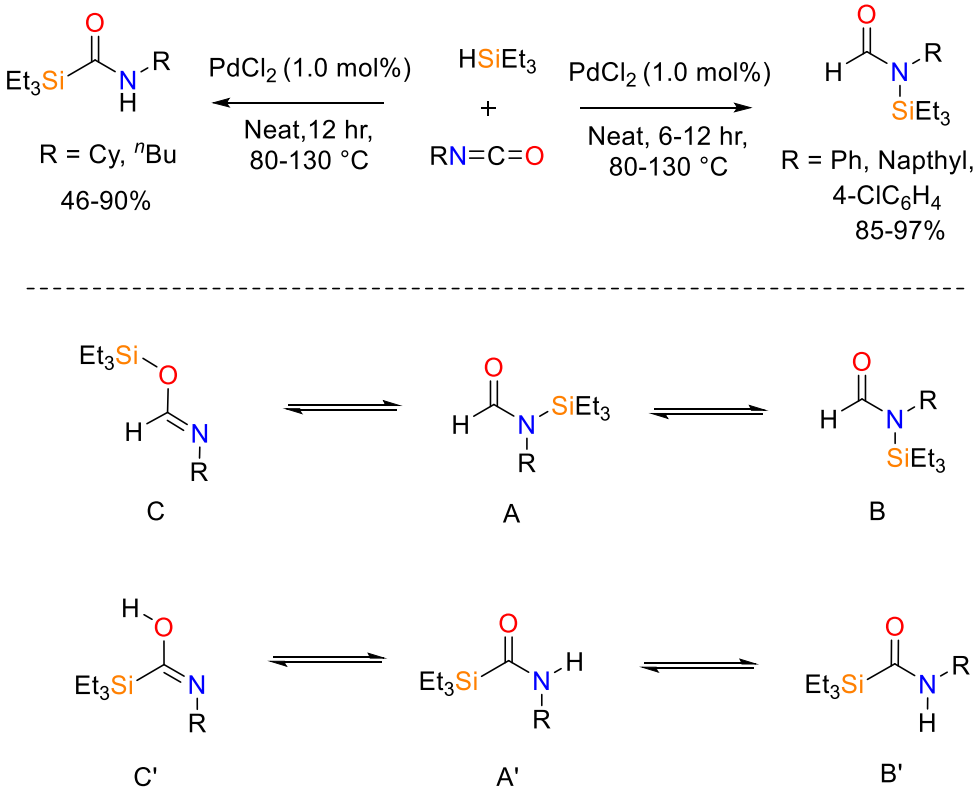
***Scheme 15**. Monohydroboration of DippN=C=NDipp to N-borylformamidine (a) followed by conversion to C-borylformamidine (b) by precatalysts **28**, **30** and **31**.*[98]

1.6 Hydrosilylation of Heterocumulenes

Seminal work in 1971 by Ojima *et al.* reported the first example of hydrosilylation of isocyanates and carbodiimides by Pd-C, $PdCl_2$ and $(Ph_3P)_3RhCl$ at elevated temperatures between 80-130 °C (**Scheme 16,** above).[101] Utilising $HSiEt_3$ with alkyl isocyanates (R = Cy, ^{n}Bu) afforded the expected *N*-triethylsilylformamides however the use of aromatic isocyanates (R = Ph, Naphthyl, 4-ClC_6H_4) gave the opposite regioselectivity yielding *C*-triethylsilylamides (**Scheme 16**, above).

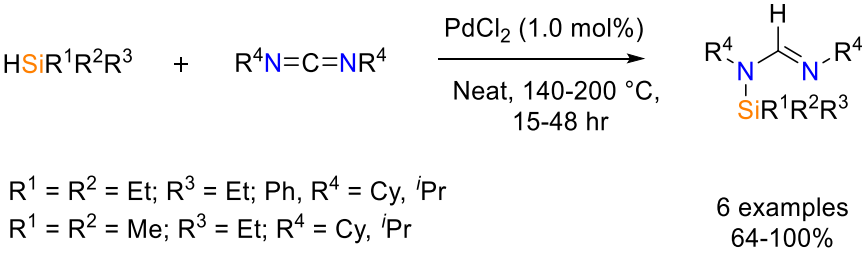
It was shown by ^{1}H NMR spectroscopy that both *N*- and *C*- silylformamides exist as a mixture of isomers (**A**-**C**). With process **A**-**B** being caused by hindered rotation around the C-N bond and process **A** to **C** being caused by amide-imidate tautomerism. While the *N*-silylformamides mainly exist as mixtures of **A**

and **C**, with the *C*-silylformamides mainly exist as a mixture of **A'** and **B'** (**Scheme 16,** below).[101]



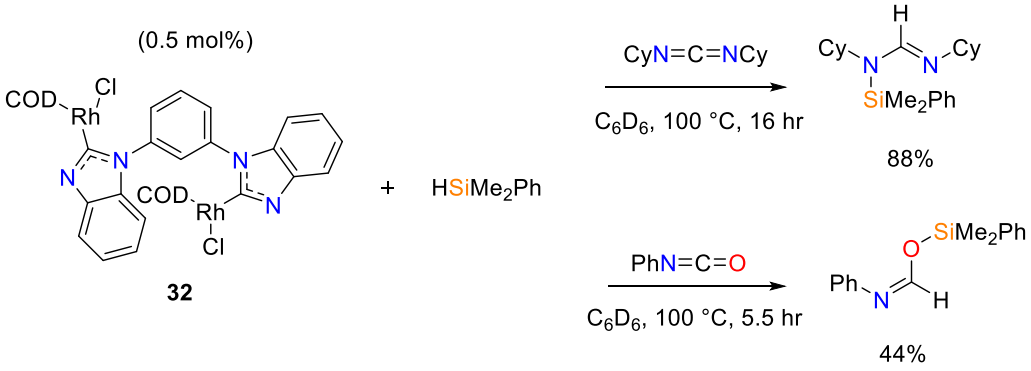
Scheme 16. *(Above) hydrosilylation of aryl isocyanates yielding N-triethylsilylamides and of alkyl isocyanates yielding N-triethylsilylformamides and (below) tautomeric forms between C-triethylsilylformamides and C- triethylsilylamides.*[101]

The hydrosilylation of carbodiimides proceeded at higher temperatures in the presence of 0.5 mol% of $PdCl_2$. In most cases, a high conversion is achieved at 140 °C in 15 hours, but the use of higher temperature (200 °C) and longer reaction times (48 hours) gave higher yields (**Scheme 17**).[101]



Scheme 17. *Hydrosilylation of carbodiimides catalysed by $PdCl_2$.*[101]

In 2013, only the second example of hydrosilylation of heterocumulenes was reported utilising bimetallic species **32** by Hollis *et al.* (**Scheme 18).** At elevated temperatures **32** catalyses the hydrosilylation of CyN=C=NCy affording the *N*-silylformamidines, but the use of PhN=C=O afforded a product of type C (**Scheme 18**), a different isomer than the expected *N*-silylformamide (type A).[102] This may be due to the increased steric bulk of the silane substituents leading to the disfavouring of isomers **A** and **B** due to steric clashes with the phenyl group.

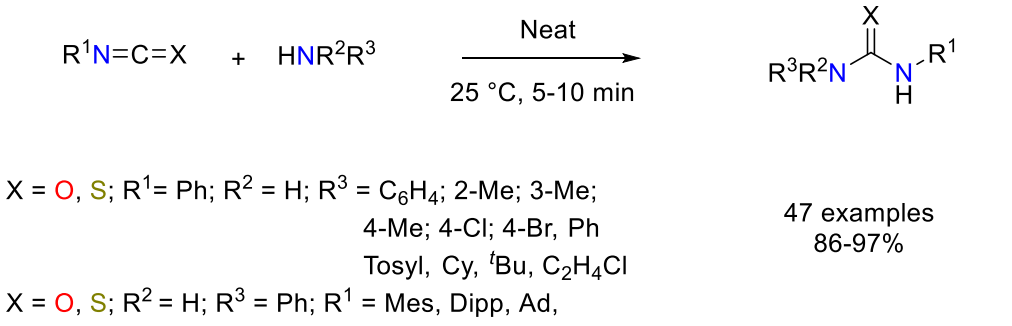


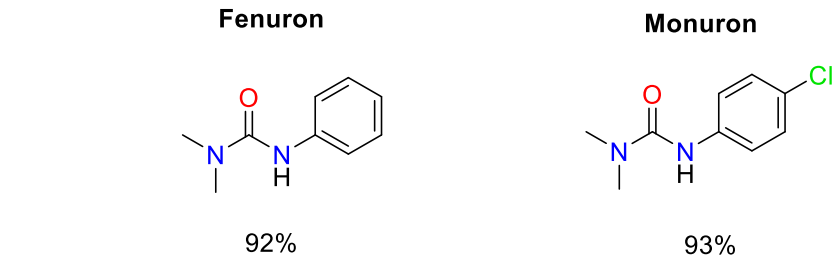
***Scheme 18**. Hydrosilylation of PhN=C=O and CyN=C=NCy by precatalyst **32**, where COD = 1,5-cyclooctadiene.*[102]

1.7 Catalyst-free N-H, B-H and P-H Hydrofunctionalisations of Heterocumulenes

Carbodiimides react with primary alkyl amines in the absence of a catalyst, to generate the corresponding guanidines under forcing reaction conditions of 120-140 °C.[103] Additionally, the direct addition of secondary cyclic amines (R = $N(C_4H_8)$, $N(C_5H_{10})$, $N(C_4H_2O)$, $N(C_4H_8NCH_3)$) to aryl carbodiimides (R = Mes, Dipp, 4-^{i}PrC_6H_4, 4-^{t}Bu-C_6H_4) at moderate temperatures (25-80 °C) is possible catalyst-free in THF solution in good to excellent yields (76-99%).[104]

In 2022 Wang *et al.* developed a catalyst-free neat approach for the hydroamination of isocyanates utilising primary alkyl and aryl amines, with both electron-donating (R = 2/3/4-Me) and electron-withdrawing groups (4-Cl, 4-Br) in 86-97% yields (**Scheme 19**).[105]



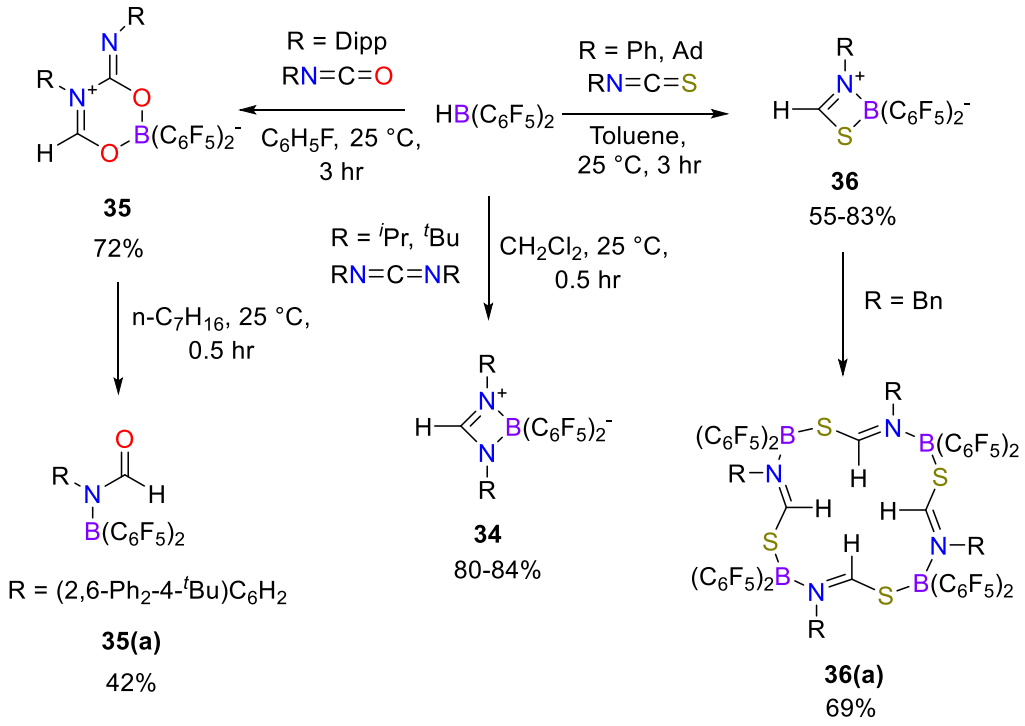


***Scheme 19**. (Above) Neat, catalyst-free hydroamination of isocyanates and isothiocyanates and (below) structures of herbicides Fenuron and Monuron.*[105]

Additionally, cyclic secondary amines could be utilised such as pyrrolidine and piperidine providing the subsequent ureas in 92% and 94% yields respectively. In a THF solution, gaseous $HNMe_2$ and either phenyl- or 4-chlorophenyl-isocyanate reacted at room temperature in 92% and 93% yields, giving the herbicides Fenuron and Monuron (**Scheme 19**, below). Further expanding the heterocumulene scope to isothiocyanates instead of isocyanates gave very similar results, proceeding to completion at room temperature in 10 mins with a near identical scope of electron donating and electron withdrawing groups being tolerated (**Scheme 19**).

Frustrated Lewis Pair (FLP)-like compounds have been synthesised by Stephan *et al.* using Piers' borane, $HB(C_6F_5)_2$ for the hydroboration of carbodiimides (R = ^{i}Pr, ^{t}Bu) forming four-membered cyclic borylformamidines

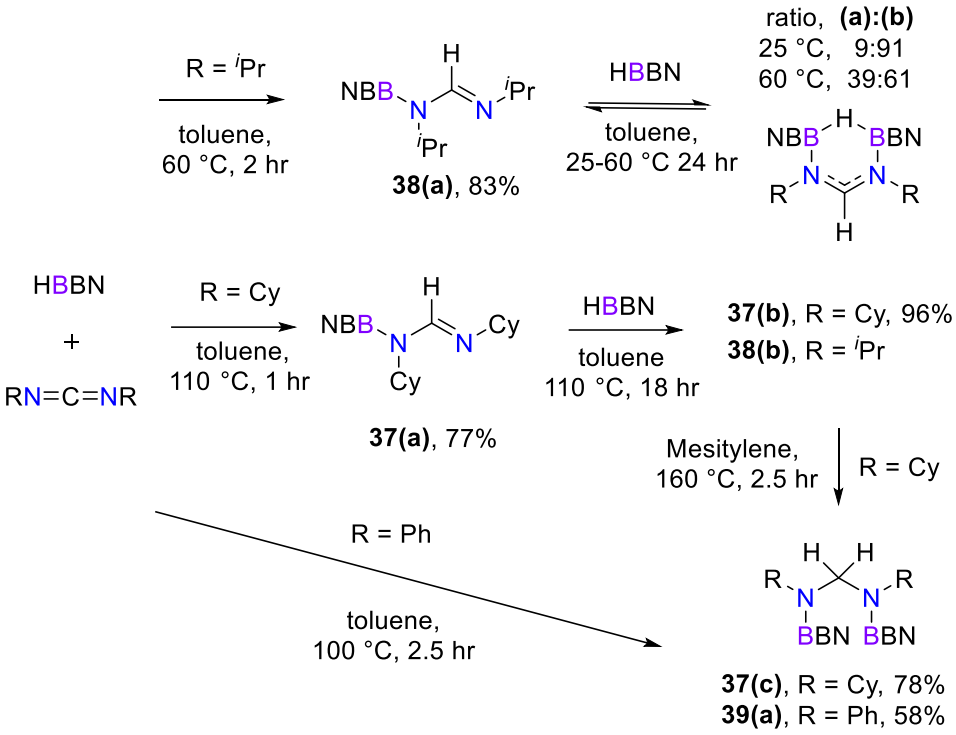
34. This reaction is catalyst-free and proceeds at ambient temperature in good yields (**Scheme 20**).[106]



***Scheme 20**. Catalyst-free hydroboration of carbodiimides with Piers' borane by Stephen et al.,[106] of isocyanates by Warren et al.[107] and of isothiocyanates by Fischer et al.[108]*

In a further extension of this work, Warren and co-workers found that when using a bulky isocyanate such as DippN=C=O, a six-membered ring formed by the insertion of two isocyanate molecules followed by oxophilic coordination of $B(C_6F_5)_2$ to yield compound **35**.[107] Using an isocyanate with a more sterically hindered aryl (2,6-Ph_2-4-^{t}BuC_6H_2), a second species **35(a)** was observed in equilibrium with **35** (**Scheme 20**). Fischer *et al.* present the only example of the hydroboration of isothiocyanates.[108] Using $HB(C_6F_5)_2$, a four-membered ring **36** forms (R = Ph, Ad) similar in structure to structures **34** from carbodiimides (**Scheme 20**, above). When R = Bn, **36** reveals a tetrameric structure in the solid state, **36(a)**, containing -S-C(H)=N(R)-$B(C_6F_5)_2$-S- motif (**Scheme 20**).

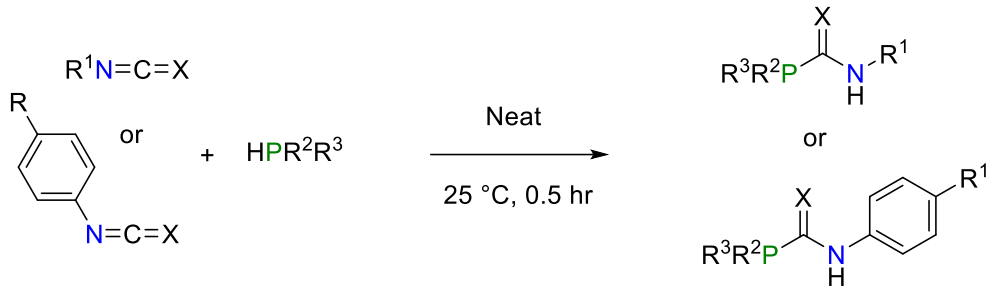
Utilising a different H–B source, HBBN (BN = 9-bicyclo[3.3.1]nonane), Koster *et al.* have shown at 110 °C CyN=C=NCy undergoes catalyst-free monohydroboration to yield **37(a)** (**Scheme 21**).[109] At longer reaction times of 18 hr with another equivalent of HBBN a cyclic double hydroboration intermediate **37(b)** is formed in excellent yields (**Scheme 21**). Subsequent heating of **37(b)** at 160 °C afforded the monomeric diborylamidine **37(c)** (58% overall yield).



***Scheme 21**. Catalyst-free HBBN hydroboration of carbodiimides by Koster et al.*[109] *and* García-Vivó *et al.*[110]

When PhN=C=NPh was used instead of CyN=C=NCy, less forcing conditions of 100 °C were required to form the free diborylamidine product **39(a)** in a moderate 58% yield (**Scheme 21**). García-Vivó *et al*. have also demonstrated that ^{i}PrN=C=N^{i}Pr shows similar reactivity to CyN=C=NCy also undergoing catalyst-free monohydroboration, however attempts at double hydroboration show **38(a)** is equilibrium with **38(b)** (**Scheme 21**).[110] A lower temperature of 25 °C favours intermediate **38(b)** in a 91:9 ratio, whilst heating at 60 °C lowers the ratio to 39:61.

Recently, catalyst- and solvent-free hydrophosphination of isocyanates and phenyl isothiocyanate have been reported with $HPPh_2$ tolerating a range of aryl and primary alkyl isocyanates, affording the products in quantitative or near-quantitative yields (**Scheme 22**).[111]



17 examples
68-99%

X = O; R_2 = R_3 = Ph; R = MeO, F, Cl, Br, CF_3,
X = O; R_2 = R_3 = Ph; R^1 = Napthyl, $(CH_2)_2Cl$, $(CH_2)_3SiMe_2Cl$
X = O; R^2 = R^3 = 4-Me/4-MeO/4-F(C_6H_4), ^{i}Pr, ^{t}Bu; R=H
X = O; R^2 = Ph, R^3 = H; R^1 = Ph (72 hr, 71%)
X = S; R^2 = R^3 = Ph R ; R^1 = Ph

Scheme 22. *Neat catalyst-free addition hydrophosphination of isocyanates and phenyl isothiocyanate.*[111]

Substrates featuring sterically demanding substituents (AdN=C=O) or secondary alkyl isocyanates (CyN=C=O) did not react. Using this methodology, dialkylphosphines HP^iPr_2 and HP^tBu_2 could also be employed affording the hydrophosphination products in high yields. The reaction with the primary phosphine H_2PPh took considerably longer than other phosphines (3 days *vs.* 30 minutes), which was postulated to be due to residual solvent in the commercial sample of H_2PPh used. Control experiments demonstrate that the key to the reaction is the solvent-free conditions (<10% solvent).

1.8 Hydrofunctionalisation Catalysis with *m*-Terphenyls

1st row transition metals are cheap and earth-abundant alternatives to scarce and expensive platinoid metals.[112,113] However, they are somewhat lacking in reactivity compared to their platinoid metal counterparts. A strategy to circumvent this low reactivity is to utilise extremely sterically bulky ligands forcing the metal into a low-coordinate state, often catalysing unusual reactions or activating challenging substrates.[114] One example of these very sterically bulky ligands is the *m*-terphenyl ligand which has the molecular formula 2,6-$Ar_2C_6H_3$. The two aryl flanking groups are in the ortho-position on the central aryl ring and the ligand forms a σ M–C bond with the metal centre. Recently Kays *et al.* have utilised iron based *m*-terphenyl complex $Fe(C_6H_3\text{-}2,6\text{-}Mes_2)_2$, precatalyst **40** (**Figure 4**) for the hydrophosphination of isocyanates with $HPPh_2$.[115]

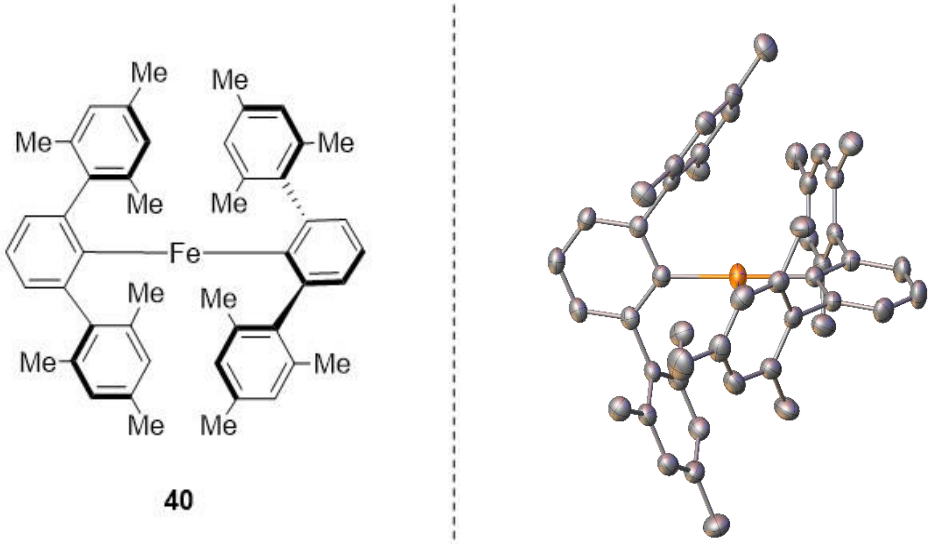
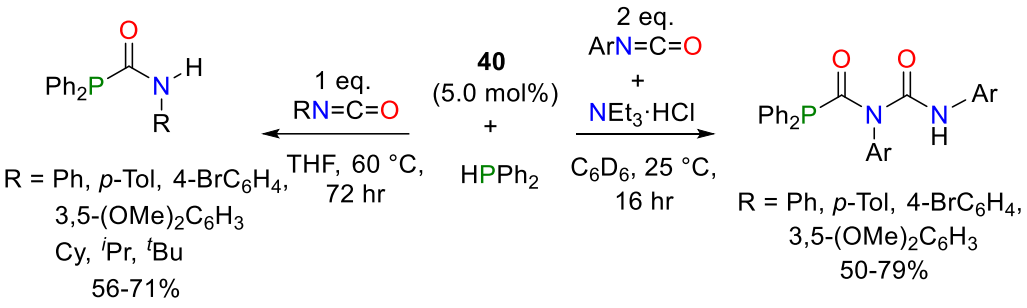


Figure 4. *(Left) Schematic and (right) crystal structure of $Fe(C_6H_3\text{-}2,6\text{-}Mes_2)_2$,* ***40****. Hydrogen atoms have been omitted for clarity and thermal ellipsoids are set at the 50% probability level.*

The hydrophosphination reaction using **40** (5 mol%) with a 1:1 mixture of isocyanate:$HPPh_2$ affords a mixture of phosphinocarboxamides and

unprecedented phosphinodicarboxamides, resulting from the overall insertion of one or two isocyanate molecules into the P–H bond.[115] For aryl isocyanate substrates, the selectivity of the reaction can be controlled by the reaction conditions: use of THF solvent affords phosphinocarboxamides and the addition of a weak acid (NEt_3·HCl) in benzene solution affords phosphinodicarboxamides (**Scheme 23**). The reactions using secondary and tertiary isocyanates are selective for phosphinocarboxamide products, and primary alkyl isocyanates (^{n}HxN=C=O) afford a mixture of phosphinocarboxamides along with the isocyanurate side product produced through cyclotrimerisation.[116]

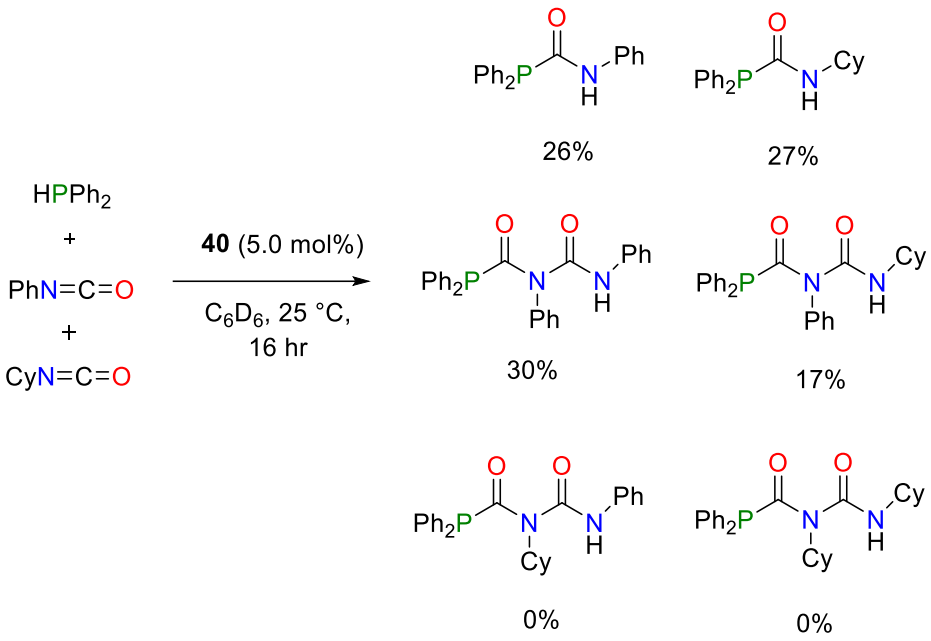


***Scheme 23**. Hydrophosphination monoinsertion (left) and diinsertion (right) selectivity by Fe(C6H3-2,6-Mes2)2, **40**.*[115]

Attempts to form mixed phosphinodicarboxamides from a 1:1:1 mixture of PhN=C=O, CyN=C=O and $HPPh_2$ yielded a mixture of four products from a proposed six with the mixed alkyl, aryl phosphinodicarboxamide product being the least favoured (**Scheme 24**).[115]

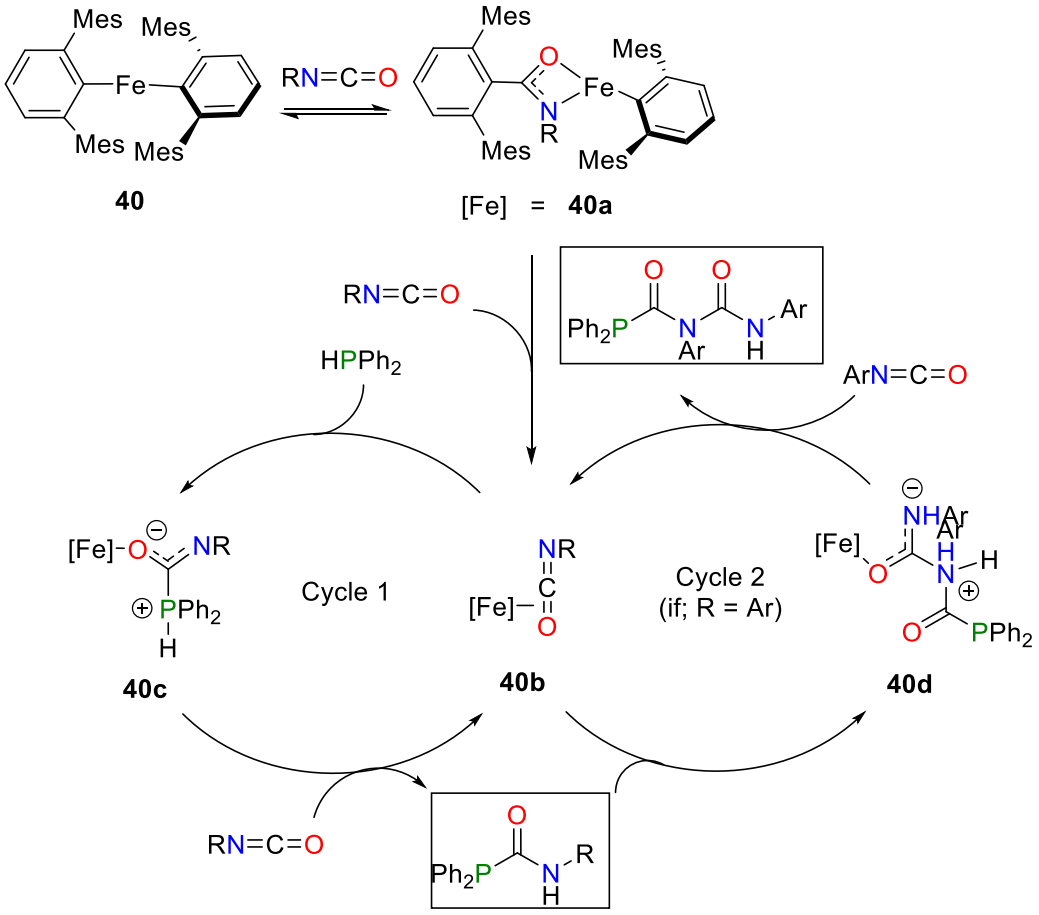
A mechanism was proposed whereby the Fe centre acts as a Lewis acid leading to coordination of the isocyanate to form the active catalyst, a subsequent nucleophilic attack occurs on intermediate **40b** and 1,3-H shift with free isocyanate coordination generates the phosphinocarboxamide (**Scheme 25).**[115] When the phosphinocarboxamide synthesised in cycle 1 contains a smaller R

group (e.g. R = aryl), the mechanism can repeat again proceeding to Cycle 2 with a nucleophilic attack on **40b** by the phosphinocarboxamide to yield **40d**, proton transfer and isocyanate coordination regenerate **40b** and produce the phosphinodicarboxamide product.

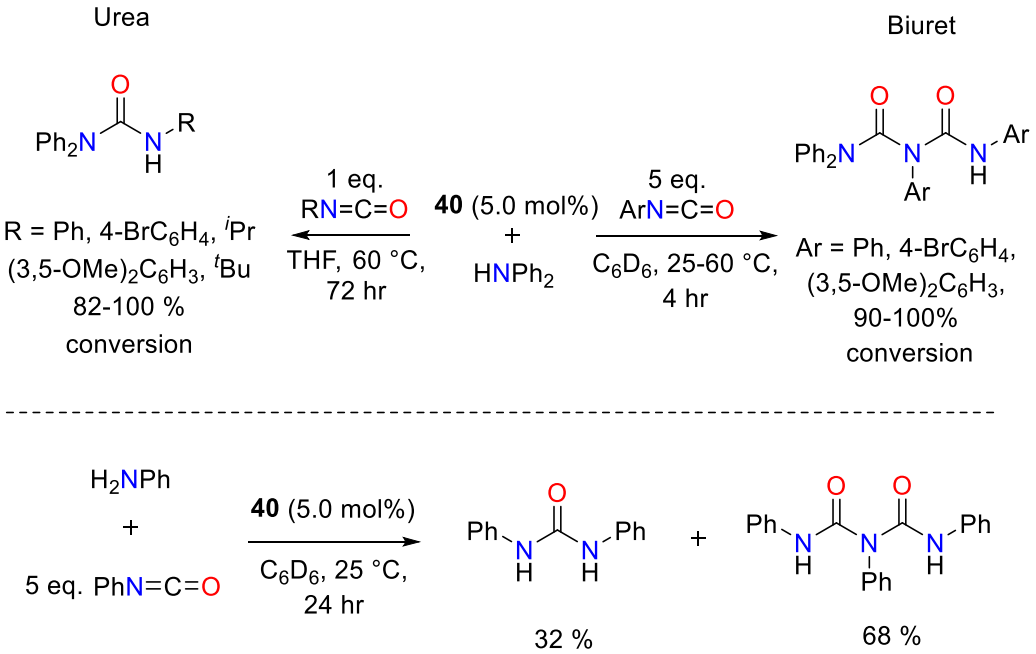


Scheme 24. *Hydrophosphination reaction of an aryl and alkyl isocyanate mixture by* ***40****.*[115]

Subsequently In 2019, **40** was also shown by Kays *et al.* to catalyse the hydroamination of isocyanates. The reaction between $HNPh_2$ and PhN=C=O afforded a mixture of two products in a 88:12 ratio, the major product was the urea product and the minor was the biuret, formed by the insertion of two equivalents of isocyanate into the N–H bond (**Scheme 26**, above).[117] Utilising a 1:5 ratio increased selectivity for the biuret to 90-100%, but this was only successful for aryl isocyanates (R = Ph, C_6H_3(3,5-$(OMe)_2$) and C_6H_4-4Br) as alkyl isocyanates ^{i}PrN=C=O and ^{t}BuN=C=O consistently only formed the corresponding ureas (**Scheme 26**, above).

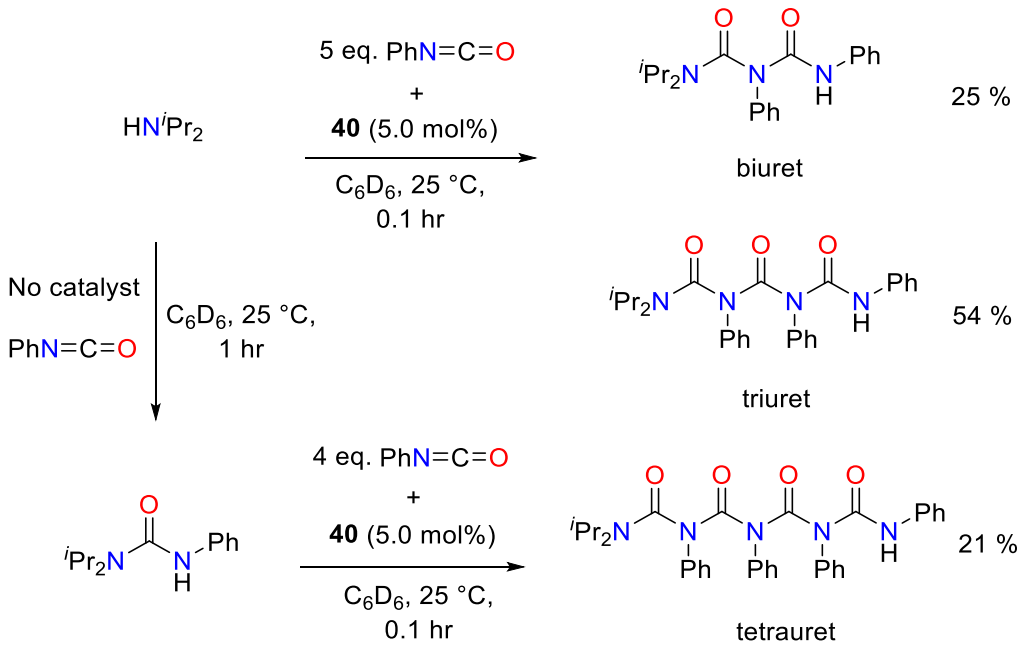


Scheme 25. *Proposed mechanism for hydrophosphination of isocyanates by* ***40****.*[115]



Scheme 26. *(Above) hydroamination of isocyanates by* ***40*** *affording the urea and biuret products and (below) double hydroamination of aniline by* ***40****.*[117]

For primary aliphatic isocyanate substrates there is a competing cyclotrimerisation reaction of the isocyanate affording isocyanurates,[118] but the secondary and tertiary aliphatic isocyanates (R = ^{i}Pr and ^{t}Bu) are unaffected by this competing process. The use of solvent was also key to reaction selectivity: use of THF results in the formation of urea products with high selectivity. The single hydroamination of PhN=C=O with aniline proceeds without a catalyst, but with the use of precatalyst Fe(C$_6$H$_3$-2,6-Mes$_2$)$_2$ in this reaction afforded the double hydroamination product – a biuret in 68% yield (**Scheme 26**, below), whereby both N–H bonds react with the isocyanate; this is contrary reactivity to the titanium precatalysts **4**, where only one N–H bond reacts. In the absence of a catalyst, the more nucleophilic HN^{i}Pr$_2$ affords the respective urea products, however using precatalyst **40** the biuret was obtained as the major product with small amounts of triuret product (**Scheme 27**).[117] A PhN=C=O: NH^{i}Pr$_2$ ratio of 5:1 affords the tetrauret in 21% yield. Use of the urea as substrate leads to fast (<10 min) conversion to the same polyinsertion products in very similar ratios.



***Scheme 27**. Polyinsertion reactions of PhN=C=O and HN^{i}Pr$_2$ catalysed by Fe(C$_6$H$_3$-2,6-Mes$_2$)$_2$.*[117]

1.9 Global Aims

The overall aim of this work is to investigate the ability of Fe-based *m*-terphenyl $Fe(C_6H_3\text{-}2,6\text{-}Mes_2)_2$ **40,** as a precatalyst for P-H unit addition reactions such as hydrophosphination (HPR_2 or H_2PR), hydrophosphinylation ($HP(O)R_2$) and hydrophosphonylation ($HP(O)R(OR)$ or $HP(O)(OR)_2$) with a range of heterocumulenes. Where possible performing parallel reactions catalyst-free at low concentrations or neat to determine if the methodology is superior. Overall forming novel products with potential biological activities in a way aligned with green and sustainable chemistry.

Initially, the P(O)-H bond scope will be screened with $HP(O)Ph_2$ with more electrophilic heterocumulenes such as PhN=C=O; catalyst-free neat or in solution and with **40** as a catalyst. The superior method will be further pursued expanding the scope to isothiocyanates. Further potentially less reactive P(O)-H substrates such as $HP(O)^iPr_2$ or $HP(O)(OEt)_2$ may also be pursued.

The less explored hydrophosphination of primary phosphines with isocyanates will be investigated catalyst-free in solution and neat and additionally with the use of a catalyst such **40**. By screening conditions ideally double hydrophosphination products can be obtained and by further increasing isocyanate concentration potentially novel diinsertion or polyinsertion type products. If successful less reactive primary alkyl phosphines will be screened such as adamantyl phosphine, $AdPH_2$.

The heterocumulene scope will be expanded to single hydrophosphination of carbodiimides initially utilising $HPPh_2$ as a starting point, to determine the reaction compatibility with **40**. Eventually expanding to an alkyl phosphine such as HP^iPr_2. Novel double hydrophosphination of carbodiimides using $FcPH_2$ will also be attempted. In all cases attempting to form only a single phosphaguanidine isomer.

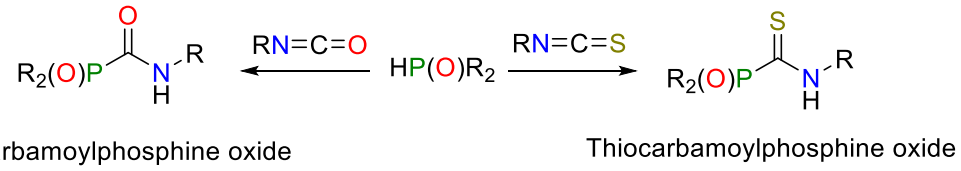
Chapter 2:

Catalyst-free P(O)-H Bond Addition of Isocyanates and Isothiocyanates

2.1 Introduction

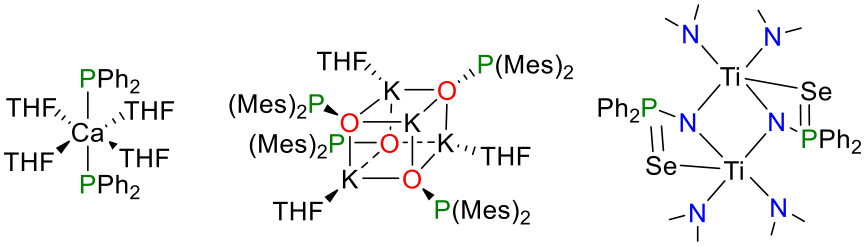
2.1.1 Hydrophosphinylation of isocyanates and isothiocyanates

Hydrophosphinylation is the addition of a secondary phosphine oxide, $HP(O)R_2$ (where R = alkyl or aryl) to an unsaturated bond. The hydrophosphinylation of isocyanates and isothiocyanates results in the direct synthesis of carbamoylphosphine oxides and thiocarbamoylphosphines (**Scheme 28**).



Scheme 28. *Hydrophosphinylation of isocyanates and isothiocyanates synthesising carbamoylphosphine oxides (left) and thiocarbamoylphosphine oxides (right), R = aryl or alkyl.*

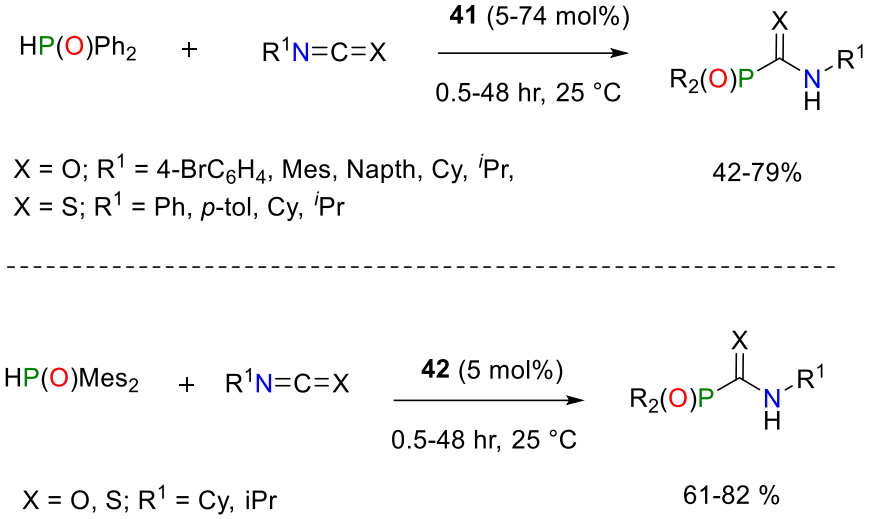
In 1963, Greenberg and co-workers reported the first synthesis of carbamoylphosphine oxides from $LiPPh_2$ with isocyanates followed by hydrolysis and oxidation with stoichiometric amounts of H_2O_2 in moderate yields after 12 hours.[119] Subsequently in 1965 the first synthesis of thiocarbamoylphosphine oxides was reported by the reaction of PhN=C=S with tetradiarylphosphines by P–P bond cleavage.[120] The first catalytic synthesis of thiocarbamoylphosphine oxides was reported in 1969 showing at elevated temperatures isothiocyanates would react with diphenylphosphine oxide in the presence of catalytic amounts of NEt_3 in moderate to excellent yields.[121] In more recent times catalytic metal-mediated hydrophosphinylation has sought to avoid the use of such stoichiometric additives and develop catalysts which tolerate a wider range of isocyanates and isothiocyanates and functional groups.



41 **42** **43**

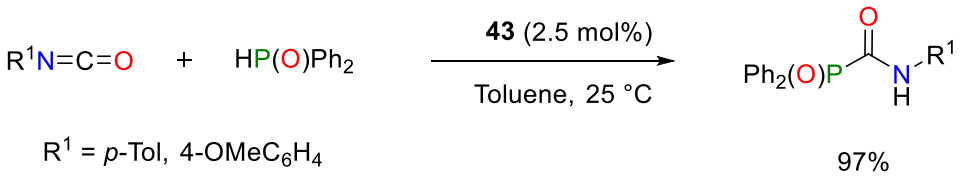
Figure 5. ***41-42*** *hydrophosphinylation catalysts by Westerhausen and co-workers*[122,123] *and* ***43*** *by Panda and co-workers.*[124]

Westerhausen and co-workers have utilised secondary phosphine oxides with calcium complex **1** (**Figure 5**) to undertake hydrophosphinylation catalysis.[122] This complex is effective in this methodology as phosphine oxides readily form complexes with calcium, whereas phosphines do not represent effective Lewis bases in calcium chemistry.[125] Additionally, a previous attempt using a calcium-based catalyst, $HPPh_2$ and phenyl isocyanate led to cyclotrimerisation.[122] The use of 5.0 mol% of complex **41** provides an effective precatalyst for the hydrophosphinylation of alkyl isocyanates (R = ^{i}Pr, ^{t}Bu, Cy) in good yields of 70-79% in 12-24 hours; however for aryl isocyanates very high precatalyst loadings of 67% and 75% are required for bulky MesN=C=O and NapthN=C=O (53% and 79%) (**Scheme 28**, above). Additionally, less bulky substrates such as PhN=C=O could not be utilised with the authors reporting a yield of a few colourless crystals of the respective carbamoylphosphine oxide. More heteroatom rich 4-bromophenyl isocyanate could be tolerated but required elevated reaction times of 48 hours with a lowered yield of 44%. Using 5.0 mol% of **41,** aryl and alkyl isothiocyanates (RN=C=S where R = ^{i}Pr, Cy, Ph, *p*-Tol) could be utilised in moderate 42-61% yields in 12-48 hours.



***Scheme 29**. Hydrophosphinylation of isocyanates and isothiocyanates mediated by **1** (above) and **2** (below).*[122,123]

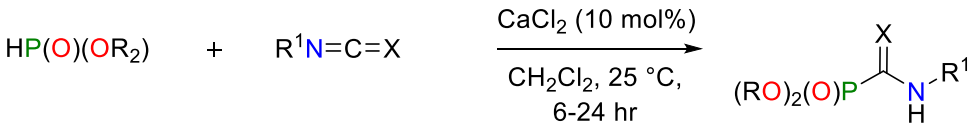
Further work by Westerhausen and co-workers with potassium-based catalyst **42** (**Figure 5**) has utilised bulkier $HP(O)Mes_2$ and alkyl isocyanates (R = ^{i}Pr, Cy), which require long reaction times of 42-48 hours to reach full conversion, in contrast to ^{i}PrN=C=S which reaches quantitative conversion in 30 mins (**Scheme 29**).[5] Complex **43** (**Figure 5**) was used in the first example of a transition metal-mediated hydrophosphinylation reaction. At 2.5 mol% loading, complex **43** has been shown to catalyse the hydrophosphinylation of aryl isocyanates (R = *p*-Tol and 4-$OMeC_6H_4$) in 97% yield (**Scheme 30**).[124]



***Scheme 30**. Hydrophosphinylation of aryl isocyanates mediated by **43**.*[124]

2.1.2 Hydrophosphonylation of isocyanates and isothiocyanates

The synthesis of carbamoylphosphonates was reported from the base catalysed reaction of aryl isocyanates (where aryl = 4-BrC_6H_4, 4-ClC_6H_4, 4-$NO_2C_6H_4$) with dialkylphosphites and either NaCN, Na_2CO_3 or NEt_3.[126,127] Only solid carbamoylphosphonates derived from aryl isocyanates could be isolated with liquid carbamoylphosphonates decomposing to starting materials upon distillation. Additionally, *via* an Arbuzov reaction of carbamoyl chlorides and trialkyl phosphites or by amidation of ethyl diethoxyphosphinylformate.[128,129] Although a range of carbamoylphosphonates could be obtained from this methodology it does suffer from the use of reactive reagents, toxicity and low selectivity that limit general use and scope. Zahedi and co-workers have reported that 5.0 mol% of $CaCl_2$ can act as a catalyst for the hydrophosphonylation of a range of alkyl and aryl isocyanates and isothiocyanates in moderate yields (**Scheme 31**).[130] However it should be noted purification of the products did require the use of column chromatography.



X = O; R = Et; R^1 = Ph, 4-Me,3-ClC_6H_3, Cy
X = O; R = Bn; R^1 = Cy, Bn
X = S; R = Et; R^1 = Ph, 4-$NO_2C_6H_4$, *p*-Tol, $(CH_2)_2$Ph
X = S; R = Bn; R^1 = Ph

37-65%

***Scheme 31**. Hydrophosphonylation of isocyanates and isothiocyanates mediated by $CaCl_2$.*

2.2 Aims

The aim of this work is to investigate the hydrophosphinylation and hydrophosphonylation of a variety of challenging functionalised isocyanates and isothiocyanates, in order to synthesise novel (thio)carbamoylphosphine oxides compounds with potential biological activities. Challenges are likely to come in different forms with the most electrophilic aryl isocyanate expected to be the most reactive but form the most side-products and the least electrophilic alkyl isothiocyanates to be least reactive but form fewer side products. The specific magnitudes of these dichotomies will determine if a catalytic route is needed or if a catalyst-free methodology can be applied using neat or low-added solvent conditions.

This work also aims to broaden the specific scope of aryl and alkyl isocyanates and isothiocyanates that can be used particularly if heteroatom groups on functionalised aryl isocyanates or isothiocyanates can be tolerated (e.g., C_6H_4; OMe, NO_2, Cl, Br, F). Additionally, for hydrophosphinylation the only secondary phosphines ever to be used have been $HP(O)Ph_2$ or $HP(O)Mes_2$, thus an aim is to utilise what could typically be seen as more difficult $HP(O)R_2$ substrate such as $HP(O)^iPr_2$ (based on the lower reactivity seen for HP^iPr_2 vs $HPPh_2$ in hydrophosphination literature).

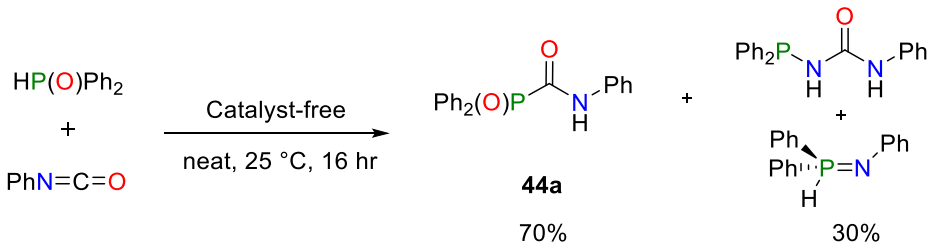
Furthermore, to see if the methodology or catalytic system for hydrophosphinylation can also be applied to a similar reaction class of hydrophosphonylation, utilising H–P(O) sources such $HP(O)(OEt)_2$ or HP(O)(OMe)Ph. Finally given the P–C bond elongation and distortion of unfunctionalised carbamoylphosphine oxides and thiocarbamoylphosphine oxides, determine using X-ray crystallography if changing the functional groups of the alkyl and aryl substituents affects the bond elongation and thus the degree of ionicity of the solid-state structures.

2.3 Results and Discussion

2.3.1 Hydrophosphinylation of isocyanates and isothiocyanates

2.3.1.1 Initial catalyst-free optimisation with phenyl isocyanate

Previous literature had suggested that hydrophosphinylation of isocyanates or isothiocyanates was unlikely to occur in the absence of a catalyst.[122] For completeness and to be certain, initial catalyst-free control reactions utilising phenyl isocyanate and diphenylphosphine oxide were performed. Surprisingly a concentrated reaction (~0.2M in C_6D_6) proceeded with good conversions of 70% to the desired phosphinylcarboxamide **44a**, despite suggestions of a lack of reactivity in the absence of a catalyst (**scheme 32**).[122] Additionally, there is the formation of two phosphorus containing side-products products in a combined 30% yield (**Scheme 32**). Further discussion of these side products is given in section 2.3.2.7.



Scheme 32. Initial catalyst-free hydrophosphinylation of neat phenyl isocyanate and diphenylphosphine oxide.

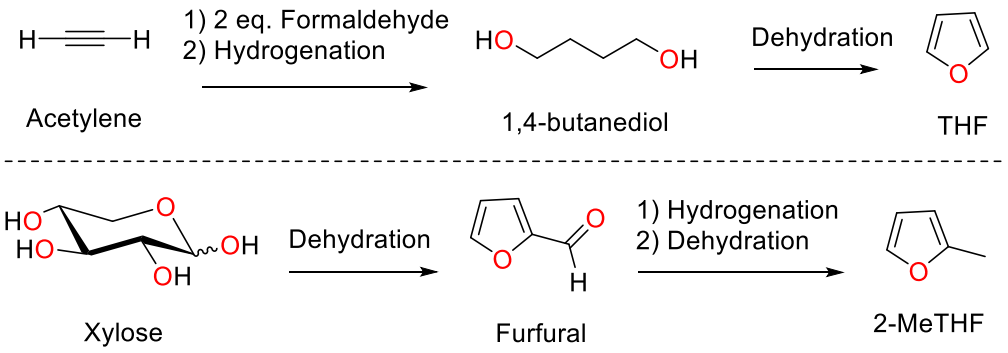
Further reactions in concentrated solutions varying the stoichiometric ratios of diphenylphosphine oxide to phenyl isocyanate showed little variation in conversion (*ca.* 0.2 M, **Table 2**, entries 1–6). Additionally, the reaction could be performed neat, with the reaction occurring faster but giving variable yields, possibly due to issues with mass transport (**Table 2**, entry 7). Reactions in air gave low conversions (**Table 2**, entry 8).

Table 2. Optimisation of the hydrophosphinylation of phenyl isocyanate under catalyst-free conditions[a]

Entry	$HP(O)Ph_2$: PhN=C=O	Solvent	Time (hr)	Conv. **44a** (%)[b]
1	1.0 : 1.0	C_6D_6	8	70
2	1.0 : 1.2	C_6D_6	8	73
3	1.0 : 1.5	C_6D_6	8	73
4	1.0 : 2.0	C_6D_6	8	71
5	1.5 : 1.0	C_6D_6	8	71
6	1.0 : 1.2	THF	8	76
7	1.0 : 1.2	Neat	3	72
8	1.0 : 1.2	Neat[c]	3	38
9	1.0 : 1.2	THF[d]	3	80
10	1.0 : 1.2	2-MeTHF[d]	3	80

[a] Reaction conditions: 1.0 eq. = 0.10 mmol, 0.5 mL solvent and 25 °C under a nitrogen atmosphere unless otherwise stated. [b] Conversion determined by ^1H NMR spectroscopy using an internal standard (mesitylene, 1.0 eq.). [c] Reaction performed in air. [d] ca. 4 eq. of solvent used.

To allow for the use of solid substrates, a near-neat method using 4 equivalents of THF was employed giving consistent conversions of 80% of **44a** (**Table 2**, entry 9). A bioderived alternative to THF (which is originally derived from the petrochemical acetylene,[131] (**Scheme 33**, above) is 2-MeTHF which is originally derived from sugars such as xylose (**Scheme 33**, below).[132]

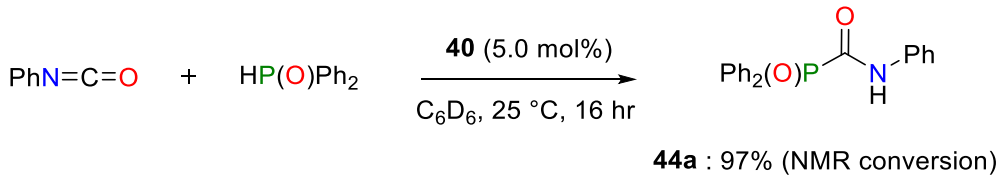


***Scheme 33**. (Above) Synthesis of THF from petrochemical derived acetylene and (below) synthesis of 2-MeTHf from bioderived xylose.*[131,132]

Replacing the use of 4 equivalents of THF with bioderived 2-MeTHF resulted in the same conversion of 80% for **44** (**Table 2**, entry 10), thus these were chosen for further substrate scope exploration.

2.3.2 Catalytic hydrophosphinylation of phenyl isocyanates with *m*-terphenyl complexes.

Previous work by Kays and co-workers has shown the low-coordinate *m*-terphenyl complex Fe(C_6H_3-2,6-Mes_2)$_2$, **40** to be an effective catalyst for the hydrophosphination of a range of isocyanates using $HPPh_2$. Given this proven tolerance for isocyanates Fe(C_6H_3-2,6-Mes_2)$_2$ was tested as a catalyst for the hydrophosphinylation of phenyl isocyanates (**Scheme 34**).



***Scheme 34**. Catalytic hydrophosphination of phenyl isocyanate by Fe((C$_6$H$_3$)(Mes)$_2$)$_2$.*

A high (90%) conversion was obtained by utilising 5.0 mol% of **40** as a precatalyst however purification by washing with ethanol gave a yield of 60% of **44a**. Comparatively, isolation utilising ethanol washing from the catalyst-free low-solvent methodology resulted in a higher 64% yield of **44a**; thus, the catalyst-free methodology was chosen for further scope exploration.

2.3.2.1 Substrate scope for the hydrophosphinylation of isocyanates

A variety of functionalised isocyanates were also tested (**Table 3**). The reaction tolerated a variety of aromatic isocyanates with electron-donating and electron-withdrawing substituents (4-Me, 2-F, 4-Br and 4-OMe-substituted phenyls). All

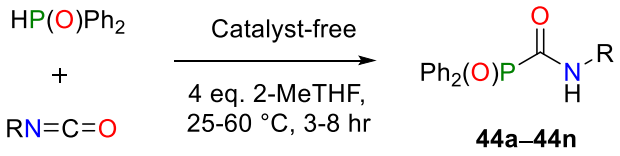
these reactions afforded pure product in reasonable yields (62-82% determined by ^{1}H NMR spectroscopy, 55–66% isolated, **Table 3**, **44a**-**44e**).

However, the more electrophilic (4-$NO_2C_6H_4$)N=C=O was not tolerated as well, with the reaction proceeding to lower conversions of **44f** (49%), as determined by ^{1}H NMR spectroscopy, and with significant phosphorus by-product formation (see section 2.3.2.7).

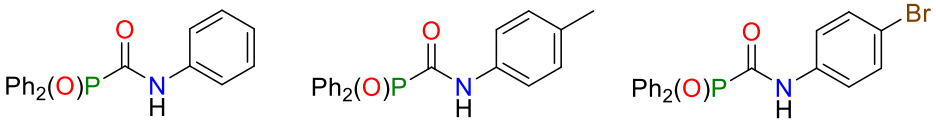
High conversions were achieved with a range of primary and secondary alkyl isocyanates (^{i}Pr, Et, ^{n}Pr, ^{n}Hx, Cy; 82–91% of **44g**-**44j** and **44m** by ^{1}H NMR spectroscopy, 65–82% isolated). To reach high conversions heating at 60 °C was required, with a loss in conversion being caused by a side reaction forming $Ph_2(O)P–P(O)Ph_2$. Bulky ^{t}BuN=C=O required longer reaction times (8 hr) to reach moderate conversions (61% by ^{1}H NMR spectroscopy, 48% isolated yield) and increasing the reaction temperature to 80 °C did not improve conversion. The chain length of primary isocyanates did not appear to affect conversion increasing from ethyl to propyl and hexyl. The benzyl functionality was tolerated, giving **44l** in a 56% isolated yield, while the heterocyclic furfuryl isocyanate afforded **44n** in a lower 35% isolated yield.

No uretdione [-NRC(O)-]$_2$ (dimerisation) or isocyanurate [-NRC(O)-]$_3$ (cyclotrimerisation) by-products were detected, even with aryl isocyanates, for which some examples are known to dimerise at room temperature without a catalyst.[133] Significantly, all products (except **44f**) were purified by washing with small quantities of ethanol. These hydrophosphinylation reactions parallel recent work on the catalyst-free hydrophosphination of alkenes, alkynes and iso(thio)cyanates.[111,134,135] However, this methodology demonstrates a broader substrate scope than these reports and, crucially, does not require column chromatography for purification, leading to a significant reduction in waste compared to previous literature procedures.[122,124]

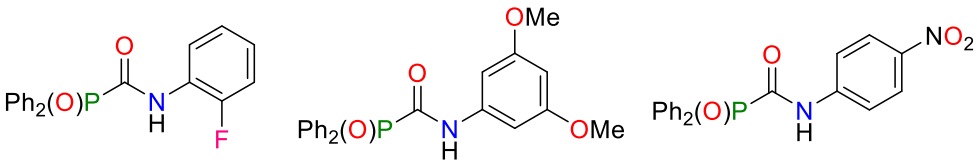
Table 3. *Hydrophosphinylation of isocyanates with diphenylphosphine oxide*[a,b]



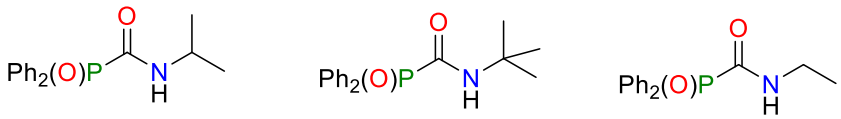
44a–44n



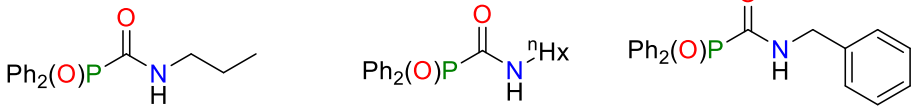
44a: 25 °C, 3 hr, 64% (80%) **44b**: 25 °C, 3 hr, 66% (82%) **44c:** 25 °C, 4 hr, 55% (62%)



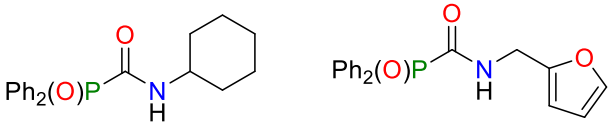
44d: 25°C, 4 hr, 61% (75%) **44e**: 25 °C, 4 hr, 63% (74%) **44f**: 25 °C, 4 hr, (49%)



44g: 60 °C, 6 hr, 67% (84%) **44h**: 60 °C, 8 hr, 48% (61%) **44i**: 60 °C, 6 hr, 71% (84%)



44j: 60 °C, 6 hr, 73% (86%) **44k**: 60 °C, 6 hr, 65% (82%) **44l**: 60 °C, 6 hr, 56% (69%)



44m: 60 °C, 6 hr, 82% (91%) **44n**: 60 °C, 6 hr, 35% (50%)

[a] *Reaction stoichiometry:* ***44a***, ***44b***, ***44d***, ***44g–44m*** *isocyanate (1.2 eq.) and* ***44c***, ***44e–44f*** *isocyanate (1.0 eq.) and HP(O)Ph₂ (1.0 eq.), 1.0 eq. = 0.30 mmol.*[b] *NMR spectroscopic yield (in brackets) determined by* ^{1}*H NMR spectroscopy using an internal standard (mesitylene, 1.0 eq.).*

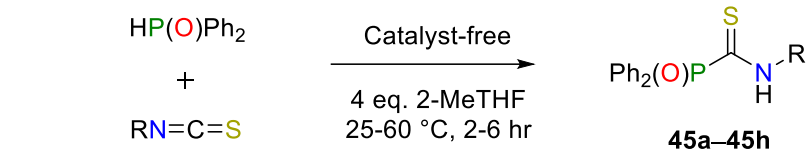
2.3.2.2 Reaction scale-up

A scaled-up reaction was performed with diphenylphosphine oxide (1.55 g, 7.67 mmol) and phenyl isocyanate (1.0 mL, 9.2 mmol). The product was purified in a similar manner to the smaller scale reactions but with a filtration first from the 2-MeTHF solvent followed by washing with ethanol to give a 10% higher yield of 74% for **44a** compared to the smaller 0.30 mmol reaction.

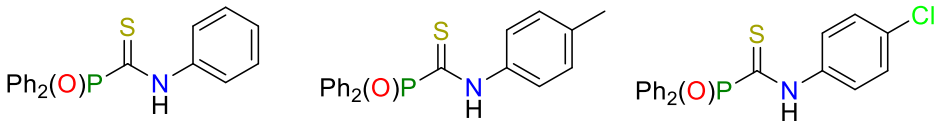
2.3.2.3 Hydrophosphinylation of isothiocyanates using $HP(O)Ph_2$

Recently, Li *et al*. reported the hydrophosphinylation of phenyl isothiocyanate and diphenylphosphine oxide to afford $Ph_2P(O)C(S)NH(Ph)$.[136] This reaction was carried out under neat conditions at 60 °C, however utilising the same methodology used for the hydrophosphinylation of isocyanates it was found that the addition of 2-MeTHF (4 eq.) afforded the desired phosphinylthiocarboxamide product (**45a**) in excellent yields (90% isolated yield) and eliminated the need for heating (**Table 4**). Subsequently, a range of aryl isothiocyanates featuring electron-donating/withdrawing substituents (4-Me, 4-Cl and 4-OMe-substituted) were tested, with all giving the expected product in excellent isolated yields (**45b**–**45d**, 90–95%, **Table 4**). Like $(4\text{-}NO_2C_6H_4)N=C=O$, $(4\text{-}NO_2C_6H_4)N=C=S$ gave low conversions with significant phosphorus containing by-product formation. A pure sample of the product (**45e**) was obtained by recrystallisation from a 1:1 THF:ethanol solution at -30 °C (31% isolated). Similarly, to alkyl isocyanates, secondary alkyl isothiocyanates required heating (60 °C, 6 h) for high conversions, although the yields are significantly lower than the corresponding alkyl isocyanates. The less bulky allyl isothiocyanate, by contrast, proceeded with near quantitative conversion (**45h**, 95% by NMR spectroscopy).

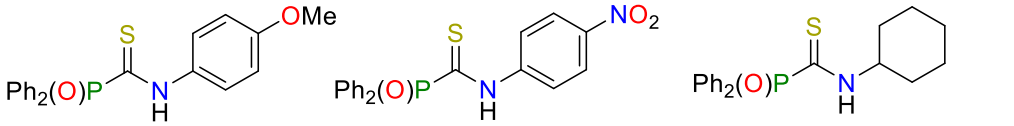
Table 4. Hydrophosphinylation of isothiocyanates with diphenylphosphine oxide.[a,b]



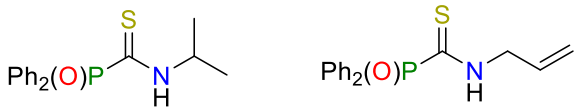
45a–45h



45a: 25 °C, 2 hr, 90% (95%) **45b**: 25 °C, 2 hr, 95% (99%) **45c**: 25 °C, 2 hr, 90% (94%)



45d: 25 °C, 2 hr, 92% (98%) **45e**: 60 °C, 6 hr, 31% (50%) **45f**: 60 °C, 6 hr, 42% (57%)



45g: 60 °C, 6 hr, 40% (65%) **45h**: 60 °C, 4 hr, 82% (95%)

*[a] Reaction stoichiometry: **45a**-**45h** isothiocyanate (1.0 eq.) and HP(O)Ph2 (1.0 eq.), 1.0 eq. = 0.30 mmol.[b] NMR spectroscopic yield (in brackets) determined by ^{1}H NMR spectroscopy using an internal standard (mesitylene, 1.0 eq.).*

2.3.2.4 Initial hydrophosphinylation of PhN=C=O using HP(O)^{i}Pr$_2$

All previous reports of hydrophosphinylation of isocyanates and isothiocyanates have been limited to secondary aryl phosphine oxides.[122–124,137] To further probe the scope of the catalyst-free methodology reactions with diisopropylphosphine oxide (HP(O)^{i}Pr$_2$) as a substrate were performed.

Table 5. Hydrophosphinylation of phenyl isocyanate utilising $HP(O)^iPr_2$ [a,b]

Entry	$HP(O)(^iPr)_2$: PhN=C=O	Solvent[c]	Temp. (°C)	Time (hr)	Conv. **46a** (%)
1	1.0 :1.0	2-MeTHF	25	3	37
2	1.0 : 1.0	2-MeTHF	25	16	40
3	1.0 : 1.0	2-MeTHF	60	16	59
4	1.0 : 1.5	2-MeTHF	60	16	44
5	1.0 : 2.0	2-MeTHF	60	16	40
6	2.0 : 1.0	2-MeTHF	60	16	52
7	1.0 : 1.0	Neat	25	3	27
8	1.0 : 1.0	Neat	25	16	37
9	1.0 : 1.0	Neat	60	16	57

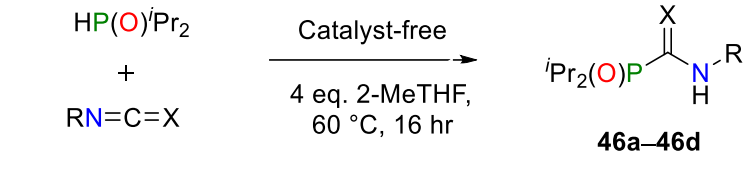
[a] Reaction conditions: 1.0 eq. = 0.105 mmol, 0.5 mL solvent and 25 °C under a nitrogen atmosphere unless otherwise stated. [b] Conversion determined by ^1H NMR spectroscopy using an internal standard (mesitylene, 1.0 eq.). [c] ca. 4 eq. of solvent used.

Initial experiments showed the reaction of phenyl isocyanate with diisopropylphosphine oxide proceeded again in the absence of a catalyst at 25 °C with 4 equivalents of 2-MeTHF as solvent. However, a lower conversion of 40% of **46a** was obtained when compared to the previous reactions to form **44a** (**Table 5**, Entries 1-2). A temperature increase to 60 °C led to a moderate increase in yield to 59% (**Table 5**, Entry 3) and varying the ratio of diisopropylphosphine oxide to phenyl isocyanate away from a 1:1 stoichiometric ratio negatively impacted yields (**Table 5**, entries 4-6). Reactions performed without solvent (**Table 5** Entries 7-9) gave similar yields to reactions performed in solvent, however, the use of a solvent allowed for the use of solid isocyanates or isothiocyanates and prevented issues with reaction homogeneity.

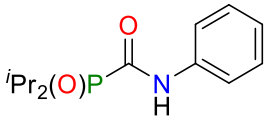
2.3.2.5 Hydrophosphinylation of isocyanates and isothiocyanates using $HP(O)^iPr_2$

Reactions with PhN=C=O (affording **46a**) and ^{i}PrN=C=O (affording **46c**) proceeded at 60 °C with modest isolated yields (41% and 61% respectively, **Table 6**). Reaction with PhN=C=S at 60 °C afforded **46b** in a very high isolated yield (95%). However, the reaction with ^{i}PrN=C=S proceeded with low conversions (36%), and the product (**46d**) could not be obtained in a pure state.

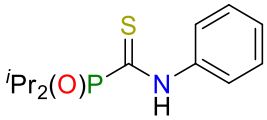
Table 6. Hydrophosphinylation of isocyanates and isothiocyanates with $HP(O)^iPr_2$[a,b,c]



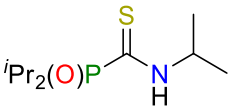
46a–46d



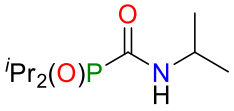
46a: 60 °C, 16 hr, 41% (60%)



46b: 60 °C, 16 hr, 99% (95%)



46c: 60 °C, 16 hr, 61% (80%)



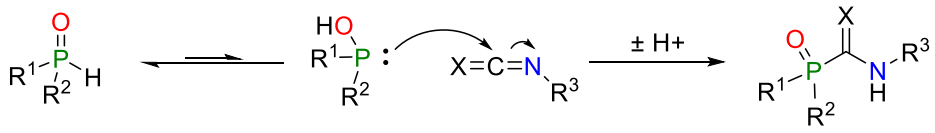
46d: 60 °C, 16 hr, (36%)

[a] Reaction stoichiometry: iso(thio)cyanate (1.0 eq.) and $HP(O)^iPr_2$ (1.0 eq.), 1.0 eq. = 0.105 mmol.[b] Reaction performed in 2-MeTHF (4.0 eq).[c] NMR spectroscopic yield (in brackets) determined by ^{1}H NMR spectroscopy using an internal standard (mesitylene, 1.0 eq.).

2.3.2.6 Proposed mechanism

To ascertain a mechanism, experiments with radical inhibitors as additives were performed for a typical reaction of phenyl isocyanate and $HP(O)Ph_2$ with either 4 equivalents of 1,4-cyclohexadiene or cumene. The reactions proceeded with

conversions of 82% and 77%, respectively. Thus, it is unlikely that the mechanism is radical based. A plausible mechanism, given the potent electrophilicity of isocyanates and isothiocyanates, involves an equilibrium between $HP(O)R^1R^2$ and its P(III)–OH tautomer.[138–141] The isocyanate or isothiocyanate then undergoes nucleophilic attack by the P(III)–OH nucleophile, followed by a proton transfer to reform the P=O bond (**Scheme 35**).



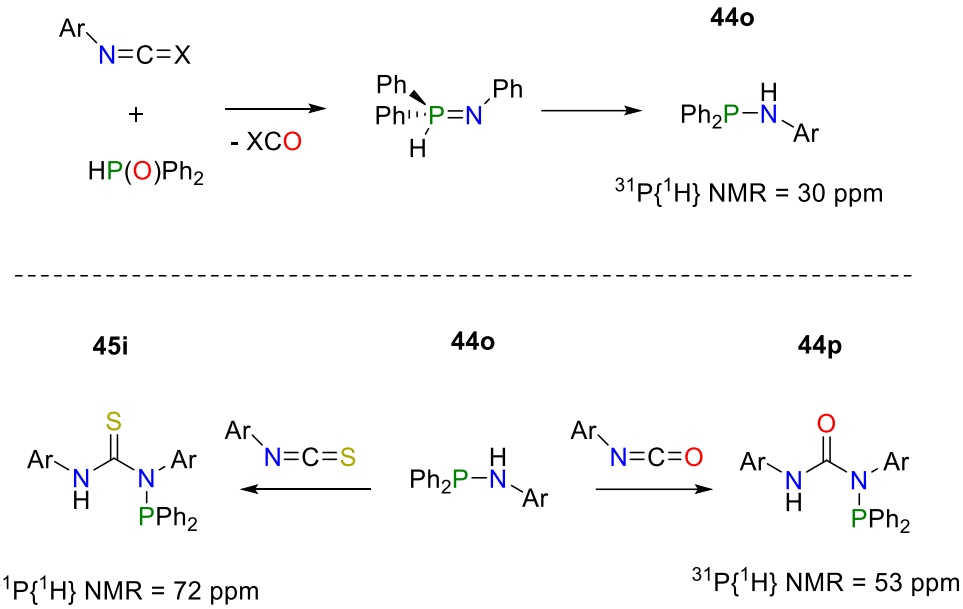
Scheme 35. *Proposed reaction mechanism for the hydrophosphinylation of isocyanates and isothiocyanates by $HP(O)R^1R^2$. X = O, S.*

2.3.2.7 By-product formation from hydrophosphinylation of aryl isocyanates and aryl isothiocyanates

In the formation of **44a**-**44e**, two side products (**44o** and **44p**, **Scheme 33**) are consistently formed in 15-20% yields (as determined by ^{31}P NMR spectroscopy) but can be easily removed by washing with ethanol. These side products have been identified by comparison of their NMR spectroscopic data with literature values.[142,143] Additionally in the formation of **45a**-**45d** two side products (**44o** and **45i**) are formed in *ca.* 1% yields (by ^{31}P NMR spectroscopy). It is plausible that **45i** is the thio-analogue of **44o**, although there is no literature precedent for **45i**, and it could not be isolated in high purity.

For **44f** and **45e** these side products are formed in significant quantities (40% and 47% yield respectively by NMR spectroscopy) and are more difficult to separate from the desired products. Tertiary phosphine oxides are known to react with isocyanates to form phosphinimides by loss of CO_2.[144–146] Thus, it is conceivable that secondary phosphine oxides could react in a similar manner

to form a phosphinimide (**Scheme 36**, above). There is a tautomeric equilibrium between the phosphinimides and **44o**, from which **44o** can perform an N–H insertion with an additional equivalent of aryl isocyanate or isothiocyanate to form species **44p** or **45i** (**Scheme 36**, below). The proposed generation of CO_2 was confirmed by experiment, in section 2.3.2.8



***Scheme 36**. (Above) Plausible reaction mechanism for the formation of side products, **44o** and (below) **44p** and **45i**. X = O or S.*[142,143]

2.3.2.8 Detection of CO_2 from hydrophosphinylation of *p*-Tolyl isocyanate

In order to confirm the proposed generation of CO_2, a Young's tap modified NMR tube was charged with either diphenylphosphine oxide (1.0 eq., 20.2 mg, 0.10 mmol) and *p*-Tolyl isocyanate (1.2 eq., 0.12 mmol, 15.1 µL) neat; or just *p*-Tolyl isocyanate (0.12 mmol, 15.1 µL). For the tube containing both $HP(O)Ph_2$ and *p*-Tolyl isocyanate effervescence was observed immediately and no such effervescence was observed just for *p*-Tolyl isocyanate alone. Each tube was briefly opened in an inert atmosphere glovebox, diluted with C_6D_6 (0.5 mL) and was immediately resealed. A 2048 scan $^{13}C\{^1H\}$ NMR spectra was recorded for

each sample. A small singlet for CO_2 was observed (124.8 ppm)[147] for the reaction between diphenylphosphine oxide and *p*-Tolyl isocyanate (**Figure 6**). No signal for CO_2 was observed for the control reaction.

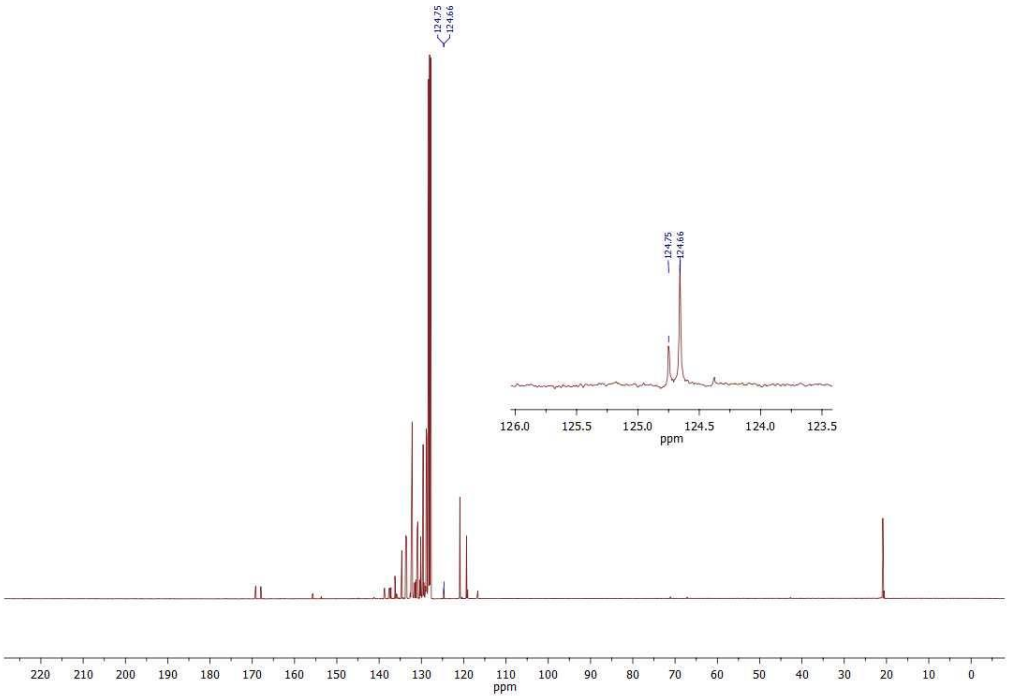


Figure 6. *$^{13}C\{^1H\}$ NMR spectrum of p-Tolyl isocyanate and diphenylphosphine oxide after 2 hours sonication at 25 °C showing a peak corresponding to CO_2 at 124.75 ppm. The peak at 124.66 is due to residual unreacted p-Tolyl isocyanate.*

2.3.3 Hydrophosphonylation of isocyanates and isothiocyanates

2.3.3.1 Initial hydrophosphonylation of phenyl isocyanate

The methodology was then expanded to hydrophosphonylation, the addition of an $HP(O)(OR)_2$ (R = alkyl or aryl) unit across a double bond. Kaboudin and Zahedi have previously described the catalytic hydrophosphonylation of isocyanates with $CaCl_2$, which required chlorinated solvents and column chromatography in the workup.[130] Initial reactions with PhN=C=O and $HP(O)(OEt)_2$ in 2-MeTHF showed no conversion at 25 °C and 3% conversion to **47a** at 60 °C (**Table 7**, entries 1 and 2). However, performing the reaction

neat at 60 °C increased conversion of **47a** to 87% (**Table 7**, entry 4). This solvent-free dependence is contrary to observations for hydrophosphinylation whereby the reaction occurs neat and in solution. However, a dependence on the reaction being performed neat has been observed before for catalyst-free hydrophosphination.[111]

Table 7. Hydrophosphonylation of phenyl isocyanate with diethyl phosphite[a,b]

Entry	$HP(O)(OEt)_2$: PhN=C=O eq.	Solvent	Temp. (°C)	Time (hr)	Conv. **47a** (%)
1	1.0 : 1.0	2-MeTHF[c]	25	3	0
2	1.0 : 1.0	2-MeTHF[c]	60	16	3
3	1.0 : 1.0	Neat	25	3	6
4	1.0 : 1.0	Neat	60	16	87
5	1.0 : 1.5	Neat	60	16	92
6	2.0 : 1.0	Neat	60	16	84

[a] Reaction conditions: 1.0 eq. = 0.232 mmol, and 25 °C under a nitrogen atmosphere unless otherwise stated.[b] Conversion determined by ^{1}H NMR spectroscopy using an internal standard (mesitylene, 1.0 eq.). [c] ca. 4 eq. of solvent used.

To probe this neat *vs.* solvent dependence for reaction success, the secondary phosphinate, methyl phenylphosphinate was tested as substrate. Initial reactions at 25 °C showed low conversions at 25 °C favouring neat conditions with a 37% conversion versus 24% of **47c** with 4 equivalents 2-MeTHF in 3 hours (**Table 8**, entry 1). However leaving the reaction for 16 hours produced near identical conversions of 53 and 52% (**Table 8**, entry 2), suggesting the neat reaction occurs more quickly but the reaction can still occur in solution albeit much slower than for diphenylphosphine oxide. Conversions could be further improved by heating at 60 °C increasing conversions to 63% and 62% (**Table 8**, entries 4-5).

Table 8. Hydrophosphonylation of phenyl isocyanate with methyl phenylphosphinate [a,b]

Entry	HP(O)Ph(OMe): PhN=C=O eq.	Temp. (°C)	Time (hr)	Conv. (%) **47c** in 2-MeTHF[c]	Conv. (%) **47c** neat
1	1.0 :1.0	25	3	24	37
2	1.0 : 1.0	25	16	53	52
3	1.0 : 1.5	25	16	49	42
4	1.0 : 1.0	60	16	62	62
5	1.0 :1.5	60	16	63	62

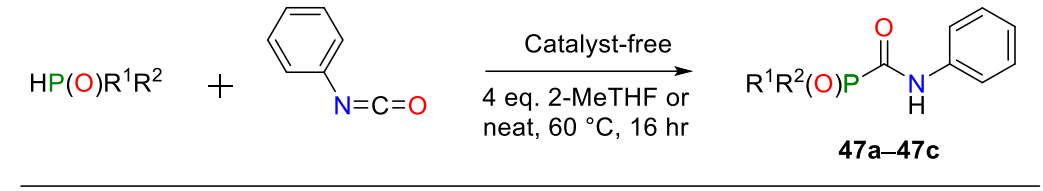
[a] Reaction conditions: 1.0 eq. = 0.232 mmol, and 25 °C under a nitrogen atmosphere unless otherwise stated.[b] Conversion determined by ^{1}H NMR spectroscopy using an internal standard (mesitylene, 1.0 eq.). [c] ca. 4 eq. of solvent used.

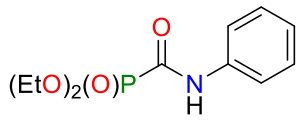
2.3.3.2 Hydrophosphonylation of phenyl isocyanate utilising HP(O)Ph(OMe) $HP(O)(OEt)_2$ and $HP(O)(OMe)_2$

Unfortunately, for these hydrophosphonylation reactions a large amount of the residual unreacted phosphorus containing starting material could not be removed from the products. Silica chromatography (utilising the method of Kaboudin and Zahedi)[130] and alumina chromatography resulted in partial decomposition of the products. Attempts at vacuum distillation also decomposed **47a**. Further attempts at recrystallisation or washing with various solvents were unsuccessful in yielding an analytically pure material (**Table 9**).

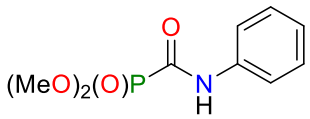
After filtration to remove a urea impurity and drying under vacuum, **47a** was obtained in 61% (containing ~11% $HP(O)(OEt)_2$ by ^{31}P NMR spectroscopy) (**Table 9**). Utilising a shorter chain and more volatile phosphite $HP(O)(OMe)_2$, **47b** was obtained in 22% yield (2% residual $HP(O)(OMe)_2$ which still could not be removed under vacuum with heating at 50 °C). A larger scale reaction (9.2 mmol) using methyl phenylphosphinate gave a 41% isolated yield of **47c** (3% HP(O)Ph(OMe) by ^{31}P NMR spectroscopy).

Table 9. Hydrophosphonylation of phenyl isocyanate [a,c]

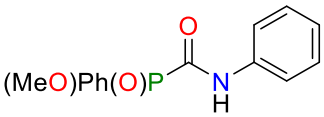




47a: 60 °C, 16 hr, (87%)



47b: 60 °C, 16 hr, 22% (48%)[b]



47c: 60 °C, 16 hr, 40%[d] (62%)

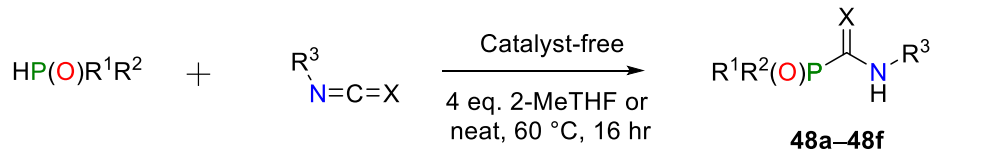
[a] Reaction stoichiometry: $HP(O)(OEt)_2$ (1.0 eq., 0.766 mmol), $HP(O)(OMe)_2$ (1.0 eq. 1.09 mmol), HP(O)Ph(OMe) (1.0 eq., 9.2 mmol) and PhN=C=O (1.0 eq).[b] Reaction performed in 2-MeTHF 4 eq.[c] NMR spectroscopic yield (in brackets) determined by ^{1}H NMR spectroscopy using an internal standard (mesitylene, 1.0 eq.).

2.3.3.3 Attempted hydrophosphonylation with PhN=C=S, ^{i}PrN=C=S, ^{i}PrN=C=O

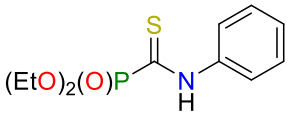
In order to further probe the scope of hydrophosphinylation a range of varying isocyanates and isothiocyanates were tested. Under the same conditions as hydrophosphinylation of phenyl isocyanate with $HP(O)(OEt)_2$, utilising phenyl isothiocyanate only yielded a 1% conversion to **48a** (by ^{1}H NMR spectroscopy, **Table 10**).

Attempts at using even less electrophilic isopropyl isocyanate and isopropyl isothiocyanate again gave very low conversions of 4% and <0.1% respectively. Similarly, comparative reactions utilising methyl phenylphosphinate, resulted in low conversions of 20%, 5% and 7% respectively (**Table 10**). Overall hydrophosphonylation does not show a trend of increasing reactivity with increasing isocyanate or isothiocyanate substrate electrophilicity, unlike hydrophosphinylation reactions.

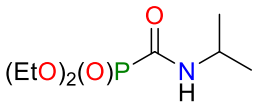
Table 10. Reactions of HP(O)Ph(OMe) and $HP(O)(OEt)_2$ with PhN=C=S, ^{i}PrN=C=O, and ^{i}PrN=C=S[a,b,c]



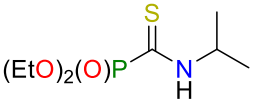
48a–48f



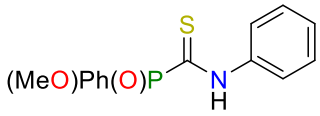
48a: 60 °C, 16 hr, (1%)



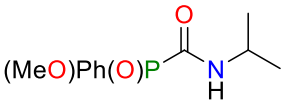
48b: 60 °C, 16 hr, (4%)



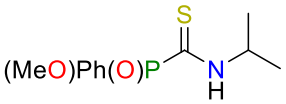
48c: 60 °C, 16 hr, (<0.1%)



48d: 60 °C, 16 hr, (20%)



48e: 60 °C, 16 hr, (5%)



48f: 60 °C, 16 hr, (7%)

[a] Reaction stoichiometry $HP(O)R^1R^2$ (1.0 eq., 0.232 mmol), isocyanate or isothiocyanate (1.0 eq., 0.232 mmol.[b] with added 2-MeTHF (4.0eq, 0.928 mmol) for substrates using HP(O)Ph(OMe) or neat for substrates using $HP(O)(OEt)_2$ as a reactant.[c] NMR spectroscopic yield (in brackets) determined by ^{1}H NMR spectroscopy using an internal standard (mesitylene, 1.0 eq.).

2.3.4 Crystallographic analysis

2.3.4.1 Diphenylphosphinyl carboxamides **44d**-**44e**, **44i**-**44j**, **44l** and **44n**

The molecular structures of the hydrophosphinylation of isocyanates were determined by X-ray crystallography. Crystals suitable for X-ray diffraction were obtained at –30 °C in varying solutions: **44d** 2:1 THF:ethanol, **44e** THF, **44i**-**44j** and **44n** ethanol and **44l** 1:1 THF: toluene. **44d-44e**, **44i**-**44j**, **44l** and **44m** all crystallise in the $P\bar{1}$ space group. The crystal structures of **44d-44e**, **44i**-**44j**, **44l** and **44n** are shown in Figures **9** and **10** with relevant bond distances and angles shown in Tables **11**-**16** respectively.

Compounds **44d** and **44l** crystallised with one molecule per asymmetric unit. **44e**, **44i** and **44n** crystallised with two molecules in the asymmetric unit with **44i** featuring a hydrogen bond donor-acceptor interaction with the adjacent molecule between P(1)–O(2)···H(1)–N(1) interactions. **44j** crystallised with four molecules per asymmetric unit with two pairs of two molecules (**Figure 7**). Each molecule features two hydrogen bonds between the adjacent molecule of the pair (e.g. P(1)–O(1)···H(2)–N(2) and P(2)–O(3)···H(1)–N(1) for molecule one) 1.953(13) Å; 2.027(13) Å at 157.13(13)°; 152.4(14)° (**Figure 7**, left) and 1.983(13) Å; 2.064(13) Å at 158.9(13)°; 146.9(13)° (**Figure 7**, right) for each respective pair. With the exception of **44i** and **44j** which already feature P(O)···(H)N interactions as part of their asymmetric unit, all the other molecules feature hydrogen bonding, 1.919(14)-2.027(14) Å at angles of 150.0(14)°-162.5(11)° by symmetry, (symmetry operations given in (Tables **11**-**13**) through P(O)···N(H) interactions similarly to **44i**-**44j**.

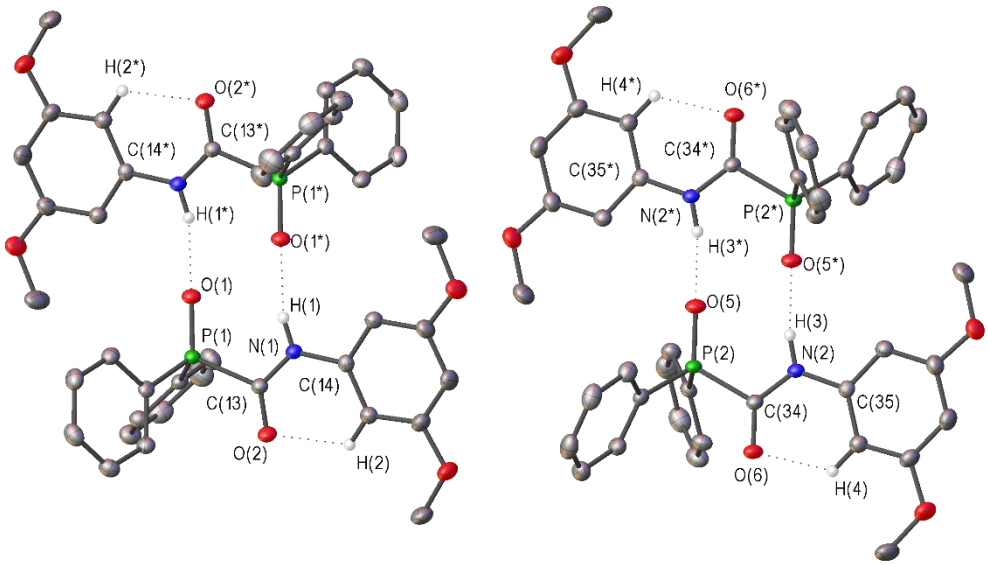


***Figure 7**. Crystal structure of **44j** containing two pairs of molecules per asymmetric unit. H atoms except H(1), H(2), H(3) and H(4) and minor disorder components have been omitted for clarity. Thermal ellipsoids are set at the 50% probability level.*

Only **44e** displayed an intramolecular hydrogen bond between the amide C(O) and C–H^{o} ortho hydrogen of the aromatic 3,5-$(OMe)_2C_6H_3$ group with values of 2.2416(9) Å and 2.1851(9) Å at 122.3° and 123.1° for each respective molecule of the asymmetric unit (**Figure 8**).

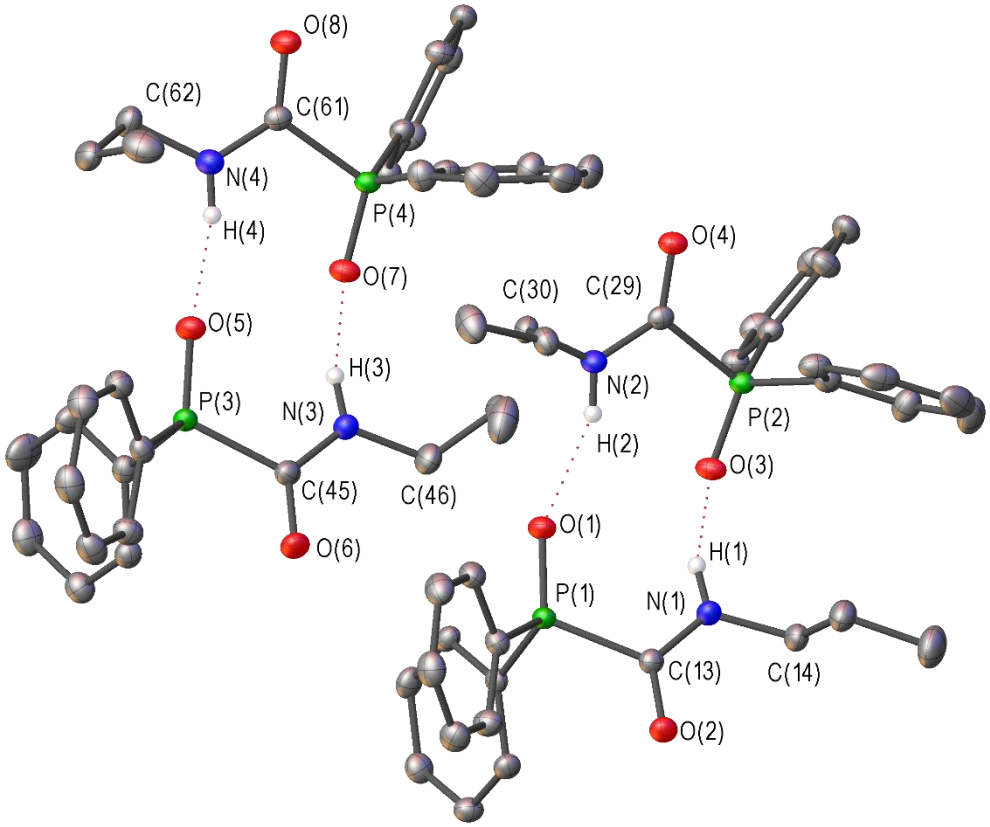


Figure 8. *Crystal structure of **44e** which contains two asymmetric units per unit cell and hydrogen by symmetry shown denoted by * in the corresponding asymmetric unit. H atoms except H(1), H(1*) H(2), H(2*) H(3), H(3*), H(4) and H(4*) have been omitted for clarity. Thermal ellipsoids are set at the 50% probability level. Symmetry operation applied 1-x, 1-y, -z.*

All of the structures feature a short P–O bond, 1.4843(14)-1.4938(8) Å as expected *vs.* 1.4881(11) Å which is the reported P–O distance in $HP(O)Ph_2$. [122] The P–C(O) bonds are elongated likely due to electrostatic repulsion between the positively polarised phosphorus and positive polarised carbon atoms. Due to the aforementioned electrostatic repulsion between positively polarised phosphorus and carbon atom the O–C–N bond angles are distorted for trigonal planar to and the P–C–N are narrowed, the P–C–O bond angles are relatively

unchanged. For all structures, there is little to no influence from the alkyl or aryl group bound to nitrogen on the bond angles or bond lengths (e.g. for C(13)-N(1) bond lengths: **44e**, R = 3,5-$OMe_2C_6H_3$ of 1.3457(17)-1.3462(17) Å versus **44i**, R = Et of 1.328(3)-1.334(3) Å).

Table 11. Selected bond lengths (Å) and angles (°) for **44d**-**44e** and **44i**, [a] Z' = 2. Symmetry operation applied: [b] 1-x, 1-y, -z; [c] 1-x, -y,1-z and [d] 2-x, 2-y, 2-z.

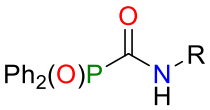
	(**44d**) R = 2-FC_6H_4	(**44e**)[a] R = 3,5-$OMe_2C_6H_3$	(**44i**)[a] R = Et
P(1)–O(1)	1.4908(9)	1.4868(9) 1.4876(10)	1.4835(14) 1.4874(14)
P(1)–C(13)	1.8706(12)	1.8616(13) 1.8614(13)	1.860(2) 1.859(2)
C(13)–O(2)	1.2198(15)	1.2238(16) 1.2250(16)	1.231(2) 1.233(2)
C(13)–N(1)	1.3520(16)	1.3457(17) 1.3462(17)	1.334(3) 1.328(3)
N(1)–C(14)	1.4227(16)	1.4209(17) 1.4224(17)	1.469(3) 1.464(3)
P(1)–C(13)–O(2)	120.57(9)	117.74(10) 116.17(10)	119.66(16) 119.85(16)
P(1)–C(13)–N(1)	113.35(9)	114.76(9) 116.81(9)	114.50(14) 114.45(14)
N(1)–C(13)–O(2)	126.07(11)	127.42(12) 127.02(12)	125.83(19) 125.7(2)

Table 12. Hydrogen-bonding geometry (Å, °) for **44d**, **44e** and **44i**. Symmetry operation applied:

[a] 1-x, 1-y, 1-z; [b] 1-x, -y, 1-z; [c] 2-x, 2-y, 2-z

D–H···A	D–H	H···A	D···A	D–H···A
(**44d**) N(1)–H(1)···O(1)[a]	0.864(13)	2.019(14)	2.8210(14)	154.0(14)
(**44e**) N(1)–H(1)···O(1)[b]	0.875(13)	1.995(14)	2.8414(14)	162.5(15)
(**44e**) N(2)–H(2)···O(5)[c]	0.885(13)	1.919(14)	2.7707(14)	161.0(15)
(**44e**) C(19)–H(19)···O(2)	0.9499(14)	2.2416(9)	2.8639(17)	122.29(9)
(**44e**) C(40)–H(40)···O(6)	0.9500(14)	2.1850(9)	2.8182(17)	123.08(9)
(**44i**) N(2)–H(2)···O(1)	0.866(18)	1.95(2)	2.70(2)	152(3)
(**44i**) N(1)–H(1)···O(3)	0.869(18)	1.98(2)	2.778(2)	151(2)

Table 13. Selected bond lengths (Å) and angles (°) for **44j**. [a] Z' = 4

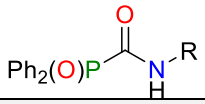
	(**44j**)[a] R = [n]Pr
P(1)–O(1)	1.4867(8), 1.4938(8), 1.4847(8), 1.4924(8)
P(1)–C(13)	1.8626(11), 1.8558(11), 1.8604(11), 1.8602(11)
C(13)–O(2)	1.2323(13), 1.2338(13), 1.2332(14), 1.2305(14)
C(13)–N(1)	1.3279(15), 1.3279(15), 1.3310(15), 1.3298(15)
N(1)–C(14)	1.4621(14), 1.4592(14), 1.4684(15), 1.483(2)
P(1)–C(13)–(2)	120.19(8), 120.75(8), 119.55(9), 118.95(8)
P(1)–C(13)–N(1)	113.99(8), 111.97(8), 114.02(8), 113.76(8)
N(1)–C(13)–O(2)	125.77(10), 127.27(10), 126.30(11), 127.19(11)

Table 14. Hydrogen-bonding geometry (Å, °) for **44j**

D–H···A	D–H	H···A	D···A	D–H···A
(**44j**) N(1)–H(1)···O(3)	0.874(12)	1.953(13)	2.7808(12)	157.5(13)
(**44j**) N(2)–H(2)···O(1)	0.855(12)	2.064(13)	2.8186(12)	146.9(13)
(**44j**) N(3)–H(3)···O(7)	0.875(12)	1.983(13)	2.8164(13)	158.9(13)
(**44j**) N(4)–H(4)···O(5)	0.853(12)	2.027(13)	2.8106(13)	152.4(14)

Table 15. Selected bond lengths (Å) and angles (°) for **44l**-**44n**. [a] Z' = 2 .

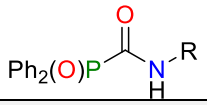
	(**44l**) R = Bn	(**44n**)[b] R = C_4H_3O	
P(1)–O(1)	1.4886(9)	1.4843(14)	1.4845(14)
P(1)–C(13)	1.8563(13)	1.862(2)	1.8577(19)
C(13)–O(2)	1.2258(16)	1.232(2)	1.233(2)
C(13)–N(1)	1.3305(17)	1.331(2)	1.330(2)
N(1)–C(14)	1.469(5)	1.469(2)	1.467(3
P(1)–C(13)–O(2)	119.98(10)	120.48(14)	118.85(14)
P(1)–C(13)–N(1)	114.21(9)	114.26(14)	116.50(14)
N(1)–C(13)–O(2)	125.71(12)	125.22(18)	124.62(18)

Table 16. Hydrogen-bonding geometry (Å, °) for **44l** and **44n**. [b] 2-x, 1-y, -z; [c] 1-x, 1-y, 2-z and [d] -x, 1-y, 1-z

D–H···A	D–H	H···A	D···A	D–H···A
(**44l**) N(1)–H(1)···O(1)[a]	0.869(13)	2.027(14)	2.8132(14)	150.0(14)
(**44n**) N(1)–H(1)···O(1)[b]	0.868(16)	1.984(17)	2.807(2)	158(2)
(**44n**) N(2)–H(2)···O(4)[c]	0.879(16)	1.959(17)	2.812(2)	163(2)

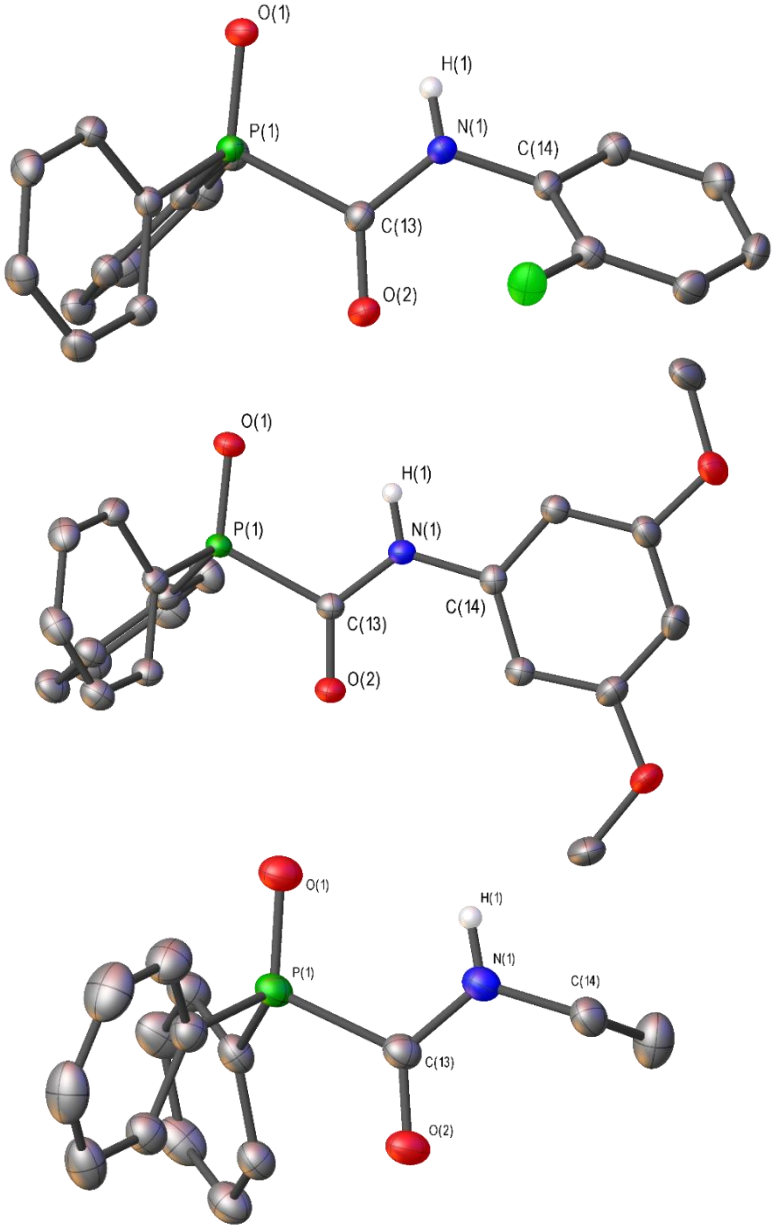


Figure 9. *Crystal structures of (from top to bottom)* ***44d, 44e*** *and* ***44i.*** *Hydrogen atoms with the exception of H(1) and minor disorder components have been omitted for clarity. Thermal ellipsoids are set at the 50% probability level.*

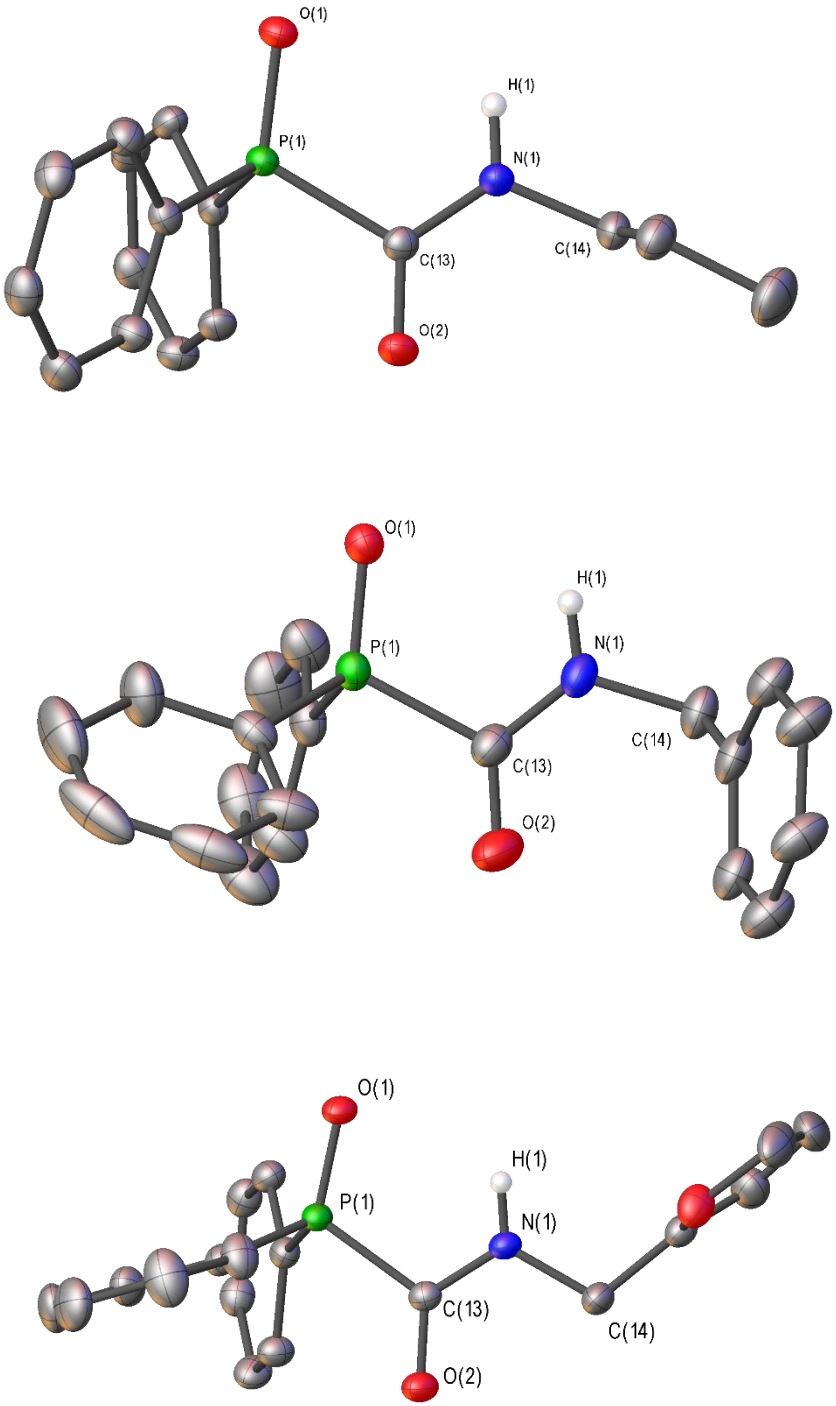


Figure 10. *Crystal structures of (from top to bottom)* ***44j, 44l*** *and* ***44n.*** *Hydrogen atoms with the exception of H(1) and minor disorder components have been omitted for clarity. Thermal ellipsoids are set at the 50% probability level.*

2.3.4.2 Diphenylphosphinyl thiocarboxamides **45c**-**45e** and **45h**

The molecular structures of the hydrophosphinylation products of isothiocyanates were determined by X-ray crystallography. Crystals suitable for X-ray diffraction were obtained at –30 °C in varying solutions of THF and ethanol. The crystal structures of **45c**-**45e** and **45h** are shown in **Figures 11-12** with relevant bond distances and angles shown in **Tables 17**-**18.**

Table 17. Selected bond lengths (Å) and angles (°) for **45c**-**45e** and **45h**.

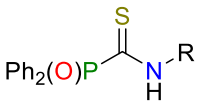
	**45c** R = 4-ClC_6H_4	**45d** R = 4-$OMeC_6H_4$	**45e** R = 4-$NO_2C_6H_4$	**45h** R = allyl
P(1)–O(1)	1.4935(9)	1.4934(8)	1.4896(9)	1.4911(8)
P(1)–C(13)	1.8486(13)	1.8469(12)	1.8422(12)	1.8472(11)
C(13)–S(1)	1.6530(13)	1.6571(12)	1.6424(12)	1.6588(11)
C(13)–N(1)	1.3366(18)	1.3352(15)	1.3492(16)	1.3208(15)
N(1)–C(14)	1.4285(17)	1.4321(15)	1.4104(16)	1.4551(15)
P(1)–C(13)–S(1)	120.16(8)	119.15(7)	116.07(7)	121.38(7)
P(1)–C(13)–N(1)	111.27(9)	112.35(8)	113.23(9)	111.28(8)
N(1)–C(13)–S(1)	128.57(10)	128.50(9)	130.69(9)	127.33(9)

Table 18. Hydrogen-bonding geometry (Å, °) for **45c**, **45d**, **45e** and **45h**. Symmetry operation applied [a]1-x, 1-y, 1-z and [b] 1-x,1-y, -z.

D–H···A	D–H	H···A	D···A	D–H···A
(**45c**) N(1)–H(1)···O(1)[a]	0.868(13)	1.956(14)	2.7827(14)	158.9(16)
(**45d**) N(1)–H(1)···O(1)[a]	0.865(13)	1.929(13)	2.7600(13)	160.8(14)
(**45e**) N(1)–H(1)···O(1)[b]	0.862(13)	1.989(14)	2.8262(14)	163.3(15)
(**45e**) C(19)–H(19)···S(1)	0.9500(13)	2.5004(3)	3.1676(13)	127.30(8)
(**45h**) N(1)–H(1)···O(1)[a]	0.853(13)	1.998(13)	2.7619(13)	148.6(14)

Similarly, to **44e, 45e** contains an intermolecular hydrogen bond of 2.5004(3) Å at 163.3(15)° between the chalcogen atom of C(X) and the *ortho*-hydrogen atom of the aryl ring; C(S) ⋯H(Ar^{o}). No such intermolecular hydrogen bonding is seen for **45d** which contains a methoxy group like **44e**. Again, all of these structures contain hydrogen bonding by symmetry through P(O)⋯N(H) interactions, all the bond lengths are statistically equivalent at ~1.97 Å (1.929(13)-1.989(14) Å). P–O bond lengths are also statistically equivalent with a short bond length of ~1.49 Å (1.48896(9)-1.4935(9) Å). P–C(S) bond lengths are comparatively 0.02 Å (1.8422(12)-1.8486(13) Å) shorter than P–C(O), likely due to the less electronegative sulfur atom giving rise to less positive charge on the carbon bond; hence there is less repulsion between P–C(S). The P(1)–C(13)–N(1) angle varies from 111.27(9)° to 113.23(9)° showing distortion away from a trigonal planar geometry, in a similar manner to that for the diphenylphosphinyl carboxamides, **44d**-**44e**, **44i**-**44j** and **44l**, **44n**.

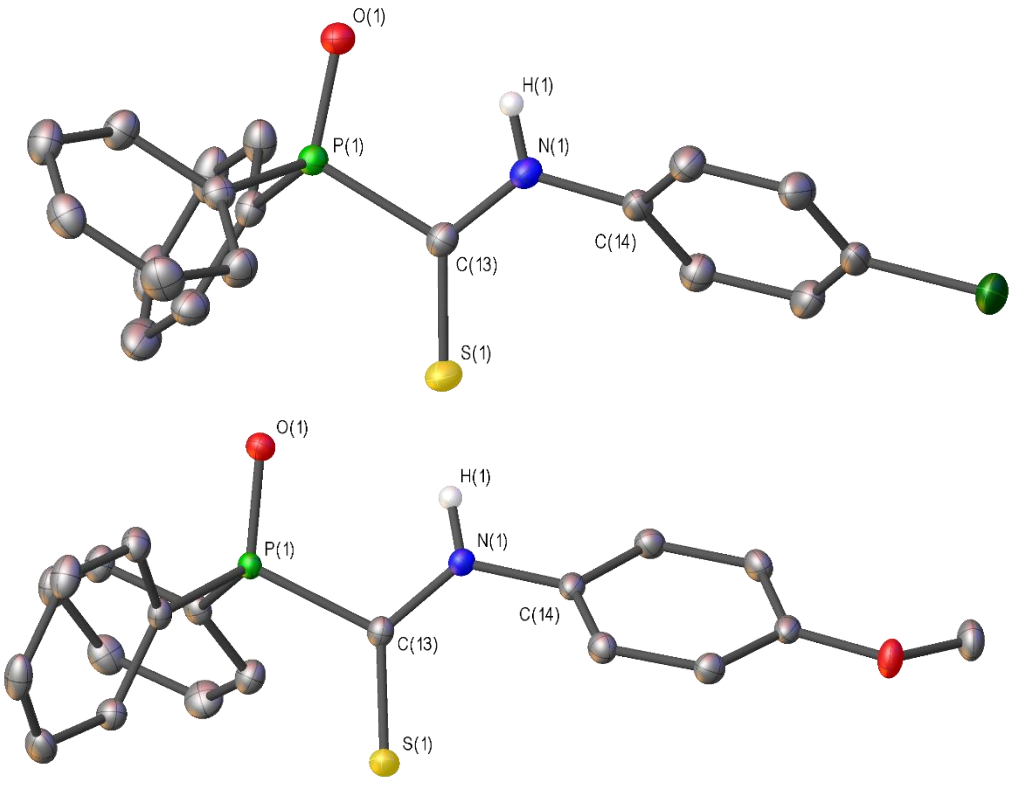


Figure 11. *Crystal structures of (from top to bottom)* ***45e*** *and* ***45h.*** *Hydrogen atoms with the exception of H(1) have been omitted for clarity. Thermal ellipsoids are set at the 50% probability level.*

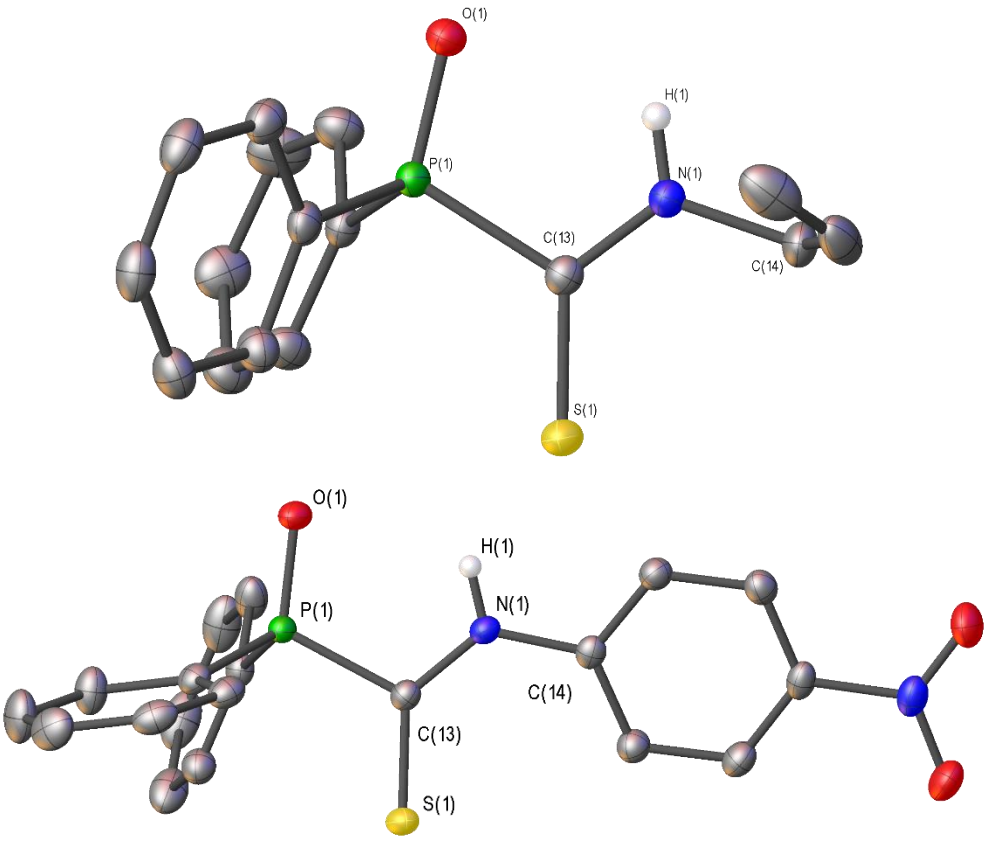


Figure 12. *Crystal structures of (from top to bottom)* ***45c and 45d.*** *Hydrogen atoms with the exception of H(1) have been omitted for clarity. Thermal ellipsoids are set at the 50% probability level.*

2.3.4.3 Diisopropylphosphinyl (thio)carboxamides **46c**-**46d** and Dimethoxylphosphonyl phenylcarboxamide **47b**

For compounds **46c**-**46d** and **47b** crystals suitable for X-ray diffraction were obtained at –30 °C from saturated ethanol solutions. Relevant bond angles and distances are shown in **Tables 19**-**20**. Similarly, to previous structures discussed in Sections 2.3.4.1 and 2.3.4.2 all contain statistically equivalent hydrogen bonds by symmetry at lengths of ~2.045 Å (2.035(13)-2.055(14) Å)

(**Table 19**). Additionally, compound **47b** contains an intermolecular hydrogen bond (2.242 Å at 122.6 °) between the C(O) amide and Ar(H) aromatic group.

The P–O bond distances for the $^{i}Pr_2P(O)$- containing compounds **46c** and **46d** averaged ~1.49 Å however $(MeO)_2P(O)$- containing **47b** the bond length is shortened to 1.47 Å. Comparatively to previous structures **44** and **45** the P-C(S) and P-C(O) bond lengths of **46c** and **46d** are statistically the same, with values of 1.8458(13) Å and 1.8611(11) Å respectively. All structures feature distorted trigonal planar geometries around the central PC(X)N moiety, with more acute P(1)–C(X)–N(1) angles of 111.38(9)-115.29(9)° and increased(1)–C(X)–X(1) angles of 126.19(10)-129.15(10)° away from an ideal 120° angle.

Table 19. Selected bond lengths (Å) and angles (°) for **46c**-**46d** and **47b**.

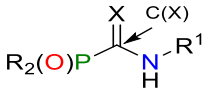
	**46c**, R = ^{i}Pr, X = S, R^1 = Ph	**46d**, R = ^{i}Pr, X = O, R^1 = ^{i}Pr	**47b**, R = OMe, X = O, R^1 = Ph
P(1)–O(1)	1.4969(9)	1.4919(8)	1.4666(10)
P(1)–C(X)	1.8458(13)	1.8611(11)	1.8507(13)
C(X)–X	1.6585(13)	1.2323(14)	1.2254(17)
C(13)–N(1)	1.3350(17)	1.3254(15)	1.3460(17)
N(1)–C(R^1)	1.4258(17)	1.4656(14)	1.4228(16)
P(1)–C(X)–X(1)	119.47(7)	119.73(8)	117.52(10)
P(1)–C(X)–N(1)	111.38(9)	114.08(8)	115.29(9)
N(1)–C(X)–X(1)	129.15(10)	126.19(10)	127.18(12)

Table 20. Hydrogen-bonding geometry (Å, °) for **46c**-**46d** and **47b**. [a] 1-x,1-y, 1-z and [b] 1-x, 1-y, -z.

D–H···A	D–H	H···A	D···A	D–H···A
(**46c**) N(1)–H(1)···O(1)[a]	0.867(11)	2.040(12)	2.8510(14)	155.3(15)
(**46d**) N(1)–H(1)···O(1)[a]	0.843(11)	2.021(12)	2.8025(12)	154.0(14)
(**47b**) N(1)–H(1)···O(1)[b]	0.853(14)	2.055(14)	2.8769(15)	161.4(15)
(**47b**) C(9)–H(9)···O(4)	0.9500(14)	2.2445(10)	2.8698(17)	122.57(9)

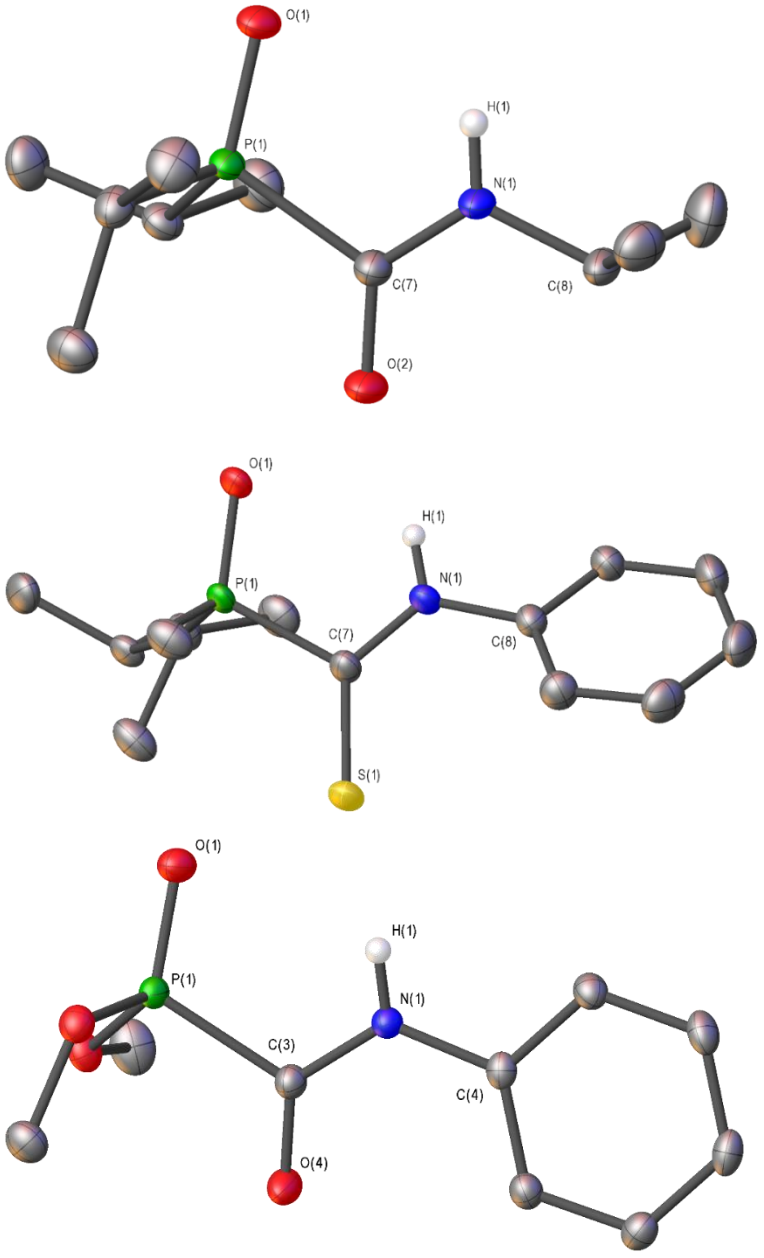


Figure 13. *Crystal structures of (from top to bottom)* ***46c***-***46d*** *and* ***47b.*** *Hydrogen atoms with the exception of H(1) have been omitted for clarity. Thermal ellipsoids are set at the 50% probability level.*

2.4 Conclusions

Hydrophosphinylation utilising $HP(O)Ph_2$ can occur under catalyst-free conditions either neat or in solution, with four equivalents of 2-MeTHF as solvent being optimal to allow the use of solid substrates. A variety of functionalised aryl and alkyl isocyanates and isothiocyanates are tolerated in moderate yields, with alkyl isocyanates and isothiocyanates requiring heating at 60 °C for good conversions. The use of substrates with very electron withdrawing groups such as 4-nitrophenyl iso(thio)cyanate is tolerated to a lesser extent, resulting in the formation of significant amounts of phosphorus containing side products. A secondary alkyl phosphine oxide, diisopropylphosphine oxide has been utilised for the first time, with excellent to moderate yields with PhN=C=O, PhN=C=S and ^{i}PrN=C=S but with low yields for ^{i}PrN=C=O.

Additive reactions with radical inhibitors cumene and 1,4-cyclohexadiene, were not slowed and gave similar conversions to reactions without inhibitors, suggesting the hydrophosphinylation reaction is not a radical mediated mechanism. In the literature, mechanisms involving secondary phosphine oxides commonly suggest the tautomerisation of secondary phosphine oxides to phosphinous acids. Thus, a mechanism here is suggested; whereby there is an equilibrium between $HP(O)R^1R^2$ and its P(III)–OH tautomer. The isocyanate or isothiocyanate then undergoes nucleophilic attack by the P(III)-OH nucleophile, followed by a proton transfer to reform the P=O bond.

The catalyst-free methodology was further expanded to hydrophosphonylation utilising diethyl phosphite as a substrate. Contrary to hydrophosphinylation, hydrophosphonylation of phenyl isocyanate reaction only proceeded in neat conditions at 60 °C giving high conversions. The same dependence was not seen for methyl phenylphosphinate, with the reaction occurring neat or in a 2-MeTHF solution. Purification attempts to remove the phosphorus containing

starting materials by chromatography, distillation or recrystallisation were unsuccessful in most cases, resulting in decomposition of the desired products. Use of less electrophilic isocyanates and isothiocyanates PhN=C=S, ^{i}PrN=C=S and ^{i}PrN=C=O, resulted in very low conversions.

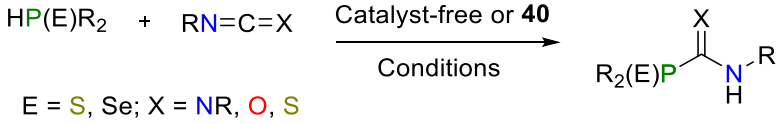
Crystallographic analysis revealed all structures to contain hydrogen bonding by symmetry or as part of the unit cell when Z'>1, from an adjacent molecule of the pair between P(O)···N(H) at lengths of ~2.0 Å (1.929(13)-2.064(13) Å and angles of 146.9(13)-162.5(15)°). Additionally, some compounds such as **44e** and **45e** contain intramolecular hydrogen bonds of 2.1851(9)-2.2416(9) Å at 123.1-123.3° and 2.5004(3) Å at 163.3(15)° respectively, between the amide or thioamide C(O/S) and C–H^{o} of the nearby aromatic ring. All structures feature an expected small P-O bond length of ~ 1.49 Å (1.4843(14)-1.4938(8) Å). For both phosphinylcarboxamides and phosphinylthiocarboxamides there is significant distortion of the expected trigonal planar environment, with an increase in N–C–O (124.62(18)-127.42(12)°) and N–C–S (127.33(9)-130.69(9)°) bond angles and decrease in P–C(O)–N (111.97(8)-116.81(9)) and P–C(S)–N (111.27(9)-113.23(9)°) bond angles; away from the idealised 120° bond angles.

Overall, this catalyst-free methodology highlights the importance of control reactions whereby, reactions performed neat and in concentrated solutions at 25 °C and 60 °C can ascertain a basic understanding of how well a reaction can perform catalyst-free and can validate whether a catalyst is needed. This is demonstrated herein by this simple methodology providing greater or equal yields and much wider substrate scope when compared to literature procedures using catalysts.

2.5 Future Work

A wide scope of isocyanates and isothiocyanates have been shown to tolerate a catalyst-free approach well, however, there is still an incompatibility with the use of more reactive electron withdrawing groups (such as 4-$NO_2C_6H_4N{=}C{=}O$). In these instances, further catalytic work either using group 1 or 2 based catalysts or metal-based *m*-terphenyl catalysts (e.g., precatalyst **40**) is necessary to obtain high yields and selectivity. This approach could also lead to opportunities involving the use of other less reactive heterocumulene substrates such as carbodiimides or H-P unit sources such as $H\text{-}P(O)(OR)_2$ sources.

Further synthetic possibilities include the alternative use of $HP(E)R_2$ (E = S, Se) compounds with heterocumulenes (**Scheme 37**). Challenges may be expected to arise from $HP(E)R_2$ substrate disproportionation, which has been shown to occur with group 1 catalysts. However, ideally this can be avoided by either a catalyst-free approach or a transition-metal based *m*-terphenyl catalyst (e.g. [Fe] (**40**), [Mn] or [Co]).



Scheme 37. *$HP(S)R_2$ and $HP(Se)R_2$ addition to heterocumulenes utilising a catalyst-free or m-terphenyl catalyst based approach.*

Finally, future work should be directed away from synthetic approaches and be based on the utilisation of these classes of compounds (particularly the novel further functionalised compounds described herein) as there seems to be a relative dearth of uses compared to analogous compounds such as ureas, thioureas and guanidines; which have numerous uses as ligands, medicines and polymers etc.

2.6 Experimental Procedures

2.6.1 Hydrophosphinylation using $HP(O)Ph_2$

2.6.1.1 Initial optimisation of catalyst-free hydrophosphinylation with $HP(O)Ph_2$ and Ph-N=C=O

NMR spectroscopic yields were calculated by integrating the ^1H NMR spectroscopic signals corresponding to the product relative to the mesitylene internal standard.

2.6.1.2 Variation of phenyl isocyanate concentration

In an inert atmosphere glovebox an oven dried Young's tap modified NMR tube was charged with diphenylphosphine oxide (1.0 eq., 20.2 mg, 0.10 mmol), C_6D_6 (0.5 mL) and phenyl isocyanate (1.0, 1.2, 1.5, or 2.0 eq.) The sealed tube was sonicated at 25 °C for 8 hours. Mesitylene (1.0 eq., 0.10 mmol) was added and a ^1H NMR spectrum recorded. Respective NMR spectroscopic yields = 70% (1.0 eq.), 73% (1.2 eq.), 71% (1.5 eq.) and 71% (2.0 eq.).

2.6.1.3 Variation of diphenylphosphine oxide concentration

In an inert atmosphere glovebox an oven dried Young's tap modified NMR tube was charged with diphenylphosphine oxide (1.5 eq., 30.3 mg, 0.15 mmol), C_6D_6 (0.5 mL) and phenyl isocyanate (1.0 eq., 10.9 µL, 0.10 mmol) The sealed tube was sonicated at 25 °*C for 8 hours.* Mesitylene (1.0 eq., 0.10 mmol) was added and a ^1H NMR spectrum recorded. NMR spectroscopic yield = 71%.

2.6.1.4 Neat reaction under an inert atmosphere

In an inert atmosphere glovebox an oven dried Young's tap modified NMR tube was charged with diphenylphosphine oxide (1.0 eq., 20.2 mg, 0.10 mmol), and phenyl isocyanate (1.2 eq., 13.4 µL, 0.12 mmol). The sealed tube was sonicated at 25 °*C* for 3 hours. Mesitylene (1.0 eq., 0.10 mmol) was added, and the reaction mixture was diluted with $CDCl_3$ (0.45 mL) and shaken vigorously until all solid dissolved. NMR spectroscopic yield = 72%

2.6.1.5 Neat reaction in air

In an inert atmosphere glovebox an oven dried Young's tap modified NMR tube was charged with diphenylphosphine oxide (1.0 eq., 20.2 mg, 0.10 mmol), and phenyl isocyanate (1.2 eq., 13.4 µL, 0.12 mmol). The sealed tube was removed from the glovebox, opened to air and sonicated at 25 °*C* for 3 hours. Mesitylene (1.0 eq., 0.10 mmol) was added and the reaction mixture was diluted with $CDCl_3$ (0.45 mL) and shaken vigorously until all solid dissolved. NMR spectroscopic yield = 38%.

2.6.1.6 Variation of solvent type and volume

In an inert atmosphere glovebox an oven dried screw cap vial was charged with diphenylphosphine oxide (1.0 eq., 20.2 mg, 0.10 mmol), phenyl isocyanate (1.2 eq., 13.4 µL, 0.12 mmol) and either THF (0.50 mL or 40.0 µL) or 2-MeTHF (40.0 µL). The sealed tube was then sonicated at 25 °C for either 3 hours (40.0 µL solvent) or 8 hours (0.5 mL solvent). Mesitylene (1.0 eq., 0.10 mmol) was added, and the reaction mixture was diluted with $CDCl_3$ (0.45 mL) and shaken vigorously until all solid dissolved. Respective NMR spectroscopic yields = 76% (THF 0.50 mL), 80% (THF 40.0 µL) and 80% (2-MeTHF 40.0 µL).

2.6.1.7 General procedure for hydrophosphinylation of isocyanates and isothiocyanates with $HP(O)Ph_2$, 44a – 45h (for NMR yields)

In an inert atmosphere glovebox an oven dried Young's tap modified NMR tube was charged with diphenylphosphine oxide (1.0 eq., 20.2 mg, 0.10 mmol), 2-MeTHF (4.0 eq., 40.3 µL, 0.40 mmol), and either liquid isocyanate (1.2 eq., 0.12 mmol) or solid isocyanate (1.0 eq., 0.10 mmol). The sealed tube was sonicated at either 25 °C for 3 hours (**44a**–**44e**) or 60 °C for 6 hours (**44g**–**44h**, **44i**–**44n**, and **45f**–**45h**) or 60 °*C* for 10 hours (**44h**) or 25 °C for 2 hours (**45a**–**45e**). Mesitylene (1 eq., 0.10 mmol) was added, and the reaction mixture was diluted with $CDCl_3$ (0.45 mL) and shaken vigorously until all solid dissolved. The yield was calculated by integrating ^1H NMR spectroscopic signals corresponding to the product relative to the mesitylene internal standard.

2.6.1.8 General procedure for hydrophosphinylation of isocyanates and isothiocyanates with $HP(O)Ph_2$, 44a – 45h (for isolated yields)

In an inert atmosphere glovebox an oven dried screw cap vial was charged with diphenylphosphine oxide (1.0 eq., 60.7 mg, 0.30 mmol), 2-MeTHF (4.0 eq., 0.121 mL, 1.20 mmol), and either liquid iso(thio)cyanate (1.2 eq., 0.36 mmol) or solid iso(thio)cyanate (1.0 eq., 0.30 mmol). The sealed vial was stirred at either 25 °*C* for 3 hours (**44a**–**44e**) or 60 °*C* for 6 hours (**44g–44h**, **44i–44n**, and **45f–45h**) or 60 °*C* for 9 hours (**44h**) or 25 °*C* for 2 hours (**45a** – **45e**). The reaction mixture was then dried under vacuum and worked up in air. The isolated solid was washed with ethanol (3 × 0.5 mL for **44a**–**44e**, **44m**–**44n**, **45g**–**45h**; 3 × 0.1 mL for **44g**–**44l**; 1 × 0.1 mL **45a**–**45d**) to afford pure product.

For **45e**, the crude solid was washed with ethanol (1 × 0.5 mL) and subsequently recrystallised from THF (0.1 mL) layered with ethanol (0.1 mL) at −30 °C to afford pure **45e** as a bright orange-red crystalline solid.

For **44f**, the crude product was washed with ethanol (3 × 5.0 mL) and then recrystallised from THF at −30 °C. However, only a few milligrams of solid precipitated, and an analytically pure sample could not be obtained.

2.6.1.9 Procedure for the gram scale hydrophosphinylation of phenyl isocyanate

In an inert atmosphere glovebox an oven dried screw cap vial was charged with phenyl isocyanate (1.2 eq., 1.0 mL, 9.2 mmol), diphenylphosphine oxide (1.0 eq., 1.55 g, 7.67 mmol), and 2-MeTHF (4.0 eq., 2.5 mL, 30.7 mmol). The sealed vial was stirred for 2 hours at room temperature. The resulting solid was filtered in air, washed with ethanol (3 × 5 mL) and dried *in vacuo* to obtain pure **44a** as a white solid (1.82 g, 74%).

2.6.2 Hydrophosphinylation with $HP(O)^iPr_2$

2.6.2.1 Initial optimisation of catalyst-free hydrophosphinylation using $HP(O)^iPr_2$

In an inert atmosphere glovebox an oven dried screw cap vial was charged with diisopropylphosphine oxide (1.0 eq., 15.0 μL, 0.105 mmol or 2.0 eq., 30.0 μL, 0.210 mmol), phenyl isocyanate (1.0 eq., 11.4 μL, 0.105 mmol or 1.5 eq., 17.1 μL, 0.158 mmol or 2.0 eq., 22.8 μL, 0.210 mmol) with 2-MeTHF (4.0 eq., 42 μL, 0.420 mmol) or neat. The sealed vial was stirred at either 25 or 60 °C for either 3 or 16 hours. Mesitylene (1.0 eq., 0.105 mmol) was added, and the reaction mixture was diluted with $CDCl_3$ (0.50 mL) and shaken vigorously until all solid

dissolved. The yield was calculated by integrating ^{1}H NMR spectroscopic signals corresponding to the product relative to the mesitylene internal standard.

2.6.2.2 General procedure for hydrophosphinylation of isocyanates and isothiocyanates with HP(O)^{i}Pr$_2$, **46a** – **46**c (for NMR yields)

In an inert atmosphere glovebox an oven dried screw cap vial was charged with diisopropylphosphine oxide (1.0 eq., 15.0 μL, 0.105 mmol) and isocyanate or isothiocyanate (1.0 eq., 0.105 mmol). The sealed vial was stirred at 60 °C for 16 hours. Mesitylene (1 eq., 0.105 mmol) was added, and the reaction mixture was diluted with $CDCl_3$ (0.50 mL) and shaken vigorously until all solid dissolved. The yield was calculated by integrating ^{1}H NMR spectroscopic signals corresponding to the product relative to the mesitylene internal standard.

2.6.2.3 General procedure for hydrophosphinylation of isocyanates and isothiocyanates with HP(O)^{i}Pr$_2$, **46a** – **46c** (for isolated yields)

In an inert atmosphere glovebox an oven dried screw cap vial was charged with diisopropyl phosphine oxide (1.0 eq., 60.0 μL, 0.628 mmol), 2-MeTHF (4.0 eq., 0.250 mL, 2.51 mmol), and iso(thio)cyanate (1.0 eq., 0.628 mmol). The sealed vial was stirred at 60 °*C* for 16 hours. The reaction mixture was then dried under vacuum and worked up in air as detailed below. The isolated solid was washed either with ethanol (2 × 0.5 mL for **46a**, 1 × 0.5 mL for **46b**) or recrystallised from the minimum amount of ethanol at -30 °C and immediately filtered (**46c**) to afford the pure product. **46a**-**46c** are less stable than **44a**- **45h** in solution and prolonged periods of time cause decomposition of the products most likely to be cyclotrimerised isocyanate and HP(O)(^{i}Pr$_2$). Thus, it has been difficult to

obtain appropriate elemental analysis, which has been successful for **46b** but not **46a** or **46c**.

2.6.3 Hydrophosphinylation with HP(O)Ph(OMe) and Hydrophosphonylation with $HP(O)(OEt)_2$ and $HP(O)(OMe)_2$

2.6.3.1 Initial optimisation

In an inert atmosphere glovebox an oven dried screw cap vial was charged with methyl phenylphosphinate (1.0 eq., 30.0 µL, 0.232 mmol) or diethylphosphite (1.0 eq., 30.0 µL, 0.232 mmol), phenyl isocyanate (1.0 eq., 25.2 µL, 0.232 mmol or 1.5 eq., 37.8 µL, 0.348 mmol or 2.0 eq., 50.4 µL, 0.464 mmol) with 2-MeTHF (4.0 eq., 93.0 µL, 0.928 mmol) or neat. The sealed vial was stirred at either 25 or 60 °C for either 3 or 16 hours. Mesitylene (1.0 eq., 0.232 mmol) was added and the reaction mixture was diluted with $CDCl_3$ (0.40 mL) and shaken vigorously until all solid dissolved. The yield was calculated by integrating ^1H NMR spectroscopic signals corresponding to the product relative to the mesitylene internal standard.

2.6.3.2 Hydrophosphinylation with HP(O)Ph(OMe) and Hydrophosphonylation with $HP(O)(OEt)_2$ with other electrophiles

In an inert atmosphere glovebox an oven dried screw cap vial was charged with methyl phenylphosphinate (1.0 eq., 30.0 µL, 0.232 mmol) or diethylphosphite (1.0 eq., 30.0 µL, 0.232 mmol), iso(thio)cyanate (1.0 eq, 0.232) with 2-MeTHF (4.0 eq., 93.0 µL, 0.928 mmol) or neat. The sealed vial was stirred at either 25 or 60 °C for either 3 or 16 hours. Mesitylene (1.0 eq., 0.232 mmol) was added, and the reaction mixture was diluted with $CDCl_3$ (0.40 mL) and shaken vigorously until all solid dissolved. The yield was calculated by integrating ^1H

NMR spectroscopic signals corresponding to the product relative to the mesitylene internal standard.

2.6.3.3 General procedure for hydrophosphinylation of phenyl isocyanate with $HP(O)(Ph)(OMe)$, $HP(O)(OEt)_2$ and $HP(O)(OMe)_2$ (for NMR yields)

In an inert atmosphere glovebox an oven dried screw cap vial was charged with methyl phenylphosphinate (1.0 eq., 30.0 μL, 0.232 mmol) or diethylphosphite (1.0 eq., 30.0 μL, 0.232 mmol) or dimethylphosphite (1.0 eq., 21.3 μL, 0.232 mmol), phenyl isocyanate (1.0 eq., 25.2 μL, 0.232 mmol) neat (**47a** – **47b**) or with 2-MeTHF (4.0 eq., 93.0 μL, 0.928 mmol, **47c**). The sealed vial was stirred at 60 °C for 16 hours. Mesitylene (1.0 eq., 0.232 mmol) was added, and the reaction mixture was diluted with $CDCl_3$ (0.50 mL, **47a**-**47b** or 0.40 mL, **47c**) and shaken vigorously until all solid dissolved. The yield was calculated by integrating ^1H NMR spectroscopic signals corresponding to the product relative to the mesitylene internal standard.

2.6.3.4 Procedure for the hydrophosphinylation of phenyl isocyanate with $HP(O)(Ph)(OMe)$, $HP(O)(OEt)_2$ and $HP(O)(OMe)_2$

Residual unreacted $HP(O)R^1R^2$ could not be removed from products by either silica or alumina chromatography, by vacuum distillation without product decomposition. Attempts at recrystallisation or by washing in various solvents were additionally unsuccessful. The procedures outlined here give the highest ratio of product to starting material.

47a: In an inert atmosphere glovebox an oven dried screw cap vial was charged with diethylphosphite (100 μL, 0.776 mmol) and phenyl isocyanate (84.4 μL, 0.776 mmol). The sealed vial was stirred at 60 °C for 16 hours. The solution

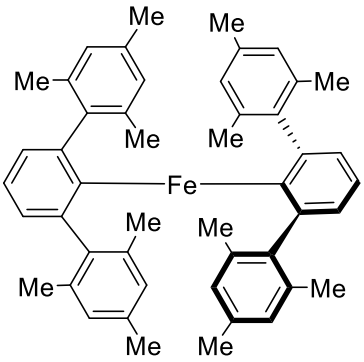
was allowed to cool to room temperature resulting in precipitation of a white solid from the yellow oil. THF (100 µL) was added to the mixture and the filtrate was separated by filtration from the solid. The yellow filtrate was then dried *in vacuo* at 50 °C with rapid stirring under vacuum for 4 hours (attempts to remove more $HP(O)(OEt)_2$ by increasing the temperature resulted in the gradual decomposition of **47a**) until a very viscous yellow oil formed (122.3 mg, 61%). Product contained approximately 11% diethylphosphite by ^{31}P NMR spectroscopy.

47b: In an inert atmosphere glovebox an oven dried screw cap vial was charged with dimethylphosphite (100 µL, 1.09 mmol) and phenyl isocyanate (118.5 µL, 1.09 mmol). The sealed vial was stirred at 60 °C for 16 hours, after 1 hour the oil turned yellow and after 16 hours formed a yellow oily-solid. The solid was washed with ethanol (3 x 0.3 mL) and dried in vacuo for 4 hours at room temperature with stirring. The resulting off-white solid was recrystalised twice from ethanol at –30 °C (further attempts at crystallisation did not improve purity), to yield clear crystals (55.8 mg, 22%). Product contained approximately 2% dimethylphosphite by ^{31}P NMR spectroscopy.

47c: In an inert atmosphere glovebox an oven dried screw cap vial was charged with methyl phenylphosphinate (1.19 mL, 9.2 mmol), phenyl isocyanate (1.0 mL, 9.2 mmol) and 2-MeTHF (3.7 mL, 36.8 mmol). Stirred for 16 hours at 60 °C resulting in a yellow oily solution and some yellow precipitate. THF (3.0 mL) was added, and the mixture was filtered. The yellow filtrate was dried *in vacuo* with rapid stirring at 40 °C for 2 hours to form a very vicious yellow oil. Ethanol (2.0 mL) was added and stirred, and subsequently left at -30 °C for 16 hours resulting in the precipitation of an off-white to yellow powder. The powder was washed with ethanol (3 x 1.0 mL) to give off-white powder. The powder was dried under vacuum and then dissolved in the minimum amount of ethanol and

left at –30 °C for 16 hours to precipitate the product as an off-white powder, (1.02 g, 41%). Product contained approximately 3% methyl phenylphosphinate by ^{31}P NMR spectroscopy.

2.6.4 Synthesis of $Fe(C_6H_3\text{-}2,6\text{-}Mes_2)_2$ (**40**)



Synthesised by a modified literature procedure. Under an argon atmosphere $[2,6\text{-}Mes_2C_6H_3Li]_2$ (2.73 g, 4.26 mmol) and $FeCl_2(THF)_{1.5}$ (1.00 g, 4.26 mmol) were charged into a Schlenk flask. THF (5.0 mL) and toluene (50 mL) were added to form a brown-yellow solution and was stirred overnight. Volatiles were removed in vacuo and the resulting brown solid was dried at 60 °C for 4 hours. The resultant brown solid was extracted into hexanes (5 x 50 mL) and the dark-yellow solution, was left to settle overnight, forming a dark-brown solid and a clear golden-yellow solution. The solution was filtered and concentrated in vacuo (~30-50 mL) and recrystallised at -30 °C (over 16-48 hours); forming golden yellow crystals. Subsequent filtration and drying in vacuo resulted in golden-yellow crystals* of $Fe(C_6H_3\text{-}2,6\text{-}Mes_2)_2$ (1.55g, 53.3%).

^{1}H NMR (400 MHz, C_6D_6, 25 °C) δ –56.2 (s, br, Δν½ = 208 Hz, 8H, *m*-H of Mes), –36.2 (s, br, Δν½ = 1230 Hz, 24H, *o*-CH_3 of Mes), –11.6 (s, Δν½ = 37 Hz, 12H, *p*-CH_3 of Mes), 33.7 (s, br, Δν½ = 272 Hz, 2H, *p*-H of C_6H_3), 139.8 (s, br, Δν½ = 957 Hz, 4H, *m*-H of C_6H_3).

*N.B: If the crystals are not golden yellow, $Fe(C_6H_3\text{-}2,6\text{-}Mes_2)_2$ needs to be purified with an additional recrystallisation, this is particularly important for catalytic work in Chapters 3 and 4.

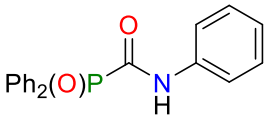
Common problems can include: pale yellow precipitate or crystals or precipitate means the concentrated solution in hexane of crude $Fe(C_6H_3\text{-}2,6\text{-}Mes_2)_2$ was too concentrated and HMes ligand impurity additionally precipitated out with $Fe(C_6H_3\text{-}2,6\text{-}Mes_2)_2$.

Slight-green tinge means water was introduced into the reaction.

Dark yellow or light yellow-brown precipitate means oxygen was introduced into the reaction (note pure golden yellow $Fe(C_6H_3\text{-}2,6\text{-}Mes_2)_2$ can crystallise from a brown solution of hexane, as long the solution is clear and not cloudy; however, the subsequent yields will be lower than a clear golden yellow solution.)

2.6.5 Yields and characterisation data for **44a**–**44n**

2.6.5.1 $Ph_2P(O)C(O)NH(Ph)$ (**44a**)



White solid: 61.0 mg, 64% (80% NMR yield).

^{1}H NMR (400 MHz, $CDCl_3$, 25 °C) δ 9.74 (s, 1H, N*H*), 8.05-7.89 (m, 4H, $P(O)Ph_2^o$), 7.72 (d, *J* = 7.9 Hz, 2H, Ph^o), 7.63-7.55 (m, 2H, $P(O)Ph_2^p$), 7.54-7.45 (m, 4H, $P(O)Ph_2^m$), 7.34 (t, ^3J(H,H) = 7.2 Hz, 2H, Ph^m), 7.16 (t, ^3J(H,H) = 7.4 Hz, 1H, Ph^p).

^{13}C{^{1}H} NMR (101 MHz, $CDCl_3$, 25 °C) δ 168.1 (d, ^1J(C,P) = 123.4 Hz, *C*O), 137.1 (d, ^3J(C,P) = 9.5 Hz, Ph^i), 132.8 (d, ^4J(C,P) = 2.8 Hz, $P(O)Ph_2^p$), 131.8 (d, ^3J(C,P) = 9.6 Hz, $P(O)Ph_2^m$), 129.0 (d,^1J(C,P) = 100.8 Hz, $P(O)Ph_2^i$), 129.0 (s, Ar *C*H), 128.8 (d, ^2J(C,P) = 12.3 Hz, $P(O)Ph_2^o$), 128.5 (s, Ar *C*H), 125.5 (s, Ar *C*H), 120.2 (s, Ar *C*H).

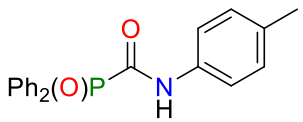
^{31}P{^{1}H} NMR (162 MHz, $CDCl_3$, 25 °C) δ 15.5.

HRMS (ESI) expected: 344.0811, found 344.0806 $[M+Na]^+$ (err [ppm] = 1.30).

IR (ATR) ν/cm^{-1} = 3172 (N–H), 1641 (C=O), 1169 (P=O).

Spectroscopic data matched previous reported literature.[122]

2.6.5.2 $Ph_2P(O)C(O)NH(4\text{-}MeC_6H_4)$ (**44b**)



White solid: 66.4 mg, 66% (82% NMR yield).

^{1}H NMR (400 MHz, $CDCl_3$, 25 °C) δ 9.25 (s, 1H, N*H*), 8.09-7.90 (m, 4H, $P(O)Ph_2^o$), 7.66-7.41 (m, 8H, $P(O)Ph_2^{m+p}$ + Ar C*H*), 7.15 (d, 2H, ^3J(H,H) = 8.2 Hz, Ar C*H*), 2.32 (s, 3H, CH_3).

^{13}C{^{1}H} NMR (101 MHz, $CDCl_3$, 25 °C) δ 167.6 (d, ^1J(C,P) = 122.8 Hz, *C*O), 135.4 (s, Ar *C*H), 134.2 (d, ^3J(C,P) = 9.5 Hz, $C_6H_4Me^i$), 132.8 (d, ^4J(C,P) = 2.8 Hz, $P(O)Ph_2^p$), 131.8 (d, ^3J(C,P) = 9.7 Hz, $P(O)Ph_2^m$), 129.7 (s, Ar *C*H), 128.8(4) (d, ^1J(C,P) = 100.2 Hz, $P(O)Ph_2^i$) 128.8(0) (d, ^2J(C,P) = 12.3 Hz, $P(O)Ph_2^o$), 119.8 (s, Ar *C*H), 21.0 (s, *C*H_3).

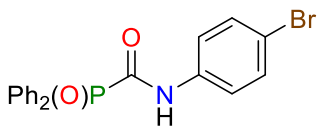
^{31}P{^{1}H} NMR (162 MHz, $CDCl_3$, 25 °C) δ 15.6.

HRMS (ESI) expected: 336.1148, found 336.1147 $[M+H]^+$ (err [ppm] = 0.4).

IR (ATR) v/cm^{-1} = 3174 (N–H), 1637 (C=O), 1167 (P=O).

Spectroscopic data matched previous reported literature.[124]

2.6.5.3 $Ph_2P(O)C(O)NH(4\text{-}BrC_6H_4)$ (**44c**)



White solid: 66.0 mg, 55% (62% NMR yield).

^{1}H NMR (400 MHz, $CDCl_3$, 25 °C) δ 9.53 (s, 1H, N*H*), 7.99-7.90 (m, 4H, $P(O)Ph_2^o$), 7.65-7.56 (m, 4H, $P(O)Ph_2^m$), 7.55-7.49 (m, 4H, $P(O)Ph_2^p$ + Ar C*H*), 7.48-7.42 (m, 2H, Ar C*H*).

^{13}C{^{1}H} NMR (101 MHz, $CDCl_3$, 25 °C) δ 168.4 (d, ^1J(C,P) = 122.2 Hz, *C*O), 135.9 (d, ^3J(C,P) = 9.6 Hz, $C_6H_4Br^i$), 133.1 (d, ^4J(C,P) = 2.9 Hz, $P(O)Ph_2^p$), 132.3 (s, Ar *C*H), 131.9 (d, ^3J(C,P) = 9.8 Hz, $P(O)Ph_2^m$), 129.0 (d, ^2J(C,P) = 12.4 Hz, $P(O)Ph_2^o$), 128.7 (d, ^1J(C,P) = 100.9 Hz, $P(O)Ph_2^i$), 121.6 (s, Ar *C*H), 118.5 (s, Ar *C*H).

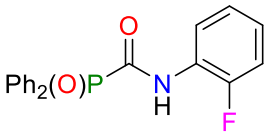
^{31}P{^{1}H} NMR (162 MHz, $CDCl_3$, 25 °C) δ 15.8.

HRMS (ESI) expected: 400.0097, found 400.0098 $[M+H]^+$ (err [ppm] = 0.3).

IR (ATR) v/cm^{-1} = 3204 (N–H), 1634 (C=O), 1168 (P=O).

Spectroscopic data matched previous reported literature.[122]

2.6.5.4 $Ph_2P(O)C(O)NH(2\text{-}FC_6H_4)$ (**44d**)



White solid: 62.1 mg, 61% (75% NMR yield). Single crystals suitable for X-ray diffraction were grown from a 2:1 THF:ethanol solution at –30 °C.

^{1}H NMR (400 MHz, $CDCl_3$, 25 °C) δ 9.59 (s, 1H, N*H*), 8.49-8.31 (m, 1H, Ar C*H*), 8.07-7.92 (m, 4H, P(O)Ph_2^o), 7.67-7.60 (m, 2H, P(O)Ph_2^p), 7.58-7.50 (m, 4H, P(O)Ph_2^m), 7.19-7.12 (m, 3H, Ar C*H*).

^{13}C{^{1}H} NMR (101 MHz, $CDCl_3$, 25 °C) δ 168.5 (d, ^1J(C,P) = 122.3 Hz, *C*O), 152.6 (d, ^1J(C,F) = 246.9 Hz, Ar *C*H), 133.0 (d, ^4J = 2.9 Hz, P(O)Ph_2^p), 131.8 (d, ^3J(C,P), P(O)Ph_2^m) = 9.7 Hz), 128.9 (d, ^2J(C,P) = 12.4 Hz, P(O)Ph_2^o), 128.6 (d, ^1J(C,P) = 101.1 Hz, P(O)Ph_2^i),126.1 (d, J = 7.5 Hz, Ar *C*H), 124.6 (d, ^3J(C,F) = 3.8 Hz, Ar *C*H), 121.6 (s, Ar *C*H), 115.4 (d, ^2J(C,F) = 18.9 Hz, Ar *C*H).

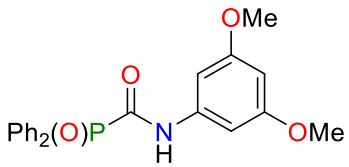
^{19}F{^{1}H} NMR (376 MHz, $CDCl_3$, 25 °C) δ −128.53.

^{31}P{^{1}H} NMR (162 MHz, $CDCl_3$, 25 °C) δ 15.8.

HRMS (ESI) expected: 340.0897, found 340.0903 $[M+H]^+$ (err [ppm] = 1.60).

IR (ATR) v/cm^{-1} = 3149 (N–H), 1666 (C=O), 1165 (P=O).

2.6.5.5 $Ph_2P(O)C(O)NH(3,5\text{-}(OMe)_2C_6H_3)$ (**44e**)



White solid: 72.1 mg, 63% (74% NMR yield). Single crystals suitable for X-ray diffraction were grown from a THF solution at –30 °C.

^{1}H NMR (400 MHz, $CDCl_3$, 25 °C) δ 9.37 (s, 1H, N*H*), 8.04-7.88 (m, 4H, P(O)Ph_2^o), 7.63-7.55 (m, 2H, P(O)Ph_2^p), 7.55-7.46 (m, 4H, P(O)Ph_2^m), 6.92 (d,

^{4}J(H,H) = 2.1 Hz, 2H, $C_6H_3^{o}$), 6.29 (t, ^{4}J(H,H) = 2.2 Hz, 1H, $C_6H_3^{p}$), 3.76 (s, 6H, OCH_3).

^{13}C{^{1}H} NMR (101 MHz, $CDCl_3$, 25 °C) δ 168.0 (d, ^{1}J(C,P) = 122.5 Hz, *C*O), 161.1 ($C_6H_3^{m}$), 138.3 (d, ^{3}J(C,P) = 9.6 Hz, $C_6H_3^{i}$), 132.9 (d, ^{4}J(C,P) = 2.9 Hz, P(O)Ph_2^{p}), 131.8 (d, ^{3}J(C,P) = 9.9 Hz, P(O)Ph_2^{m}), 128.8 (d, ^{2}J(C,P) = 12.4 Hz, P(O)Ph_2^{o}), 128.6 (d, ^{1}J(C,P) = 100.7 Hz, P(O)Ph_2^{i}) 98.4 (s, $C_6H_3^{p}$), 98.0 (s, $C_6H_3^{o}$), 55.46 (s, O*C*H_3).

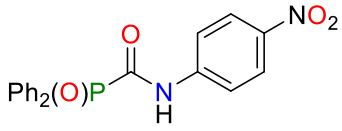
^{31}P{^{1}H} NMR (162 MHz, $CDCl_3$, 25 °C) δ 15.9.

HRMS (ESI) expected: 382.1203, found 382.1202 $[M+H]^+$ (err [ppm] = 0.2).

IR (ATR) v/cm^{-1} = 3188 (N–H), 1648 (C=O), 1174 (P=O).

Elemental analysis $C_{21}H_{20}NO_4P$: calcd. C 66.14, H 5.29, N 3.67; found: C 65.79, H 5.24, N 3.66 %.

2.6.5.6 $Ph_2P(O)C(O)NH(4\text{-}NO_2C_6H_4)$ (**44f**)



Selected *in situ* values. (49% NMR yield).

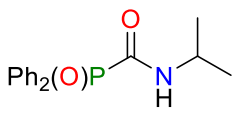
^{1}H NMR (400 MHz, $CDCl_3$, 25 °C) δ 9.78 (s, 1H, N*H*), 8.27 (d,^{3}J(H,H) = 9.2 Hz, 2H, Ar C*H*), 8.01-7.93 (m, 4H, P(O)Ph_2^{o}), 7.90 (d, ^{3}J(H,H) = 9.2 Hz, 2H, Ar C*H*), 7.69-7.62 (m, 2H, P(O)Ph_2^{p}), 7.60-7.53 (m, 4H, P(O)Ph_2^{m}).

^{13}C{^{1}H} NMR (101 MHz, $CDCl_3$, 25 °C) δ 169.5 (d, ^{1}J(C,P) = 121.9 Hz, *C*O).

^{31}P{^{1}H} NMR (162 MHz, $CDCl_3$, 25 °C) δ 16.3.

HRMS (ESI) expected: 389.0662, found 389.0662 $[M+Na]^+$ (err [ppm] = 0.1).

2.6.5.7 $Ph_2P(O)C(O)NH(^{i}Pr)$ (**44g**)



Colourless crystalline solid: 57.8 mg, 67% (84% NMR yield).

^{1}H NMR (400 MHz, $CDCl_3$, 25 °C) δ 7.94-7.85 (m, 4H, P(O)Ph_2^o), 7.61-7.53 (m, 2H, P(O)Ph_2^p), 7.52-7.44 (m, 5H, P(O)Ph_2^m + N*H*), 4.32-4.08 (m, 1H, C*H*$(CH_3)_2$), 1.22 (d, ^{3}J(H,H) = 6.6 Hz, 6H, CH(C*H*$_3)_2$).

^{13}C{^{1}H} NMR (101 MHz, $CDCl_3$, 25 °C) δ 168.8 (d, ^{1}J(C,P) = 120.8 Hz, *C*O), 132.7 (d, ^{4}J(C,P) = 2.8 Hz, P(O)Ph_2^p), 131.8 (d, ^{3}J(C,P) = 9.7 Hz, P(O)Ph_2^m), 129.5 (d, ^{1}J(C,P) = 99.7 Hz, P(O)Ph_2^i), 128.8 (d, ^{2}J(C,P) = 12.2 Hz, P(O)Ph_2^o), 42.3 (d, ^{3}J(C,P) = 5.0 Hz, *C*H$(CH_3)_2$), 22.6 (s, CH(*C*H$_3)_2$).

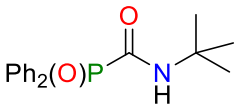
^{31}P{^{1}H} NMR (162 MHz, $CDCl_3$, 25 °C) δ 14.9.

HRMS (ESI) expected: 310.0967, found 310.0972 $[M+Na]^+$ (err [ppm] = 1.4).

IR (ATR) v/cm^{-1} = 3194 (N–H), 1641 (C=O), 1171 (P=O).

Spectroscopic data matched previous reported literature.[122]

2.6.5.8 $Ph_2P(O)C(O)NH(^tBu)$ (**44h**)



Colourless crystalline solid: 43.4 mg, 48% (61% NMR yield).

^{1}H NMR (400 MHz, $CDCl_3$, 25 °C) δ 7.92-7.84 (m, 4H, P(O)Ph_2^o), 7.60-7.53 (m, 2H, P(O)Ph_2^p), 7.48 (m, 4H, P(O)Ph_2^m), 7.41 (s, 1H, N*H*), 1.42 (s, 9H, C(C*H*$_3)_3$).

^{13}C{^{1}H} NMR (101 MHz, $CDCl_3$, 25 °C) δ 168.8 (d, ^{1}J(C,P) = 119.6 Hz, *C*O), 132.5 (d, ^{4}J(C,P) = 2.9 Hz, P(O)Ph_2^p), 131.7 (d, ^{3}J(C,P) = 9.5 Hz, P(O)Ph_2^m), 129.5 (d, ^{1}J(C,P) = 98.7 Hz, P(O)Ph_2^i), 128.7 (d, ^{2}J(C,P) = 12.2 Hz, P(O)Ph_2^o), 53.4 (d, ^{3}J(C,P) = 6.9 Hz, *C*$(CH_3)_3$), 28.6 (s, C(*C*H$_3)_3$).

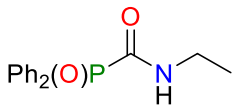
^{31}P{^{1}H} NMR (162 MHz, $CDCl_3$, 25 °C) δ 14.5.

HRMS (ESI) expected: 302.1304, found 302.1307 $[M+H]^+$ (err [ppm] = 0.8).

IR (ATR) v/cm^{-1} = 3203 (N-H), 1643 (C=O), 1171 (P=O).

Spectroscopic data matched previous reported literature.[122]

2.6.5.9 2.4.4.9 – $Ph_2P(O)C(O)NH(Et)$ (**44i**)



Colourless crystalline solid: 58.2 mg, 71% (84% NMR yield). Single crystals suitable for X-ray diffraction were grown from an ethanol solution at -30 °C.

^{1}H NMR (400 MHz, $CDCl_3$, 25 °C) δ 8.00-7.85 (m, 4H, $P(O)Ph_2^o$), 7.72 (s, 1H, N*H*), 7.61-7.52 (m, 2H, $P(O)Ph_2^p$), 7.52-7.44 (m, 4H, $P(O)Ph_2^m$), 3.43 (m , 2H, CH_2), 1.21 (t, ^3J(H,H) = 7.4Hz, 3H, CH_3).

^{13}C{^{1}H} NMR (101 MHz, $CDCl_3$, 25 °C) δ 169.4 (d, ^1J(C,P) = 121.1 Hz, *C*O), 132.6 (d, ^4J(C,P) = 2.9 Hz, $P(O)Ph_2^p$), 131.7 (d, ^3J(C,P) = 9.7 Hz, $P(O)Ph_2^m$), 129.3 (d,^1J(C,P) = 99.8 Hz, $P(O)Ph_2^i$), 128.7 (d, ^2J(C,P) = 12.2 Hz, $P(O)Ph_2^o$), 34.6 (d, ^3J(C,P) = 5.2 Hz, *C*H_2), 14.5 (s, *C*H_3).

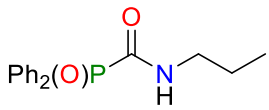
^{31}P{^{1}H} NMR (162 MHz, $CDCl_3$, 25 °C) δ 14.9.

HRMS (ESI) expected: 274.0991, found 274.0993 $[M+H]^+$ (err [ppm] = 0.5).

IR (**ATR)** v/cm^{-1} = 3211 (N–H), 1684 (C=O), 1176 (P=O).

Elemental analysis $C_{15}H_{16}NO_2P$: calcd. C 65.93, H 5.90, N 5.13; found: C 65.65, H 5.84, N 5.14 %.

2.6.5.10 $Ph_2P(O)C(O)NH(^nPr)$ (**44j**)



Colourless crystalline solid: 62.9 mg, 73% (86% NMR yield). Single crystals suitable for X-ray diffraction were grown from an ethanol solution at –30 °C.

^{1}H NMR (400 MHz, $CDCl_3$, 25 °C) δ 7.96-7.86 (m, 4H, $P(O)Ph_2^o$), 7.71 (s, 1H, N*H*) 7.61-7.53 (m, 2H, $P(O)Ph_2^p$), 7.52-7.43 (m, 4H, $P(O)Ph_2^m$), 3.35 (q, ^3J(H,H) = 6.7 Hz, 2H, CH_2CH$_3$), 1.59 (m, 2H, CH_2CH$_2$), 0.93 (t, ^3J(H,H) = 7.4 Hz, 3H, CH$_2$CH_3).

^{13}C{^{1}H} NMR (101 MHz, $CDCl_3$, 25 °C) δ 169.6 (^1J(C,P) = 121.3 Hz, *C*O), 132.6 (d, ^4J(C,P) = 2.9 Hz, $P(O)Ph^p$), 131.7 (d, ^3J(C,P) = 9.8 Hz, $P(O)Ph_2^m$), 129.4 (d,

^{1}J(C,P) = 99.9 Hz, P(O)Ph^{i}), 128.7 (d, ^{2}J(C,P) = 12.3 Hz, P(O)Ph^{o}), 41.3 (d, ^{3}J(C,P) = 5.2 Hz, *C*H_2CH$_2$), 22.6 (s, CH$_2$*C*H$_2$), 11.3 (s, *C*H$_3$).

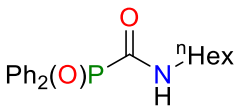
^{31}P{^{1}H} NMR (162 MHz, $CDCl_3$, 25 °C) δ 15.1.

HRMS (ESI) expected: 310.0967, found 310.0967 $[M+Na]^+$ (err [ppm] = 0.3).

IR (ATR) ν/cm^{-1} = 3244 (N–H), 1639 (C=O), 1169 (P=O).

Elemental analysis $C_{16}H_{18}NO_2P$: calcd. C 66.89, H 6.32, N 4.88; found: C 66.71, H 6.35, N 4.90 %.

2.6.5.11 Ph$_2$P(O)C(O)NH(^{n}Hex) (**44k**)



Colourless crystalline solid: 64.2 mg, 65% (82% NMR yield).

^{1}H NMR (400 MHz, $CDCl_3$, 25 °C) δ 7.97-7.85 (m, 4H, P(O)Ph$_2^{o}$), 7.71 (s, 1H, N*H*), 7.61-7.53 (m, 2H, P(O)Ph$_2^{p}$), 7.52-7.42 (m, 4H, P(O)Ph$_2^{m}$), 3.37 (q, ^{3}J*(H,H)* = 6.4 Hz, 2H, C*H*$_2$CH$_2$(CH$_2$)$_3$CH$_3$), 1.62-1.50 (m, 2H, CH$_2$C*H*$_2$CH$_2$(CH$_2$)$_3$CH$_3$), 1.37-1.19 (m, 6H, C*H*$_2$CH$_2$(C*H*$_2$)$_3$CH$_3$), 0.86 (q, *J* = 7.3 Hz, 3H, C*H*$_2$CH$_2$(CH$_2$)$_4$C*H*$_3$).

^{13}C{^{1}H} NMR (101 MHz, $CDCl_3$, 25 °C) δ 169.3 (d, ^{1}J(C,P) = 121.0 Hz, *C*O), 132.6 (d, ^{4}J(C,P) = 2.8 Hz, P(O)Ph$_2^{p}$), 131.7 (d, ^{3}J(C,P) = 9.5 Hz, P(O)Ph$_2^{m}$), 129.3 (d, ^{1}J(C,P) = 99.8 Hz, P(O)Ph$_2^{i}$), 128.7 (d, ^{2}J(C,P) = 12.2 Hz, P(O)Ph$_2^{o}$), 39.7 (d, ^{3}J(C,P) = 5.2 Hz, N*C*H$_2$-), 31.3 (^{n}Hex *C*H), 29.23 (^{n}Hex *C*H), 26.47 (^{n}Hex *C*H), 22.49 (^{n}Hex *C*H), 13.97 (s, (CH$_2$)*C*H$_3$).

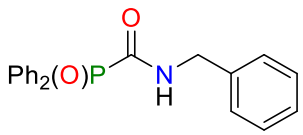
^{31}P{^{1}H} NMR (162 MHz, $CDCl_3$, 25 °C) δ 15.2.

HRMS (ESI) Expected: 330.1617, found 330.1615 $[M+H]^+$ (err [ppm] = 0.6).

IR (ATR) ν/cm^{-1} = 3235 (N–H), 1643 (C=O), 1171 (P=O).

Elemental analysis $C_{19}H_{24}NO_2P$: calcd. C 69.28, H 7.34, N 4.25; found: C 69.20, H 7.44, N 4.39 %.

2.6.5.12 $Ph_2P(O)C(O)NH(CH_2)Ph$ (**44l**)



White solid: 56.3 mg, 56% (69% NMR yield).

^{1}H NMR (400 MHz, $CDCl_3$, 25 °C) δ 8.38 (t, 1H, ^3J(H,H) = 6.1 Hz, N*H*), 7.98-7.85 (m, 4H, P(O)Ph_2^o), 7.64-7.55 (m, 2H, P(O)Ph_2^p), 7.55-7.45 (m, 4H, P(O)Ph_2^m), 7.35-7.27 (m, 5H, Ph), 4.58 (d, 2H, ^3J(H,H) = 6.5 Hz, CH_2).

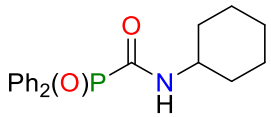
^{13}C{^{1}H} NMR (101 MHz, $CDCl_3$, 25 °C) δ 169.6 (d, ^1J(C,P) = 120.5 Hz, *C*O), 136.6 (Ar *C*H), 132.70 (d, ^4J(C,P) = 2.9 Hz), 131.7 (d, ^2J(C,P) = 9.8 Hz, P(O)Ph_2^o), 128.8 (d, ^3J(C,P) = 4.6 Hz, P(O)Ph_2^m), 128.7 (Ar *C*H), 128.6 (d, ^{1}J(C,P) = 100.7 Hz, P(O)Ph_2^i), 128.1 (s, Ar *C*H), 127.9 (s, Ar *C*H), 43.7 (d, ^3J(C,P) = 5.5 Hz, *C*H_2).

^{31}P{^{1}H} NMR (162 MHz, $CDCl_3$, 25 °C) δ 15.3. HRMS (ESI) Expected: 358.0967, found 358.0975 $[M+Na]^+$ (err [ppm] = 2.1).

IR (ATR) ν/cm^{-1} = 3179 (N–H), 1647 (C=O), 1158 (P=O).

Elemental analysis $C_{20}H_{18}NO_2P$: calcd. C 71.63, H 5.41, N 4.18; found: C 71.73, H 5.38, N 4.46 %.

2.6.5.13 $Ph_2P(O)C(O)NH(Cy)$ (**44m**)



White powder**:** 80.5 mg, 82% (91% NMR yield).

^{1}H NMR (400 MHz, $CDCl_3$, 25 °C) δ 7.95-7.86 (m, 4H, P(O)Ph_2^o), 7.60-7.53 (m, 2H, P(O)Ph_2^p), 7.53-7.44 (m, 5H, P(O)Ph_2^m + N*H*), 3.98-3.81 (m, 1H, N-C*H*), 1.99-1.87 (m, 2H, Cy), 1.80-1.68 (m, 2H, Cy), 1.67-1.56 (m, 1H, Cy), 1.44-1.11 (m, 5H, Cy).

^{13}C{^{1}H} NMR (101 MHz, $CDCl_3$, 25 °C) δ 168.7 (d, ^1J(C,P) = 120.7 Hz, *C*O), 132.7 (d, ^4J(C,P) = 2.8 Hz, P(O)Ph_2^p), 131.8 (d, ^{3}J(C,P) = 9.7 Hz, P(O)Ph_2^m) 129.6 (d, ^1J(C,P) = 99.6 Hz, P(O)Ph_2^i), 128.8 (d, ^{2}J(C,P) = 12.3 Hz, P(O)Ph_2^o) 49.2 (d, ^3J(C,P) = 5.0 Hz, Cy^i), 32.9 (s, Cy), 25.4 (s, Cy), 24.9 (s, Cy).

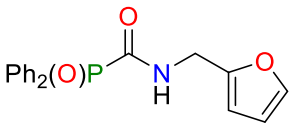
$^{31}P\{^{1}H\}$ NMR (162 MHz, $CDCl_3$, 25 °C) δ 15.1.

HRMS (ESI) expected: 328.1461, found 328.1459 $[M+H]^+$ (err [ppm] = 0.6).

IR (ATR) v/cm^{-1} = 3191 (N–H), 1642 (C=O), 1170 (P=O).

Spectroscopic data matched previous reported literature.[122]

2.6.5.14 $Ph_2P(O)C(O)NH(CH_2)(C_4H_3O)$ (**44n**)



White powder: 34.2 mg, 35% (51% NMR yield). Single crystals suitable for X-ray diffraction were grown from an ethanol solution at –30 °C.

^{1}H NMR (400 MHz, $CDCl_3$, 25 °C) δ 8.06-7.81 (m, 5H, $P(O)Ph_2^{o}$ + N*H*), 7.61-7.55 (m, 2H, $P(O)Ph_2^{p}$), 7.53-7.46 (m, 4H, $P(O)Ph_2^{m}$), 7.37-7.35 (m, 1H, CH=C*H*-O), 6.33-6.29 (m, 1H, CH-C*H*=CH), 6.27 – 6.23 (m, 1H, C=C*H*-CH), 4.55 (d, ^{3}J(H,H) = 5.7 Hz, 2H, CH_2).

$^{13}C\{^{1}H\}$ NMR (101 MHz, $CDCl_3$, 25 °C) δ 169.6 (d, ^{1}J(C,P) =120.1 Hz, *C*O), 149.7 (CH=*C*-O, 142.9 (CH=*C*H-O), 132.7 (d, ^{4}J(C,P) = 2.9 Hz, $P(O)Ph_2^{p}$), 131.7 (d, ^{3}J(C,P) = 9.6 Hz, $P(O)Ph_2^{m}$), 130.0 (d, ^{1}J(C,P) = 100.2 Hz, $P(O)Ph_2^{i}$), 128.7 (d, ^{2}J(C,P) = 12.3 Hz, $P(O)Ph_2^{o}$), 110.5 (s, C_4H_3O *C*H), 108.4 (s, C_4H_3O *C*H), 36.4 (d, ^{3}J(C,P) = 5.7 Hz, *C*H_2).

$^{31}P\{^{1}H\}$ NMR (162 MHz, $CDCl_3$, 25 °C) δ 15.5.

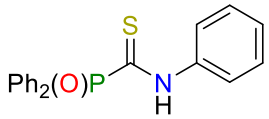
HRMS (ESI) expected: 348.0760, found 348.0755 $[M+Na]^+$ (err [ppm] = 1.5).

IR (ATR) v/cm^{-1} = 3158 (N–H), 1632 (C=O), 1178 (P=O).

Elemental analysis $C_{18}H_{16}NO_3P$: calcd. C 66.46, H 4.96, N 4.31; found: C 66.13, H 4.94, N 4.29 %.

2.6.6 Yields and characterisation data for **45a**–**45h**

2.6.6.1 $Ph_2P(O)C(S)NH(Ph)$ (**45a**)



Yellow crystalline solid**:** 91.0 mg, 90% (95% NMR yield).

^{1}H NMR (400 MHz, $CDCl_3$, 25 °C) δ 11.28 (s, 1H, N*H*), 8.13-8.06 (m, 2H, Ph, C*H*), 8.06-7.97 (m, 4H, $P(O)Ph_2^o$), 7.63-7.55 (m, 2H, $P(O)Ph_2^p$), 7.53-7.45 (m, 4H, $P(O)Ph_2^m$), 7.42 (t, ^3J(H,H) = 8.0 Hz, 2H, Ph C*H*), 7.29 (t, ^{3}J(H,H) = 7.3 Hz, 1H, Ph^p).

^{13}C{^{1}H} NMR (101 MHz, $CDCl_3$, 25 °C) δ 194.1 (d, ^1J(C,P) = 89.8 Hz, *C*S), 138.5 (d, ^2J(C,P) = 11.5 Hz, $P(O)Ph_2^o$), 133.0 (d, ^3J(C,P) = 9.5 Hz, $P(O)Ph_2^m$), 132.8 (d, ^4J(C,P) = 2.9 Hz, $P(O)Ph_2^p$), 129.2 (s, Ar *C*H), 129.1 (d, ^1J(C,P) = 104.7, $P(O)Ph_2^i$) 128.6 (d, ^3J(C,P) = 8.0 Hz, Ph^i), 127.5 (s, Ar *C*H), 121.8 (s, Ar *C*H).

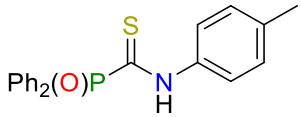
^{31}P{^{1}H} NMR (162 MHz, $CDCl_3$, 25 °C) δ 21.6.

HRMS (ESI) expected: 338.0763, found 338.0758 $[M+H]^+$ (err [ppm] = 1.4).

IR (ATR) v/cm^{-1} = 3076 (N–H), 1523 (C=S), 1178 (P=O).

Spectroscopic data matched previous reported literature.[122]

2.6.6.2 $Ph_2P(O)C(S)NH(4\text{-}MeC_6H_4)$ (**45b**)



Yellow crystalline solid**:** 100.1 mg, 95% (99% NMR yield).

^{1}H NMR (400 MHz, $CDCl_3$, 25 °C) δ 11.14 (d, ^3J(P,H) = 8.4 Hz, 1H, N*H*), 8.06-7.93 (m, 6H, $P(O)Ph_2^o$+ Ar C*H*), 7.63-7.56 (m, 2H, $P(O)Ph_2^p$), 7.53-7.45 (m, 4H, $P(O)Ph_2^m$), 7.22 (d, ^3J(H,H) = 8.3 Hz, 2H, Ar C*H*), 2.36 (s, 3H, CH_3).

^{13}C{^{1}H} NMR (101 MHz, $CDCl_3$, 25 °C) δ 193.2 (d, ^1J(C,P) = 90.2 Hz, *C*S), 137.7 (s, Ar *C*H), 136.1 (d, ^3J(C,P) = 11.5 Hz,$C_6H_4Me^i$), 133.0 (d, ^3J(C,P) = 9.4 Hz, $P(O)Ph_2^m$), 132.8 (d, ^4J(C,P) = 2.8 Hz, $P(O)Ph_2^p$), 129.0 (d, ^1J(C,P) = 106.1 Hz, $P(O)Ph_2^i$), 128.5 (d, ^2J(C,P) = 12.5 Hz, $P(O)Ph_2^o$), 121.7 (s, Ar *C*H), 21.4 (s, *C*H_3).

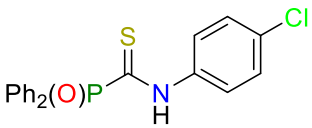
$^{31}P\{^{1}H\}$ NMR (162 MHz, $CDCl_3$, 25 °C) δ 21.5.

HRMS (ESI) expected: 374.0739, found 374.0739 $[M+Na]^+$ (err [ppm] = 0.1).

IR (ATR) ν/cm^{-1} = 3055 (N–H), 1508 (C=S), 1166 (P=O).

Spectroscopic data matched previous reported literature.[122]

2.6.6.3 $Ph_2P(O)C(S)NH(4\text{-}ClC_6H_4)$ (**45c**)



Yellow crystalline solid**:** 100.4 mg, 90% (94% NMR yield). Single crystals suitable for X-ray diffraction were grown from a 1:1 THF:ethanol solution at -30 °C.

^{1}H NMR (400 MHz, $CDCl_3$, 25 °C) δ 11.23 (d, ^{3}J(P,H) = 8.2 Hz, 1H, N*H*), 8.06 (d, ^{3}J(H,H) = 8.9 Hz, 2H, Ar C*H*), 8.03-7.96 (m, 4H, $P(O)Ph_2^{o}$), 7.63-7.57 (m, 2H, $P(O)Ph_2^{p}$), 7.52-7.47 (m, 4H, $P(O)Ph_2^{m}$), 7.38 (d, ^{3}J(H,H) = 8.9 Hz, 2H, Ar C*H*).

$^{13}C\{^{1}H\}$ NMR (101 MHz, $CDCl_3$, 25 °C) δ 194.7 (d, ^{1}J(C,P) = 89.5 Hz, *C*S), 137.0 (d, ^{3}J(C,P) = 11.6 Hz, $C_6H_4Cl^{i}$), 133.0 (d, ^{3}J(C,P) = 9.3 Hz, $P(O)Ph_2^{m}$), 132.9 (d, ^{4}J(C,P) = 2.3 Hz, $P(O)Ph_2^{p}$), 132.5, (s, Ar *C*H) 128.9 (d, ^{1}J(C,P) = 108.4 Hz, $P(O)Ph_2^{i}$), 129.3 (s, Ar *C*H), 128.6 (d, ^{2}J(C,P) = 12.7 Hz, $P(O)Ph_2^{o}$), 123.1 (s, Ar *C*H).

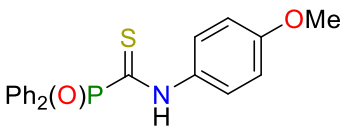
$^{31}P\{^{1}H\}$ NMR (162 MHz, $CDCl_3$, 25 °C) δ 21.7.

HRMS (ESI) expected: 394.0193, found 394.0191 $[M+Na]^+$ (err [ppm] = 0.5).

IR (ATR) ν/cm^{-1} = 3049 (N–H), 1509 (C=S), 1166 (P=O).

Elemental analysis $C_{19}H_{15}ClNOPS$: calcd. C 61.38, H 4.07, N 3.77; found: C 61.05, H 3.96, N 3.72 %.

2.6.6.4 $Ph_2P(O)C(S)NH(4\text{-}MeOC_6H_4)$ (**45d**)



Yellow crystalline solid**:** 101.4 mg, 92% (98% NMR yield). Single crystals suitable for X-ray diffraction were grown from a 4:1 THF:ethanol solution at –30 °C.

^{1}H NMR (400 MHz, $CDCl_3$, 25 °C) δ 11.14 (d, ^3J(P,H) = 8.7 Hz, 1H, N*H*), 8.11-7.92 (m, 6H, $P(O)Ph_2^o$ + Ar C*H*), 7.61-7.55 (m, 2H, $P(O)Ph_2^p$), 7.53-7.45 (m, 4H, $P(O)Ph_2^m$), 6.95-6.89 (m, 2H, Ar C*H*), 3.82 (s, 3H, OCH_3).

^{13}C{^{1}H} NMR (101 MHz, $CDCl_3$, 25 °C) δ 192.2 (d, ^1J(C,P) = 90.3 Hz, *C*S), 158.4 (s, $C_6H_4^p$), 132.9 (d, ^3J(C,P) = 9.4 Hz, $P(O)Ph_2^m$), 132.7 (d, ^4J(C,P) = 2.8 Hz, $P(O)Ph_2^p$), 131.8 (d, ^3J(C,P) = 11.9 Hz, $C_6H_4^i$), 129.1 (d, ^1J(C,P) = 108.1 Hz, $P(O)Ph_2^i$), 128.4 (d, ^2J(C,P) = 12.7 Hz, $P(O)Ph_2^o$), 123.3 (s, Ar *C*H), 114.0 (s, Ar *C*H), 55.5 (s, O*C*H$_3$).

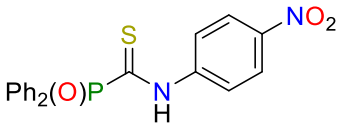
^{31}P{^{1}H} NMR (162 MHz, $CDCl_3$, 25 °C) δ 21.5.

HRMS (ESI) expected: 368.0869, found 368.0871 $[M+H]^+$ (err [ppm] = 0.7).

IR (ATR) v/cm^{-1} = 3062 (N–H), 1503 (C=S), 1165 (P=O).

Elemental analysis $C_{19}H_{15}N_2O_3PS$: calcd. C 65.38, H 4.94, N 3.81; found: C 65.11, H 4.89, N 3.82 %.

2.6.6.5 $Ph_2P(O)C(S)NH(4\text{-}NO_2C_6H_4)$ (**45e**)



Bright orange-red solid**:** 35.6 mg, 31% (50% NMR yield). Single crystals suitable for X-ray diffraction were grown from a 1:1 THF:ethanol solution at –30 °C.

^{1}H NMR (400 MHz, $CDCl_3$, 25 °C) δ 11.57 (d, ^3J(P,H) = 7.9 Hz, 1H, N*H*), 8.39-8.32 (m, 2H, Ar C*H*), 8.31-8.26 (m, 2H, Ar C*H*), 8.03-7.93 (m, 4H, $P(O)Ph_2^o$), 7.67-7.57 (m, 2H, $P(O)Ph_2^p$), 7.56-7.46 (m, 4H, $P(O)Ph_2^m$).

^{13}C{^{1}H} NMR (101 MHz, $CDCl_3$, 25 °C) δ 197.0 (d, ^1J(C,P) = 88.4 Hz, *C*S), 145.3 (s, $C_6H_4^p$), 143.3 (d, ^3J(C,P) = 11.9 Hz, $C_6H_4^i$), 133.0 (d, ^4J(C,P) = 2.8 Hz,

P(O)Ph_2^p), 132.8 (d, ^3J(C,P) = 9.6 Hz, P(O)Ph_2^m), 128.6 (d, ^2J(C,P) = 12.8 Hz, P(O)Ph_2^o), 128.5 (d, ^1J(C,P) = 108.9 Hz, P(O)Ph_2^i), 124.9 (s, Ar *C*H), 121.0 (s, Ar *C*H).

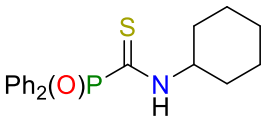
$^{31}P\{^1H\}$ NMR (162 MHz, $CDCl_3$, 25 °C) δ 22.4.

HRMS (ESI) expected: 405.0433, found 405.0432 $[M+Na]^+$ (err [ppm] = 0.3).

IR (ATR) v/cm^{-1} = 3056 (N–H), 1507 (C=S), 1170 (P=O).

Elemental analysis $C_{20}H_{18}NO_2PS$: calcd. C 59.68, H 3.95, N 7.33; found: C 59.53, H 3.91, N 7.18 %.

2.6.6.6 $Ph_2P(O)C(S)NH(Cy)$ (**45f**)



Yellow solid**:** 43.3 mg, 42% (57% NMR yield).

^1H NMR (400 MHz, $CDCl_3$, 25 °C) δ 9.44 (s, 1H, *N*H), 8.05-7.89 (m, 4H, P(O)Ph_2^o), 7.64-7.53 (m, 2H, P(O)Ph_2^p), 7.52-7.42 (m, 4H, P(O)Ph_2^m), 4.62-4.30 (m, 1H, Cy), 2.14-2.03 (m, 2H, Cy), 1.84-1.74 (m, 2H, Cy), 1.73-1.62 (m, 1H, Cy), 1.47-1.34 (m, 4H, Cy), 1.31-1.20 (m, 1H, Cy).

$^{13}C\{^1H\}$ NMR (101 MHz, $CDCl_3$, 25 °C) δ 195.3 (d, ^1J(C,P) = 87.3 Hz, *C*S), 132.9 (d, ^3J(C,P) = 9.5 Hz, P(O)Ph_2^m), 132.7 (d, ^4J(C,P) = 2.8 Hz, P(O)Ph_2^p), 129.5 (d, ^1J(C,P) = 107.5 Hz, P(O)Ph_2^i), 128.5 (d, ^2J(C,P) = 12.5 Hz, P(O)Ph_2^o), 54.1 (d, ^3J(C,P) = 5.3 Hz, Cy^i), 31.3 (s, Cy *C*H_2), 25.47 (s, Cy *C*H_2), 24.7 (s, Cy *C*H_2).

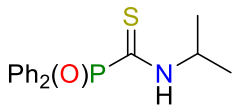
$^{31}P\{^1H\}$ NMR (162 MHz, $CDCl_3$, 25 °C) δ 20.7.

HRMS (ESI) expected: 344.1232, found 344.1232 $[M+H]^+$ (err [ppm] = 0.3).

IR (ATR) v/cm^{-1} = 3014 (N–H), 1515 (C=S), 1176 (P=O).

Spectroscopic data matched previous reported literature.[122]

2.6.6.7 $Ph_2P(O)C(S)NH(^iPr)$ (**45g**)



Yellow solid**:** 36.4 mg, 40% (65% NMR yield).

^{1}H NMR (400 MHz, $CDCl_3$, 25 °C) δ 9.47 (s, 1H, N*H*), 8.03-7.86 (m, 4H, P(O)Ph_2^o), 7.60-7.54 (m, 2H, P(O)Ph_2^p), 7.50-7.42 (m, 4H, P(O)Ph_2^m), 4.78-4.67 (m, 1H, C*H*$(CH_3)_2$), 1.33 (d, ^3J(H,H) = 6.6 Hz, 6H, CH(C$H_3)_2$).

^{13}C{^{1}H} NMR (101 MHz, $CDCl_3$, 25 °C) δ 195.3 (d, ^1J(C,P) = 87.6 Hz, *C*S), 132.7 (d, ^3J(C,P) = 9.5 Hz, P(O)Ph^m), 132.6 (d, ^4J(C,P) = 2.8 Hz, P(O)Ph_2^p), 129.3 (d, ^1J(C,P) = 107.6 Hz, P(O)Ph_2^i), 128.4 (d, ^2J(C,P) = 12.7 Hz, P(O)Ph_2^o), 47.2 (d, ^3J(C,P) = 5.5 Hz, *C*H$(CH_3)_2$), 21.0 (s, CH(*C*$H_3)_2$).

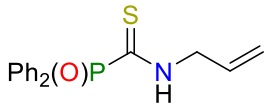
^{31}P{^{1}H} NMR (162 MHz, $CDCl_3$, 25 °C) δ 20.6.

HRMS (ESI) expected: 304.0919, found 304.0920 $[M+H]^+$ (err [ppm] = 0.2).

IR (ATR) v/cm^{-1} = 3124 (N-H), 1510 (C=S), 1168 (P=O).

Spectroscopic data matched previous reported literature.[122]

2.6.6.8 $Ph_2P(O)C(S)NH(CH_2CH{=}CH_2)$ (**45h**)



Yellow solid**:** 74.1 mg, 82% (95% NMR yield). Single crystals suitable for X-ray diffraction were grown from an ethanol solution at –30 °C.

^{1}H NMR (400 MHz, $CDCl_3$, 25 °C) δ 9.94 (s, 1H, N*H*), 8.08-7.82 (m, 4H, P(O)Ph_2^o), 7.61-7.53 (m, 2H, P(O)Ph_2^p), 7.52-7.43 (m, 4H, P(O)Ph_2^m), 5.99-5.85 (m, C*H*=CH_2, 1H), 5.34-5.15 (m, CH=CH_2, 2H), 4.38 (td, *J* = 5.8, 1.5 Hz, CH_2-CH, 2H).

^{13}C{^{1}H} NMR (101 MHz, $CDCl_3$, 25 °C) δ 197.2 (d, ^1J(C,P) = 87.9 Hz, *C*S), 132.8 (d, ^3J(C,P) = 9.6 Hz, P(O)Ph_2^m), 132.7 (s, CH=*C*H_2), 130.8 (s, *C*H=CH_2), 129.4 (d, ^1J(C,P) = 107.9 Hz, P(O)Ph_2^i), 128.5 (d, ^2J(C,P) = 12.5 Hz, P(O)Ph_2^o), 119.3 (s, CH=*C*H_2), 47.8 (d, ^3J(C,P) = 5.9 Hz, *C*H_2-CH).

$^{31}P\{^{1}H\}$ NMR (162 MHz, $CDCl_3$, 25 °C) δ 21.0.

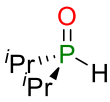
HRMS (ESI) expected: 324.0582, found 324.0583 $[M+Na]^+$ (err [ppm] = 0.1).

IR (ATR) ν/cm^{-1} = 3137 (N–H), 1512 (C=S), 1178 (P=O).

Elemental analysis $C_{16}H_{16}NOPS$: calcd. C 63.77, H 5.35, N 4.65; found: C 63.63, H 5.33, N 4.61 %.

2.6.7 Yields and characterisation data for $HP(O)(^{i}Pr)_2$ and **46a**–**46c**

2.6.7.1 $HP(O)(^{i}Pr)_2$



Synthesised by a modified literature procedure.[148] Under an argon atmosphere, chlorodiisopropylphosphine (5.0 mL, 31.4 mmol) was dissolved in dried degassed CH_2Cl_2 (25 mL). The solution was cooled to 0 °C and H_2O (0.65 mL, 34.5 mmol) was added dropwise over 1 hour. The resulting mixture was stirred at room temperature overnight. In air, $NaHCO_3$ (2.65g, 31.4 mmol) was added and stirred vigorously for 5 minutes, $MgSO_4$ was then added to dry the solution. The solution was then filtered, and the solvent was removed in Vacuo, to yield diisopropylphosphine oxide as a yellow oil (3.22g, 76%).

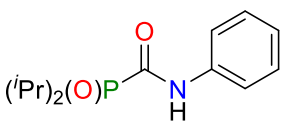
^{1}H NMR (400 MHz, C_6D_6, 25 °C) δ 6.34 (d, ^{1}J(P,H) = 467 Hz, P*H*), 1.84-1.68 (m, 2H C*H*$(CH_3)_2$), 1.04-0.89 (m, 12H, CH(C*H*$_3)_2$).

$^{13}C\{^{1}H\}$ NMR (101 MHz, $CDCl_3$, 25 °C) 24.1 (d, ^{1}J(C,P) = 61.7 Hz, *C*H$(CH_3)_2$), 15.9 (s, CH(*C*$H_3)_2$), 14.8 (d, ^{2}J(C,P) = 3.6 Hz, CH(*C*$H_3)_2$.

$^{31}P\{^{1}H\}$ NMR (162 MHz, $CDCl_3$, 25 °C) δ 55.9.

Spectroscopic data matched previous reported literature.[149]

2.6.7.2 $(^{i}Pr)_2P(O)C(O)NH(Ph)$ (**46a**)



White solid: 65.2 mg, 41% (59% NMR yield).

^{1}H NMR (400 MHz, $CDCl_3$, 25 °C) δ 9.06 (s, 1H, N*H*), 7.67-7.64 (m, 2H, Ph^{o}), 7.39-7.34 (m, 2H, Ph^{m}), 7.20-7.16 (m, 1H, Ph^{p}), 2.35 (m, 2H, C*H*$(CH_3)_2$), 1.28 (m, 12H, CH(C*H*$_3)_2$).

^{13}C{^{1}H} NMR (101 MHz, $CDCl_3$, 25 °C) δ 168.9 (d, ^{1}J(C,P) = 101.1 Hz, *C*O), 136.7 (d, ^{3}J(C,P) = 8.1 Hz, Ph^{i}), 129.31 (s, Ar *C*H), 125.6 (s, Ar *C*H), 119.0 (s, Ar *C*H), 24.7 (d, ^{1}J(C,P) = 61.1 Hz, *C*H$(CH_3)_2$), 16.2 (d, ^{2}J(C,P) = 2.7 Hz, CH(*C*H$_3)_2$), 15.0 (d, ^{2}J(C,P) = 2.8 Hz, CH(*C*H$_3)_2$).

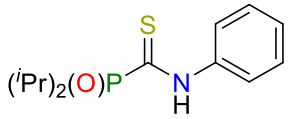
^{31}P{^{1}H} NMR (162 MHz, $CDCl_3$, 25 °C) δ 51.4.

HRMS (ESI) expected: 276.1135, found 276.1126 $[M+Na]^+$ (err [ppm] = 3.3).

IR (ATR) v/cm^{-1} = 3159 (N–H), 1642 (C=O), 1145 (P=O).

Elemental analysis $C_{13}H_{20}NO_2P$: calcd. C 61.65, H 7.96, N 5.53; found: C 61.11, H 8.05, N 5.29 %.

2.6.7.3 (^{i}Pr)$_2$P(O)C(S)NH(Ph) (**46b**)



Yellow solid: 161 mg, 95% (99% NMR yield).

^{1}H NMR (400 MHz, $CDCl_3$, 25 °C) δ 10.82 (s, 1H, N*H*), 8.06-8.02 (m, 2H, Ph^{o}), 7.45-7.41 (m, 2H, Ph^{m}), 7.32-7.28 (m, 1H, Ph^{p}), 2.63-2.53 (m, 2H, C*H*$(CH_3)_2$), 1.33-1.23 (m, 12H, CH(C*H*$_3)_2$).

^{13}C{^{1}H} NMR (101 MHz, $CDCl_3$, 25 °C) δ 195.5 (d, ^{1}J(C,P) = 70.0 Hz, *C*S), 138.3 (d, ^{3}J(C,P) = 9.7 Hz, Ph^{i}), 129.2 (s, Ar *C*H), 127.5 (s, Ar *C*H), 121.9 (s, Ar *C*H), 25.6 (d, ^{1}J(C,P) = 65.9 Hz, *C*H$(CH_3)_2$), 16.5 (d, ^{2}J(C,P) = 3.6 Hz, CH(*C*H$_3)_2$), 15.3 (d, ^{2}J(C,P) = 2.6 Hz, CH(*C*H$_3)_2$).

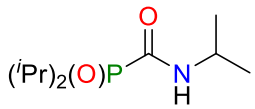
^{31}P{^{1}H} NMR (162 MHz, $CDCl_3$, 25 °C) δ 55.3.

HRMS (ESI) expected: 292.0895, found 292.0897 $[M+Na]^+$ (err [ppm] = 0.50).

IR (ATR) v/cm^{-1} = 3087 (N–H), 1593 (C=S), 1144 (P=O).

Elemental analysis $C_{13}H_{20}NOPS$: calcd. C 57.97, H 7.48, N 5.20; found: C 58.07, H 7.69, N 5.14 %.

2.6.7.4 (^{i}Pr)$_2$P(O)C(S)NH(^{i}Pr) (**46c**)



Colourless crystals: 83.3 mg, 61% (80% NMR yield).

^{1}H NMR (400 MHz, $CDCl_3$, 25 °C) δ 7.20 (s, 1H, NH), 4.25-4.16 (m, 1H, N-C*H*(CH_3)), 2.31-2.21 (m, 2H, P-(C*H*(CH_3)$_2$)$_2$), 1.27-1.16 (m, 18H, N-CH(C*H*$_3$)$_2$ + P(CH(C*H*$_3$)$_2$)$_2$).

^{13}C{^{1}H} NMR (101 MHz, $CDCl_3$, 25 °C) δ 169.3 (d, ^{1}J(C,P) = 100.8 Hz, CO), 41.8 (d, ^{3}J(C,P) = 4.2 Hz, N-*C*H(CH_3)$_2$), 24.5 (d, ^{1}J(C,P) = 61.2 Hz, P(*C*H(CH_3)$_2$)$_2$), 22.7 (s, NCH(*C*H$_3$)$_2$), 16.1 (d, ^{2}J(C,P) = 2.7 Hz, PCH(*C*H$_3$)$_2$), 15.0 (d, ^{2}J(C,P) = 2.8 Hz, PCH(*C*H$_3$)$_2$).

^{31}P{^{1}H} NMR (162 MHz, $CDCl_3$, 25 °C) δ 50.1.

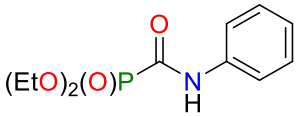
HRMS (ESI) expected: 276.1124, found 276.1116 $[M+Na]^+$ (err [ppm] = 3.00).

IR (ATR) ν/cm^{-1} = 3193 (N–H), 1633 (C=O), 1145 (P=O).

2.6.8 Crude yields and characterisation data for **47a**–**47c**

Due to the aforementioned difficulties with the isolation **47a–47c** could not be isolated pure, however crude product could be isolated in differing purities, the initial NMR yields and the final ratios of product to HP(O)(R_2) impurity are given below.

2.6.8.1 (EtO)$_2$P(O)C(O)NH(Ph) (**47a**)



Yellow oil: 122.3 mg, 61% (**47a**: HP(O)(OEt)$_2$, 1.00 : 0.11) (87% NMR yield).

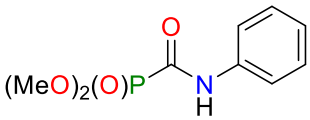
^{1}H NMR (400 MHz, $CDCl_3$, 25 °C) δ 9.41 (s, 1H, N*H*), 7.70-7.67 (m, 2H, Ph^{o}), 7.35-7.30 (m, 2H, Ph^{m}), 7.17-7.12 (m, 1H, Ph^{p}), 4.32-4.21 (m, 4H, C*H*$_2$CH$_3$), 1.39-1.33 (m, 6H, CH$_2$C*H*$_3$).

$^{13}C\{^{1}H\}$ NMR (101 MHz, $CDCl_3$, 25 °C) δ 164.2 (d, ^{1}J(C,P) = 226.7 Hz, *C*O), 136.8 (d, ^{3}J(C,P) = 13.3 Hz, Ph^{i}), 129.0 (s, Ar *C*H), 125.5 (s, Ar *C*H), 120.3 (s, Ar *C*H), 64.7 (d, ^{2}J(C,P) = 6.8 Hz, *C*$H_2$$CH_3$), 16.3 d, ^{3}J(C,P) = 5.8 Hz, CH_2*C*H_3).

$^{31}P\{^{1}H\}$ NMR (162 MHz, $CDCl_3$, 25 °C) δ –1.9.

Spectroscopic data matched previous reported literature.[150]

2.6.8.2 (MeO)$_2$P(O)C(O)NH(Ph) (**47b**)



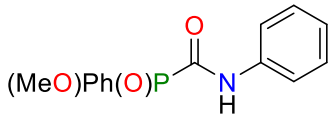
Colourless crystals: 55.8mg, 22% (**4b**: HP(O)(OMe)$_2$, 1.00:0.02) (48% NMR yield).

^{1}H NMR (400 MHz, $CDCl_3$, 25 °C) δ 9.06 (s, 1H, N*H*), 7.65 (d, ^{3}J(H,H) = 8.02 Hz, 2H, Ph^{o}), 7.36 (t, ^{3}J(H,H) = 7.75 Hz, 2H, Ph^{m}), 7.19 (t, ^{3}J(H,H) = 7.42 Hz 1H, Ph^{p}), 3.93 (d, ^{3}J(P,H) = 10.98 Hz, 2H, CH_3).

$^{13}C\{^{1}H\}$ NMR (101 MHz, $CDCl_3$, 25 °C) δ 163.4 (d, ^{1}J(C,P) = 227.5 Hz, *C*O), 136.6 (d, ^{3}J(C,P) = 13.2 Hz, Ph^{i}), 129.3 (s, Ar *C*H), 125.9 (s, Ar *C*H), 120.3 (s, Ar *C*H), 54.9 (d, ^{2}J(C,P) = 6.6 Hz, *C*H_3).

$^{31}P\{^{1}H\}$ NMR (162 MHz, $CDCl_3$, 25 °C) δ -0.5.

2.6.8.3 (MeO)PhP(O)C(O)NH(Ph) (**47c**)



Off-white powder: 1.02g, 41% (**47b**:HP(O)(Ph)(OMe), 1.00:0.03) (62% NMR yield).

^{1}H NMR (400 MHz, $CDCl_3$, 25 °C) δ 9.16 (s, 1H, N*H*), 8.03-7.98 (m, 2H, Ar), 7.66-7.64 (m, 3H, Ar), 7.55-7.50 (m, 2H, Ar), 7.36-7.32 (m, 2H, Ar), 7.19-7.15 (m, 1H, Ar).

$^{13}C\{^{1}H\}$ NMR (101 MHz, $CDCl_3$, 25 °C) δ 165.8 (d, ^{1}J(C,P) = 160.1 Hz), 136.5 (d,^{3}J(C,P) = 10.0 Hz, Ph^{i}), 133.8 (d,^{4}J(C,P) = 2.9 Hz, Ph^{p}), 132.6 (d,^{3}J(C,P) =

10.4 Hz, P(O)(OMe)Ph^{m}), 129.2 (Ph *C*H), 128.8 (d,^{2}J(C,P) = 13.5 Hz, P(O)(OMe)Ph^{o}), 125.9 (d,^{1}J(C,P) = 137.7 Hz, P(O)(OMe)Ph^{i}), 125.7 (s, Ph *C*H), 119.8 (s, Ph *C*H).

^{31}P{^{1}H} NMR (162 MHz, $CDCl_3$, 25 °C) δ 20.1.

HRMS (ESI) expected: 298.0604, found 298.0598 $[M+Na]^+$ (err [ppm] = 1.80).

IR (ATR) v/cm^{-1} = 3176 (N–H), 1653 (C=O), 1251 (P=O).

2.6.9 Mechanistic Experiments

2.6.9.1 Hydrophosphinylation of isocyanates in the presence of cumene

In an inert atmosphere glovebox, an oven dried Young's tap modified NMR tube was charged with *p*-Tolyl isocyanate (1.2 eq., 15.1 µL, 0.12 mmol), diphenylphosphine oxide (1.0 eq., 20.2 mg, 0.10 mmol), 2-MeTHF (4.0 eq., 40.3 µL, 0.40 mmol), and cumene (4.0 eq., 0.40 mmol). The sealed tube was sonicated at 25 °C for 3 hours. Trimethoxybenzene (1.0 eq., 16.8 mg, 0.10 mmol) was added and the reaction mixture was diluted with $CDCl_3$ (0.5 mL) and shaken vigorously. ^{1}H NMR spectra were recorded to evaluate the yield in solution (integrating relative to the trimethoxybenzene internal standard). NMR yield = 77%.

2.6.9.2 Hydrophosphinylation of isocyanates in the presence of 1,4-cyclohexadiene

In an inert atmosphere glovebox an oven dried Young's tap modified NMR tube was charged with *p*-Tolyl isocyanate (1.2 eq., 15.1 µL, 0.12 mmol), diphenylphosphine oxide (1.0 eq., 20.2 mg, 0.10 mmol), 2-MeTHF (4.0 eq., 40.3 µL, 0.40 mmol), and cyclohexadiene (4.0 eq., 0.40 mmol). The sealed tube was sonicated at 25 °C for 3 hours. Trimethoxybenzene (1.0 eq., 16.8 mg, 0.10

mmol) was added and the reaction mixture was diluted with $CDCl_3$ (0.5 mL) and shaken vigorously. ^1H NMR spectra were recorded to evaluate the NMR yield (integrating relative to the trimethoxybenzene internal standard). NMR yield = 82%.

2.6.9.3 Detection of CO_2 from hydrophosphinylation of *p*-TolN=C=O

In an inert atmosphere glovebox an oven dried Young's tap modified NMR tube was charged with either diphenylphosphine oxide (1.0 eq., 20.2 mg, 0.10 mmol) and *p*-Tolyl isocyanate (1.2 eq., 0.12 mmol, 15.1 µL); or just *p*-Tolyl isocyanate (0.12 mmol, 15.1 µL). In the tube containing both diphenylphosphine oxide and *p*-Tolyl isocyanate, effervescence was observed immediately. No such effervescence was observed for *p*-Tolyl isocyanate alone. Both reactions were sonicated for 2 hours at room temperature. Each Young's tap modified NMR tube was opened briefly, diluted with C_6D_6 (0.5 mL) and immediately resealed. A $^{13}C\{^1H\}$ NMR spectrum was recorded with 2048 scans and a delay of 1s, for each sample on a Bruker AV(III)400HD spectrometer equipped with a cryoprobe. A small singlet for CO_2 was observed (124.8 ppm)[147] for the reaction between diphenylphosphine oxide and *p*-Tolyl isocyanate No signal for CO_2 was observed for the control reaction containing only *p*-Tolyl isocyanate.

2.6.10 Summary of spectroscopic data

Table 21. Selected spectroscopic data for **44a**–**44n**, **45a**–**45h**, **46a**–**46c** and **47a**–**47c**

	NMR conv. (%)	δ_P (ppm	δ_C (C=X) (ppm)	^1J(C,P) (Hz)	δ_H (N*H*) (ppm)	ν_{NH} (cm^{-1})	ν_{CX} (cm^{-1})	ν_{PO} (cm^{-1})
44a	80	15.5	168.1	123.4	9.74	3172	1641	1169
44b	82	15.6	167.6	122.8	9.25	3174	1637	1167
44c	62	15.8	168.4	122.2	9.53	3204	1634	1168
44d	75	15.8	168.5	122.3	9.59	3149	1666	1165
44e	74	15.9	168.0	122.5	9.37	3188	1648	1177
44f	49	16.3	169.5	121.9	9.78	-[a]	-[a]	-[a]
44g	84	14.9	168.8	120.8	-[b]	3194	1641	1171
44h	61	14.5	168.8	119.6	7.41	3203	1643	1172
44i	84	14.9	169.4	121.1	7.75	3211	1684	1176
44j	86	15.1	169.6	121.3	7.71	3244	1639	1169
44k	82	15.2	169.3	121.0	7.71	3235	1643	1171
44l	91	15.1	168.7	120.7	-[b]	3191	1642	1170
44m	69	15.3	169.6	120.5	8.38	3179	1647	1158
44n	51	15.5	169.6	120.1	7.95	3158	1632	1178
45a	95	21.6	193.1	89.8	11.28	3076	1523	1178
45b	99	21.5	193.2	90.2	11.14	3055	1508	1166
45c	94	21.7	194.7	89.5	11.23	3049	1509	1166
45d	98	21.5	192.2	90.3	11.14	3062	1503	1165
45e	50	22.4	197.0	88.4	11.60	3056	1507	1165
45f	57	20.7	195.3	87.3	9.44	3104	1515	1176
45g	65	20.6	195.3	87.6	9.47	3124	1510	1168
45h	95	21.0	197.2	87.9	9.94	3137	1512	1178
46a	59	51.4	168.9	101.1	9.06	3159	1642	1145
46b	99	55.3	195.5	70.0	10.82	3087	1593	1144
46c	80	50.1	169.3	61.2	7.20	3193	1633	1145
47a	87	-1.9	164.2	226.7	9.41	-[a]	-[a]	-[a]
47b	48	-0.5	163.4	227.5	9.06	-[a]	-[a]	-[a]
47c	62	20.1	165.8	160.1	9.16	3176	1653	1251

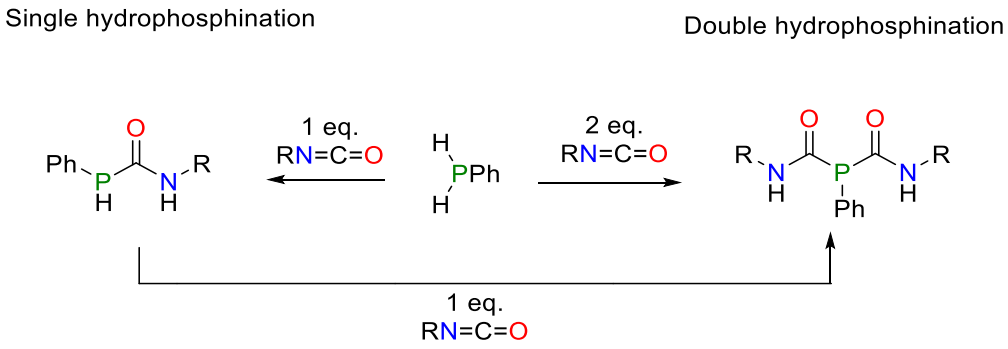
[a] IR values could not be reliably determined from the impure sample.[b] NH ^{1}H NMR peak overlaps with aromatic signals of P-bound phenyl groups.

Chapter 3:

Hydrophosphination and Diinsertion-cyclisation of Isocyanates

3.1 Introduction

The addition of secondary phosphine (R_2PH) across an unsaturated substrate can only undergo a single hydrophosphination, as there is only one available P–H bond for reaction. However, the addition of primary phosphines (RPH_2), which contain two P–H bonds that can be activated presents a greater chemoselective challenge as either one (single hydrophosphination) or two bonds (double hydrophosphination) can undergo reaction (**Scheme 38**).

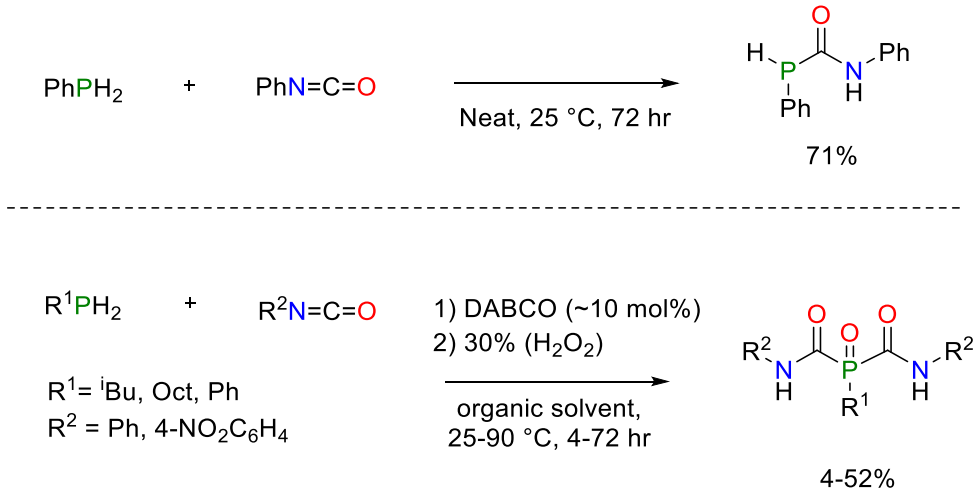


***Scheme 38**. (Left) single hydrophosphination of isocyanates; reacting with one P–H bond, (right) double hydrophosphination of isocyanates; reacting with two P–H bonds and (bottom) sequential addition of 2 eq. of isocyanate to form the double hydrophosphination product overall.*

Additionally, with further challenges due to primary phosphines being highly pyrophoric, having very unpleasant odours and lack of synthetic routes, these compounds are significantly underutilised when compared to similar counterparts such as primary amines; even with very common substrates such as alkenes and alkynes.

Examples of hydrophosphination reactions with isocyanates utilising primary phosphines are few. Recent work by Nakazawa *et al.* describes that even very small amounts of solvent hamper the catalyst-free reaction between $PhPH_2$ and PhN=C=O; resulting in a 71% yield after 72 hours (**Scheme 39**, above).[111] Additionally, these reactions only form the single hydrophosphination product

even when treated with two equivalents of isocyanates (**Scheme 39,** above).[111] A patent from 1962 by Buckler and Epstein describes the use of 10 mol% of triethylenediamine (DABCO) as a precatalyst at elevated temperatures for the hydrophosphination of aryl isocyanates (PhN=C=O and 4-NO_2N=C=O) in low to moderate yields (**Scheme 39**, below).[151] Additionally, significant amounts of aryl urea side product form and subsequently the desired phosphine products can only be separated by oxidative work-up with stoichiometric H_2O_2. The literature on this area appears contradictory with some patents describing catalyst-free approaches in solution with subsequent oxidation to yield the double hydrophosphination products as oxides, thus again the double hydrophosphination products cannot be obtained.

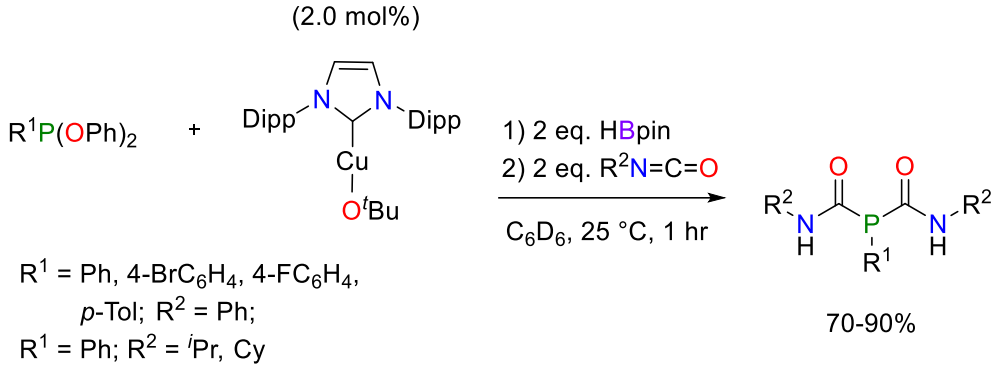


Scheme 39. *(Above) Neat catalyst-free single hydrophosphination of PhN=C=O with $PhPH_2$ by Nakazawa et al. and (below) DABCO catalysed hydrophosphination of isocyanates.*[111,151]

As discussed previously in Chapters 1.7 and 2 regarding catalyst-free approaches, in theory a catalyst-free approach can be superior to catalytic methodologies (given similar conditions and yields), however, the catalyst-free methodology needs to be robust enough that it can be easily reproducible, otherwise the catalytic methodology is the more appropriate choice. Given the lack of demonstrated isocyanate scope and long reaction times for catalyst-free

hydrophosphination using primary phosphines, there is ample room for the development of catalytic approaches.

In 2022 Liptrot *et al.* reported a methodology for the catalytic hydrophosphination of isocyanates using aryl-substituted primary phosphines (**Scheme 40**).[152] The primary phosphines are generated *in situ* by the reduction of phosphonites by HBpin utilising a NHC-Cu(I)-based precatalyst. Subsequently, in one-pot reactions, RN=C=O (R = Ph, Cy, ^{i}Pr) undergoes double hydrophosphination in high yields.



***Scheme 40**. 1) Reduction of phosphinites using HBpin to primary aryl phosphines and 2) In situ hydrophosphination of isocyanates by primary phosphines by Liptrot et al.*[152]

However, alkyl primary phosphines such as ^{i}PrPH$_2$ and CyPH$_2$ could be used to yield the double hydrophosphination product as the major product but gave inconsistent results and additionally other phosphorus containing species with longer reaction times. Other limitations include no reactivity with the bulkier ^{t}BuN=C=O substrate, even after 24 hours.[152]

It is also worth noting that Liptrot *et al.* performed a catalyst-free control reaction with a 1:2 neat mixture of PhPH$_2$ and PhN=C=O at 25 °C for 16 hours in a manner analogous to Nakazawa *et al.* and only reported a 3% conversion by ^{31}P NMR spectroscopy to the double hydrophosphination product.[111,152]

3.2 Aims

The aim of this work is to investigate the hydrophosphination of alkyl and aryl isocyanates utilising primary phosphines. In comparison to highly established secondary phosphines, primary phosphines will have more chemoselective challenges and are likely to be accompanied by an additional need for forcing conditions to obtain high yields, exacerbating the chemoselective challenges. Depending on these factors, a catalyst-free or catalytic methodology will be initially tested utilising previously established precatalyst **40** with either neat or low-added solvent conditions.

This work also aims to utilise a less pyrophoric and less malodourous but still reactive source of primary phosphine, ferrocenylphosphine ($FcPH_2$) as the main reagent; in place of more pyrophoric and malodourous phenylphosphine. Additionally other more challenging primary phosphines such as adamantyl phosphine will be investigated.

Through these investigations, an aim was to probe conditions that could allow for chemoselectivity between single hydrophosphination or double hydrophosphination by changing the reaction solvent and reaction stoichiometry.

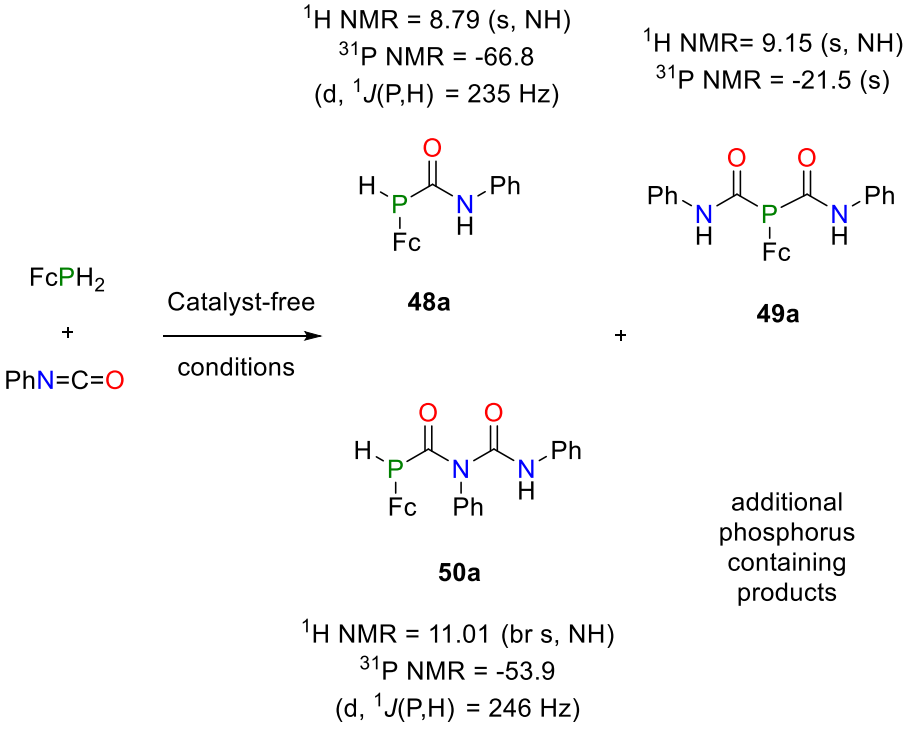
The investigation of a novel double-diinsertion reaction by increasing isocyanate concentration and neat reactions will also be performed. Additionally, Stoichiometric reactions and poisoning experiments to probe a mechanism for catalysis, if a viable methodology can be made with precatalyst **40**.

3.3 Results and Discussion

3.3.1 Hydrophosphination of isocyanates with ferrocenylphosphine

3.3.1.1 Initial catalyst-free hydrophosphination of PhN=C=O.

Initial catalyst-free attempts in solution and low (~0.83M) and high (~6.9M) concentrations, yielded low (≤1%) amounts of the desired single hydrophosphination product, – 66.8 ppm (d, ^{1}J(P,H) = 235 Hz) (**48a**) double hydrophosphination product, 21.5 (s) ppm (**49a**) and single hydrophosphination diinsertion product **50a** – 54.0 ppm (d, ^{1}J(P,H) = 246 Hz) (**Scheme 41**) (**Table 22**, entries 1-4). There is additional conversion of the $FcPH_2$ starting material to products related to dehydrocoupling and other non-N-H containing phosphorus species which are discussed in further detail in section **3.3.3**.



Scheme 41. *General reaction of catalyst-free hydrophosphination of PhN=C=O by $FcPH_2$, yielding a mixture of the single hydrophosphination product* ***48a****, double hydrophosphination product* ***49a****, the single hydrophosphination-diinsertion product* ***50a*** *and other phosphorus containing products.*

Performing the reaction under neat conditions at 25 °C resulted in a higher conversion of $FcPH_2$ (21%) but entries 1-4 afforded little to none of the desired hydrophosphination products **48a**-**50a** (**Table 22**, entry 5). Increasing the temperature of the solvent-free reaction to 60 °C resulted in a large increase of conversion to 80% with conversions of 11% to **48a**, 45% to **49a** and <1% to **50a**. (**Table 22**, entry 6).

Table 22. Catalyst-free hydrophosphination of phenyl isocyanate with ferrocenylphosphine.[a,b,c,d]

Entry	$FcPH_2$: PhN=C=O	Solvent	Conv. (%)	Yield **48a** (%)	Yield **49a** (%)	Yield **50a** (%)
1	1:2	2-MeTHF	7	1	1	1
2	1:2	2-MeTHF[c]	10	0	0	0
3	1:2	C_6D_6	6	0	<0.1	0
4	1:2	C_6D_6[c]	14	0	1	0
5	1:2	Neat	20	0	<0.1	0
6[d]	1:2	Neat	80	11	45	<1
7[d]	1:4	Neat	94	4	25	43
8[d]	1:8	Neat	80	1	20	30

[a] Reaction conditions: 1.0 eq. = 0.138 mmol, and solvent volume = 0.5 mL under a nitrogen atmosphere at 25 °C unless otherwise stated. [b] Conversion determined by ^{31}P NMR spectroscopy using the relative ratios of ^{31}P containing products. [c] ca. 4 eq. of solvent used. ***48a*** *= single hydrophosphination product and* ***49b*** *= double hydrophosphination product.[d] Performed at 60 °C.*

In an effort to further optimise the neat reaction, the equivalents of PhN=C=O used were increased from 2 to 4 which increased the conversion to 94%, but with a large switch in hydrophosphination product selectivity; with conversions of **48a** decreasing to 4%, of **49a** decreasing to 25% but **50a** increasing to 43% (**Table 22**, entry 7). Further increasing the isocyanate concentration to 8 equivalents gave a lower conversion of 80% but with similar relative distributions of **48a**, **49a** and **50a** at 1%, 20% and 30% respectively. (**Table 22**, entry 8).

An increased scale ($FcPH_2$; 1.0 eq = 0.889 mmol) reaction (**Table 22**, entry 7) was performed with the aim of separating either **48a** or **49a** from the eight other phosphorus containing impurities (see **Figure 14** for a ^{31}P NMR spectrum of entry 7). Attempts at isolation of either products by successive rounds of column chromatography or recrystallisations were unsuccessful in separating the products.

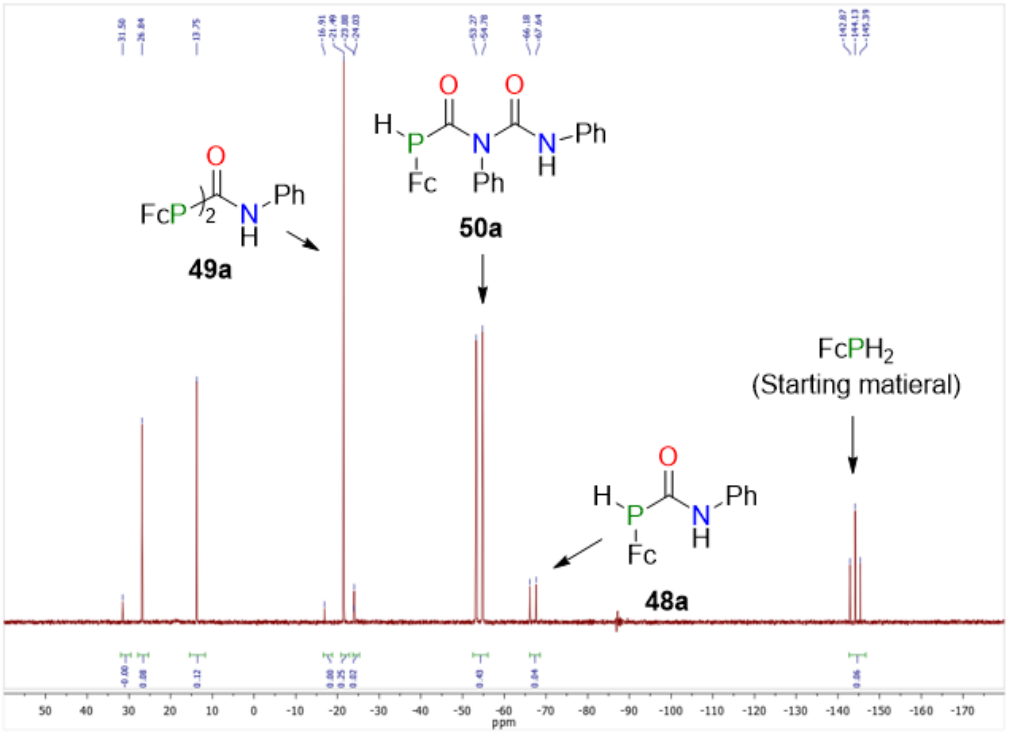


Figure 14. *Proton coupled ^{31}P NMR spectrum of the catalyst-free neat hydrophosphination of PhN=C=O with $FcPH_2$ (**Table 16**, entry 7).*

3.3.1.2 Initial catalytic hydrophosphination of PhN=C=O with $FcPH_2$

Given the lack of chemoselectivity for **48a**, **49a** or **50a** by catalyst-free reactions in section **3.3.1.1**, the iron precatalyst **40** was employed to try and improve selectivity and additionally conversions. Initially, an NMR scale reaction was performed between $FcPH_2$ and PhN=C=O in a 1:2 ratio with 5 mol% catalyst loading. $FcPH_2$ (31.8 mg, 0.146 mmol) in C_6D_6 (0.25 mL) and PhN=C=O (31.7µL, 0.292 mmol) were added to a Young's NMR tube followed by **40** (5.0

mg, 7.32 µmol) in C_6D_6 (0.25 mL) and inverted 5 times. After 16 hours the reaction reached quantitative conversion with the disappearance of the $FcPH_2$ starting material peak at –145.6 ppm, accompanied by a colour change from light orange to dark orange.

The ^{31}P NMR spectrum of the reaction mixture showed three new peaks, the highest intensity peak is at –22.2 ppm with a conversion of 89% which can be assigned to the double hydrophosphination product, **49a** (**Table 23**, entry 1). Additionally, there is another minor product at 25.0 (s) ppm which can be assigned to a rare diinsertion-cyclisation product **52a** (which is further discussed in Section 3.3.3). The assignment of the double hydrophosphination product is also accompanied by the expected appearance of a resonance at 9.06 ppm in the ^{1}H NMR spectrum, which has been assigned to an N-H. Additionally there is a 3rd smaller unknown peak (3% conversion) at 31.2 ppm, which cannot easily be assigned to any hydrophosphination type product.

Table 23. Catalytic hydrophosphination of ferrocenylphopshine by phenyl isocyanate[a,b]

Entry	$FcPH_2$: PhN=C=O eq.	Temp. (°C)	Cat. mol%	Conv. (%)	Yield **49a** (%)	Yield **52a** (%)
1	1.0 : 2.0	25	5.0	99	89	6
2	1.0 : 2.0	60	5.0	99	88	7
3	1.0 : 2.0	25	1.0	73	56	2
4	1.0 : 3.0	25	5.0	99	72	15
5	1.0 : 3.0	60	5.0	99	82	8

[a] Reaction conditions: 1.0 eq. = 0.136 mmol and solvent volume = 0.5 mL under a nitrogen atmosphere unless otherwise stated. [b] Conversion determined by ^{31}P NMR spectroscopy using an internal standard (addition 1.0 eq. of PPh_3 in 0.15 mL C_6D_6 after 16 hours).

In an attempt to further increase selectivity for the formation of **49a**, a range of conditions were tested (**Table 23**). Heating at 60 °C had little effect on conversion to compound **49a** and a slight increase in the amount of **52a** obtained (**Table 23,** entry 2). Additionally, lowering catalyst loading to 1.0 mol% significantly decreased conversions overall and the amount of the double hydrophosphination product **49a** to 56% (**Table 23**, entry 3). Increasing the number of equivalents of isocyanate to 3 at either 25 °C or 60 °C decreased the conversion of the double hydrophosphination product to 72% and 82%, respectively and increased the diinsertion-cyclisation product conversions to 15% and 8%, respectively. Thus, the conditions described in **Table 23**, entry 1 were found to be optimal for conversion to the double hydrophosphination product (see **Figure 15**, for ^{31}P NMR spectrum).

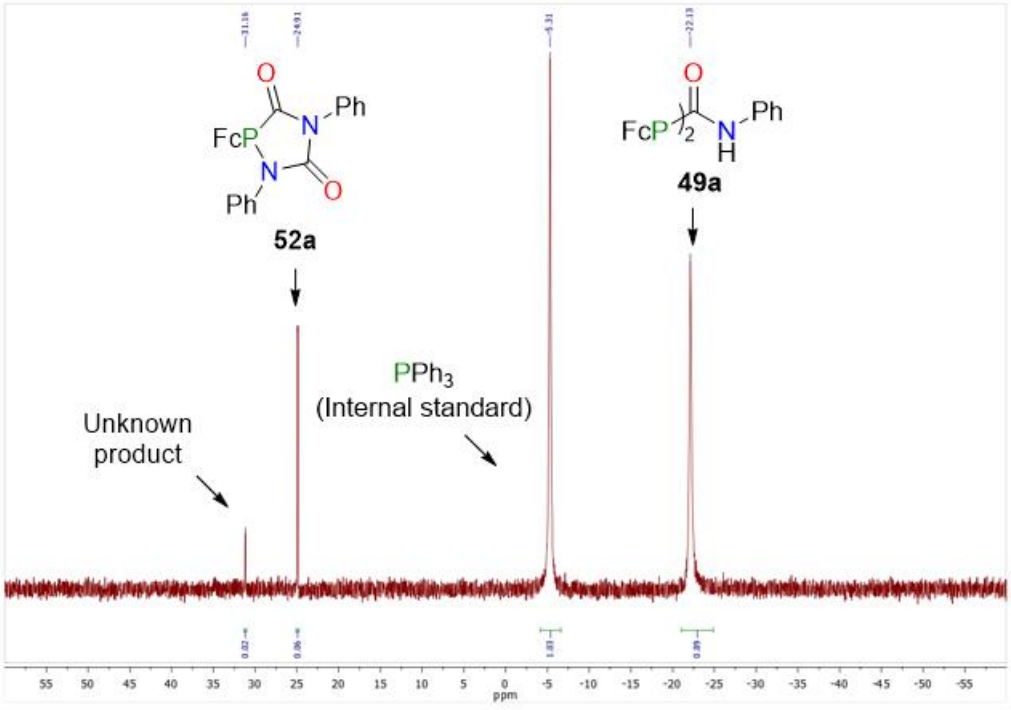
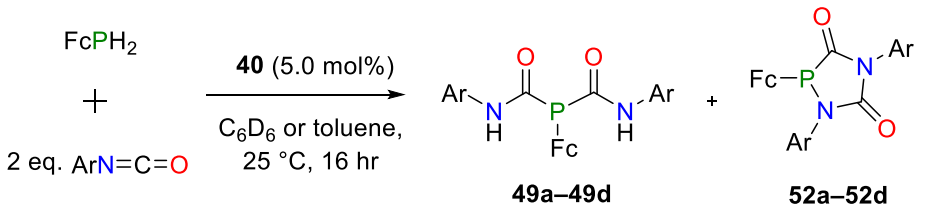


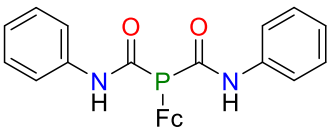
Figure 15. *Catalytic hydrophosphination of phenyl isocyanate with $FcPH_2$, utilising conditions*

3.3.1.3 Catalytic double hydrophosphination of aryl isocyanates

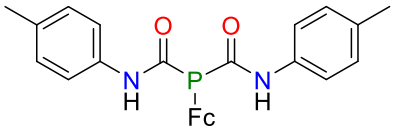
A range of functionalised aryl isocyanates were also tested, utilising the conditions described in **Table 23**, entry 1, with the reaction found to tolerate both electron donating and electron withdrawing substituents (C_6H_4; 4-Me, 3-Cl, 4-OMe) (**Table 24**).

Table 24. Double hydrophosphination of aryl isocyanates utilising $FcPH_2$[a,b,c,d]

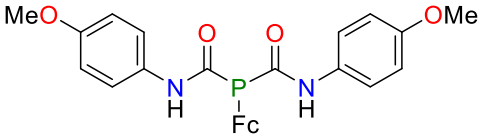




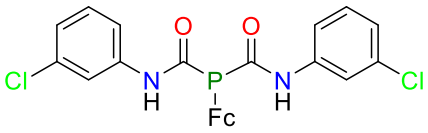
49a: 25 °C, 16 hr, 60% (**49a**:**52a,** 87:4)



49b: 25 °C, 16 hr, 66% (**49b**:**52b**, 84:7)



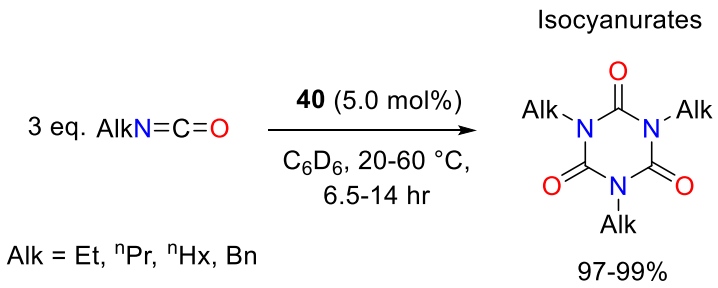
49c: 25 °C, 16 hr, 63% (**49c**:**52c**, 84:11)



49d: 25 °C, 16 hr, 56% (**49d**:**52d**, 73:11)

*[a] Reaction conditions for conversions: 1.0 eq. $FcPH_2$ = 0.136 mmol, and C_6D_6 (0.5 mL) under a nitrogen atmosphere unless otherwise stated.[b] Reaction conditions for isolated yields: 1.0 eq. $FcPH_2$ = 0.936 mmol and toluene (4.0 mL).[c] Conversion determined by ^{31}P NMR spectroscopy using an internal standard (addition 1.0 eq. of PPh_3 in 0.15 mL C_6D_6 after 16 hours).[d] ratios given in brackets are NMR conversions of (**49** and **52**) respectively.*

As determined by ^{31}P NMR spectroscopy, all reached high conversions to the double hydrophosphination products, in the range of 84-87% for Ph, 4-MeC_6H_4, 4-OMeC_6H_4, with a slightly lower conversion for the 3-ClC_6H_4-substituted isocyanate (73%) due to the formation of a larger amount of cyclotrimerised isocyanurate forming as a side product, reducing the amount of isocyanate available for hydrophosphination. This could be seen as a surprising result as in previous work by Kays *et al.* precatalyst **40** has been shown to be an efficient catalyst for the selective cyclotrimerisation of primary alkyl isocyanates with no conversion for aromatic isocyanates even with heating to 60 °C for 48 hours (**Scheme 42**).



Scheme 42. *Previous work by Kays et al. utilising precatalyst* ***40*** *for the selective cyclotrimerisation of primary alkyl isocyanates, to yield isocyanurates.*[118]

For the isolation of the double hydrophosphination products, **49a**-**49d,** scaled up reactions were performed (1.0 eq. $FcPH_2$ = 0.936 mmol, substituting C_6D_6 for toluene). Initially, the products were purified by washing with hexane in order to remove organic soluble phosphorus containing impurities, followed by recrystallisation from 1:1 toluene:hexane mixtures at –30 °C. However, in many cases a small amount (typically ~5% yield) of isocyanurate impurity was precipitated or crystallised out of solution alongside the desired double hydrophosphination products.

In order to circumvent this issue, as the products are stable in air, column chromatography was performed on silica with 2% ethyl acetate:toluene mixture

as eluent, to afford the **49a**-**49d** in moderate isolated yields (56-66%) with no isocyanurate impurity present.

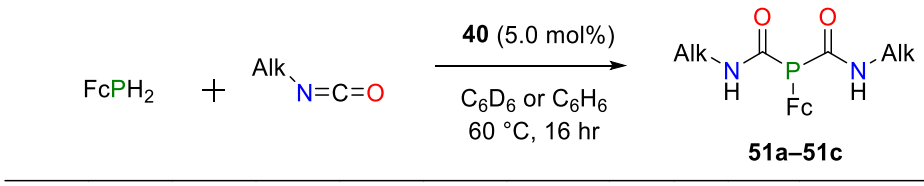
3.3.1.4 Catalytic double hydrophosphination of alkyl isocyanates

Due to precatalyst **40** demonstrating high reactivity towards aryl isocyanates, to further expand the scope alkyl isocyanates were also tested. Initially an NMR scale reaction between cyclohexyl isocyanate and $FcPH_2$ with 5.0 mol% of **40** at 25 °C, was performed, which, after 16 hours showed only a 68% conversion to the double hydrophosphination product **51a**. The $^{13}C\{^1H\}$ NMR spectra of this reaction indicated that there were no concomitant diinsertion-cyclisation or isocyanurate products formed (**Table 25**). Increasing the reaction temperature to 60 °C resulted in a large increase in conversion to product **51a** (97% as determined by ^{31}P NMR) with the other 3% due to $FcPH_2$ dehydrocoupling products (**Table 25**). Analogous reactions with ^{i}PrN=C=O and ^{t}BuN=C=O reached excellent conversions of 99% (**51b**) and 96% (**51c**) respectively, with the ^{t}BuN=C=O reaction requiring a slightly longer reaction time of 20 hours vs 16 hours for ^{i}PrN=C=O.

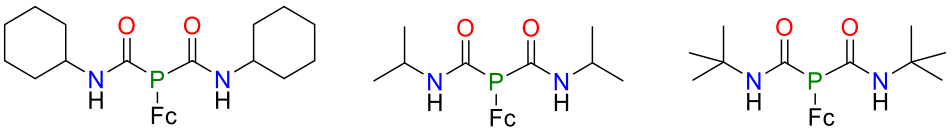
Given the lower yields of side products for reactions with alkyl isocyanates compared with their aryl analogues, the subsequent double hydrophosphination products **51a**-**51c** could be isolated without the use of column chromatography. The products are air-sensitive so anaerobic conditions were necessary, but washing with degassed water, extracting the products into toluene and subsequent recrystallisation from a 1:5 hexane:toluene mixture at –30 °C afforded the isolated products in moderate yields (64-73%). It should be noted a 5-10% reduction in isolated yield was observed for the scaled-up reactions when the reaction solvent was changed from benzene to toluene. This is possibly due to the lower boiling point of benzene versus toluene and the higher

pressure being needed in the Young's reaction flask for the reaction to reach completion.

Table 25. Double hydrophopshination of alkyl isocyanates utilising $FcPH_2$



51a–51c



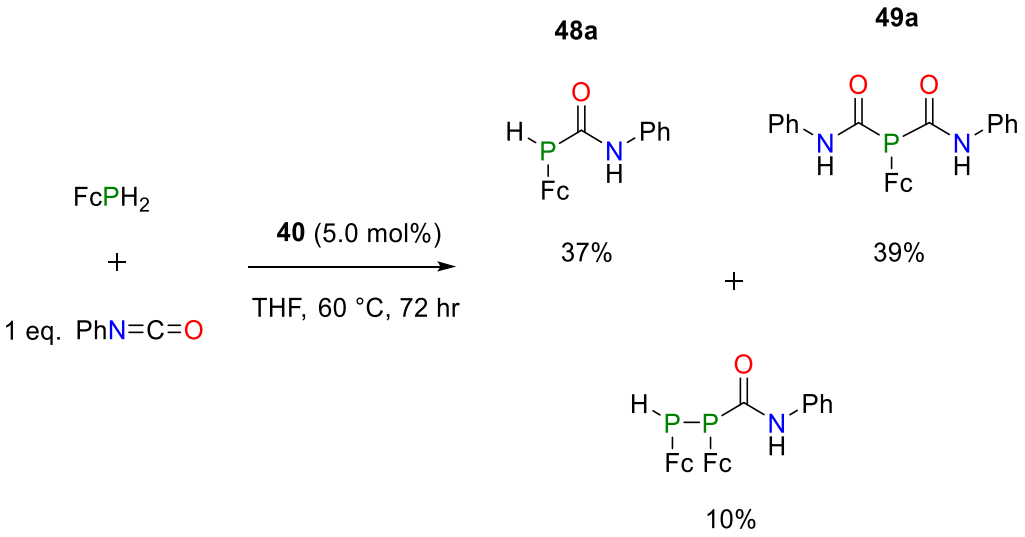
51a: 60 °C, 16 hr, 73% (97%) **51b**: 60°C, 16 hr, 63% (99%) **51c**: 60 °C, 20 hr, 65% (96%)

[a] Reaction conditions for conversions: 1.0 eq. $FcPH_2$ = 0.136 mmol, and C_6D_6 (0.5 mL) under a nitrogen atmosphere unless otherwise stated.[b] Reaction conditions for isolated yields: 1.0 eq. $FcPH_2$ = 0.936 mmol and benzene (4.0 mL).[c] Conversion determined by ^{31}P NMR spectroscopy using an internal standard (addition 1.0 eq. of PPh_3 in 0.15 mL C_6D_6 after 16 hours).

3.3.2 Solvent variation to THF

To probe the effect of solvent on the reaction, the solvent was changed from C_6D_6 or toluene to more polar THF. Again, the reaction (1:2 ratio of $FcPH_2$: PhN=C=O with 5.0 mol% **40**) was performed in a Youngs NMR tube but with a sealed C_6D_6 insert. The reaction took significantly longer to reach a high conversion compared to the reaction in C_6D_6, reaching 87% conversion of the double hydrophosphination product, **49a** after 3 days at 60 °C (*cf* 16 hours at 25 °C in C_6D_6). A similar observation is seen with the hydrophosphination of isocyanates utilising $HPPh_2$. When changing the solvent from C_6D_6 to THF the reaction time increases from 16 hours to 72 hours and requires a temperature increase from 25 to 60 °C.[115]

When performing the reaction in THF with a reduced stoichiometry of isocyanate (1:1 ratio of $FcPH_2$: PhN=C=O with 5.0 mol% **40**) at 60 °C for 3 days a 1:1.05 mixture of single hydrophosphination, **48a** and double hydrophosphination, **49a** is observed (37 and 39% conversion), suggesting that whilst THF presents the potential to coordinate to the metal centre, there remains sufficient space within the coordination sphere to allow the formation of the bulkier double hydrophosphination product. Additionally, there is a signal with an integration of *ca.* 10% (two doublets of doublets at –88.1 and -91.8 ppm) which can be assigned to products resulting from dehydrocoupling potentially of **48a** with residual unreacted $FcPH_2$ starting material (**Scheme 43**).

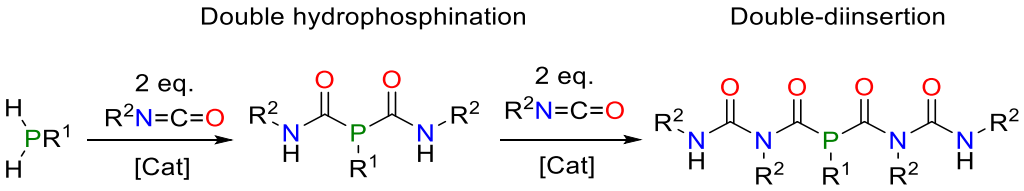


Scheme 43. *Hydrophosphination of phenyl isocyanate by $FcPH_2$ in THF forming a near 1:1 mixture of single and double hydrophosphination products,* ***48a*** *and* ***49a****.*

3.3.3 Diinsertion-cyclisation of aryl isocyanates with $FcPH_2$

3.3.3.1 Introduction

One of the original aims of this work was to further expand the diinsertion type compounds that precatalyst **40** was capable of synthesising.[115,117] One of the products being aimed for was a double-diinsertion product, whereby two equivalents of isocyanate insert into the P–H bonds to form the double hydrophosphination, with subsequent insertion of a further two isocyanate molecules, leading to four isocyanate molecules overall reacting with one primary phosphine molecule (**Scheme 44**).

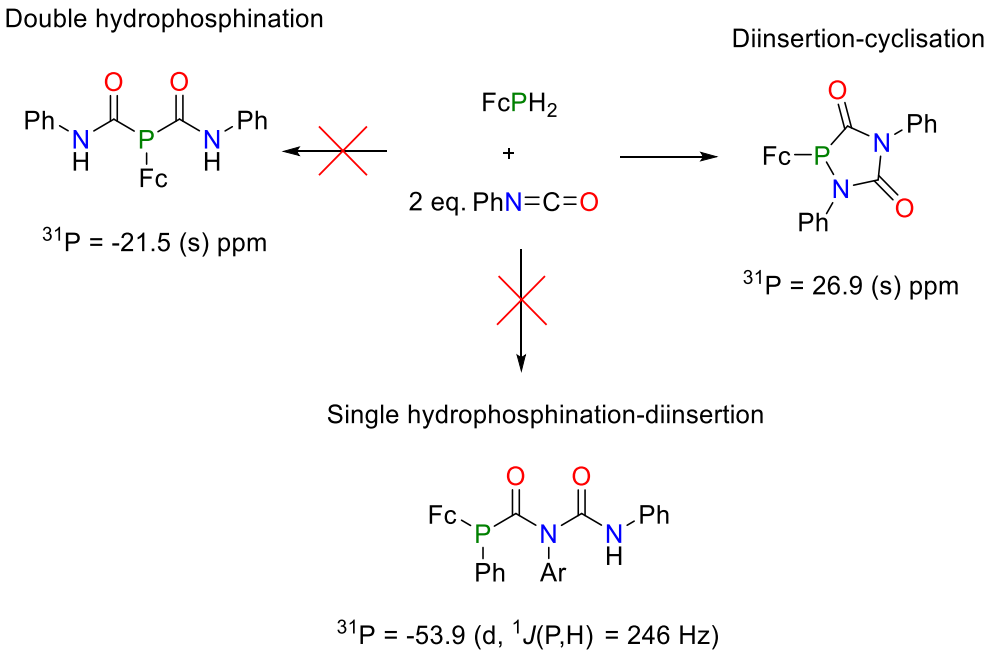


Scheme 44. *Proposed structure of target double-diinsertion product.*

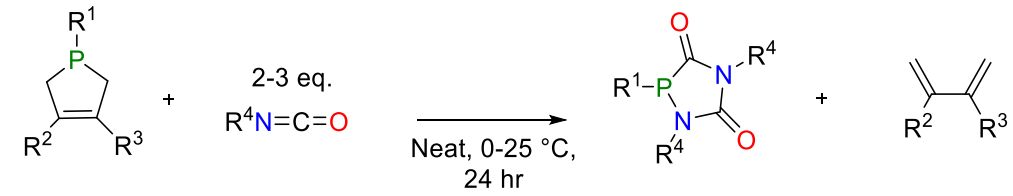
As previously stated, for the double hydrophosphination of aryl isocyanates, in the crude reaction there is typically between 2-15% of phosphorus containing side products at ~25 ppm in the ^{31}P NMR spectrum (Section 3.3.1.2, **Table 23**).

After isolating a crude (~95% purity by ^{31}P NMR spectroscopy) amount of this peak at ~25 ppm (**51a)** by column chromatography, the corresponding ^{1}H NMR spectrum showed two aryl groups from isocyanate molecules per ferrocenyl group but with no peaks which could be due to an N-H moiety. Excluding the possible presence of a hydrophosphination-type product. Further analysis of the product by $^{13}C\{^{1}H\}$ NMR spectroscopy showed two distinct PC=O and NC=O doublets at 178.6 ($^{1}J_{CP}$ = 2.1 Hz) and 155.0 ($^{1}J_{CP}$ = 5.7 Hz), with similar values to those previously seen for diinsertion (~185 ($^{1}J_{CP}$ = 29 Hz) P*C*=O and ~151 Hz *C*=O, **Scheme 45**).[115]

From the literature there is only one example of this phosphorus heterocycle (1,4,2-diazaphospholidine-3,5-dione).[153] Under neat conditions unsaturated phospholene moieties (R^1 = ^{n}Bu, Me, Ph) were stirred with primary aliphatic isocyanates (R = Me or ^{n}Bu) resulting in the formation of the desired 1,4,2-diazaphospholidine-3,5-diones in 85-99% yields; with the subsequent stoichiometric formation of diene side products (**Scheme 46**).[153]



Scheme 45. *Plausible structures from the reaction of 1.0 eq. of $FcPH_2$ and 2.0 eq. of PhN=C=O.*

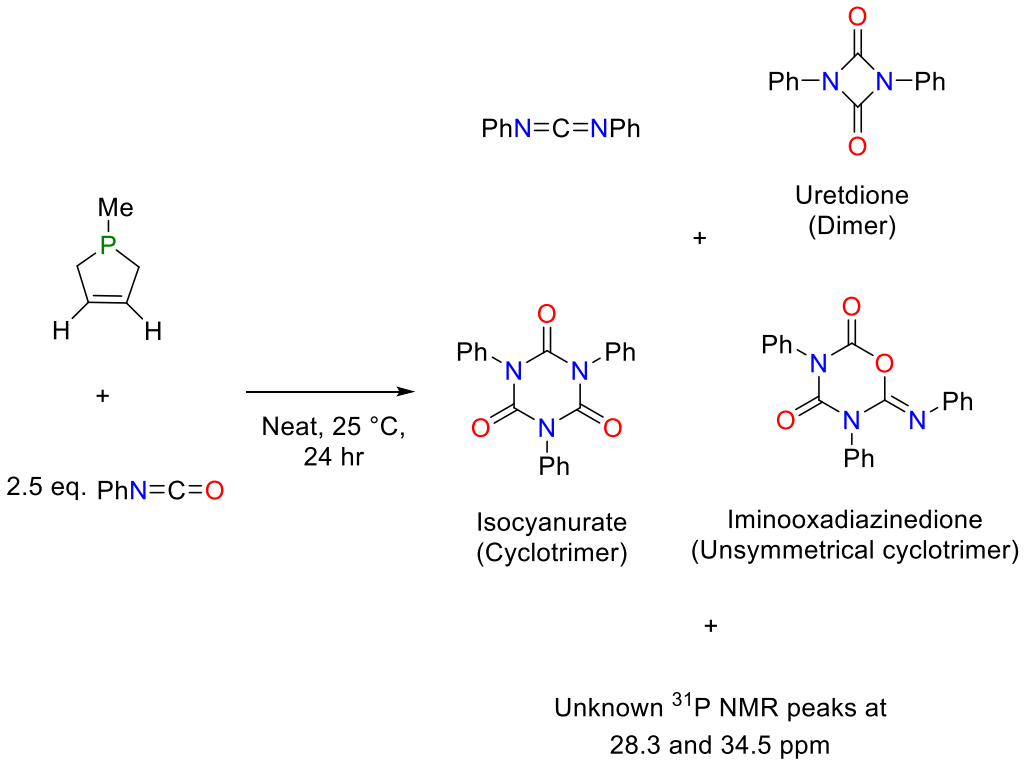


R^1 = ^{n}Bu; R^2 = R^3 = Me; R^4 = Me
R^1 = Me; R^2 = R^3 = H; R^4 = Me, ^{n}Bu
R^1 = Ph; R^2 = R^3 = Me; R^4 = Me

Scheme 46*. Previous work by Richter Reaction of phospholes with MeN=C=O or ^{n}BuN=C=O to yield 1,4,2-Diazaphospholidine-3,5-diones.*[153]

Further attempts at the synthesis using CyN=C=O and ^{i}PrN=C=O were very slow (31% conversion by ^{31}P NMR spectroscopy after 48 hours, when utilising ^{i}PrN=C=O) and attempts using ^{t}BuN=C=O were completely unsuccessful as determined by ^{1}H, ^{31}P NMR and GC-MS analysis.[153]

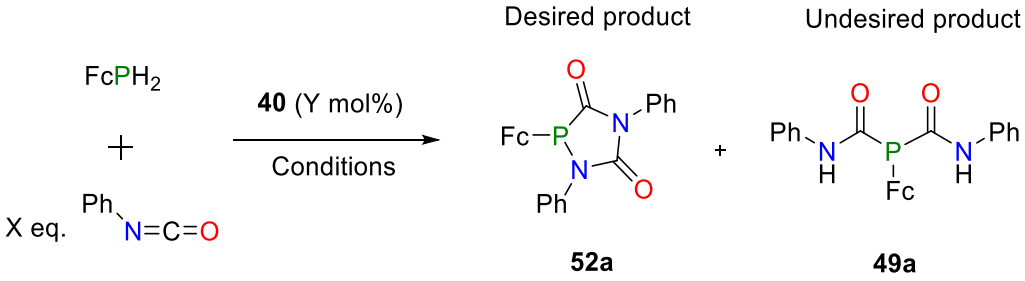
Richter also reports that the reaction between PhN=C=O and alkyl phospholes is very exothermic, producing two peaks in the ^{31}P NMR spectrum at 38.3 and 34.5 ppm, unrelated to any desired products. GC-MS analysis revealed the presence of a range of products: diphenyl carbodiimide, triphenyl isocyanurate (cyclotrimer product), triphenyl iminooxadiazinedione (unsymmetrical cyclotrimer) and diphenyl uretdione (dimer) (S**cheme 47**), highlighting the significant effect changing the organic group of isocyanates from alkyl to aryl can have on reactivity.



Scheme 47. *Previous work by Richter for the reaction of phenyl isocyanate and 1-methyl-2,5-dihydro-1H-phosphole. Products were identified by GC/MS analysis and ^{31}P NMR spectroscopy.*[153]

3.3.3.2 Initial diinsertion-cyclisation optimisation

Initial attempts at increasing the ratio of diinsertion-cyclisation product **51a** to double hydrophosphination product **49a** by either increasing temperature from 25 °C to 60 °C or catalyst loading of **40** from 5.0 mol% to 10 mol% gave low conversions (6 and 8%) after 16 hours of the desired product (**Table 20**, entries 1 and 2. **Scheme 48**, for a general reaction outline).



Scheme 48. *General outline for diinsertion-cyclisation optimisation, conditions given in* ***Table 26*****.**

The first moderate increase in the amount of **52a** came from increasing the ratio of $FcPH_2$:PhN=C=O from 1:2 to 1:6, yielding a 41% conversion of **52a** after 16 hours and importantly (for potential future separation and isolation) a decrease in **49a** (**Table 26**, entry 3). An increase in the reaction temperature from 60 °C to 85 °C for 16 hours gave a slight increase in conversion to 44% and a further increase in catalyst loading from 5.0 mol% to 10 mol% afforded a higher conversion to 58% of **51a** (**Table 26**, entries 4 and 5).

Given the previous success of neat and highly concentrated reactions in **Chapter 2**, a reaction was performed with a ratio of 1:6 $FcPH_2$:PhN=C=O in the absence of solvent at 60 °C at a lower catalyst loading of 5.0 mol%, resulting in a high conversion of 78% of **52a** (**Table 26**, entry 6). However, attempts at repeating this reaction gave various conversions between 52-78% likely due to mass transport issues.

Table 26. Initial Diinsertion-cyclisation optimisation of phenyl isocyanate with $FcPH_2$[a,b]

Entry	$FcPH_2$: PhN=C=O eq.	Temp. (°C)	Cat. mol%	Sol.	Yield **49a** (%)	Yield **52a** (%)
1	1.0:2.0	60	5.0	C_6D_6	86	6
2	1.0:2.0	25	10	C_6D_6	74	8
3	1.0:6.0	60	5.0	C_6D_6	35	41
4	1.0:6.0	80	5.0	C_6D_6	21	44
5	1.0:6.0	80	10	C_6D_6	12	58
6	1.0:6.0	60	5.0	Neat	17	78
7	1.0:50	60	5.0	Neat	35	63
8	1.0:8.0	85	10	C_6D_6[c]	12	80

[a] Reaction conditions: 1.0 eq. = 0.146 mmol, and solvent volume = 0.5 mL; reactions performed under a nitrogen atmosphere for 16 hours unless otherwise stated. [b] Conversion determined by ^{31}P NMR spectroscopy using an internal standard (addition 1.0 eq. of PPh_3 in 0.15 mL C_6D_6 after 16 hours). [c] 0.25 mL used.

In an effort to circumvent the homogeneity issues giving varying yields (from 52% up to 78%, (**Table 26**, entry 6), the PhN=C=O substrate was utilised as the "solvent" with 50 equivalents vs phosphine used, however the reaction gave a lower conversion of 63% for **52a** and, unfortunately, a higher conversion of undesired **49a** (35%. **Table 26**, entry 8). An alternative approach where 20 equivalents of C_6D_6 and slightly more PhN=C=O (8 equivalents) were used giving a comparably high conversion of 80% of **52a**; albeit with the need for a higher 10 mol% catalyst loading of **40** (**Table 26**, entry 8). In this scenario, the volume of C_6D_6 is enough to dissolve all the starting materials and all the subsequent less soluble products preventing the reaction from prematurely ending due to mass transport issues.

Repeated reactions showed the reaction consistently gave an 80% conversion to **52a**, thus conditions from **Table 20**, entry 8 were chosen as the ideal

conditions for further isocyanate substrate scope analysis. A ^{31}P NMR spectrum for the optimal reaction conditions is shown in **Figure 16**.

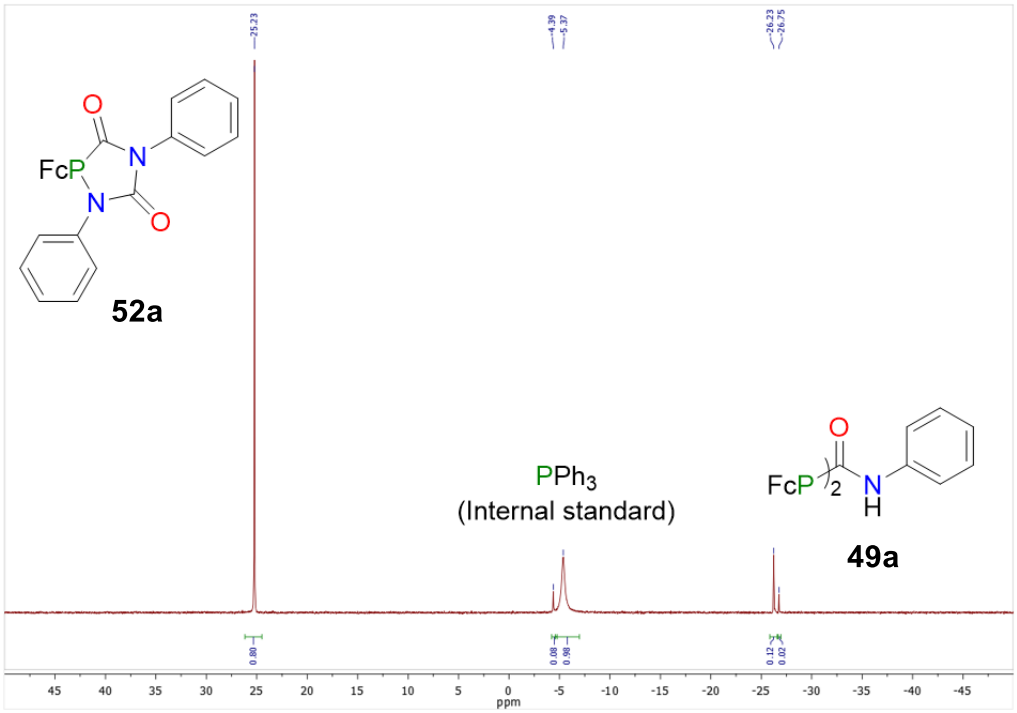
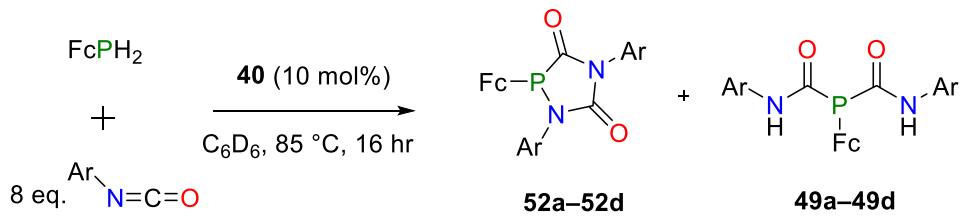


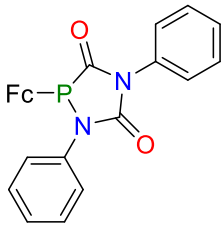
Figure 16. *^{31}P NMR spectrum of a 1:8 $FcPH_2$: PhN=C=O with 10 mol% **40** reaction at 85 °C after 16 hours.*

3.3.3.3 Diinsertion-cyclisation of aryl isocyanates

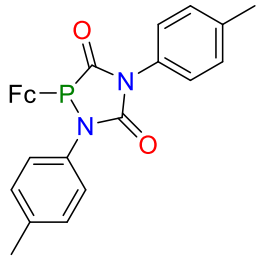
As determined by ^{31}P NMR spectroscopy, all reactions reached similar high conversions to the double hydrophosphination products (in the range 78-80% for RN=C=O where R = Ph, 4-MeC_6H_4, 4-$(MeO)C_6H_4$) with minimal amounts of double hydrophosphination products formed (12-16%) (**Table 27**). The use of 3-ClC_6H_4N=C=O gave a higher conversion of 89% with only 5% double hydrophosphination product forming (**Table 27**).

Table 27. Diinsertion-cyclisation of aryl isocyanates utilising $FcPH_2$[a,b,c]

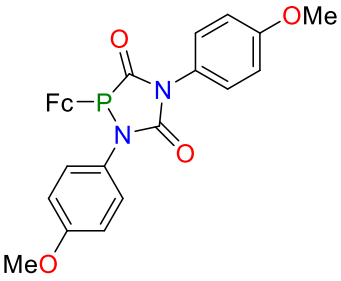




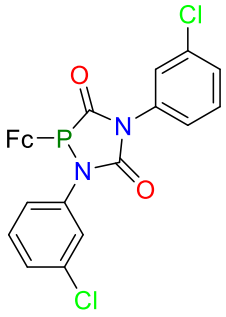
52a: 85 °C, 16 hr, (**52a:49a**, 80:12)



52b: 85 °C, 16 hr, (**52b:49b**, 78:14)



52c: 85 °C, 16 hr, (**52c:49c**, 79:16)



52d: 85°C, 16 hr, (**52d:49d**, 89:5)

*[a] Reaction conditions for conversions: 1.0 eq. $FcPH_2$ = 0.146 mmol, and C_6D_6 (0.25 mL) under a nitrogen atmosphere unless otherwise stated.[b] Reaction conditions for isolated yields: 1.0 eq. $FcPH_2$ = 2.30 mmol and benzene (4.0 mL).[c] Ratios given in brackets as ratios of product **52** to **49** and determined by ^{31}P NMR spectroscopy using an internal standard (addition 1.0 eq. of PPh_3 in 0.15 mL C_6D_6 after 16 hours).*

3.3.4 Hydrophosphination of isocyanates with $AdPH_2$

3.3.4.1 Initial catalyst-free hydrophosphination with $AdPH_2$

Given the significant electronic and steric differences between $AdPH_2$ and $FcPH_2$, it is still important to ascertain the need for a catalyst by performing

initial control reactions; even though they have been performed for $FcPH_2$ already. Initial attempts in a solution of C_6D_6 at 25 °C and 60 °C were unsuccessful yielding only 2% of an unknown product at -4.6 ppm and performing the reaction neat at 25 °C led to only 2% of products likely related to dehydrocoupling of $AdPH_2$ (**Table 28**, entries 1-3).

Table 28. Catalyst-free hydrophosphination of phenyl isocyanate with $AdPH_2$[a,b]

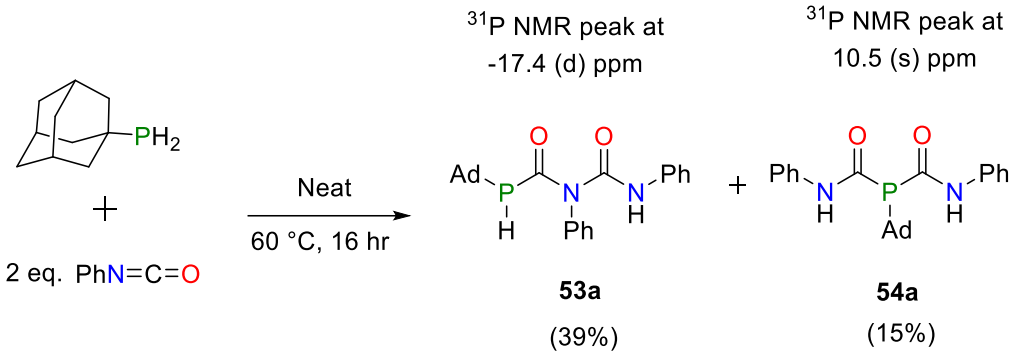
Entry	$AdPH_2$: PhN=C=O eq.	Temp. (°C)	Solv.	Conv. (%)	Yield **53a** (%)	Yield **54a** (%)
1	1.0 : 2.0	25	C_6D_6	0	0	0
2	1.0 : 2.0	60	C_6D_6	2[c]	0	0
3	1.0 : 2.0	25	Neat	2[c]	0	0
4	1.0 : 2.0	60	Neat	55[c]	39	15

[a] Reaction conditions for conversions: 1.0 eq. $AdPH_2$ = 0.0732 mmol, and C_6D_6 (0.50 mL) under a nitrogen atmosphere unless otherwise stated.[b] Conversion determined by ^{31}P NMR spectroscopy by relative ^{31}P peaks.[c] Additional conversion to minor unknown products at ^{31}P NMR = -4.6(s) and -15.7(s) ppm (<0.1-2%)

However, heating at 60 °C led to 15% of a peak at 10.5 ppm and 39% of a new doublet at -17.4 ppm (^1J(P,H) = 232 Hz). The product contains one P–H bond, which is evidenced by the presence of a doublet at 3.30 ppm in the ^1H NMR spectrum (^1J(P,H)) = 232 Hz). Additionally, there is a broad resonance at 11.45 ppm, assigned to an N–H bond, suggesting a diinsertion type product, ($(PPh_2C(O)N(Ph)C(O)NH(Ph)$ ^1H NMR = 11.57 ppm (s, NH)).[115] Overall, this suggests the peak at –17.4 ppm is a single hydrophosphination diinsertion type compound **53a** (**Scheme 49**).

Further evidence that the ^{31}P NMR spectroscopy peak -17.4 ppm is product **53a** is provided by $^{13}C\{^1H\}$ NMR spectroscopy, which shows two types of C(O) doublet peaks at 186.4 ppm (^1J(C,P) = 34.3 Hz, P*C*O) and 174.3 ppm (^3J(C,P) = 28.0 Hz, N*C*O) typical of diinsertion products.[115] The other major ^{31}P NMR

containing peak (10.5 ppm) in the ^{1}H NMR spectrum corresponds to a distinctive broad N-H resonance at 9.53 ppm and can be assigned to the double hydrophosphination product **54a** (**Scheme 49** and **Figure 17**).



Scheme 49. *Neat catalyst-free hydrophosphination of phenyl isocyanate by $AdPH_2$, where Ad = 1-adamantyl.*

It should be noted that whilst the formation of **53a** is novel, there are some issues with mixing. After 16 hours, the reaction mixture becomes highly viscous and subsequent heating for 16 hours does not further increase conversion. This limits the usefulness of this reaction as a significant proportion of pyrophoric and pungent $AdPH_2$ is left unreacted.

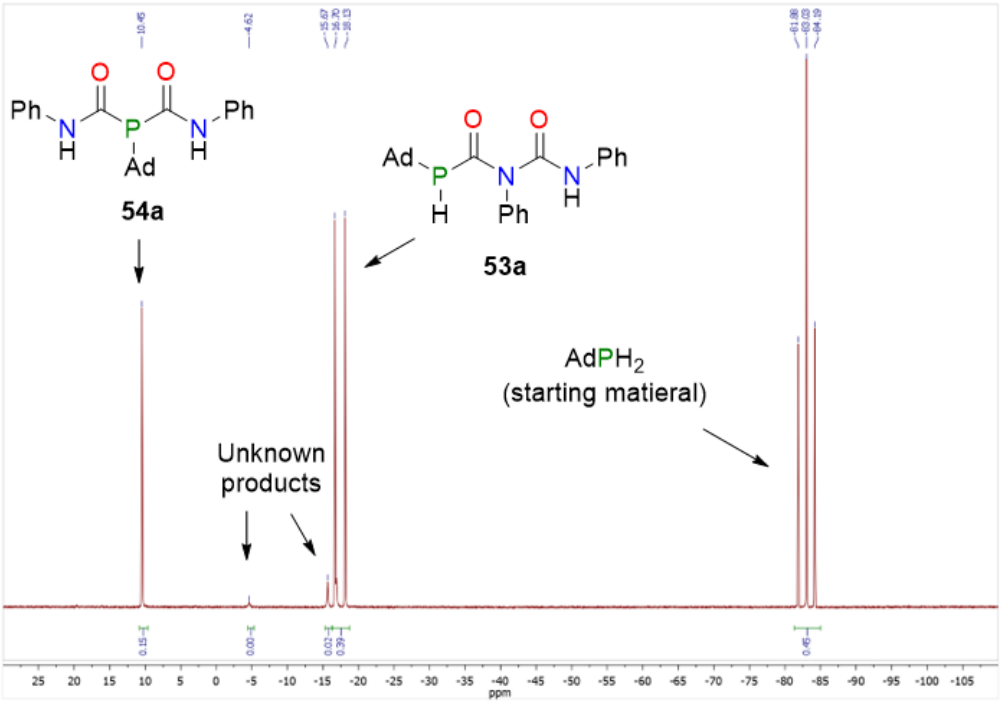


Figure 17. *Neat catalyst-free addition of $AdPH_2$ to PhN=C=O (**Table 28**, entry 4).*

3.3.4.2 Initial Catalytic Hydrophosphination with $AdPH_2$ and PhN=C=O

Initial conditions of 5.0 mol% catalyst loading of **40** for 16 hours at 25 °C in C_6D_6 only reached 5% conversion from $AdPH_2$ forming an unknown species at -70.4 ppm (2%, *J* = 136 and 59.5 Hz) and 3% of the single hydrophosphination diinsertion product **53a** (^{31}P NMR = -17.3(d) ^{1}J(P,H) = 231 Hz), see section 3.3.4.1) (**Table 29**, entry 1, for a general scheme of the identified products formed from reactions of **Table 30**, see **Scheme 50**). This demonstrates that $AdPH_2$ is a much less reactive substrate compared to $FcPH_2$, which underwent 100% conversion with analogous conditions (section 3.3.1.2).

Table 29. Initial Catalytic hydrophosphination of PhN=C=O by $AdPH_2$[a,b]

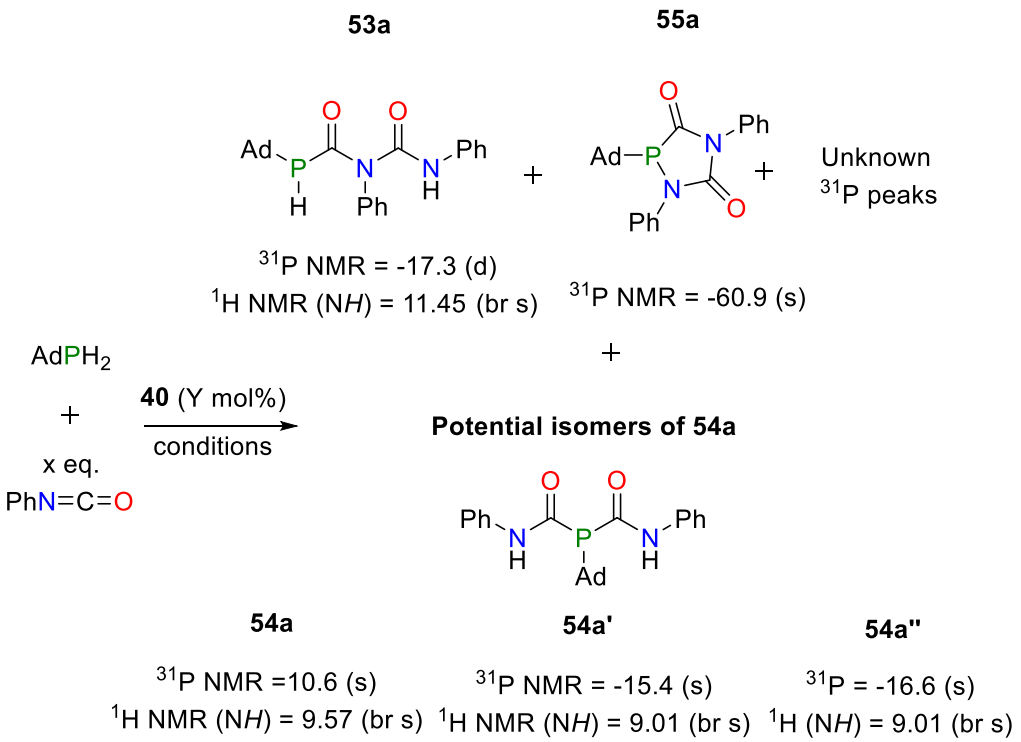
Entry	$AdPH_2$: PhN=C=O	Cat. loading	Temp. (°C)	Time (hr)	Conv. from $AdPH_2$ (%)
1	1.0 : 2.0	5.0	25	16	5
2	1.0 : 2.0	5.0	60	16	61
3	1.0 : 2.0	10.0	60	32	90
4	1.0 : 4.0	10.0	60	32	98

[a] Reaction conditions for conversions: 1.0 eq. $AdPH_2$ = 0.0732 mmol, and C_6D_6 (0.50 mL) under a nitrogen atmosphere unless otherwise stated.[b] Conversion determined by ^{31}P NMR spectroscopy by relative ^{31}P peaks.

Increasing the reaction temperature to 60 °C for 16 hours increased the conversion from $AdPH_2$ to 61%, with the highest NMR conversion (31%) being due to the product with a singlet resonance at 10.6 ppm in the ^{31}P NMR spectrum. Correspondingly, the ^{1}H NMR spectrum shows resonances assigned to an N–H moiety at 9.57 ppm, suggesting the double hydrophosphination product **54a** has been formed (**Table 30**, entry 2).

Table 30. ^{31}P NMR spectrum peaks and relative conversions of products from the initial catalytic hydrophosphination of PhN=C=O by $AdPH_2$, continued from **Table 29**

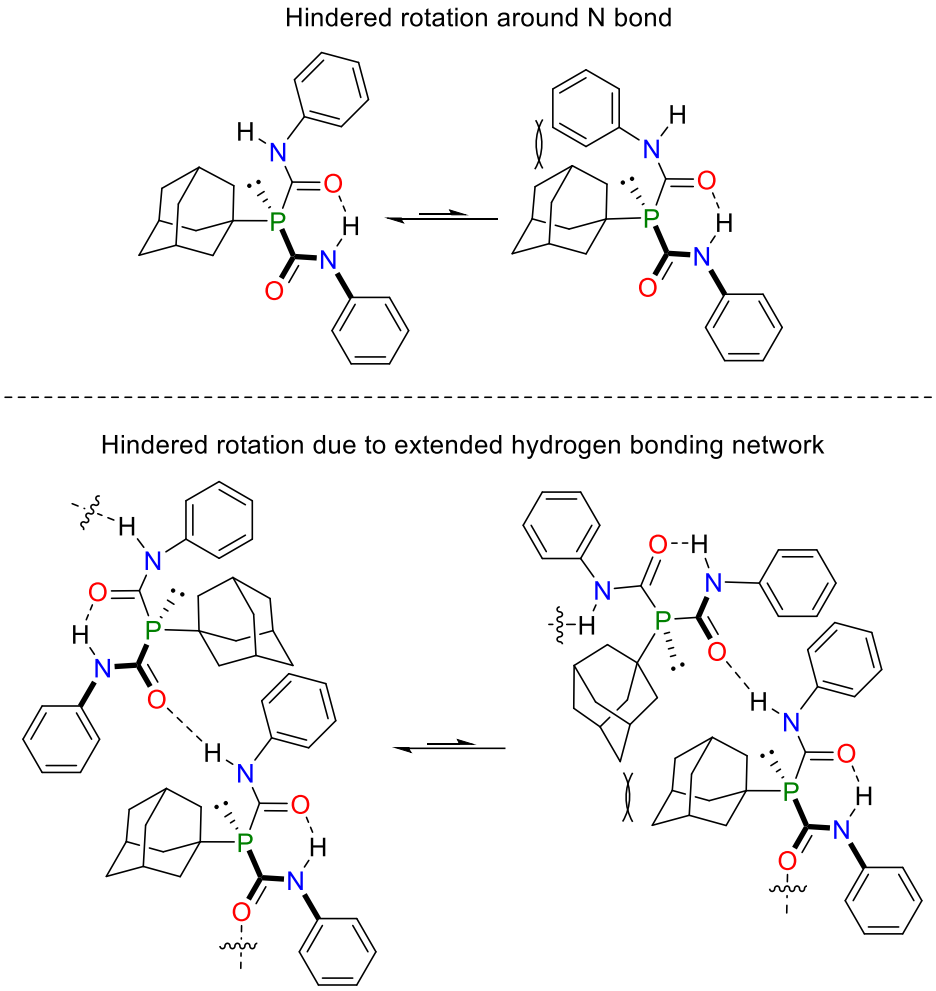
^{31}P NMR Peak (ppm) / product	Entry 1 Conv. (%)	Entry 2 Conv. (%)	Entry 3 Conv. (%)	Entry 4 Conv. (%)
81.0 (s)	-	-	-	3
79.8 (s)	-	-	-	3
74.1 (s)	-	-	-	2
--70.4 (dd)	2	5	10	-
53a (-17.3 d)	3	3	-	-
54a'' (-16.5 s)	-	-	8	-
54a' (-15.3 s)	-	18	11	12
54a (10.6 s)	-	31	53	56
42.9 (s)	<0.1	<0.1	3	11
55a (60.9 s)	<0.1	4	4	10
82.6 (s)	-	-	1	1
83.5 (s)	-	-	1	1



***Scheme 50**. General reaction PhN=C=O with $AdPH_2$ utilising precatalyst **40** under conditions stated in **Table 29-30**, along with ^{31}P NMR spectroscopic assignments.*

The second highest conversion is 18% to a singlet peak at ^{31}P = -15.3 ppm in the corresponding ^{1}H spectrum corresponds to a broad singlet at 9.01 ppm, suggesting the product is a double hydrophosphination product but is not a monoinsertion product, however this product has already been assigned to **54a**. Potentially there could be rotational isomerism due to the steric bulk of the adamantyl group, causing hindered rotation around the C-N bond (**Scheme 51** above). Additionally, depending on how the hydrogen bonding in the system is organised, there could be further intramolecular hydrogen bonding (see section 3.3.6.2 for an X-ray crystal structure example of this with ferrocene instead of adamantyl) in which steric clashes between neighbouring adamantyl groups could occur (**Scheme 51**, below). Further analysis is needed such as variable temperature NMR spectroscopy, X-ray crystal structures and computational analysis to determine the energy barriers to rotation and what potential isomers correspond to which products; but for the purpose of future discussion the product corresponding to ^{31}P = -15.4 ppm, will be referred to as **54a'**.

Increasing catalyst loading to 10 mol% and doubling the reaction time from 16 hours to 32 hours increases reaction conversion to 90% with the double hydrophosphination product, **54a**, being the largest resonance (48%); with the other isomer **54a'** at a lower conversion (11%, **Table 30**, entry 3). Interestingly there is an 8% conversion to a ^{31}P NMR peak at -16.5(s) ppm which corresponds to an NH peak at 9.01ppm in the ^{1}H NMR spectrum like **54a**' (potentially two similar broad N*H* peaks, overlapping to look like one very broad singlet), thus can be assigned to another isomer of double hydrophosphination, **54a**'' (**Table 30**, entry 3).



Scheme 51. *Potential atropisomers of double hydrophosphination product* ***54a****, (above) due to hindered rotation around the free nitrogen bond and adamantyl group and (below) due to hindered rotation from extending hydrogen bonding networks with adamantyl to adamantyl steric hindrance.*

Further increasing the ratio of $AdPH_2$:PhN=C=O to 1:4 achieves a 98% conversion leaving no residual $AdPH_2$, forming a 68% mixture of double hydrophosphination product isomers (**54a**; 56% and **54a**'; 12%. **Table 30**, entry 4). There is a 10% conversion to a ^{31}P NMR spectrum peak at 60.4 ppm with no corresponding NH type peaks in the ^{1}H NMR spectrum, further analysis by $^{13}C\{^{1}H\}$ reveals a PC(O) peak at 174.2ppm (d, $^{1}J(C,P)$ =4.9 Hz) and a PNC(O) peak at 166.1 ppm (s) suggesting this product is the diinsertion-cyclisation product **55a**.

Attempts to separate this product mixture by column chromatography were unsuccessful due to the mildly air-sensitive nature of the products and additional attempts to purify by recrystallisations by CH_2Cl_2: hexane layering and toluene:hexane mixtures at -30 °C were also unsuccessful.

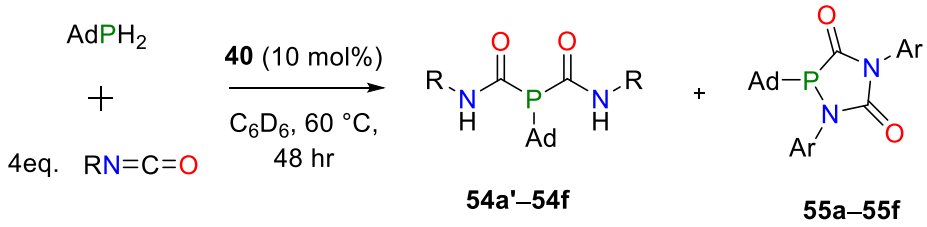
3.3.4.3 Diinsertion-cyclisation of aryl isocyanates and double hydrophosphination of alkyl isocyanates with $AdPH_2$

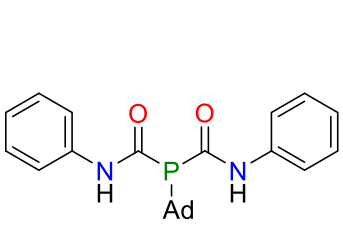
Given the reduced success for reactions between $AdPH_2$ and PhN=C=O, (compared to reactions with $FcPH_2$ and PhN=C=O), other functionalised isocyanates were investigated. Under analogous conditions (**40** 10 mol%, $AdPH_2$: isocyanate ratio of 1:4 and heating at 60 °C for 48 hours) the reactions between $AdPH_2$ and RN=C=O (R = 3-ClC_6H_4, 4-$OMeC_6H_4$ and *p*-Tol) demonstrated a complete shift in product selectivity, all forming ~72% of the diinsertion-cyclisation products, **55b** -**55d** and showing no peaks at ~10-11ppm in the ^1H NMR spectrum, which could be assigned to double hydrophosphination products (**Table 31**). The main impurities were as yet unassigned peaks at resonances in the range of 42-43 ppm in the ^{31}P NMR spectrum with relative conversions of 14, 10 and 8%. 3-ClC_6H_4N=C=O gave a 72% conversion to the cyclic product **55d** with minor (14%) formation of a product at 42.9 ppm (as determined by ^{31}P NMR spectroscopy). Similar results were observed for the *p*-Tol and 4-$OMeC_6H_4$ derivatives.

The use of alkyl isocyanates typically requires more forcing conditions involving higher temperatures or catalyst loadings, however, under the same conditions as those used for the aryl isocyanates, CyN=C=O underwent double hydrophosphination which formed the **54b** product in 81% conversion (**Table 31**). In addition, 13% of the product distribution was due to a diinsertion-cyclisation product, which is unusual for less electrophilic alkyl isocyanates as

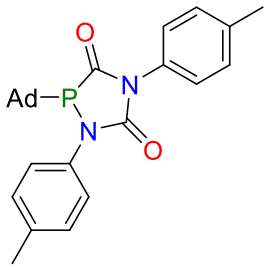
evidenced in previous work by Kays *et al*.[115,117] Utilising the bulkier ^{t}BuN=C=O slowed the reaction, whereby after 36 hours at 60 °C, 71% conversion to the double hydrophosphination product **54c** was achieved, with no diinsertion-cyclisation products observed by ^{31}P NMR spectroscopy (**Table 31**).

Table 31. Hydrophosphination-cyclisation of aryl isocyanates utilising $AdPH_2$[a,b,c]

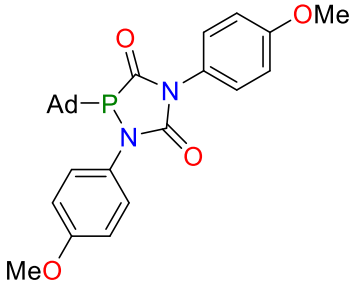




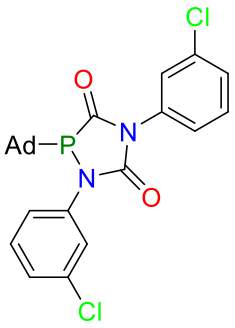
54a': (**54a'**:**55a**, 58:10)



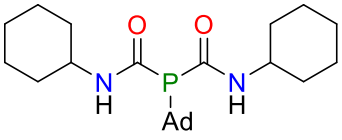
55b: (**54b**:**55b**, 0:72)



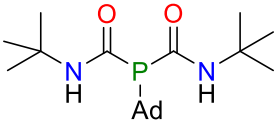
55c: (**54c**:**55c**, 0:72)



55d: (**54d**:**55d**, 0:72)



54e: (**54e**:**55e**, 81:13)



54f: (**54f**:**55f**, 71:0)

*[a] Reaction conditions for conversions: 1.0 eq. $AdPH_2$ = 0.146 mmol, and C_6D_6 (0.5 mL) under a nitrogen atmosphere unless otherwise stated.[b] Relative conversion determined by ^{31}P NMR spectroscopic NMR conversions are given as ratios of double hydrophosphination product (**54**) diinsertion-cyclisation product (**55**).*

3.3.5 Mechanistic studies

3.3.5.1 Poisoning experiments

To ascertain if the catalytic mechanism proceeds by a homogeneous, a heterogeneous or a radical mechanism, various additives to poison the reaction were added to a standard double hydrophosphination reaction of $FcPH_2$ and PhN=C=O. (**Table 32**). A baseline reaction was performed to obtain a minimum time required for 99% conversion, for which at ~8 hours 99% conversion was reached at 25 °C (**Table 32** entry 1).

A mercury drop test indicates whether the catalysis proceeds *via* a homogeneous or heterogeneous mechanism, as elemental mercury has been shown to selectively poison heterogeneous catalysts because elemental mercury forms an amalgam and inhibits the reaction.[154,155] However the mercury drop test is not conclusive for iron as elemental mercury does not always form an amalgam with iron, but there are some reported examples where this does happen.[156,157]

Carbon disulfide can be used as an alternative to mercury.[154,158] This is a small ligand which can coordinate to the metal and poison the catalyst. If the reaction is heterogeneous then only a fraction of the active sites are available on the surface of the particles. If the reaction is slowed with only 0.1 equivalents of the ligand with respect to the catalyst this suggests that all the active sites have been blocked and it is a heterogeneous catalyst. Whereas a homogeneous catalyst would only be inhibited with at least 1 equivalent of CS_2. The phosphine $PPhMe_2$ can be used in a similar way to CS_2.[159]

In all of these poisoning experiments, after 8 hours at 25 °C the reaction reaches and gives near identical conversions to the control reaction at 87-89% for **49a** and 5-6% **51a** (**Table 32**, entries 2-4). Additionally, no visible metal

precipitate is seen, suggesting that a homogeneous mechanism is in operation. The catalysis was also performed in the presence of cumene and 1,4-cyclohexadiene (1,4-CHDN), which can act as radical traps (**Table 32**, Entries 5-6).[160] In the presence of these compounds, longer reaction times would indicate that the catalysis undergoes a radical mechanism. The addition of 1,4-cyclohexadiene and cumene does not affect the reaction time, suggesting that the reaction does not proceed *via* a radical mechanism.

Table 32. Hydrophosphination of PhN=C=O with $FcPH_2$ and poisoning additives[a,b]

Entry	$FcPH_2$: PhN=C=O	Additive	Amount	t (hr)	Conv. (%)	Yield **49a**:**51a**
1	1.0 : 2.0	None	None	8	99	86:6
2	1.0 : 2.0	Hg(0)	*ca*. 1 drop	8	99	88:5
3	1.0 : 2.0	CS_2	0.732 µmol	8	99	89:5
4	1.0 : 2.0	$PPhMe_2$	0.732 µmol	8	99	87:6
5	1.0 : 2.0	Cumene	73.2 µmol	8	99	96:2
6	1.0 : 2.0	1,4-CHDN	73.2 µmol	8	99	87:6

*[a] Reaction conditions for conversions: 1.0 eq. $FcPH_2$ = 0.146 mmol, 2.0 eq PhN=C=O = 0.292 mmol, 5.0 mol% **40** (7.32 µmol) and C_6D_6 (0.5 mL) under a nitrogen atmosphere unless otherwise stated.[b] Conversion determined by ^{31}P NMR spectroscopy by relative ^{31}P peaks.*

3.3.5.2 Stoichiometric studies

To further elucidate a plausible mechanism of catalysis a 1:1:1 stoichiometric reaction between $Fe(C_6H_3\text{-}2,6\text{-}Mes_2)_2$ (**40**), PhN=C=O and $FcPH_2$ in C_6D_6 (0.6 mL) was performed. The reaction resulted in a colour change from light orange to very dark orange. The ^1H NMR spectrum of this reaction displayed no new paramagnetically shifted resonances, but after 3 hours of reaction, three new peaks could be observed in the ^{31}P NMR spectrum. Two of these resonances are triplets at –3.2 ppm (J = 49.1 Hz) and 38.8 ppm (J = 48.3 Hz) in a near 1:1 integration ratio; which are unlikely to be coordinated $FcPH_2$ (Free $FcPH_2$ = -

143.6 t ^{1}J(P,H) = 203 Hz) (**Figure 18**). Additionally, there is a singlet at 13.5 ppm which does not relate to any values typically seen for phosphinocarboxamides. It is unlikely these ^{31}P NMR peaks relate to a product that is bound directly to the Fe metal centre of **40** as they are not paramagnetically shifted. These changes are not observed when either PhN=C=O or $FcPH_2$ are just added to **40** suggesting the peaks could be related to a phosphaurea-type compound coordinating to the iron centre.

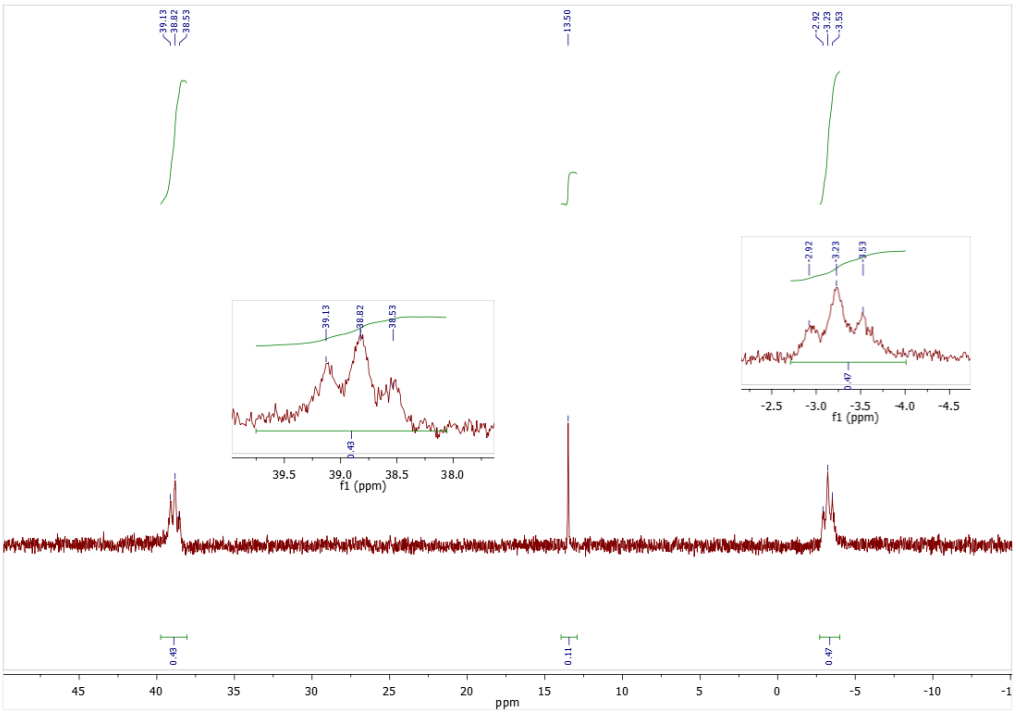


***Figure 18**. ^{31}P NMR spectra of 1:1:1 stoichiometric reaction of $FcPH_2$, PhN=C=O and $Fe((C_6H_3)(Mes)_2)_2$ in C_6D_6 after 3 hours.*

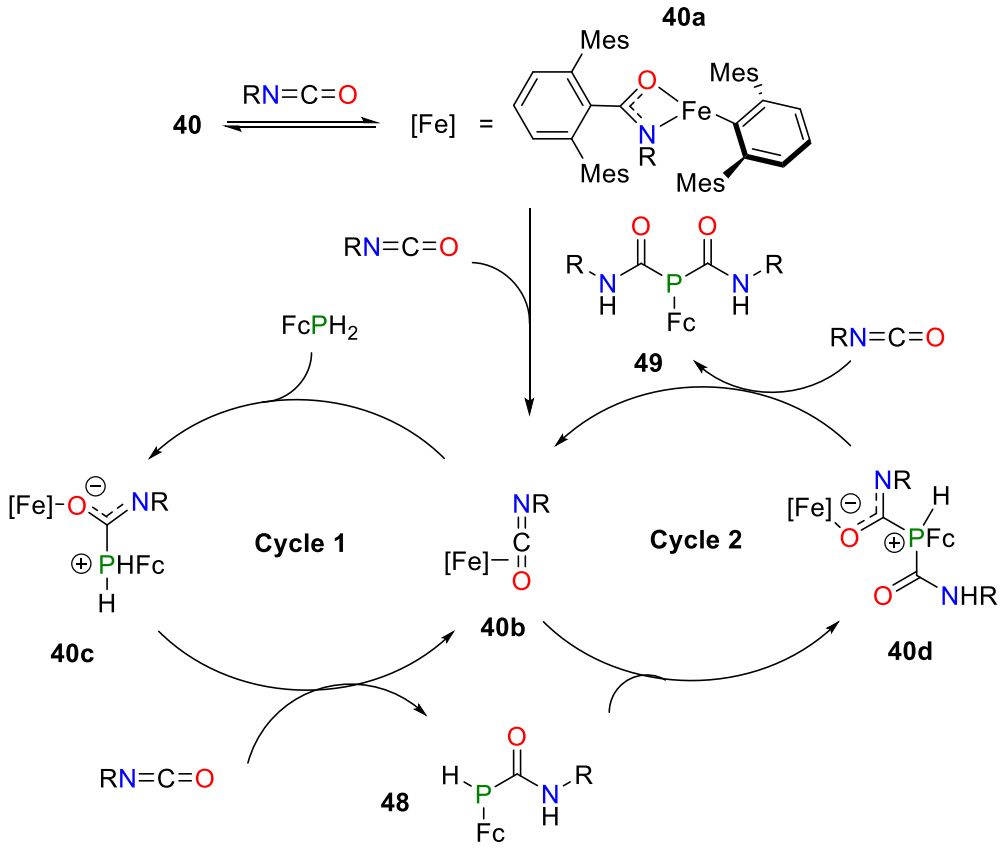
Other typically observed mechanisms for hydrophosphination involve the formation of a metal amido intermediate, resulting in the formation of a protonated ligand. For this catalytic system, this would result in the formation of protonated *m*-terphenyl ligand, however in these stoichiometric NMR experiments and monitored NMR experiments no protonated *m*-terphenyl product (2,6-Mes_2CH_4) is seen, suggesting this type of mechanism is unlikely.

3.3.5.3 Potential mechanism for double hydrophosphination

Whilst these mechanistic studies are not conclusive in suggesting an active species for the catalytic reaction, the catalysis does have very similar characteristics to previously reported hydrophosphination and hydroamination of isocyanates.[115,117] Thus, it can be envisaged a similar mechanism is in operation for the double hydrophosphination of isocyanates (**Scheme 52,** Cycle **1** and **2**).

In hydrophosphination of isocyanate (and isothiocyanate and carbodiimide) mechanistic literature the initial step is typically 1 of 2 steps either: 1) protonation of a ligand of the precatalyst allowing for the coordination of R_2P^- (predominantly for carbodiimides)[90–92,152,161–165] or insertion of the heterocumulene into the metal ligand bond.[91,115,166] Given the lack of evidence for initial protonation by $FcPH_2$ (with no HMes ligand being liberated). Thus, given the additional high oxidation of Fe(II) and co-coordinative unsaturation, the first step could be the isocyanate coordinating to the iron metal centre to form species (**40b**), with the metal centre acting as a Lewis acid**.**[167,168] $FcPH_2$ undergoes a nucleophilic attack on the activated isocyanate (**40c**); a subsequent 1,3-proton shift with displacement by a free isocyanate molecule generates the single-hydrophosphination product **48** (identified as an intermediate in slower reactions with THF as solvent by ^{31}P NMR: -54.0 ppm (d, ^1J(P,H) = 246 Hz) (**Scheme 52**, **Cycle 1**). These steps can be considered analogous to the single hydrophosphination of isocyanates with $HPPh_2$ forming $Ph_2PC(O)NH(R)$ previously reported by Kays *et al*.[115]

In analogous steps, free **48** is able to again undergo a P-H based nucleophilic attack on **40b** followed by another 1,3-proton shift (**40d**) and isocyanate coordination to reform **40b** and the double hydrophosphination product (**49**). (**Scheme 52**, **Cycle 2**).



Scheme 52. *Potential mechanism for the double hydrophosphination of isocyanates (**Cycle 1** and **2**).*

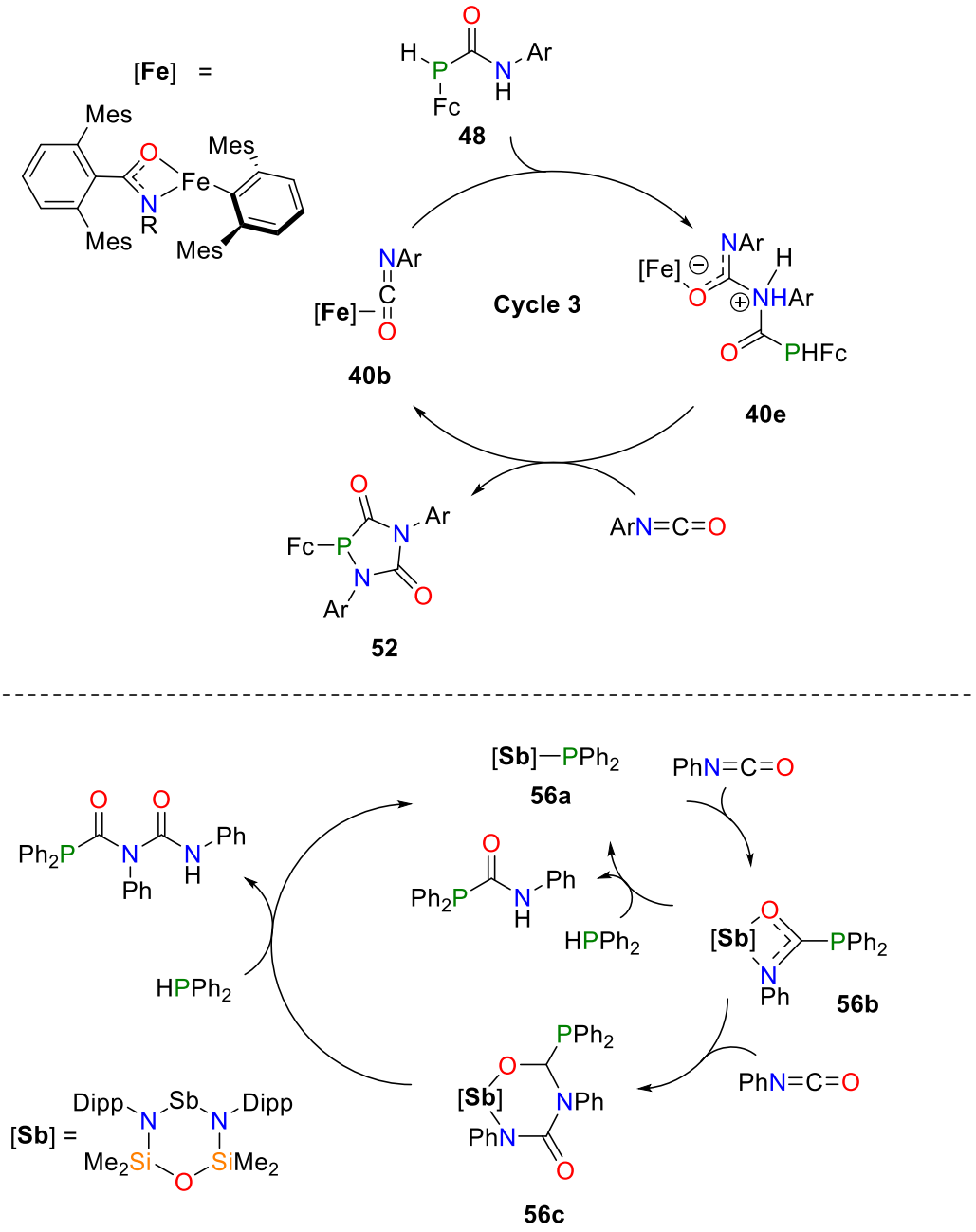
3.3.5.4 Potential mechanisms for diinsertion or diinsertion-cyclisation

The purpose of this section is to put forward general ideas and discussion regarding the diinsertion reactivity of isocyanates with phosphines, as such the mechanism for diinsertion-cyclisation (**Scheme 53**, above) is very tentatively proposed and further investigation is needed particularly the isolation of X-ray crystal structure of intermediates and computational analysis.

Alternatively, after **Cycle 1** is complete (**Scheme 52**) releasing the single hydrophosphination product **48**, instead of P–H-based nucleophilic attack on **40b**, an N–H based nucleophilic attack on **40b** may occur, forming a diinsertion type zwitterion complex **40e** (**Scheme53, Cycle 3**). In order to proceed to **cycle 2b** the R group used must be small, as such only diinsertion-cyclisation

products have been detected (by ^{31}P NMR spectroscopy) when R = aryl. Additionally, to this steric selectivity when a coordinating solvent such as THF is utilised, solvation of **40b** can occur significantly slowing the overall reaction and stopping the formation of any diinsertion-cyclisation products even when R = aryl. A further subsequent 1,3 proton shift of **40e** and isocyanate coordination; followed by dehydrocoupling reforms **40b** and forms the diinsertion-cyclisation product **52**.

So far, the discussion has been focused on similar mechanistic steps to previous Kays *et al.* work regarding single hydrophosphination diinsertion of isocyanates,[115] given the similarities regarding aryl group diinsertion and non-coordinating solvent selectivity for double hydrophosphination and diinsertion-cyclisation presented in this chapter (see sections 3.3.5.1 - 3.3.5.3). However in 2022 Coles *et al.* utilising antinomy-based compound **56a** have proposed an alternate route to diinsertion type compounds with a sequential isocyanate coordination from the active catalyst (**56a**) via intermediates **56b** and **56c** finishing the cycle with protonation with $HPPh_2$ to release the diinsertion product (**Scheme 53**, below).[165] Such sequential isocyanate insertion mechanistic steps are often proposed in the cyclotrimerisation of isocyanates, where multiple equivalents of isocyanates also have to be utilised in the mechanism.[118,169–171] This has relevance for the proposed mechanism of diinsertion-cyclisation with $FcPH_2$ (**Scheme 53**, top), as there is always a small amount of cyclotrimer formed in the reaction (~5-10%, when R = aryl and not when R = alkyl), suggesting some sequential isocyanate insertions could alternatively be involved in the mechanism.



Scheme 53. *(Above) proposed mechanism for the diinsertion-cyclisation of isocyanates with $FcPH_2$, via a zwitterionic intermediate and (below) diinsertion of isocyanates with $HPPh_2$ via competitive sequential isocyanate diinsertion versus $HPPh_2$ protonation by Coles et al.*[165]

3.3.6 Crystallographic studies

3.3.6.1 Ferrocenyl diarylphosphinocarboaxmides **49a**-**49d**

The molecular structures of the double hydrophosphination of isocyanates **49a**-**49d** were determined by X-ray diffraction using crystals obtained at room temperature from the slow diffusion of hexane into a solution of the compound in CH_2Cl_2. The crystal structures of **49a**-**49d** are shown in **Figures 19**-**20** with relevant bond angles and distances shown in **Tables 33**-**34.**

Table 33. Selected bond lengths (Å) and angles (°) for **49a**-**49d**.

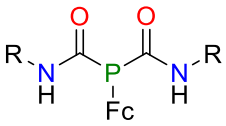
	**49a** R = Ph	**49b** R = *p*-Tol	**49c** R = 4-OMeC$_6$H$_4$	**49d** R = 3-ClC$_6$H$_4$
P(1)–C(1)	1.8825(15)	1.8649(17)	1.8636(18)	1.8942(16)
C(1)–O(1)	1.2165(18)	1.232(2)	1.229(2)	1.218(2)
C(1)–N(1)	1.3526(18)	1.341(2)	1.341(2)	1.356(2)
N(1)–C(2)	1.4152(18)	1.431(2)	1.437(2)	1.410(2)
P(1)–C(1)–O(1)	119.75(11)	120.00(12)	120.16(13)	121.44(12)
P(1)–C(1)–N(1)	114.16(10)	115.35(12)	115.57(13)	113.31(11)
N(1)–C(1)–O(1)	125.68(13)	124.35(15)	124.00(16)	125.14(14)

Table 34. Hydrogen-bonding geometry (Å, °) for **49a**-**49d**

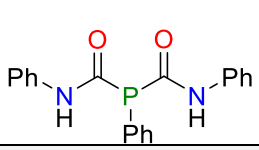
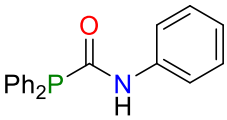
D–H···A	D–H	H···A	D···A	D–H···A
(**49a**) N(1)–H(1)···O(2)	0.862(14)	2.042(16)	2.8179(16)	149.3(17)
(**49b**) N(1)–H(1)···O(2)	0.842(16)	2.017(18)	2.7818(19)	151(2)
(**49c**) N(1)–H(1)···O(2)	0.864(16)	2.05(2)	2.788(2)	142(2)
(**49d**) N(1)–H(1)···O(2)	0.862(15)	2.091(18)	2.7912(18)	138.0(18)

All compounds crystalised with one molecule per asymmetric unit; whereas the analogous phenyl variant PhP(C(O)NH(Ph) by Liptrot *et al.* (**Table 35**) contains four molecules per asymmetric unit arranged as a crown like structure with intramolecular hydrogen bonds and additionally linked through intermolecular hydrogen bonds.[152] Compounds **49a**-**49d** all contain similar intramolecular C(1)–O(1)···H(2)–N(2) hydrogen bonds between 2.017(18)-2.091(18) Å at 138.0(18)-151(2)° (**Table 34**) which are ~0.1 Å smaller comparatively to analogous PhP(C(O)NH(Ph) with 1.8935(16)-1.9715(15) Å at 146.5-162.5°.

The effect of the substituted aryl group seems to have little to no effect on bond distances *e.g.* C(1)-N(1) for **49a** (R = Ph) 1.3526(18) Å and **49d** (R = 3-ClC_6H_4) 1.356(2) Å versus more electron donating **49b** (R = *p*-Tol) 1.341(2) Å and **49c** (R = 4-$MeOC_6H_4$) 1.341(2) Å being slightly smaller (~0.01 Å). For the C(1)–O(1) bond, the bond lengths are statistically equivalent at 1.2165(18) Å (**49a**), 1.232(2) Å (**49b**), 1.229(2) Å (**49c**).and 1.218(2) Å (**49d**).

For all compounds **49a**-**49d** there is noticeable trigonal distortion around the central phosphinocarboxamide P(CO)N moiety, with smaller P(1)–C(1)–N(1) angles of 113.31(11)-115.57(13)° and larger N(1)–C(1)–O(1) angles of 124.35(15)-125.68(13)°; versus the idealised 120° bond angles.

Table 35. *Comparative* selected bond lengths (Å) and angles (°) for $PhPC((O)NH(Ph))_2$ and $Ph_2PC(O)NH(Ph)$ by Liptrot *et al*. and Kays *et al*.[115,152]

		
P(1)–C(1)	1.880(2)-1.885(2)	1.8882(14)
C(1)–O(1)	1.224(3)-1.232(3)	1.2254(17)
C(1)–N(1)	1.343(3)-1.339(3)	1.3456(17)
N(1)–C(2)	1.414(3)-1.419(3)	1.4184(18)
C(O)···H(N)	1.8935(16)-1.9715(15)	–
P(1)–C(1)–O(1)	115.86(15)-121.62(18)	121.92(10)
P(1)–C(1)–N(1)	113.33(15)-117.90(16)	114.15(9)
N(1)–C(1)–O(1)	123.82(19)-126.2(2)	123.56(13)
N(1)···H(1)···O(2)	144.8-150.9	–

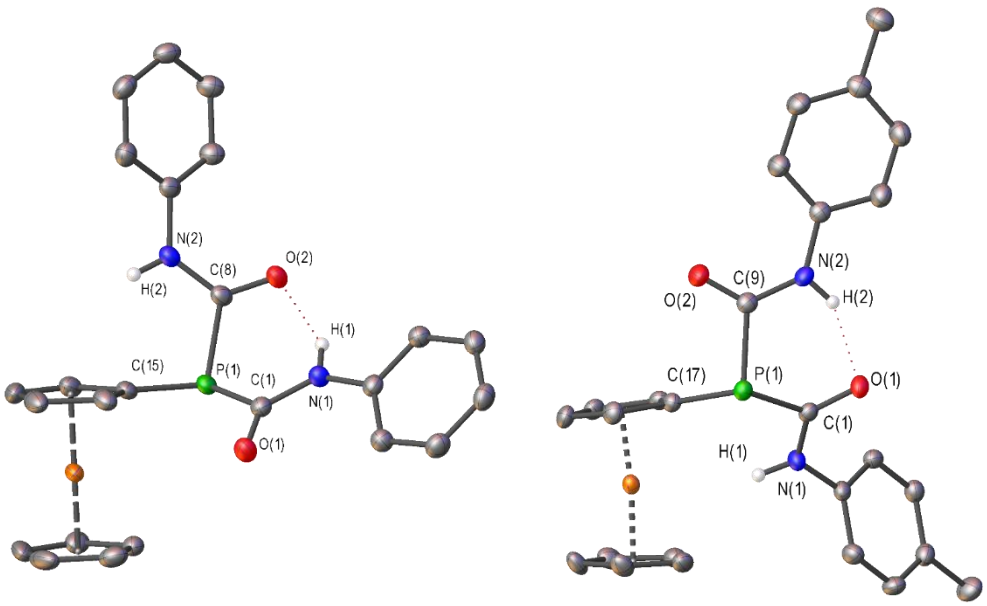


Figure 19. *Crystal structures of (left to right)* ***49a*** *and* ***49b*** *Hydrogen atoms with the exception of H(1) and H(2) have been omitted for clarity. Thermal ellipsoids are set at the 50% probability level.*

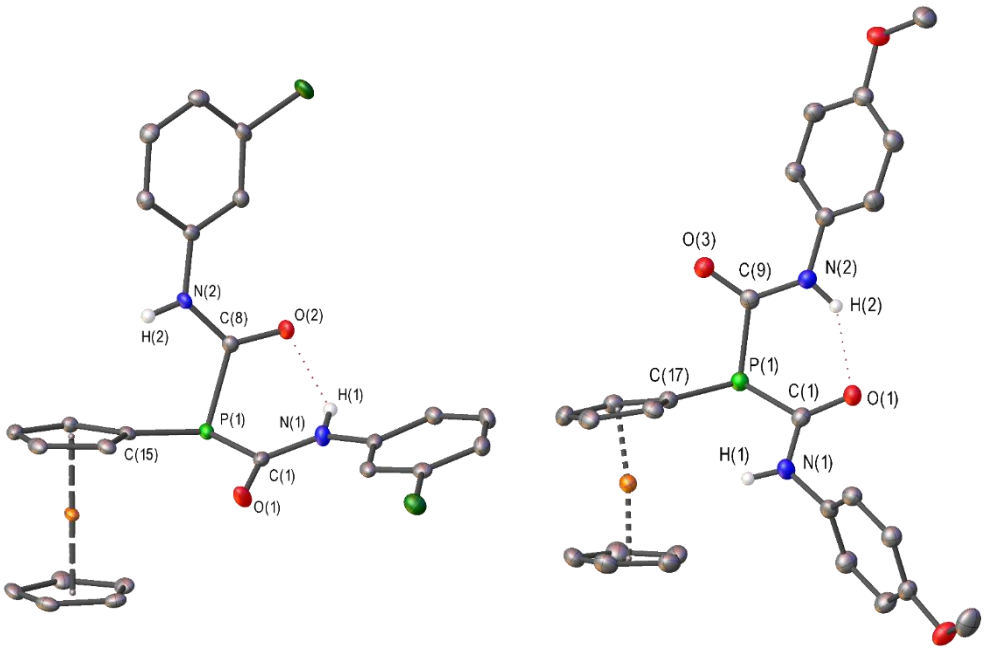


Figure 20. *Crystal structures of (left to right)* ***49c*** *and* ***49d****. Hydrogen atoms with the exception of H(1) and H(2) have been omitted for clarity. Thermal ellipsoids are set at the 50% probability level.*

3.3.6.2 Ferrocenyl dialkylcarboxamides **51a**-**51b**

Similarly to aryl double hydrophosphination products **49a**-**49d**, (R = Ph, *p*-Tol, 4-OMeC_6H_4 and 3-ClC_6H_4) the alkyl variant **51a** (R = Cy) features an intramolecular C(8)–O(2)···H(1)–N(1) interaction at 2.09(2) Å at 142(2)° (**Table 37**) which is statistically equivalent to **49a**-**49d** 2.017(18)-2.091(18) Å at 138.0(18)-151(2)°.

For **51b** (R = ^{i}Pr) has both intramolecular C(1)–O(1)···H(2)–N(2) hydrogen bonding like **49a**-**49d** and **51a** but also hydrogen bonding by symmetry through N(1)–H(1)···O(2*)–C(5*) at 1.979(15) Å at 166.0(19)° from one molecule of **51b** to another molecule of **51b** (**Figure 21**, right). As a consequence, the intramolecular C(1)–O(1)···H(2)–N(2) hydrogen bond is shortened significantly from 2.09(2) Å (for **51a**) to 1.925(17) Å (**Table 28**); however the bond angle

remains largely consistent with a value of 151(2)° (138.0(18)-151(2)° for **49a**-**49d** and **51a**).

Additionally, this can be seen in bond length changes to the PC(O) phosphinocarboxamide core. In comparison to **51a** the P(1)–C(1) bond for **51b** is lengthened from 1.8810(19) Å to 1.9015(15) Å and C(1)–O(1) from 1.224(2) Å to 1.2416(18) Å (**Table 36**). Further comparative trigonal distortion of the phosphinocarboxamide core is seen for **51b.** With an increase in the P(1)–C(1)–O(1) angle to 124.29(11) for **51b** (from 118.07(14)-121.44(12)° for **49a**-**49d** and **51a**) and a decrease in the P(1)–C(1)–N(1) angle to 112.64(11)° for **51b** (from 117.75(15)-113.31(11)° for **51a** and **49a**-**49d**, **Table 36**).

Table 36. Selected bond lengths (Å) and angles (°) for **7f** and **7g**.[a]

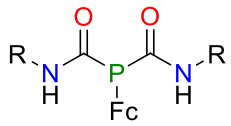
	**51a** R = Cy	**51b** R = *i*Pr
P(1)–C(1)	1.8810(19)	1.9015(15)
C(1)–O(1)	1.224(2)	1.2416(18)
C(1)–N(1)	1.336(3)	1.3254(19)
N(1)–C(2)	1.470(3)	1.4684(19)
P(1)–C(1)–O(1)	118.07(14)	124.29(11)
P(1)–C(1)–N(1)	117.75(15)	112.64(11)
N(1)–C(1)–O(1)	123.91(18)	123.06(14)

Table 37. Hydrogen-bonding geometry (Å, °) for **51**-**51b.** [a] Symmetry operation applied $\frac{1}{2}-x,\frac{1}{2}-y,\frac{1}{2}-z$

D–H···A	D–H	H···A	D···A	D–H···A
(**51a**) N(1)–H(1)···O(2)	0.868(17)	2.09(2)	2.827(2)	142(2)
(**51b**) N(1)–H(1)···O(2)	0.865(15)	1.925(17)	2.7158(17)	151(2)
(**51b**) N(2)–H(2)···O(1)[a]	0.864(14)	1.979(15)	2.8248(17)	166.019

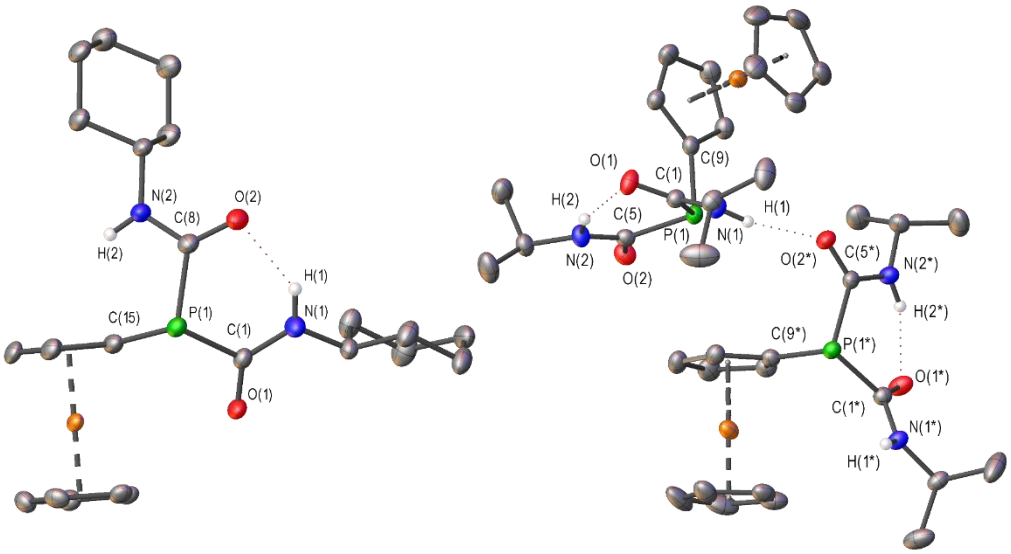


Figure 21. *Crystal structures of (left)* ***51a*** *and (right)* ***51b****. Hydrogen atoms with the exception of H(1)/H(1*) and H(2)/H(2*) have been omitted for clarity. Thermal ellipsoids are set at the 50% probability level.*

3.3.6.3 Mixed addition product: 1-(4,6-dioxo-1,3,5-triphenyl-1,3,5-triazinan-2-yl)-1-ferrocenyl-*N*-phenylphosphinocarboxamide, **56**

In an attempt to obtain the X-ray crystal structure of the diinsertion-cyclisation product **52a**, a reaction of 10 mol% **40**, 6.0 eq. PhN=C=O and 1.0 eq. $FcPH_2$ was performed. Following column chromotography of the crude product with hexane:chloroform. A fraction suspected of possibly being **52a** was collected, and after slow evaporation of the solvent, a small quantity of orange crystals formed, X-ray crystallographic analysis revealed the compound to not be **52a**, but instead serendipitous formation of 1-(4,6-dioxo-1,3,5-triphenyl-1,3,5-triazinan-2-yl)-1-ferrocenyl-*N*-phenylphosphinocarboxamide, compound **56** (**Figure 22**). **56** is novel and there are no examples in the literature of a species that has undergone a mixed reaction from single hydrophosphination and an isocyanurate-type insertion. The plausible insertion of the isocyanurate side product into the P-H bond (from $FcPH_2$) has resulted in the formation of a new

C-H bond along with the subsequent loss of one of the carbonyl moieties of the ring from the isocyanurate substrate (**Figure 22**).

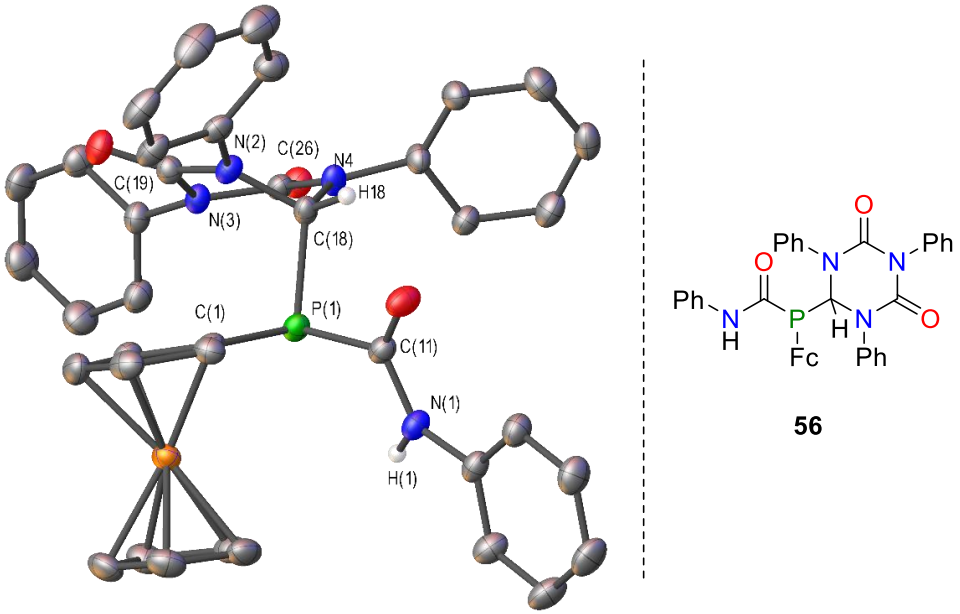
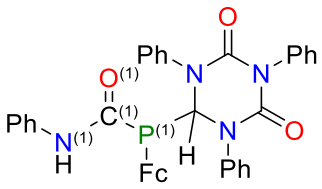
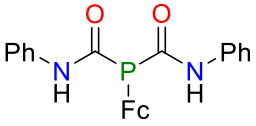


Figure 22. *(left) Crystal structure of* ***56,*** *minor disorder components and hydrogen atoms with the exception of H(1), H(2) and H(18) have been omitted for clarity. Thermal ellipsoids are set at the 50% probability level. (Right) schematic structure of* ***56****.*

The phosphinocarboxamide moiety of **56** has statistically identical bond lengths to the phosphinocarboxamide moiety of **52a**. With bond lengths of 1.893(2) Å for the P(1)-C(1) bond (*vs.* 1.8825(15) Å for **52a**), 1.223(3) Å for the C(1)-O(1) bond (*vs*. 1.2165(18) Å for **52a**) and 1.354(3) Å for the C(1)-N(1) bond (*vs*. 1.3526(18) Å for **52a**) (**Table 38**). Furthermore, trigonal distortion is seen the N-C(O)-P core with both lengthened P(1)–C(1)–O(1) and N(1)–C(1)–O(1) angles at 122.91(17)° and 124.9(2)°, as well as a shortened P(1)–C(1)–N(1) angle at 112.22(17), giving analogous trigonal distortion to that observed for **52a** (**Table 38**).

Table 38. Selected bond lengths (Å) and angles (°) for the 1-(phosphinocarboxamide) moieties of **56** and **52a**

	 **56**	 **52a**
P(1)–C(1)	1.893(2)	1.8825(15)
C(1)–O(1)	1.223(3)	1.2165(18)
C(1)–N(1)	1.354(3)	1.3526(18)
P(1)–C(1)–O(1)	122.91(17)	119.75(11)
P(1)–C(1)–N(1)	112.22(17)	114.16(10)
N(1)–C(1)–O(1)	124.9(2)	125.68(13)

The 1-(4,6-dioxo-1,3,5-triazinan-2-yl) moiety of **56** contains a symmetrical ring structure of C-N bonds (**Table 39**). The “ortho” C-N bond lengths for C(2)-N(2) and C(2)-N(4) are statistically identical at 1.458(3) Å and 1.449(3) Å respectively. The “Meta” statistically identical C-N bond lengths for N(2)-C(3) and N(4)-C(4) are significantly shortened to 1.357(3) Å and 1.356(3) Å. The “Para” statistically identical C-N bond lengths for C(3)-N(3) and C(4)-N(3) are somewhere in between “ortho” and “meta” values at 1.417(3) Å and 1.422(3) Å.

The “ortho” C-N bond lengths are ~0.4 Å longer than C-N bonds of triphenyl isocyanurate (~1.389(2)-1.395(3) Å, **Table 39**), suggesting a higher degree of single bond character. Comparatively, the “meta” C-N bond lengths are significantly shortened by ~0.4 Å compared to triphenyl isocyanurate suggesting higher double bond character and the “para” C-N bonds are only slightly lengthed at ~0.1 Å in comparison. The C=O bond lengths of **56** are unaffected, being statistically identical to C=O bond lengths of triphenyl isocyanurate at 1.224(4) Å and 1.213(3) Å *vs*. 1.204(2)-1.210(2) Å.

Table 39. Selected bond lengths (Å) and angles (°) for the 1-(4,6-dioxo-1,3,5-triazinan-2-yl) moiety of **56** and triphenyl isocyanurate

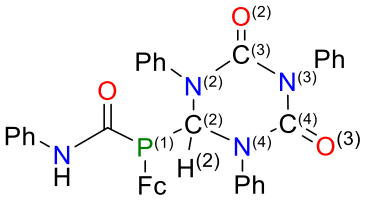
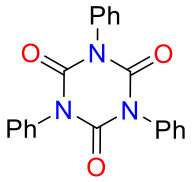
	 **56**	
P(1)-C2)	1.918(2)	-
C(2)-H(2)	0.980(2)	-
C(2)-N(2)	1.458(3)	~1.389(2)-1.395(3)
N2-C(3)	1.357(3)	-
C(3)-N(3)	1.417(3)	-
N(3)-C(4)	1.422(3)	-
C(4)-N(4)	1.356(3)	-
N(4)-C(2)	1.449(3)	-
C(3)=O(2)	1.224(4)	~1.204(2)-1.210(2)
C(4)=O(3)	1.213(3)	-
P(1)–C(1)–O(1)	122.91(17)	-
P(1)–C(1)–N(1)	112.22(17)	-
N(1)–C(1)–O(1)	124.9(2)	-
N(4)-C(2)-N(2)	108.11(18)	-
C(2)-N(2)-C(3)	116.33(18)	-
N(2)-C(3)-N(3)	113.07(19)	115.05(16)-115.19(17)
C(3)-N(3)-C(4)	121.96(19)	124.38(16)-125.11(16)
N(3)-C(4)-N(4)	112.96(19)	-
C(4)-N(4)-C(2)	117.48(19)	-

Table 40. Hydrogen-bonding geometry (Å, °) for **51**-**51b.** [a] Symmetry operation applied 1-X,1-Y,1-Z

D–H···A	D–H	H···A	D···A	D–H···A
N(1)–H(1)···O(2)[a]	0.882(17)	2.153(19)	2.994(3)	160(3)
C(13)–H(13)···O(1)	0.93000(3)	2.3053(17)	2.9049(17)	121.79(4)

56 crystallises as a pair via hydrogen bonding from one molecule's amide N-H group to a carbonyl C=O moiety of a 1-(4,6-dioxo-1,3,5-triazinan-2-yl) group of another molecule of **56**, at a bond length 2.9049(17) Å at 121.79(4)° (**Table 40** and **Figure 23**). Additionally, there is an internal hydrogen bond from the C=O carboxamide moiety to the nearby aryl *ortho* hydrogen C(13)–H(13)···O(1) at a bond length of 2.994(3) Å and angle of 121.79(4)° (**Table 40**). Previously discussed **49a**-**49d** and **51a**-**51b** also contain a similar phosphinocarboxamide moiety however unlike **56** no C(13)–H(13)···O(1) internal hydrogen bonding is present. It is however present for carbamoylphosphine oxide **44e** (at a bond length of 2.8182(17)-2.8639(17) Å at 122.29(9)-123.08(9)°, Chapter 2.3.4.1, **Table 12**) and for thiocarbamoylphosphine oxide **45e** (at a bond length of 3.167(13) Å at 127.30(8)°, Chapter 2.3.4.2, **Table 18**).

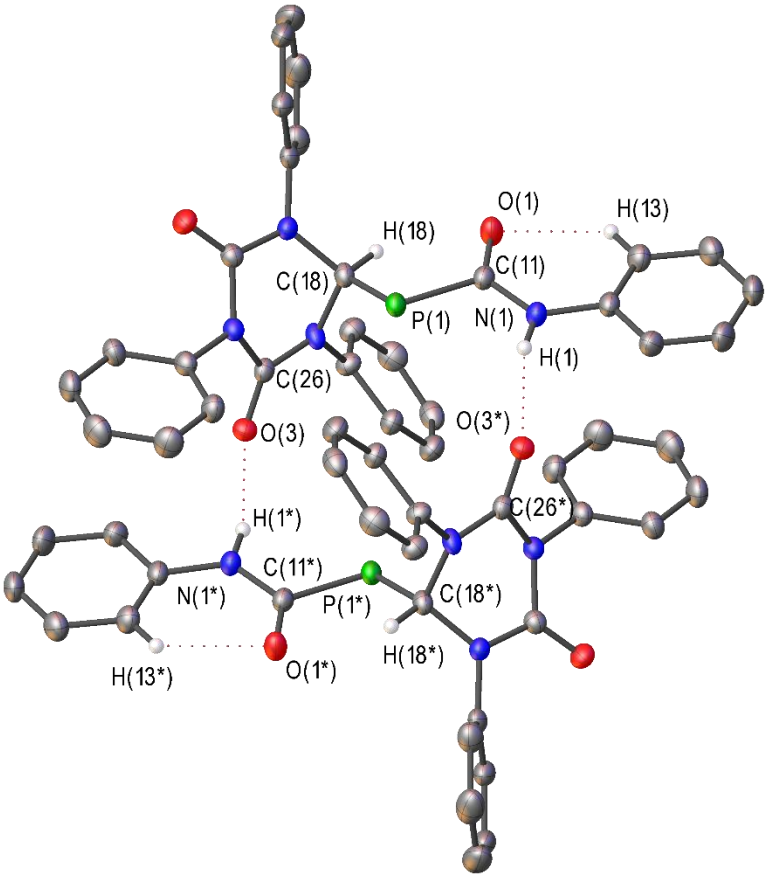


Figure 23. *Crystal structure of* ***56****, with symmetry operator 1-X,1-Y,1-Z applied. The ferrocenyl moiety, minor disorder components and hydrogen atoms with the exception of H(1), H(2), H(13) and H(18) have been omitted for clarity. Thermal ellipsoids are set at the 50% probability level.*

3.4 Conclusions

Initial catalyst-free hydrophosphination reactions of PhN=C=O with $FcPH_2$ in solution (at 25 °C or 60 °C) were unsuccessful. Attempts with $FcPH_2$ at 60 °C neat gave an 80% conversion: however, forming only an 11% and 46% mixture of the single (**48a**) and double (**49a**) hydrophosphination products. Thus, a catalyst was deemed necessary for hydrophosphination reactions with $FcPH_2$.

Precatalyst **40** (5.0 mol%, at 60 °C for 16 hours) catalysed the double hydrophosphination of PhN=C=O yielding desired product **49a** in excellent conversions (89% along with 6% of unexpected and rare **51a** a product from diinsertion-cyclisation). functionalised isocyanates were well tolerated for both electron withdrawing (R = 3-Cl, 73%) and electron donating groups (R = 4-OMe and 4-Me, 84 and 84%, 55-66% isolated yields). Further to this, alkyl isocyanates (R = Cy, ^{i}Pr and ^{t}Bu) were very well tolerated albeit requiring a higher temperature of 60 °C (6-97% conversions and 63-73% yield).

Surprisingly under more forcing conditions such as increasing catalyst loading of **40**, temperature or isocyanate concentration none of the expected double-diinsertion or polyinsertion[115,117] products formed; instead novel diinsertion products formed, **51**. In highly concentrated solutions (~4M in C_6D_6 with 1.0 eq., $FcPH_2$ + 6.0 eq. aryl isocyanate) with increased loading of **40** (10 mol%), moderate to excellent conversions of the diinsertion-cyclisation products, **51a**-**51d** could be formed with functionalised isocyanates being well tolerated. (R = Ph, 4-OMe, 4-Me, 3-Cl; 78-89%). Additionally, there is aryl isocyanate selectivity for diinsertion-cyclisation; with alkyl isocyanates not undergoing diinsertion-cyclisation at all.

Solvent selectivity is crucial to single or double hydrophosphination selectivity whereby changing the solvent from non-coordinating C_6D_6 to coordinating THF

slows the reaction down. Whereby (at 60 °C) after 3 days a 1:1 mixture of the single (**48a**) to double (**49a**) hydrophosphination products form.

Changing the P-H unit scope from $FcPH_2$ to $AdPH_2$ showed some neat catalyst-free reactivity at 60 °C forming 40% single and 15% double hydrophosphination product; however, conversions could not be improved further. As expected, the use of the primary alkyl phosphine $AdPH_2$ proved more difficult than with $FcPH_2$ requiring 10 mol% of precatalyst **40** (at 60 °C with an increased time of 48 hr) to afford a higher ratio of desired double hydrophosphination along with a small amount of the diinsertion-cyclisation products.

Interestingly, under the same conditions utilising functionalised aryl isocyanates (R = 4-OMe, 4-Me, 3-Cl) only the diinsertion-cyclisation products formed in 72% conversion with no double hydrophosphination products. However, under the same conditions utilising alkyl isocyanates (R = Cy and ^{t}Bu) changed the selectivity back to double hydrophosphination in high conversions (81 and 71%). Suggesting the electronics of the aryl group affect the selectivity more when $AdPH_2$ is used (*vs.* $FcPH_2$) however for R = Cy a small amount (13%) of the diinsertion-cyclisation was present (contrary to findings for $FcPH_2$ and alkyl isocyanates).

X-ray crystal structures of $FcP(C(O)NH(R))_2$ double hydrophosphination products **49a**-**49d** (R = Ph, *p*-Tol, 4-OMe, 3-Cl) and **50a**-**50b** (R = Cy, ^{i}Pr) were obtained. All (except **50b**) contain very similar bond angles and lengths comparable to $PhP(C(O)NH(Ph))_2$ (e.g. C(1)–N(1) 1.336(3)-1.356(2) Å for **49a**-**49d** and **50a** versus 1.339(3)-1.343(3) Å) and slightly shorter intramolecular C(1)–O(1)···H(2)–N(2) hydrogen bonds (2.042(16)-2.091(18) Å for **49a**-**49d** and **50a** versus 1.8935(16)-1.9715(15) Å). Additionally, trigonal distortion across the PC(O)N moiety is also seen, consistent with the literature for

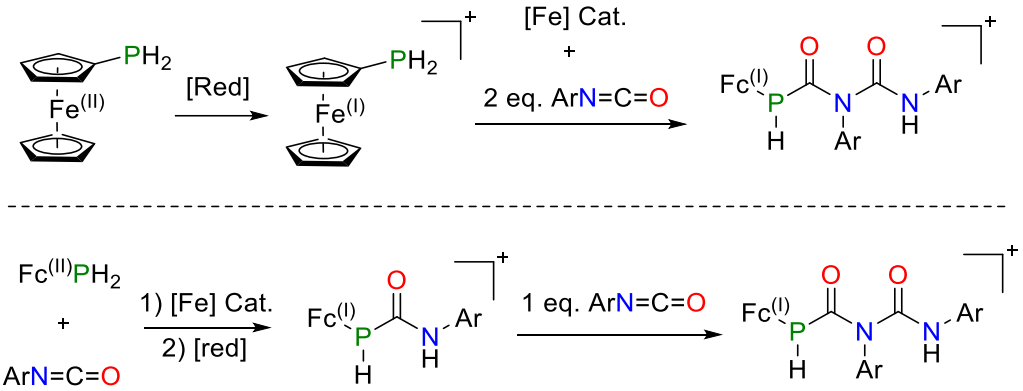
$PhP(C(O)NH(Ph))_2$ (e.g. N(1)-C(1)-O(1) 13.91(18)-125.68(13)° for **49a**-**49d** and **50a** versus 123.82(19)-126.2(2)°).[152]

In addition to an intramolecular hydrogen bond **50b** also contains a shorter hydrogen bond by symmetry through N(1)–H(1)···O(2*)–C(5*) to another molecule of **50b**, resulting in further trigonal distortion (e.g. for P(1)-C(1)-O(1) an angle of 124.29(11) ° versus 118.07(14)-121.44(12) ° for **49a**-**49d** and **50a**).

Overall, all these reactions demonstrate that whilst hydrophosphination of isocyanates with primary phosphines can proceed somewhat catalyst-free neat, the reaction typically forms impractical and low yielding mixtures of the desired hydrophosphination products. However, the use of a precatalyst **40** can selectively synthesise the expected and desired products such as single hydrophosphination or double hydrophosphination products. In addition (and depending on the nature of the particular R group, of RN=C=O) unexpected and rare diinsertion-cyclisation products can be formed. Highlighting the unpredictable (but potentially promising for future novel reactions) nature of hydrophosphination-type reactions with isocyanates

3.5 Future Work

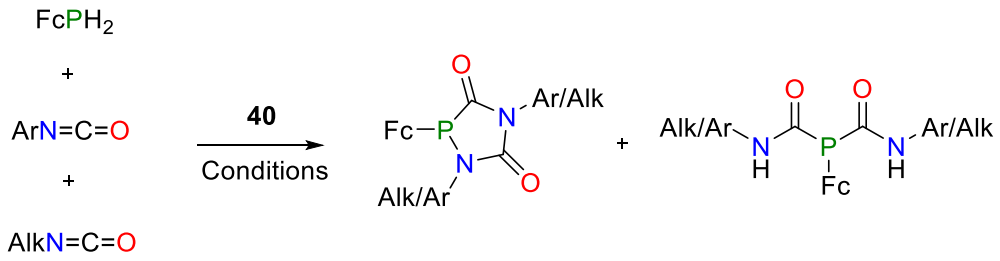
Further work on chemoselectivity between hydrophosphination and diinsertion type products is needed, potentially reducing the Fe(II) atom of the ferrocenyl moiety (of $FcPH_2$ or FcPH(C(O)NH(Ar)) to Fe(I) may reduce the nucleophilicity of the Phosphorus atom. Plausibly deactivating the P-H bond from nucleophilic attack and thus favouring nucleophilic attack on the carboxamide amide moiety overall favouring a single hydrophosphination-diinsertion type product (**Scheme 54**). Further to this thinking increasing the electrophilicity of the aryl isocyanate substrate with electron withdrawing groups such as $-NO_2$, could further bias diinsertion products (or even polyinsertion products).



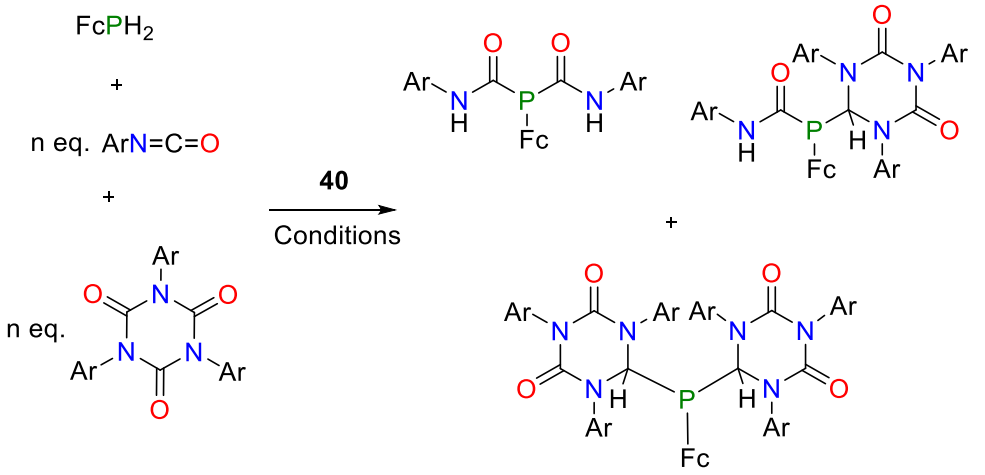
Scheme 54. *(Above) Proposed initial reduction of ferrocenyl phosphine followed by single hydrophosphination-diinsertion or (below) initial single hydrophosphination-monoinsertion with reduction of ferrocene motif of the phosphinocarboxamide followed by diinsertion.*

Other emergent ideas for the development of novel products or methodologies derive from utilising Mixed substrate reactions. In which 1 equivalent of alkyl isocyanate and aryl isocyanate or two different aryl isocyanates could be utilised to synthesise asymmetric products; as well as investigating if this mixed approach affects chemoselectivity for double hydrophosphination versus diinsertion-cyclisation. (**Scheme 55**, above).

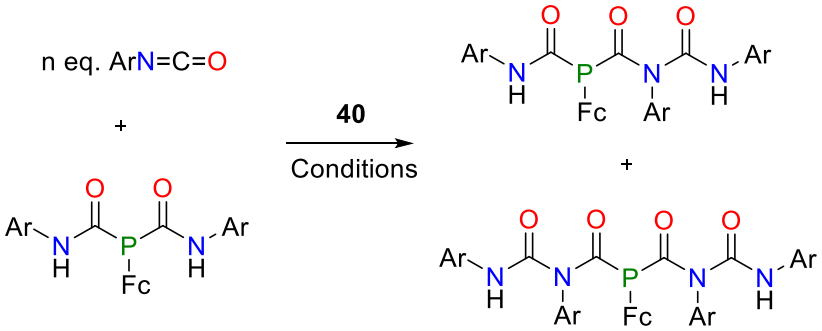
Mixed alkyl, aryl isocyanate hydrophosphiantion or diinsertion-cylisation



Hydrophosphination with isocyanurate insertion



Linear diinsertion



Scheme 55. *(Above) Mixed reactions with alkyl and aryl isocyanates synthesising mixed alkyl/aryl diinsertion-cyclisation and double hydrophosphination products, (middle) reactions with aryl isocyanate and aryl cyclotrimers as substrates, attempting to synthesise similar mixed products to X (Ar = Ph) and (bottom) utilising the double hydrophosphination product as the initial phosphorus source (instead of $FcPH_2$) to try and form linear diinsertion products; instead of cyclic diinsertion products.*

In further expansion based on the serendipitous synthesis of crystals of **56** (containing a cyclotrimer-like and carboxamide motif), instead of just being limited to isocyanates as the electrophilic substrate; the electrophilic substrates could be a mixture of aryl isocyanate and cyclotrimer (**Scheme 55,** middle). With the rationale behind the methodology of just either reproducing the synthesis of **56** or forming another species whereby two equivalents of isocyanurate have undergone insertion into two P-H bonds.

Despite forcing conditions linear diinsertion type compounds were never observed only cyclic (unlike previous literature with $HPPh_2$).[115] In pursuit of these types of compounds it would be interesting to determine if using the double hydrophosphination products as the initial phosphorus-based starting material instead of $FcPH_2$ with multiple equivalents of isocyanate could help circumvent the cyclisation problem (**Scheme 55,** below)

3.6 Experimental Procedures

3.6.1 Double hydrophosphination with $FcPH_2$

3.6.1.1 Initial catalyst-free Variation of solvent type and concentration

In an inert atmosphere glovebox, an oven dried Young's tap modified NMR tube was charged with $FcPH_2$ (1.0 eq., 31.8 mg, 0.146 mmol) and PhN=C=O (2.0 eq., 31.7 µL, 0.292 mmol) in 2-MeTHF (4.0 eq., 0.6 mL) or C_6D_6 (4.0 eq., 0.6 mL). The sealed tube was left at 25 °C for 16 hours. PPh_3 (1.0 eq., 0.146 mmol) was added and a ^{31}P NMR spectrum was recorded. Respective NMR spectroscopic yields (conv. from $FcPH_2$: conv. to **48a**: conv to **49a** %) = (8: 1: 2 %), (14: 0: 0 %), (6: 0: 0 %) and (14: 0: 0 %) respectively.

3.6.1.2 Initial neat catalyst-free variation of temperature

In an inert atmosphere glovebox, an oven dried screw cap vial was charged with $FcPH_2$ (1.0 eq., 31.8 mg, 0.146 mmol) and PhN=C=O (2.0 eq., 31.7 µL, 0.292 mmol). The sealed vial was left at 25 °C or heated to 60 °C for 16 hours and PPh_3 (1.0 eq.) and C_6D_6 (0.6 mL) were added and a ^{31}P NMR spectrum was recorded. Respective NMR spectroscopic yields (conv. from $FcPH_2$: conv. to **48a**: conv to **49a** %) = (21: 0: 1 %) and (80: 11: 46 %) respectively.

3.6.1.3 Initial neat catalyst-free variation of phenyl isocyanate concentration

In an inert atmosphere glovebox, an oven dried screw cap vial was charged with $FcPH_2$ (1.0 eq., 31.8 mg, 0.146 mmol) and PhN=C=O (4.0 eq. or 8.0 eq.). The sealed vial was heated to 60 °C for 16 hours PPh_3 (1.0 eq.) and C_6D_6 (0.6 mL) was added and a ^{31}P NMR spectrum was recorded. Respective NMR

spectroscopic yields (conv. from $FcPH_2$: conv. to **48a**: conv to **49a** %) = (94: 43: 25 %) and (78: 34: 23 %).

3.6.1.4 Initial catalytic variation of temperature and phenyl isocyanate concentration

In an inert atmosphere glovebox, an oven dried Young's tap modified NMR tube was charged with $FcPH_2$ (1.0 eq., 31.8 mg, 0.146 mmol) and PhN=C=O (2.0 eq., or 3.0 eq.). The sealed tube was left at 25 °C or heated to 60 °C for 16 hours. PPh_3 (1.0 eq.) and C_6D_6 (0.6 mL) were added and a ^{31}P NMR spectrum was recorded. Respective NMR spectroscopic yields (conv. from $FcPH_2$: conv. to **49a**: conv to **51a** %) = (99: 89: 6 %), (99: 72: 15 %), (99, 88: 7) and (99: 82: 8%) respectively.

3.6.1.5 General procedure for the double hydrophosphination of isocyanates with $FcPH_2$ (NMR yields)

In an inert atmosphere glovebox, an oven dried Young's tap modified NMR tube was charged with $Fe(C_6H_3\text{-}2,6\text{-}Mes_2)_2$, (0.05 eq., 5.0 mg, 0.00732 mmol) $FcPH_2$ (1.0 eq., 31.8 mg, 0.146 mmol) and isocyanate (2.0 eq., 0.292 mmol) in C_6D_6 (0.6 mL). The sealed tube was either left at 25 °C (**49a**-**49d**) or heated at 60 °C (**51a**-**51c**). PPh_3 (1.0 eq. 0.146 mmol) was then added and a ^{31}P NMR spectrum was recorded. The yield was calculated by integrating the ^{31}P NMR spectroscopic signals corresponding to the product relative to the PPh_3 internal standard. Respective NMR spectroscopic yields for conv. **49a-49d** (conv. to **49a-d**: conv to **52a-d**) and conv. **51a**-**51c** = **49a** (87:4 %), **49b** (84:7 %), **49c** (84:11 %), **49d** (73:11 %), **51a** (97%), **51b** (99%) and **51c** (96%).

3.6.1.6 Double hydrophosphination of aryl isocyanates with $FcPH_2$ (isolated yields) **49a**-**49d**

To a solution of $FcPH_2$ (1.0 eq., 204 mg, 0.936 mmol) and $Fe(C_6H_3\text{-}2,6\text{-}Mes_2)_2$ (0.05 eq., 30 mg, 0.044 mmol) in toluene (4.0 mL) was added to aryl isocyanate (2.0 eq., 1.8 mmol) and the reaction stirred at room temperature overnight. During this time the solution was observed to change from orange to dark red-orange. The remaining procedure was carried out in air, as the product is air stable. Volatiles were removed *in vacuo* to afford the crude product as a dark orange flocculent solid. This was then dissolved in the minimum amount of CH_2Cl_2 purified by flash column chromatography (silica gel 60, eluting with 2-4% ethyl acetate in toluene) to afford pure **49a**-**49d** as a dark orange solid. Crystals suitable for single crystal X-ray diffraction were grown from slow diffusion of hexane into a concentrated solution of **49a**-**49d** in dichloromethane, (*ca* 1:1 hexane:dichloromethane).

3.6.1.7 Double hydrophosphination of alkyl isocyanates with $FcPH_2$ (isolated yields) **51a**-**51c**

In an inert atmosphere glovebox, a 25 mL oven dried Young's tap modified flask was charged with $Fe(C_6H_3\text{-}2,6\text{-}Mes_2)_2$, (0.05 eq., 30.0 mg, 0.044 mmol), $FcPH_2$ (1.0 eq., 204 mg, 0.936 mmol) and isocyanate (2.0 eq., 0.292 mmol) in C_6H_6 (4.0 mL) and the reaction stirred at 60 °C overnight. The remaining procedure was carried out under an inert atmosphere as the products are mildly air-sensitive. Degassed H_2O (5.0 mL) was added to the reaction mixture for *ca* 5 minutes and then the two layers were allowed to separate. The upper organic layer was filtered into a Schlenk flask containing $MgSO_4$ (~10 g) and the remaining aqueous layer was washed with toluene (2 x 5 mL, R = ^{i}Pr or tBu) or (4 × 5.0 mL, R = Cy) and the organic extracts combined into the flask containing

$MgSO_4$. The organic-$MgSO_4$ mixture was stirred (*ca* 5 minutes) and filtered. Volatiles were removed *in vacuo* to afford the crude product as a dark orange-red to dark brown solid. This was then dissolved in the minimum amount of 1:5 hexane: toluene (~5.0 mL). Storing the subsequent solution at -30 °C for 24-48 hours resulted in the formation of dark brown-orange crystals suitable for X-ray diffraction.

3.6.1.8 *In situ* single hydrophosphination of PhN=C=O in THF

In an inert atmosphere glovebox, an oven dried Young's tap modified NMR tube was charged with $Fe(C_6H_3\text{-}2,6\text{-}Mes_2)_2$ (0.05 eq., 2.5 mg, 0.00037 mmol), $FcPH_2$ (1.0 eq., 16.1 mg, 0.074 mmol) and PhN=C=O (1.0 eq., 0.074 mmol) in THF (0.6 mL). The sealed tube was heated at 60 °C for 72 hours. Utilising a sealed C_6D_6 insert the conversion was quantified by relative integration of the ^{31}P NMR spectrum. Respective NMR spectroscopic yields: conv. from $FcPH_2$ = 86%; conv. to **48a** = 40% and conv to **49a** = 44%.

3.6.2 Diinsertion-cyclisation with $FcPH_2$

3.6.2.1 Catalytic diinsertion-cyclisation optimisation variation of isocyanate concentration, catalyst loading, solvent concentration or temperature

In an inert atmosphere glovebox, an oven dried Young's tap modified NMR tube was charged with $FcPH_2$ (1.0 eq., 31.8 mg, 0.146 mmol), PhN=C=O (2.0 eq., 6.0 eq., 8.0 eq. or 50 eq.) and $Fe(C_6H_3\text{-}2,6\text{-}Mes_2)_2$ (0.05 eq or 0.10 eq) in C_6D_6 (0.5 mL or 0.25 mL or neat). The sealed vial was left at 25 °C or heated to 60 °C or 80 °C for 16 hours. PPh_3 (1.0 eq.) and if necessary C_6D_6 (0.25 mL or 0.50 mL) was added and a ^{31}P NMR spectrum was recorded. (See **Table 41**, for relative conversions of **49a** and **52a**)

Table 41. *Initial catalytic diinsertion-cyclisation of PhN=C=O with $FcPH_2$*

Entry	$FcPH_2$: PhN=C=O eq.	Temp. (°C)	Cat. mol%	Solv.	Conv. **49a** (%)	Conv. **52a** (%)
1	1.0:2.0	60	5.0	C_6D_6	86	6
2	1.0:2.0	25	10	C_6D_6	74	8
3	1.0 :6.0	60	5.0	C_6D_6	35	41
4	1.0 :6.0	85	5.0	C_6D_6	21	44
5	1.0:6.0	85	10	C_6D_6	12	58
6	1.0:6.0	60	5.0	Neat	17	78
7	1.0:50	60	5.0	Neat	35	63
8	1.0:8.0	85	10	C_6D_6[c]	12	80

3.6.2.2 General procedure for the diinsertion-cyclisation of aryl isocyanates with $FcPH_2$ (NMR yields)

In an inert atmosphere glovebox, an oven dried screw cap vial was charged with $Fe(C_6H_3\text{-}2,6\text{-}Mes_2)_2$ (0.1 eq., 10.0 mg, 0.0146 mmol), $FcPH_2$ (1.0 eq., 31.8 mg, 0.146 mmol) and isocyanate (8.0 eq., 1.168 mmol) in C_6D_6 (0.25 mL). The sealed vial was heated at 85 °C. PPh_3 (1.0 eq. 0.146 mmol) and C_6D_6 (0.25 mL) was then added and a ^{31}P NMR spectrum was recorded. The yield was calculated by integrating the ^{31}P NMR spectroscopic signals corresponding to the product relative to the PPh_3 internal standard. Respective NMR spectroscopic yields for conv. (conv. to **52a**: conv to **49a** %) = **52a** (80:12 %), **52b** (78:14 %), **52c** (79:16 %) and **52d** (89:5 %).

3.6.2.3 Diinsertion-cyclisation of phenyl isocyanate with $FcPH_2$ (isolated yield)

In an inert atmosphere glovebox, an oven dried 5.0 mL screw cap vial was charged with $FcPH_2$ (1.0 eq., 61.4 mg, 0.294 mmol), PhN=C=O (6.0 eq., 192

µL, 1.764 mmol and $Fe(C_6H_3\text{-}2,6\text{-}Mes_2)_2$ (0.1 eq., 20 mg, 0.0292 mmol). The sealed vial was heated to 85 °C for hours. In a Schlenk flask the dark orange solid formed was dried i*n vacuo* at 60 °C for 3 hours forming a foam-like flocculent solid (expanding to a volume of ~5.0 mL). The flocculent solid was washed with degassed ethanol whilst at the same time physically stirring the solid with a spatula under a flow of argon. After filtration and drying 58.6 mg (44%) of **52a** was obtained as a light orange solid.

3.6.3 Double hydrophosphination and diinsertion-cyclisation with $AdPH_2$

3.6.3.1 Initial catalyst-free optimisation variation of temperature and of solvent

In an inert atmosphere glovebox, an oven dried Young's tap modified NMR tube was charged with $AdPH_2$ (1.0 eq., 0.0732 mmol) and PhN=C=O (2.0 eq., 0.146 mmol) in C_6D_6 (0.6 mL) or neat. The sealed tube was left at 25 °C or heated at 60 °C for 16 hours. A ^{31}P NMR spectrum was recorded with conversions being relative. Respective NMR spectroscopic yields for (conv. from $AdPH_2$: conv. to **53a**: conv to **54a** %) = (0:0:0 %), (2,0,2 %), (2, 0, 0%) and (55:39:15 %)

3.6.3.2 Initial catalytic optimisation reactions for double hydrophosphination with $AdPH_2$ and PhN=C=O variation catalyst loading, temperature or time

In an inert atmosphere glovebox, an oven dried Young's tap modified NMR tube was charged with $AdPH_2$ (1.0 eq., 0.0732 mmol), PhN=C=O (2.0 eq. or 4.0 eq.) $Fe(C_6H_3\text{-}2,6\text{-}Mes_2)_2$ (0.05 eq. or 0.10 eq.) and C_6D_6 (0.6 mL). The sealed tube was either left at 25 °C or heated at 60 °C for either 16 or 32 hours. A ^{31}P NMR spectrum was recorded with conversions being relative. Respective NMR

spectroscopic yields for (conv. from $AdPH_2$: conv. to **54a'**: conv to **54a** %) (5, 0, 0 %), (57, 5, 33%), (90, 4, 48 %) and (100, 13, 58 %).

3.6.3.3 General procedure for the double hydrophosphination or diinsertion-cyclisation of isocyanates with $AdPH_2$ (NMR yields)

In an inert atmosphere glovebox, an oven dried Young's tap modified NMR tube was charged with $AdPH_2$ (1.0 eq., 0.0732 mmol), PhN=C=O (4.0 eq.) $Fe(C_6H_3\text{-}2,6\text{-}Mes_2)_2$ (0.10 eq.) and in C_6D_6 (0.6 mL). The sealed tube was heated at 60 °C for 32 hours. A ^{31}P NMR spectrum was recorded with conversions being relative. Respective NMR spectroscopic yields for (conv. to double hydrophosphination : diinsertion-cyclisation product %) **54a** (58:10 %), **55b** (0:72 %), **55c** (0:72 %), **55d** (0:72 %), **54b** (81:13 %) and **54c** (71:0 %).

3.6.4 Stoichiometric NMR reactions

3.6.4.1 Stoichiometric reaction of $FcPH_2$ and $Fe(C_6H_3\text{-}2,6\text{-}Mes_2)_2$

$Fe(C_6H_3\text{-}2,6\text{-}Mes_2)_2$ (1.0 eq., 33.25 mg, 0.0487 mmol) was dissolved in C_6D_6 (0.6 mL) in a Young's NMR tube along with $FcPH_2$ (1.0 eq., 10.62 mg, 0.0487 mmol). The reaction was carried out at room temperature and was monitored by ^1H and ^{31}P NMR spectroscopy.

3.6.4.2 Stoichiometric reaction of PhN=C=O and $Fe(C_6H_3\text{-}2,6\text{-}Mes_2)_2$

$Fe(C_6H_3\text{-}2,6\text{-}Mes_2)_2$ (1.0 eq., 33.25 mg, 0.0487 mmol) was dissolved in C_6D_6 (0.6 mL) in a Young's NMR tube along with PhN=C=O (1.0 eq., 5.29 µL, 0.0487 mmol). The reaction was carried out at room temperature and was monitored by ^1H and ^{31}P NMR spectroscopy.

3.6.4.3 Stoichiometric reaction of PhN=C=O, $FcPH_2$ and $Fe(C_6H_3\text{-}2,6\text{-}Mes_2)_2$

$Fe(C_6H_3\text{-}2,6\text{-}Mes_2)_2$ (1.0 eq., 33.25 mg, 0.0487 mmol) was dissolved in C_6D_6 (0.6 mL) in a Young's NMR tube along with $FcPH_2$ (1.0 eq., 10.62 mg, 0.0487 mmol) and PhN=C=O (1.0 eq., 5.29 µL, 0.0487 mmol). The reaction was carried out at room temperature and was monitored by ^{1}H and ^{31}P NMR spectroscopy.

3.6.5 Catalytic hydrophosphination with additives

3.6.5.1 Catalytic hydrophosphination of isocyanates in the presence of Hg(0)

$Fe(C_6H_3\text{-}2,6\text{-}Mes_2)_2$ (0.05 eq., 33.25 mg, 0.0487 mmol) was dissolved in C_6D_6 (0.6 mL) in a Young's NMR tube along with $FcPH_2$ (31.8 mg, 0.146 mmol) and PhN=C=O (31.7 µL, 0.292 mmol). A drop of elemental mercury) was then added to the reaction mixture. The reaction was carried out at room temperature and monitored by ^{31}P NMR spectroscopy. Conversion was quantified by integration of ^{31}P NMR spectra using PPh_3 as an internal standard.

3.6.5.2 Catalytic hydrophosphination of isocyanates in the presence of CS_2

$Fe(C_6H_3\text{-}2,6\text{-}Mes_2)_2$ (0.05 eq., 5.0 mg, 0.00732 mmol) was dissolved in C_6D_6 (0.6 mL) in a Young's NMR tube along with $FcPH_2$ (31.8 mg, 0.146 mmol) and PhN=C=O (31.7 µL, 0.292 mmol) and CS_2 (0.05 M in toluene, 14.6 µL, 0.000732 mmol). The reaction was carried out at room temperature and monitored by ^{31}P NMR spectroscopy. Conversion was quantified by integration of ^{31}P NMR spectra using PPh_3 as an internal standard.

3.6.5.3 Catalytic hydrophosphination of isocyanates in the presence of $PhPMe_2$

$Fe(C_6H_3\text{-}2,6\text{-}Mes_2)_2$ (0.05 eq., 5.0 mg, 0.00732 mmol) was dissolved in C_6D_6 (0.6 mL) in a Young's NMR tube along with $FcPH_2$ (31.8 mg, 0.146 mmol) and PhN=C=O (31.7 µL, 0.292 mmol) and $PPhMe_2$ (0.05M in toluene, 14.6 µL, 0.732 µmol). The reaction was carried out at room temperature and monitored by ^{31}P NMR spectroscopy. Conversion was quantified by integration of ^{31}P NMR spectra using PPh_3 as an internal standard.

3.6.5.4 Catalytic hydrophosphination of isocyanates in the presence of cumene

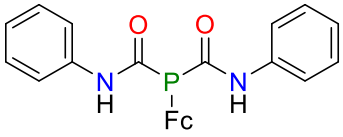
$Fe(C_6H_3\text{-}2,6\text{-}Mes_2)_2$ (0.05 eq., 5.0 mg, 0.00732 mmol) was dissolved in C_6D_6 (0.6 mL) in a Young's NMR tube along with $FcPH_2$ (31.8 mg, 0.146 mmol) and PhN=C=O (31.7 µL, 0.292 mmol) and cumene (10.7 µL, 0.0733 mol). The reaction was carried out at room temperature and monitored by ^{31}P NMR spectroscopy. Conversion was quantified by integration of ^{31}P NMR spectra using PPh_3 as an internal standard.

3.6.5.5 Catalytic hydrophosphination of Carbodiimides in the presence of 1,4-cyclohexadiene

$Fe(C_6H_3\text{-}2,6\text{-}Mes_2)_2$ (0.05 eq., 5.0 mg, 0.00732 mmol) was dissolved in C_6D_6 (0.6 mL) in a Young's NMR tube along with $FcPH_2$ (31.8 mg, 0.146 mmol) and PhN=C=O (31.7 µL, 0.292 mmol) and 1,4-cyclohexadiene (6.9 µL, 0.0733 mol). The reaction was carried out at room temperature and monitored by ^{31}P NMR spectroscopy. Conversion was quantified by integration of ^{31}P NMR spectra using PPh_3 as an internal standard.

3.6.6 Yields and characterisation for **49a**-**49d**

3.6.6.1 FcP(C(O)N(H)Ph)$_2$ (**49a**)



Dark-orange solid, 60% (87% NMR yield). Single crystals suitable for X-ray diffraction were grown from a 1:1 CH_2Cl_2:hexane solution at 25 °C.

^{1}H NMR (400 MHz, $CDCl_3$, 25 °C) δ 9.08 (s, 2H, N*H*), 7.51-7.47 (m, 4H, Ph^o), 7.36-7.30 (m, 4H, Ph^m), 7.16-7.11 (m, 2H, Ph^p), 4.62–4.60 (m, 2H, Cp *H*), 4.54-4.51 (m, 2H, Cp *H*), 4.42 (s, 5H, Cp *H*).

^{13}C{^{1}H} NMR (101 MHz; $CDCl_3$, 25 °C) δ 174.0 (d, ^1J(C,P) = 17.9 Hz, *C*O), 137.4 (s, Ph^i), 129.2 (s, Ph^m), 125.1 (s, Ph^p), 120.3 (s, Ph^o), 73.5 (d, ^1J(C,P) = 15.6 Hz, Cp *C*), 72.5 (d, ^2J(C,P) = 5 Hz, Cp *C*), 70.4 (s, Cp *C*), 67.2 (d, ^3J(C,P) = 6.5 Hz, Cp *C*).

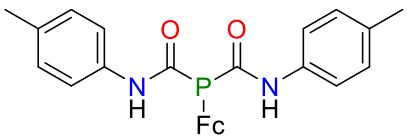
^{31}P{^{1}H} NMR (162 MHz; $CDCl_3$, 25 °C) δ -21.5 (s).

HRMS (ESI) expected 479.0582, found: 479.0581 [M + Na] (err [ppm] = 0.40).

Elemental analysis $C_{24}H_{21}N_2O_2PFe$: calcd. C 63.18, H 4.64, N 6.14; found C 62.98, H 4.56, N 6.05 %.

IR (ATR) ν/cm^{-1} 3366 (NH), 1656 (CO).

3.6.6.2 FcP(C(O)N(H)*p*-Tol)$_2$ (**49b**)



Dark-orange solid, 66% (84% NMR yield). Single crystals suitable for X-ray diffraction were grown from a 1:1 CH_2Cl_2:hexane solution at 25 °C.

^{1}H NMR (400 MHz, $CDCl_3$, 25 °C) δ 9.06 (s, 2H, N*H*), 7.37 (m, 4H, $C_6H_4{}^o$), 7.12 (m, 4H, $C_6H_4{}^m$), 4.63-4.56 (m, 2H, Cp *H*), 4.53-4.49 (m, 2H, Cp *H*), 4.41 (s, 5H, Cp *H*), 2.31 (s, 6H, C*H*$_3$).

$^{13}C\{^1H\}$ NMR (101 MHz; $CDCl_3$, 25 °C) δ 173.8 (d, ^1J(C,P) = 18.0 Hz, *C*O), 134.9 (d, ^3J(C,P) = 2.1 Hz, $C_6H_4^i$), 134.8 (s, C_6H_4), 129.7 (s, C_6H_4), 120.4 (s, C_6H_4) , 73.5 (d, ^1J(C,P) = 15.5 Hz, Cp C), 72.4 (d, ^2J(C,P) = 5.0 Hz, Cp C), 70.3 (s, Cp C), 67.5 (d, ^3J(C,P) = 6.6 Hz, Cp C), 21.1 (s, CH_3).

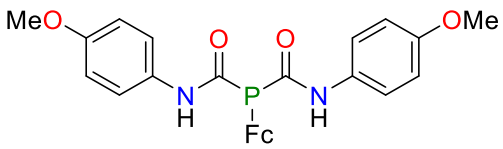
$^{31}P\{^1H\}$ NMR (162 MHz; $CDCl_3$, 25 °C) δ -22.2 (s).

HRMS (ESI) expected 507.0895, found: 507.0888 [M+Na] (err [ppm] = 1.50).

Elemental analysis $C_{26}H_{25}N_2O_2PFe$: calcd. C 64.48; H, 5.20, N 5.78; found 64.35; H 5.20, N 6.18 %.

IR (ATR) ν/cm^{-1} 3368 (NH), 1662 (CO).

3.6.6.3 FcP(C(O)N(H)(4-OMeC$_6$H$_4$))$_2$ (**49c**)



Dark-orange solid, 63% (84% NMR yield). Single crystals suitable for X-ray diffraction were grown from a 1:1 CH_2Cl_2:hexane solution at 25 °C.

^1H NMR (400 MHz, $CDCl_3$, 25 °C) δ 9.06 (s, 2H, N*H*), 7.47-7.34 (m, 4H, Ph^o), 6.91- 6.75 (m, 4H, $C_6H_4^m$), 4.64-4.51 (m, 2H, Cp *H*), 4.51 (m, 2H, Cp *H*), 4.40 (s, 5H, Cp *H*), 3.79 (s, 6H, OC*H*$_3$).

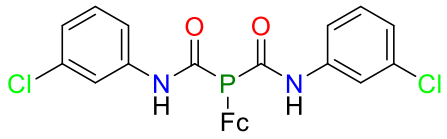
$^{13}C\{^1H\}$ NMR (101 MHz; $CDCl_3$, 25 °C) δ 173.7 (d, ^1J(C,P) = 17.6 Hz, *C*O), 156.9 (s, $C_6H_4^p$), 130.6 (d, ^3J(C,P) = 2.2 Hz, $C_6H_4^i$), 122.0 (s, C_6H_4), 114.3 (s, C_6H_4), 73.5 (d, ^1J(C,P) = 15.4 Hz, Cp *C*), 72.4 (d, ^2J(C,P) = 4.7 Hz, Cp *C*), 70.3 (s, Cp *C*), 67.5 (d, ^3J(C,P) = 6.6 Hz, Cp *C*), 55.6 (S, O*C*H$_3$).

$^{31}P\{^1H\}$ NMR (162 MHz; $CDCl_3$, 25 °C) δ -22.3 (s).

HRMS (ESI) expected: 539.0794, found: 539.0802 [M+Na] (err [ppm] = 1.60).

Elemental analysis $C_{26}H_{25}N_2O_4PFe$: calcd. C 60.48, H 4.88, N 5.43; found C 60.20, H 4.81, N 5.36 %.

3.6.6.4 FcP(C(O)N(H)3-$ClC_6H_4)_2$ (**49d**)



Dark-orange solid, 56% (73% NMR yield). Single crystals suitable for X-ray diffraction were grown from a 1:1 CH_2Cl_2:hexane solution at 25 °C.

^{1}H NMR (400 MHz, $CDCl_3$, 25 °C) δ 9.03 (s, 2H, N*H*), 7.63 (m, 2H, C_6H_4), 7.33 (m, 2H, C_6H_4), 7.33-7.23 (m, 2H, C_6H_4), 4.64 (m, 2H, Cp *H*), 4.51 (m, 2H, Cp *H*), 4.43 (s, 5H, Cp *H*).

^{13}C{^{1}H} NMR (101 MHz, $CDCl_3$, 25 °C) δ 174.2 (d, ^1J(C,P) = 19.4 Hz, *C*O), 138.3 (d, ^3J(C,P) = 2.2 Hz, $C_6H_4^i$), 134.9 (s, C_6H_4), 130.2 (s, C_6H_4), 125.2 (s, C_6H_4), 120.3 (s, C_6H_4), 118.2 (s, C_6H_4), 73.4 (d, ^1J(C,P) = 16.0 Hz, Cp *C*), 72.7 (d, ^2J(C,P) = 5.0 Hz, Cp *C*), 70.5 (s, Cp *C*), 66.5 (d, ^3J(C,P) = 6.3 Hz, Cp *C*).

^{31}P{^{1}H} NMR (162 MHz, $CDCl_3$, 25 °C) δ -20.2.

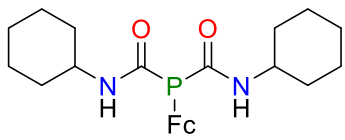
HRMS (ESI) expected: 546.9819, found: 546.9819 [M+Na] err [ppm] = 2.90).

Elemental Analysis $C_{24}H_{19}N_2O_2Cl_2PFe$: calcd. C 54.89, H 3.65, N 5.33; found C 54.78, H 3.45, N 5.19 %.

IR (ATR) v/cm^{-1} 3369 (NH), 1668 (CO).

3.6.7 Yields and characterisation for **51a-51c**

3.6.7.1 FcP(C(O)N(H)Cy)$_2$ (**51a**)



Dark-orange solid, 73% (97% NMR yield). Single crystals suitable for X-ray diffraction were grown from a 1:5 hexane:toluene solution at -30 °C.

^{1}H NMR (400 MHz, C_6D_6, 25 °C) δ 7.42 (s, 2H, N*H*), 4.45 (m, 2H, Cp *H*), 4.31 (s, 5H, Cp *H*), 4.17 (m, 2H, Cp *H*), 4.08-3.93 (m, 2H, Cy^i C*H*), 1.74 (m, 4H, Cy CH_2), 1.50-1.34 (m, 4H, Cy CH_2), 1.33-1.17 (m, 2H, Cy CH_2), 1.16-0.96 (m, 8H, Cy CH_2), 0.95-0.79 (m, 4H, Cy CH_2).

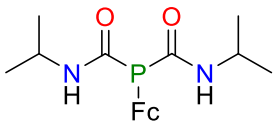
$^{13}C\{^1H\}$ NMR (101 MHz, C_6D_6, 25 °C) δ 174.5 (d, ^1J(C,P) = 15.3 Hz, *C*O), 73.4 (d, ^1J(C,P) = 14.9 Hz, Cp *C*), 71.8 (d, ^2J(C,P) = 4.5 Hz, Cp *C*), 70.7 (s, Cp *C*), 69.9 (d, ^3J(C,P) = 7.7 Hz, Cp *C*), 48.9 (s, Cy *C*H_2), 32.8 (d, ^3J(C,P) = 8.8 Hz, Cy^i *C*H), 25.7 (s, Cy *C*H_2), 24.7 (d, ^4J(C,P) = 2.8 Hz, Cy *C*H_2).

$^{31}P\{^1H\}$ NMR (162 MHz, C_6D_6, 25 °C) δ -27.0 (s).

HRMS (ESI) expected: 491.1521, found: 491.1515 [M+Na] (err [ppm] = 1.40).

Elemental analysis $C_{24}H_{33}N_2O_2PFe$: calcd C 61.55, H 7.10, N 5.98; found C 61.91, H 7.15, N 5.71 %.

3.6.7.2 FcP(C(O)N(H)^{i}Pr)$_2$ (**51b**)



Dark-orange solid, 64% (99% NMR yield). Single crystals suitable for X-ray diffraction were grown from a 1:5 hexane:toluene solution at -30 °C.

^1H NMR (400 MHz, C_6D_6, 25 °C) δ 7.29 (s, 2H, N*H*), 4.41 (m, 2H, Cp *H*), 4.27 (m, 5H, Cp *H*), 4.20-4.14 (*m*, 2H, C*H*$(CH_3)_2$), 4.12 (m, 2H, Cp *H*), 0.90 (d, ^3J(H,H) = 6.6 Hz, 6H, CH(C*H*$_3)_2$), 0.87 (d, ^3J(H,H) = 6.5 Hz, 6H, CH(C*H*$_3)_2$).

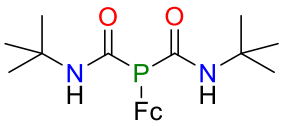
$^{13}C\{^1H\}$ NMR (101 MHz, C_6D_6, 25 °C) δ 174.6 (d, ^3J(C,P) = 15.4 Hz), 73.4 (d, ^1J(C,P) = 15.2 Hz, Cp *C*), 71.8 (d, ^2J(C,P) = 4.9 Hz, Cp *C*), 70.6 (s, Cp C), 69.6 (d, ^3J(C,P) = 7.4 Hz, Cp C), 42.3 (s, CH(*C*$H_3)_2$), 22.5 (d, ^3J(C,P) = 6.8 Hz, *C*H$(CH_3)_2$).

$^{31}P\{^1H\}$ NMR (162 MHz, C_6D_6, 25 °C) δ -26.8 (s).

HRMS (ESI) expected: 411.0895, found: 411.0889 [M+Na] (err [ppm] = 1.60).

Elemental Analysis $C_{18}H_{25}N_2O_2PFe$: calcd C 55.69, H 6.49, N 7.22; found C 55.86, H 6.30, N 7.04 %.

3.6.7.3 FcP(C(O)N(H)^{t}Bu)$_2$ (**51c**)



Dark-orange solid, 65% (96% NMR yield).

^{1}H NMR (400 MHz, C_6D_6, 25 °C) δ 7.19 (s, 2H, N*H*), 4.42-4.37 (m, 2H, Cp *H*), 4.29 (s, 5H, Cp *H*), 4.16-4.10 (m, 2H, Cp *H*), 1.25 (s, 18H, C(C*H*$_3$)$_3$).

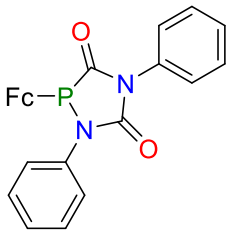
^{13}C{^{1}H} NMR (101 MHz, C_6D_6, 25 °C) δ 175.1 (d, ^{1}J(C,P) = 17.4 Hz, *C*O), 73.1 (d, ^{1}J(C,P) = 14.5 Hz, Cp *C*), 71.6 (d, ^{2}J(C,P) = 4.0 Hz, Cp *C*), 70.7 (s, Cp *C*), 70.5 (s, Cp *C*), 52.6 (s, *C*(CH$_3$)$_3$), 28.8 (s, C(*C*H$_3$)$_3$).

^{31}P{^{1}H} NMR (162 MHz, C_6D_6, 25 °C) δ -24.9 (s).

HRMS (ESI) expected: 439.1208, found: 439.1214 [M+Na] (err [ppm] = 1.40).

3.6.8 Yields and characterisation for **52a**-**52d**

3.6.8.1 FcP-(C(O)N(Ph)C(O)N(Ph)- (**52a**)



Light orange solid 58.6 mg, 44% (80% NMR yield).

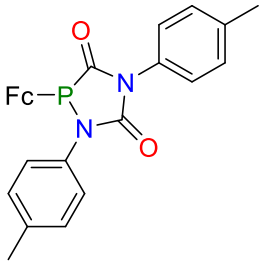
^{1}H NMR (400 MHz, $CDCl_3$, 25 °C) δ 7.56-7.48 (m, 2H, Ph^{p}), 7.46-7.33 (m, 8H, Ph^{m+o}).

^{13}C{^{1}H} NMR (101 MHz, $CDCl_3$, 25 °C) δ 178.6 (d, ^{1}J(C,P) = 2.1 Hz, P*C*O), 155.0 (d, ^{2}J(C,P) = 5.7 Hz, N*C*O), 137.4 (d, ^{2}J(C,P) = 9.0 Hz, Ph^{i}), 133.2 (s, Ph), 129.2 (d, ^{3}J(C,P) = 3.5 Hz, Ph^{o}), 128.8 (s, Ph), 127.6 (s, Ph), 126.8 (s, Ph), 125.9 (d, ^{3}J(C,P) = 5.1 Hz, Ph^{i}), 124.5 (s, Ph) 74.8 (d, ^{1}J(C,P) = 32.5 Hz, Cp *C*), 72.9 (d, ^{3}J(C,P) = 7.7 Hz, Cp *C*), 72.8 (s, Cp *C*), 71.8 (d, ^{2}J(C,P) = 31.1 Hz, Cp *C*), 70.2 (s, Cp *C*), 69.8 (s, Cp *C*).

^{31}P{^{1}H} NMR (162 MHz, $CDCl_3$ 25 °C) δ 26.9 (s).

HRMS (ESI) expected: 477.0426, found 477.0423 [M+Na] (err [ppm] = 0.60).

3.6.8.2 FcP-(C(O)N(*p*-Tol)C(O)N(*p*-Tol)- (**52b**)



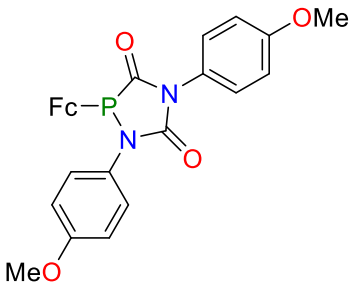
Selected *in situ* values (78% NMR yield).

$^{13}C\{^{1}H\}$ NMR (101 MHz, C_6D_6, 25 °C) δ 176.1 (d, ^{1}J(C,P) = 13.9 Hz, P*C*O), 155.0 (d, ^{2}J(C,P) = 5.8 Hz, N*C*O).

$^{31}P\{^{1}H\}$ NMR (162 MHz, C_6D_6, 25 °C) δ 24.9 (s).

HRMS (ESI) expected: 483.0901, found: 483.0919 [M+H] (err [ppm] = 3.80).

3.6.8.3 FcP-(C(O)N(4-OMeC_6H_4)C(O)N(4-OMeC_6H_4)- (**52c**)



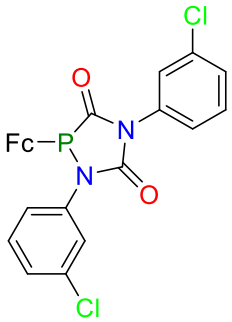
Selected *in situ* values (79% NMR yield).

$^{13}C\{^{1}H\}$ NMR (101 MHz, C_6D_6, 25 °C) δ 175.9 (d, ^{1}J(C,P) = 15.8 Hz, P*C*O), 154.2 (d, ^{2}J(C,P) = 5.8 Hz, N*C*O).

$^{31}P\{^{1}H\}$ NMR (162 MHz, C_6D_6, 25 °C) δ 25.4 (s).

HRMS (ESI) expected: 537.0637, found: 537.0641 [M+Na] (err [ppm] = 0.60).

3.6.8.4 FcP-(C(O)N(3-ClC_6H_4)C(O)N(3-ClC_6H_4)- (**52d**)



Selected *in situ* values (89% NMR yield).

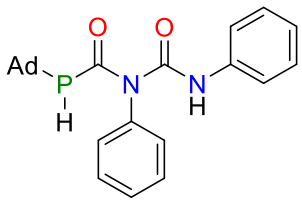
$^{13}C\{^{1}H\}$ NMR (101 MHz, C_6D_6, 25 °C) δ 176.4 (d, ^{1}J(C,P) = 13.9 Hz, P*C*O), 155.4 (d, ^{2}J(C,P) = 5.3 Hz, N*C*O).

$^{31}P\{^{1}H\}$ NMR (162 MHz, C_6D_6, 25 °C) δ 27.3 (s).

HRMS (ESI) expected: 544.9646, found: 544.9673 [M+Na] (err [ppm] = 4.60).

3.6.9 Yields and characterisation for **53a** and **54a-54c**

3.6.9.1 AdP(H)(C(O)N(Ph)C(O)NH(Ph) (**53a**)



Selected *in situ* values (39% NMR yield).

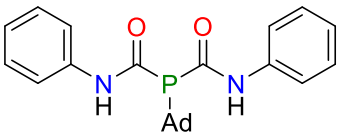
^{1}H NMR (400 MHz, C_6D_6, 25 °C) δ 11.57 (s, N*H*), 3.30 (d, ^{1}J(P,H) = 232 Hz, P*H*).

^{13}C{^{1}H} NMR (101 MHz, C_6D_6, 25 °C) δ 186.4 (d, ^{1}J(C,P) = 34.3 Hz, P*C*O), 174.3 (d, ^{2}J(C,P) = 28.6 HZ, N*C*O).

^{31}P NMR (162 MHz, C_6D_6, 25 °C) -17.4 (d, J(P,H) = 232 Hz).

^{31}P{^{1}H} NMR (162 MHz, C_6D_6, 25 °C) -17.4 (s).

3.6.9.2 AdP(C(O)NH(Ph)$_2$ (**54a/54a'/54a''**)



Selected *in situ* values: Major isomer **54a** (53% NMR yield).

^{1}H NMR (400 MHz, C_6D_6, 25 °C) δ 9.53 (s, N*H*).

^{13}C{^{1}H} NMR (101 MHz, C_6D_6, 25 °C) δ 174.2 (d, ^{1}J(C,P) = 5.1 Hz, P*C*O).

^{31}P{^{1}H} NMR (162 MHz, C_6D_6, 25 °C) δ 10.6 (s).

Minor isomer **54a'** (11% NMR yield).

^{1}H NMR (400 MHz, C_6D_6, 25 °C) δ 9.00 (s, N*H*).

^{31}P{^{1}H} NMR (162 MHz, C_6D_6, 25 °C) -15.4 (s).

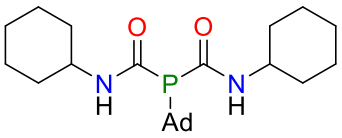
Minor isomer **54a''** (8% NMR yield).

^{1}H NMR (400 MHz, C_6D_6, 25 °C) δ 9.00 (s, N*H*).

^{31}P{^{1}H} NMR (162 MHz, C_6D_6, 25 °C) -16.6 (s).

HRMS (ESI) expected: 457.2015, found: 457.2003 [M+Na] (err [ppm] = 2.80).

3.6.9.3 AdP(C(O)N(H)Cy)$_2$ (**54b**)



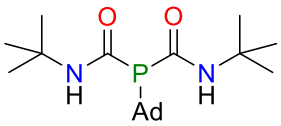
Selected *in situ* values (81% NMR yield).

^{1}H NMR (400 MHz, C_6D_6, 25 °C) δ 7.78 (s, 2H, N*H*).

^{13}C{^{1}H} NMR (101 MHz, C_6D_6, 25 °C) δ 173.6 (d, ^{1}J(C,P) = 20.5 Hz, P*C*O).

^{31}P{^{1}H} NMR (162 MHz, C_6D_6, 25 °C) δ 5.5 (s).

3.6.9.4 AdP(C(O)N(H)^{t}Bu)$_2$ (**54c**)



Selected *in situ* values (71% NMR yield).

^{1}H NMR (400 MHz, C_6D_6, 25 °C) δ 7.32 (s, 2H, N*H*).

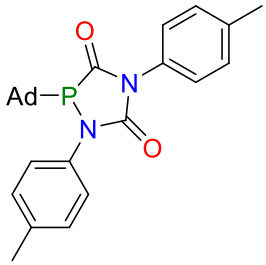
^{13}C{^{1}H} NMR (101 MHz, C_6D_6, 25 °C) δ 174.6 (d, ^{1}J(C,P) = 25.0 Hz, P*C*O).

^{31}P{^{1}H} NMR (162 MHz, C_6D_6, 25 °C) δ 8.2 (s).

HRMS (ESI) expected: 367.2509, found: 367.2524 [M+H] (err [ppm] = 4.10).

3.6.10 Yields and characterisation for **55b**-**55d**

3.6.10.1 AdP-(C(O)N(*p*-Tol)C(O)N(*p*-Tol)- (**55b**)

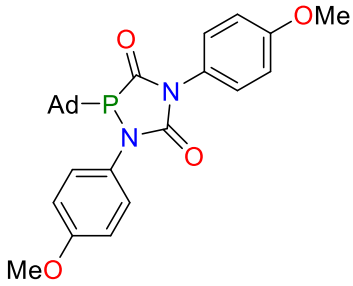


Selected *in situ* values (72% NMR yield).

$^{13}C\{^{1}H\}$ NMR (101 MHz, C_6D_6, 25 °C) δ 174.1 (d, ^{1}J(C,P) = 4.8 Hz, P*C*O), 166.0 (s, N*C*O).

$^{31}P\{^{1}H\}$ NMR (162 MHz, $CDCl_3$ 25 °C) δ 60.6 (s).

3.6.10.2 AdP-(C(O)N(4-OMeC_6H_4)C(O)N(4-OMeC_6H_4)- (**55c**)

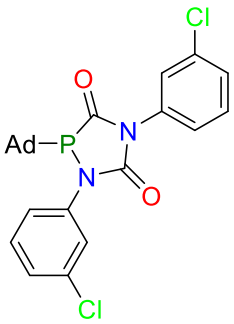


Selected *in situ* values (72% NMR yield).

$^{13}C\{^{1}H\}$ NMR (101 MHz, C_6D_6, 25 °C) δ 174.1 (d, ^{1}J(C,P) = 4.5 Hz, P*C*O), 166.1 (s, N*C*O).

$^{31}P\{^{1}H\}$ NMR (162 MHz, $CDCl_3$ 25 °C) δ 60.3 (s).

3.6.10.3 AdP-(C(O)N(3-ClC_6H_4)C(O)N(3-ClC_6H_4)- (**55d**)



Selected *in situ* values (72% NMR yield).

$^{13}C\{^{1}H\}$ NMR (101 MHz, C_6D_6, 25 °C) δ 173.9 (d, ^{1}J(C,P) = 4.8 Hz, P*C*O), 166.2 (s, N*C*O).

$^{31}P\{^{1}H\}$ NMR (162 MHz, C_6D_6, 25 °C) δ 61.8 (s).

3.6.11 Summary of spectroscopic data

	NMR yield (%)	δ_P (ppm)	δ_C (PC=O) (ppm)	^1J(C,P) (Hz)	δ_C (NC=O) (ppm)[a]	^2J(C,P) (Hz)[a]	δ_H (N*H*) (ppm)[b]
49a	87	-21.5	174.0	17.9	-	-	9.08
49b	84	-22.2	173.8	18.0	-	-	9.06
49c	84	-22.3	173.7	17.6	-	-	9.06
49d	73	-20.2	174.2	19.4	-	-	9.03
51a	97	-27.0	174.5	15.3	-	-	7.42
51b	99	-26.8	174.6	15.4	-	-	7.29
51c	96	-24.9	175.1	17.4	-	-	7.19
52a	80	26.9	178.6	2.1	155.0	5.7	-
52b	78	24.9	176.1	13.9	155.0	5.8	-
52c	79	25.4	175.9	15.8	154.2	5.8	-
52d	89	27.3	176.6	13.9	155.4	5.3	-
54a	58	10.6	174.2	5.1	-	-	9.00
54b	81	5.5	173.6	20.5	-	-	7.78
54c	71	8.2	174.6	25.0	-	-	7.32
55b	72	60.7	174.1	4.8	166.0	-	-
55c	72	60.3	174.1	4.5	166.1	-	-
55d	72	61.8	173.9	4.8	166.2	-	-

[a]Not applicable to **49a**-**49d**, **51a**-**51c** and **54a**-**54c**. [b] Not applicable to **52a**-**52d** and **55b**-**55d**.

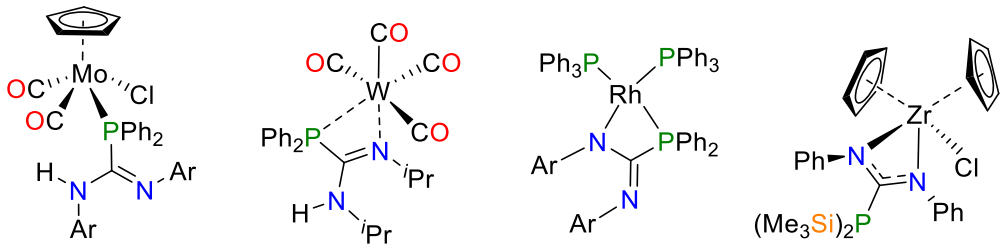
Chapter 4:

Hydrophosphination of Carbodiimides

4.1 Introduction

4.1.1 Hydrophosphination of carbodiimides with secondary phosphines

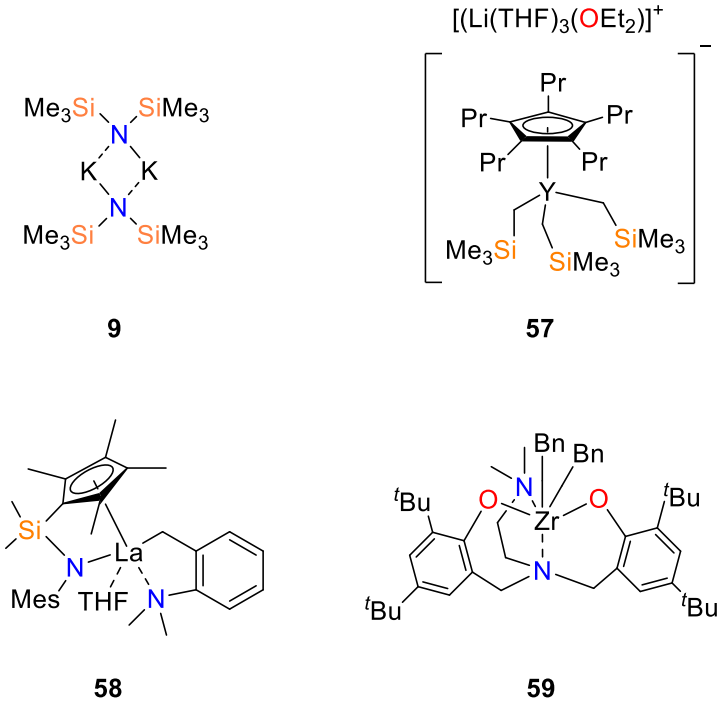
In comparison to substrates such as alkenes or alkynes that have been widely investigated for hydrophosphination chemistry, the hydrophosphination of carbodiimides is somewhat lacking. Currently, there is only a handful of reactions limited to s-block,[90,91,172] f-block[92,93,161,162] and zirconium catalysts.[173] The hydrophosphination of carbodiimides is an economical route to synthesise phosphaguanidines, which are important building blocks in transition metal complexes and synthons for challenging organic transformations (**Scheme 56**).[47,174–176]



***Scheme 56**. Phosphaguanidine ligands in transition metal complexes.*[47,177]

The first reported catalytic example of hydrophosphination of carbodiimides was by Hou *et al.* in 2006 (**Figure 24**).[90] Utilising 1.0 mol% of **9**, a wide scope of secondary aryl phosphines, $HPAr_2$ (where Ar = 2/3/4-Me-, 4-OMe-, 4-Cl-, 4-Br, 3,5-Me_2- and 3,5-OMe_2-substituted aryls) were shown to react with ^{i}PrN=C=N^{i}Pr (**Scheme 57**), affording the products in near-quantitative yields.

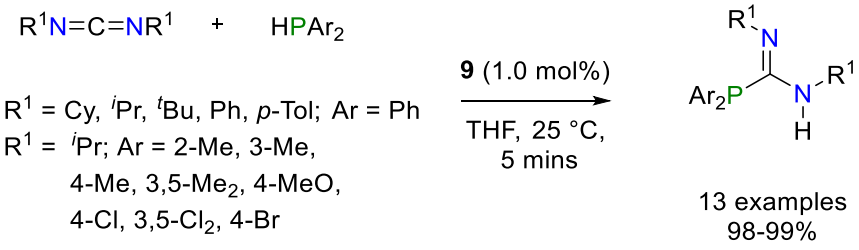
Additionally, a range of symmetric and asymmetric carbodiimides could be used: $R^1N{=}C{=}NR^2$ where R^1, R^2 = Cy, *p*-Tol; ^{t}Bu, Et; Ph, Cy. For the more challenging mixed alkyl/aryl phosphine HPPh(Et) and dialkyl phosphine HP$^{i}Bu_2$, a higher (3.0 mol%) loading of **9** was required for the hydrophosphination of ^{i}PrN=C=N^{i}Pr.



9 **57**

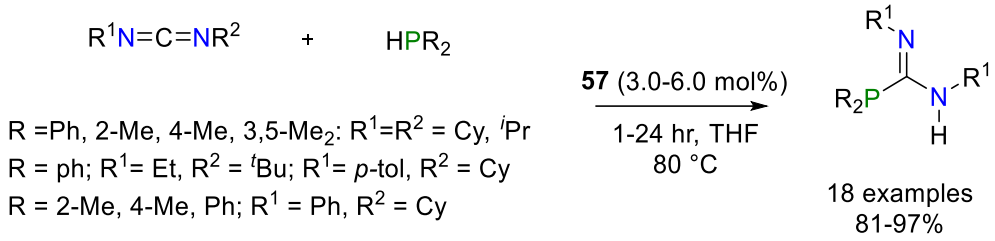
58 **59**

***Figure 24**. Carbodiimide hydrophosphination precatalysts; **9** by Hou et al.,[90] **57** by Zhang et al.,[162] **58** by Hou et al.,[161] and **59** by Shen et al.[173]*



***Scheme 57.** Hydrophosphination of carbodiimides by precatalyst **9**.[90]*

The anionic precatalyst **57** demonstrated greater activity than the corresponding neutral lanthanide complex (**Figure 21**).[162] The use of symmetrical substrates ^{i}PrN=C=N^{i}Pr and CyN=C=NCy afforded the phosphaguanidine products in excellent yields (**Scheme 58**). For unsymmetrical carbodiimides R^{1}N=C=NR^2 (R^1 = Ph, Cy; R^2 = Ph, pentyl, *p*-Tol, Cy) lower yields of product were obtained, albeit with concomitant doubling of catalyst loading (to 6.0 mol%) and increase of the reaction time, owing to the lower electrophilicity of the mixed aryl, alkyl carbodiimides (**Scheme 58**).



Scheme 58. *Hydrophosphination of carbodiimides by* ***57***.[162]

For precatalyst **57** the use of functionalised aryl phosphines did not significantly affect yields. However, the attempted reaction of very bulky DippN=C=NDipp with $HPPh_2$ was not tolerated, either due to increased steric bulk or lowered carbodiimide electrophilicity.[162]

Utilising 1.0 mol% of **58** (**Figure 24**) at 80 °C with a wide range of substituted diarylphosphines ($HPAr_2$; where Ar = 2-MeC_6H_4, 3-MeC_6H_4, 4-MeC_6H_4, 4-$MeOC_6H_4$, 4-ClC_6H_4, 4-BrC_6H_4 and 3-5-$Cl_2C_6H_3$) and ^{i}PrN=C=N^{i}Pr the reaction was not influenced by the position of the ring-substitution on the phosphine substrate (95-99%).[161] Similarly, to the precatalyst **9**, the reactions with mixed aryl, alkyl phosphine, HPPh(Et) required more forcing conditions of 110 °C for good conversions (86%).

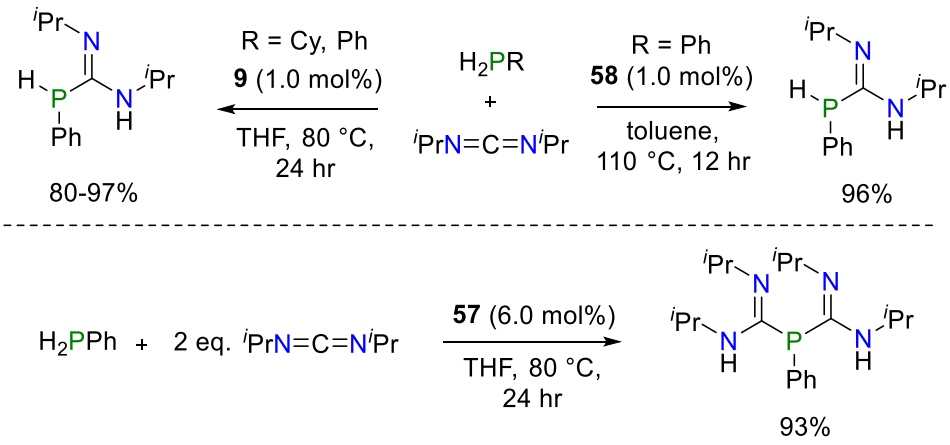
Use of 10 mol% of neutral zirconium precatalyst **59** (**Figure 24**) at 110 °C in the hydrophosphination of ^{i}PrN=C=N^{i}Pr gave low yields (<11%), but the addition of 10 mol% $[Ph_3C][B(C_6F_5)_4]$ to generate the cationic precatalyst of **58** increased yields to 75% (CyN=C=NCy; at 110 °C) and 90% (for PhN=C=NPh; at 60 °C).[173]

4.1.2 Hydrophosphination of carbodiimides with primary phosphines

There have been only three examples of hydrophosphination of carbodiimides with primary phosphines reported in the literature; these use precatalysts **9**, **58** and **57** (**Scheme 59**).[90,161,162] Two of these examples are limited to only single hydrophosphination, the first of which was reported by Hou *et al.* in 2006.[90]

Utilising 1.0 mol% of **9** at increased temperatures of 80 °C and reaction time of 24 hours (*vs* 0.1 hr at 25 °C for single hydrophosphination with $HPPh_2$) $^{i}PrN{=}C{=}N^{i}Pr$ undergoes single hydrophosphination with primary phosphines H_2PPh and H_2PCy in 97% and 80% yields respectively (with 15% double hydrophosphination product when H_2PCy is used) (**Scheme 59**). In 2008, further work by Hou *et al.* utilised lanthanum-based precatalyst **58** for the single hydrophosphination of $^{i}PrN{=}C{=}N^{i}Pr$ with H_2PPh in a 96% yield (**Scheme 59,** above). However, compared to previous work with precatalyst **9** an increased temperature of 110 °C was required; albeit with a shorter time of 12 hours.

The first and only example of double hydrophosphination of a primary phosphine (in high conversions and not as a 15% side product in the case of precatalyst **9** with H_2PCy) was described by Zhang *et al.* in 2015 (**Scheme 59**, below). An increased catalyst loading of 6.0 mol% of **57** was needed (from 3% for secondary phosphines) yielding the double hydrophosphination product in a 93% yield from 2 equivalents of $^{i}PrN{=}C{=}N^{i}Pr$ with H_2PPh. Across these three examples, it is evident that only carbodiimide $^{i}PrN{=}C{=}N^{i}Pr$ has been used, and the catalyst loadings and temperatures are vastly increased compared to those with secondary phosphines. This highlights the additional difficulties of using primary phosphines as hydrophosphination substrates.



Scheme 59. *(above) Single hydrophosphination of $^{i}PrN{=}C{=}N^{i}Pr$ by precatalysts **9** and **58** by Hou et al.*[90,161] *(below) double hydrophosphination of $^{i}PrN{=}C{=}N^{i}Pr$ by precatalyst **57** by Zhang et al.*[162]

4.2 Aims

Carbodiimides are more synthetically challenging to utilise and less electrophilic than isocyanates, thus are expected to very likely need a catalyst, however for completeness catalyst-free neat and in-solution control reactions were still performed to investigate the need to use a catalyst.

Precatalyst, **40** was a suitable choice for initial reactions with carbodiimides (given **40**'s proven tolerance for heterocumulenes such as isocyanates, see Chapter 3). Initial aims focused on testing the secondary aryl phosphine $HPPh_2$ for single hydrophosphination with carbodiimides. Proving the viability of **40** for further testing with other P-H substrates and the first example of a 1st row transition metal complex performing a hydrophosphination of carbodiimide. Based on this success the P-H was further increased to the less reactive alkyl secondary phosphines HP^iPr_2; with the reaction being far less successful

Perhaps the most ambitious aim of this work was to utilise some of the most challenging P-H substrates (for hydrophosphination of carbodiimides). Such as primary phosphines (e.g., with $FcPH_2$) attempting to form novel double hydrophosphination products, with uses as ligands with varying bonding modes. Other general aims include increasing the scope of carbodiimides utilised to examples not only limited to symmetrical alkyl carbodiimides, but unsymmetrical carbodiimides such as ^{t}BuN=C=NEt. Additionally, underutilised diaryl carbodiimides such as PhN=C=NPh will be investigated.

The final aim and consideration of this work was the formation of isomers of the respective single hydrophosphination and double hydrophosphination products. From the eight possible isomers (for one respective phosphaguanidine ligand) it was expected from E_{syn}-(α or β), E_{anti}-(α or β), Z_{syn}-(α or β), Z_{anti}-(α or β) that typically E_{syn}-(α) or Z_{anti}-(β) isomers would form, as these have been shown to be often the lowest resting conformational state.[178]

4.3 Results and Discussion

4.3.1 Single hydrophosphination of carbodiimides with $HPPh_2$

4.3.1.1 Attempted catalyst-free hydrophosphination of $^{i}PrN=C=N^{i}Pr$ with $HPPh_2$

Control reactions were performed neat or in C_6D_6 at 25 or 60 °C for 16 hours (**Table 42**, entries 1-4). However, unlike isocyanates there was no conversion to any products from $HPPh_2$ as observed through ^{31}P NMR spectroscopic monitoring. Increasing the reaction time to 72 hours for the neat reaction at 60 °C still gave a 0% conversion as determined by ^{31}P NMR spectroscopy (**Table 42**, entry 5).

Table 42. Initial attempted catalyst-free hydrophosphination of $^{i}PrN=C=N^{i}Pr$ with $HPPh_2$[a,b,c]

Entry	$HPPh_2$: $^{i}PrN=C=N^{i}Pr$	Temp. (°C)	Solvent	Conv. From $HPPh_2$ (%)
1	1.0 :1.0	25	C_6D_6	0
2	1.0 : 1.0	60	C_6D_6	0
3	1.0 : 1.0	25	neat	0
4	1.0 : 1.0	60	neat	0
5[c]	1.0 : 1.0	60	neat	0

[a] Reaction conditions for conversions: 1.0 eq. of $HPPh_2$ or $^{i}PrN=C=N^{i}Pr$ = 0.734 mmol, and C_6D_6 (0.60 mL) for 16 hours under a nitrogen atmosphere unless otherwise stated.[b] Conversion determined by ^{31}P NMR spectroscopy by relative integration of ^{31}P NMR peaks.[c] Reaction time increased to 72 hours.

4.3.1.2 Initial catalytic hydrophosphination of $^{i}PrN=C=N^{i}Pr$ with $HPPh_2$

Initial NMR experiments with $HPPh_2$, $^{i}PrN=C=N^{i}Pr$ and 5 mol% of **40** were performed at 25 °C, after 4 hours showing a darkening from clear yellow to dark brown in solution. After 16 hours the ^{31}P NMR spectrum showed 12%

consumption of $HPPh_2$ (d, –38.8ppm) and the formation of a peak at –18.2 (d, ^3J(P,H) = 8.2 Hz, N*H*) which can be assigned to single hydrophosphination product, **60a** (**Table 43,** entry 1).

Table 43. Initial catalytic hydrophosphination of ^{i}PrN=C=N^{i}Pr with $HPPh_2$[a,b]

Entry	Temp. (°C)	Cat. (mol%)	Time (hr)	Conv. (%)	**60a:** $(PhP)_2$
1	25	5.0	16	12	12:0
2	60	5.0	16	>99	98:2

[a] Reaction conditions for conversions: 1.0 eq. of $HPPh_2$ or ^{i}PrN=C=N^{i}Pr = 0.734 mmol, and C_6D_6 (0.60 mL) for 16 hours under a nitrogen atmosphere unless otherwise stated.[b] Conversion determined by ^{31}P NMR spectroscopy by relative integration of the ^{31}P NMR peaks.

Increasing the reaction temperature to 60 °C gave quantitative conversions of $HPPh_2$ to 98% of **60a** along with 2% of a species at –15.0 (s) ppm which can be assigned to Ph_2P-PPh_2 from dehydrocoupling of $HPPh_2$ (**Table 43**, entry 2) (**Figure 25**). Due to the simple reaction conditions needed for a near quantitative conversion to desired product **60a**, the conditions of **Table 43**, entry 2 were chosen for application in further carbodiimide substrate scope testing.

In principle 8 isomers of the single hydrophosphination product **60a** can exist E_{syn}(α/β), E_{anti}(α/β), Z_{syn}(α/β), Z_{anti}(α/β) (**Figure 26**).[178] However after comparison to the literature the ^{31}P NMR spectroscopic value indicates that most likely the E_{syn}(α) isomer has been formed.[162] This is typically the lowest energy isomer, the structure of which could be confirmed by X-ray diffraction measurements. The next lowest energy isomer would be the Z_{anti}(β) isomer which would be expected to have a change in ^{31}P NMR values approximately 15 ppm more positive than the value observed value of –18.2, at approximately –4 to –5 ppm.[178]

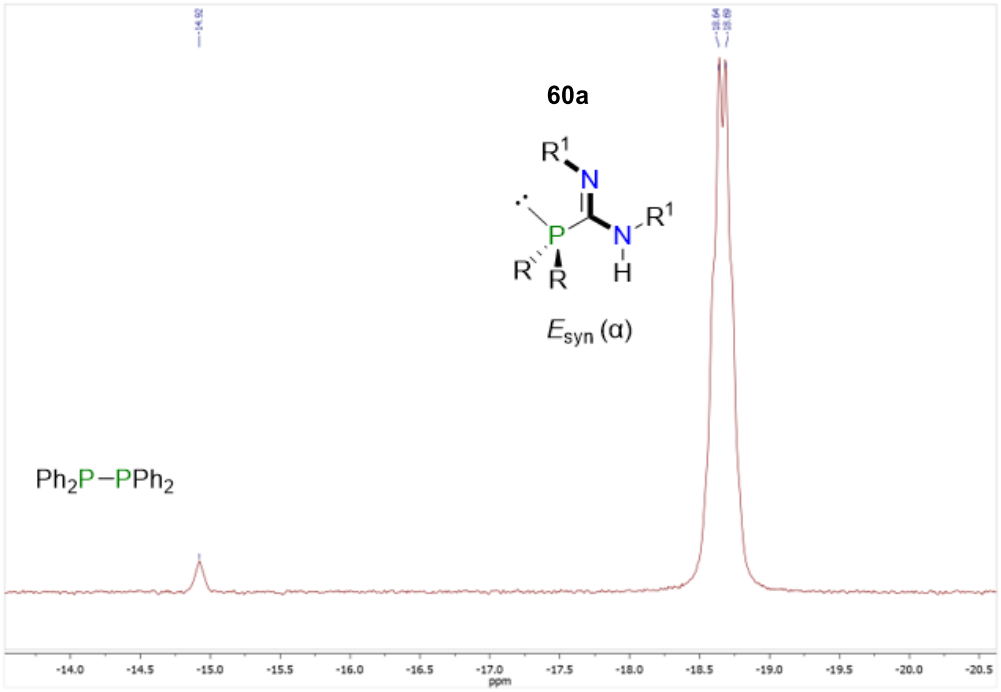


Figure 25. *^{31}P NMR spectrum of the reaction of the Table 43, entry 2.*

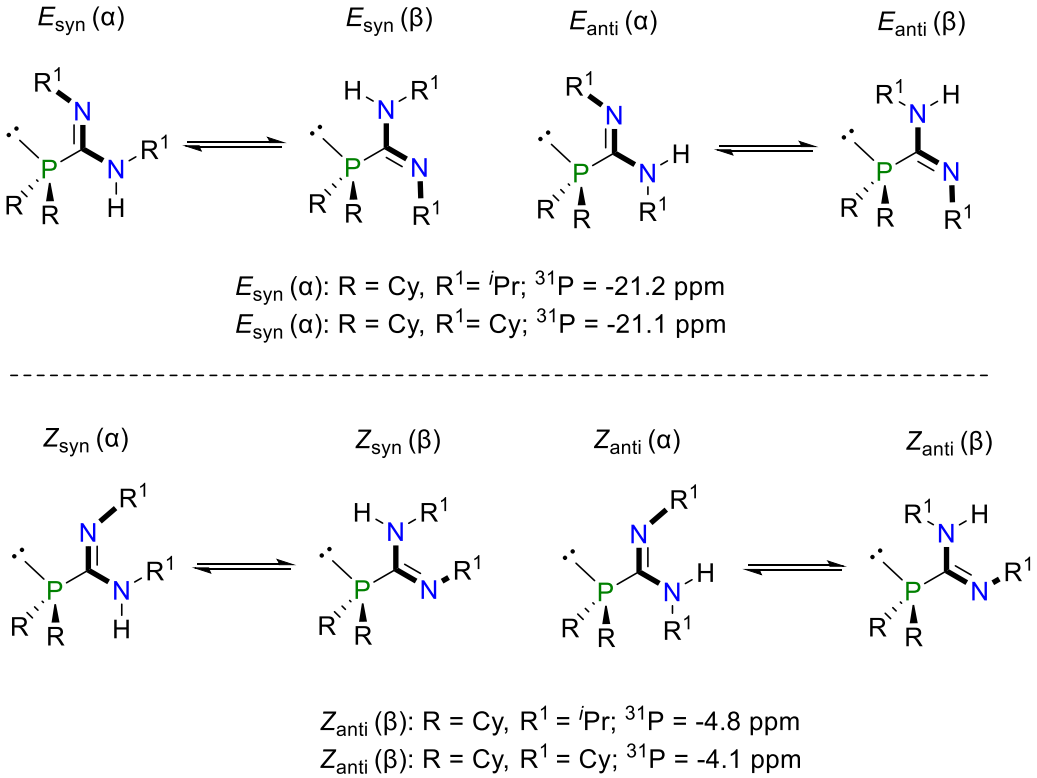


Figure 26*. Configurational isomerism (E_{syn}, E_{anti}, Z_{syn} and Z_{anti}) and conformational isomerism (α or β) of phosphaguanidines with given ^{31}P NMR spectroscopic values for two most common isomers E_{syn}(α) and Z_{anti}(β).*[178]

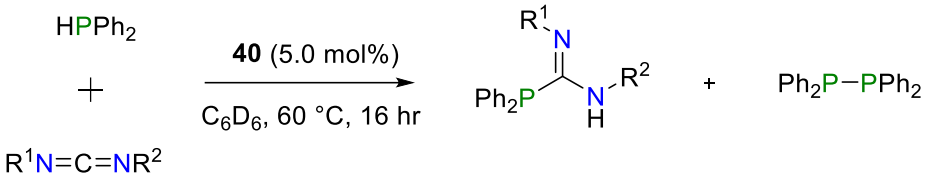
4.3.1.3 Catalytic single hydrophosphination of carbodiimides with $HPPh_2$

The reaction was extended to other alkyl carbodiimides, utilising CyN=C=NCy under the same conditions as ^{i}PrN=C=N^{i}Pr (5.0 mol% **40**, 60 °C and 16 hours) gave near quantitative conversions to the single hydrophosphination product **60b** (99%**;** ^{31}P NMR = –18.3 ppm, E_{syn}(α) isomer) along with 1% of $Ph_2P–PPh_2$ (**Table 44**).

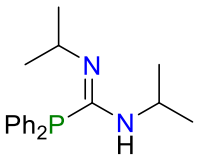
Use of the asymmetric alkyl carbodiimide ^{t}BuN=C=NEt gave 91% yield of a single hydrophosphination product **60c** (^{31}P NMR = –16.2ppm; E_{syn}-(α) isomer) requiring a longer reaction time of 24 hours with concomitant formation of $Ph_2P–PPh_2$ (6%) (**Table 44**). The use of 2D NMR (COSY, HSQC and HMBC) identified the particular regioisomer formed was the isomer whereby; the N–H bond formed on the "NCN" motif is by the bulkier *tert*-butyl group. Additionally, there is <0.1% of the opposite regioisomer (δ_P = –14.4 ppm; $Ph_2PC(=N^{t}Bu)(-N(Et)H)$), showing high regioselectivity by precatalyst **40**. Furthermore, there is only 1% of the Z_{anti}-(β) isomer formed (δ_P = –5.4 ppm).

Under the same conditions used for dialkyl carbodiimides, the diaryl carbodiimide PhN=C=NPh gave a 99% conversion to the expected product **60d**, in all cases of single hydrophosphination the isomer identified can be assigned to the E_{syn}-(α) isomer. It should be noted as well that even when multiple (2 or 5) equivalents of carbodiimide are used for PhN=C=NPh, unlike the hydrophosphination of isocyanates, no diinsertion type products form. This is likely due to the much lower electrophilicity of carbodiimides as well as increased steric bulk.

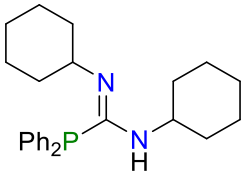
Table 44. Catalytic hydrophosphination of carbodiimides with $HPPh_2$.[a,b]



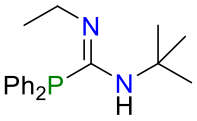
60a–60d



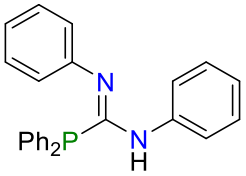
60a: 60 °C, 16 hr, (**60a**:$[PPh_2]_2$, 98:2)



60b: 60 °C, 16 hr, (**60b**:$[PPh_2]_2$, 99:1)



60c: 60 °C, 24 hr, (**60c**:$[PPh_2]_2$, 91:6)



60d: 60°C, 16 hr, (**60d:**$[PPh_2]_2$, 99:1)

*[a] Reaction conditions for conversions: 1.0 eq. of $HPPh_2$ or $R^1N=C=NR^2$ = 0.734 mmol, and C_6D_6 (0.60 mL) under a nitrogen atmosphere unless otherwise stated.[b] Conversion determined by ^{31}P NMR spectroscopy by relative integration of ^{31}P NMR peaks; conversions given in brackets as percentage conversion to (**60**: Ph_2P-PPh_2).*

4.3.1.4 Scaled up isolation catalytic hydrophosphination of CyN=C=NCy with $HPPh_2$

To obtain isolated yields and assess the practicality of the procedure, the reaction was scaled up. Utilising CyN=C=NCy (1.0 eq., 1.00 g, 4.85 mmol) and $HPPh_2$ (1.0 eq., 0.84 mL, 4.9 mmol) with **40** (5.0 mol%, 0.165 g, 0.24 mmol) in toluene (10 mL) at 60 °C for 24 hours. Degassed water (30 mL) was used to remove any Fe(II)-containing impurities formed from the catalyst and then the

product was extracted into toluene (2 × 20 mL). After subsequent drying of the organic layer (with $MgSO_4$) removal of volatiles in vacuo gave a crude light brown solid. After dissolving in the minimum amount of hot (*ca.* 60 °C) hexane; recrystallisation at –30 °C gave **60b** as an off-white crystalline solid in a high yield (1.567 g, 83%). This procedure has shown the methodology with **40** is practicable, scalable and isolated yields are comparable to NMR yields.

4.3.2 Catalytic hydrophosphination of carbodiimides with HP^iPr_2

4.3.2.1 Initial attempted hydrophosphination of ^{i}PrN=C=N^{i}Pr with HP^iPr_2

Given the good tolerance of precatalyst **40** for the hydrophosphination of varying carbodiimides with $HPPh_2$ and providing excellent conversions, the P-H substrate was changed to the secondary alkyl phosphine, HP^iPr_2. Secondary alkyl phosphines have been shown to be more challenging for hydrophosphination catalysis with heterocumulenes in general (and particularly carbodiimides).[90,91,161] For completeness, before utilising precatalyst **40**, catalyst-free control reactions were performed neat and in solution (C_6D_6) at 25 °C and 60 °C for 16 hours; with no conversion being apparent from the ^{31}P NMR spectra (**Table 45**, entries 1-4).

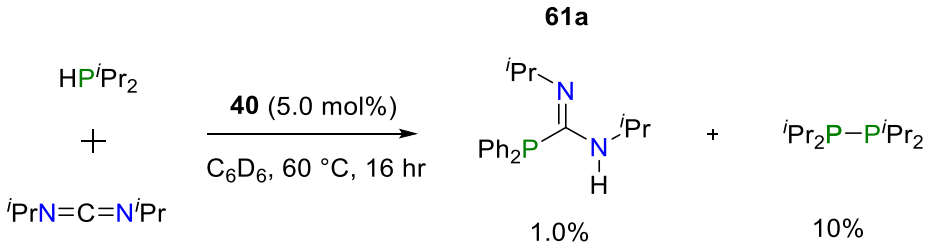
The addition of 5.0 mol% of precatalyst **40** to the reaction of HP^iPr_2 and ^{i}PrN=C=N^{i}Pr **for** 16 hours at 25 °C resulted in a 0% conversion by ^{31}P NMR spectroscopy to any products (**Table 45**, entry 5). Increasing the temperature from 25 °C to 60 °C resulted in an increase in conversion from HP^iPr_2 to 11% (**Table 45**, entry 6). However, 10% of the product identified was the result of dehydrocoupling of HP^iPr_2 yielding $^iPr_2P–P^iPr_2$; with only 1% being the signal related to the single hydrophosphination product **61a** with a ^{31}P NMR spectroscopic peak at 3.3 (s) ppm suggesting a possible Z_{anti} isomer (**Scheme 60**) and **Table 45**, entry 6). This is in stark contrast to reactions with $HPPh_2$

where under the same conditions (5.0 mol% **40** and 60 °C) near quantitative conversion to hydrophosphination products was observed (section 4.3.1.3).

Table 45. Attempted catalyst-free and catalytic hydrophosphination of ^{i}PrN=C=N^{i}Pr with HP^{i}Pr$_2$.[a,b]

Entry	Temp. (°C)	Solv.	**40** (mol%)	Conv. (%)	Conv. **61a**: (^{i}Pr$_2$P)$_2$ (%)
1	25	Neat	0	0	0 : 0
2	60	Neat	0	0	0 : 0
3	25	C_6D_6	0	0	0 : 0
4	60	C_6D_6	0	0	0 : 0
5	25	C_6D_6	5.0	0	0 : 0
6	60	C_6D_6	5.0	11	1 : 10

[a] Reaction conditions for conversions: 1.0 eq. of HP^{i}Pr$_2$ or ^{i}PrN=C=N^{i}Pr = 0.734 mmol, and if a solvent is used, C_6D_6 (0.60 mL) for 16 hours under a nitrogen atmosphere unless otherwise stated.[b] Conversion determined by ^{31}P NMR spectroscopy by relative integration of the ^{31}P NMR peaks.



Scheme 60. *Reaction of ^{i}PrN=C=N^{i}Pr, HP^{i}Pr$_2$ and 5.0 mol% **40** in C_6D_6 at 60 °C for 16 hours.*

4.3.2.2 Single hydrophosphination of CyN=C=NCy and ^{t}BuN=C=NEt with HP^{i}Pr$_2$

Investigations to determine if other carbodiimides could possibly be reactive with HP^{i}Pr$_2$ an analogous reaction to that shown in **Table 45**, entry 6 was performed with CyN=C=NCy (**Table 46**, entry 1). Unfortunately, however no

conversion was achieved, with no dehydrocoupling products forming or hydrophosphination products observed. Subsequently, increasing the reaction time from 16 hours to 72 hours at 60 °C gave conversion to a product at δ_P = –12.4 ppm (singlet, 10%), which is assigned to the single hydrophosphination product **61b** (**Scheme 61**, right) and additionally is assigned to E_{syn}-(α) isomer (with 1% of the Z_{anti}-(β) isomer forming at δ_P = 3.9 ppm (singlet) (**Table 46**, entry 2). The effect of doubling the precatalyst loading of **40** from 5.0 mol% to 10 mol% was tested, but this still only gave a very low conversion to **61b** (5% by ^{31}P NMR spectroscopy).

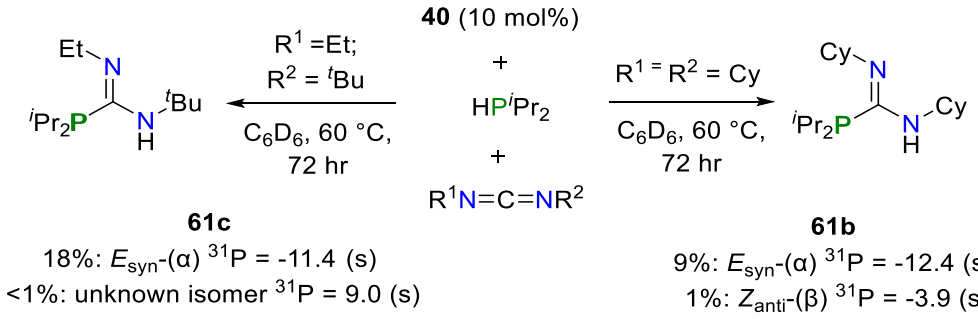
Changing the carbodiimide substrate to ^{t}BuN=C=NEt with 5.0 mol% of **40** at 60 °C gave a very low (3%) conversion to the single hydrophosphination product **61c** as determined by ^{31}P NMR spectroscopy (–11.4 ppm, singlet, E_{syn}-(α) isomer) (**Table 46**, entry 4). Increasing the reaction time to 72 hours gave an increased conversion of **61c** to 18%, as well as <1% of an additional ^{31}P resonance at 9.0 ppm (singlet) which cannot be assigned to the other common isomer Z_{anti}-(β) (**Scheme 61**, left. **Table 34,** entry 5).

Table 46. Catalytic hydrophosphination of CyN=C=NCy or ^{i}PrN=C=N^{i}Pr with HP^{i}Pr$_2$[a,b]

Entry	$R^1N=C=NR^2$	Temp. (°C)	Time (hr)	Cat. (mol%)	Conv. **61** (%)
1	Cy, Cy	60	16	5.0	0
2	Cy, Cy	60	72	5.0	10
3	Cy, Cy	80	16	10	5
4	^{t}Bu, Et	60	16	5.0	3
5	^{t}Bu, Et	60	72	5.0	18
6	^{t}Bu, Et	80	16	10	2

[a] Reaction conditions for conversions: 1.0 eq. of HP^{i}Pr$_2$ or ^{i}PrN=C=N^{i}Pr = 0.147 mmol, and C_6D_6 (0.60 mL) for 16 hours under a nitrogen atmosphere unless otherwise stated.[b] Conversion determined by ^{31}P NMR spectroscopy by relative ^{31}P NMR peaks.

As with the reactions detailed for CyN=C=NCy, doubling the catalyst loading to 10 mol% and increasing the temperature to 80 °C only marginally improved yields giving only a 2% conversion by ^{31}P NMR spectroscopy.



Scheme 61. *(Left) Hydrophosphination of ^{t}BuN=C=NEt by conditions of* ***Table 34****, entry 5 and (right) hydrophosphination of CyN=C=NCy by conditions of* ***Table 34****, entry 2.*

4.3.3 Double hydrophosphination of carbodiimides with $FcPH_2$

4.3.3.1 Initial catalyst-free control reaction

For completeness, control reactions with $FcPH_2$ and ^{i}PrN=C=N^{i}Pr (in a 1:2 ratio) were performed neat or in C_6D_6 at 25 or 60 °C for 16 hours, after which 0% conversions from $FcPH_2$ to any products was observed (**Table 35**, entries 1-4). Thus catalyst-free hydrophosphination of carbodiimides with $FcPH_2$ was not pursued further.

Table 47. Initial attempted catalyst-free hydrophosphination of ^{i}PrN=C=N^{i}Pr with $HPPh_2$[a,b]

Entry	$FcPH_2$: ^{i}PrN=C=N^{i}Pr	Temp. (°C)	Solvent	Conv. From $HPPh_2$ (%)
1	1.0 :2.0	25	C_6D_6	0
2	1.0 : 2.0	60	C_6D_6	0
3	1.0 : 2.0	25	neat	0
4	1.0 : 2.0	60	neat	0

[a] Reaction conditions for conversions: 1.0 eq. of $FcPH_2$ = 0.292 mmol and C_6D_6 (0.50 mL) for 16 hours under a nitrogen atmosphere unless otherwise stated[b] Conversion determined by ^{31}P NMR spectroscopy by relative integration of the ^{31}P NMR peaks.

4.3.3.2 Initial catalytic hydrophosphination of CyN=C=NCy with $FcPH_2$

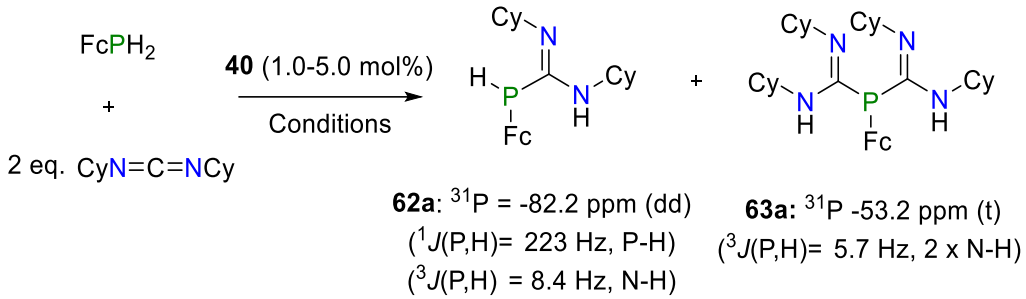
The Initial catalytic reaction of CyN=C=NCy and $FcPH_2$ with 5.0 mol% of **40** at 25 °C resulted in 21% conversion from $FcPH_2$ in 16 hours (**Table 48**, entry 1). This reaction resulted in the formation of two ^{31}P NMR spectroscopic resonances: 7% conversion at –82.2 ppm (dd), $^{1}J(P,H)$= 222.7 Hz, P–H and $^{3}J(P,H)$ = 5.7 Hz, N–H which can be assigned to the single hydrophosphination product, **62a** and 14% conversion to 53.2 ppm (t), $^{3}J(P,H)$ = 8.4 Hz, 2 × N–H for the double hydrophosphination product, **63a** (**Table 48,** entry 1 and **Scheme 62**).

Increasing the temperature of the reaction to 60 °C from 25 °C resulted in a large increase in conversion to 97%; forming 96% of **63a** and only 1% of **62a** (**Table 48**, entry 2). Attempts to decrease the catalyst loading at 60 °C to 2.5 mol% and 1.0 mol% of **40** led to decreases in conversions to 59% and 12%, respectively, giving; conversions of 58% and 10%, respectively, to **62a**: **63a** (**Table 48**, entries 3-4).

Table 48. Initial catalytic hydrophosphination of CyN=C=NCy with $FcPH_2$.[a,b]

Entry	$FcPH_2$: CyN=C=NCy	Temp. (°C)	Cat. (mol%)	Conv. (%)	Yield **62a**:**63a** (%)
1	1.0 :2.0	25	5.0	21	7:14
2	1.0 : 2.0	60	5.0	97	1:96
3	1.0 : 2.0	60	2.5	59	1:58
4	1.0 : 2.0	60	1.0	12	2:10

[a] Reaction conditions for conversions: 1.0 eq. of $FcPH_2$ = 0.146 mmol and C_6D_6 (0.50 mL) for 16 hours under a nitrogen atmosphere unless otherwise stated.[b] Conversion determined by ^{31}P NMR spectroscopy by relative integration of the ^{31}P NMR peaks.

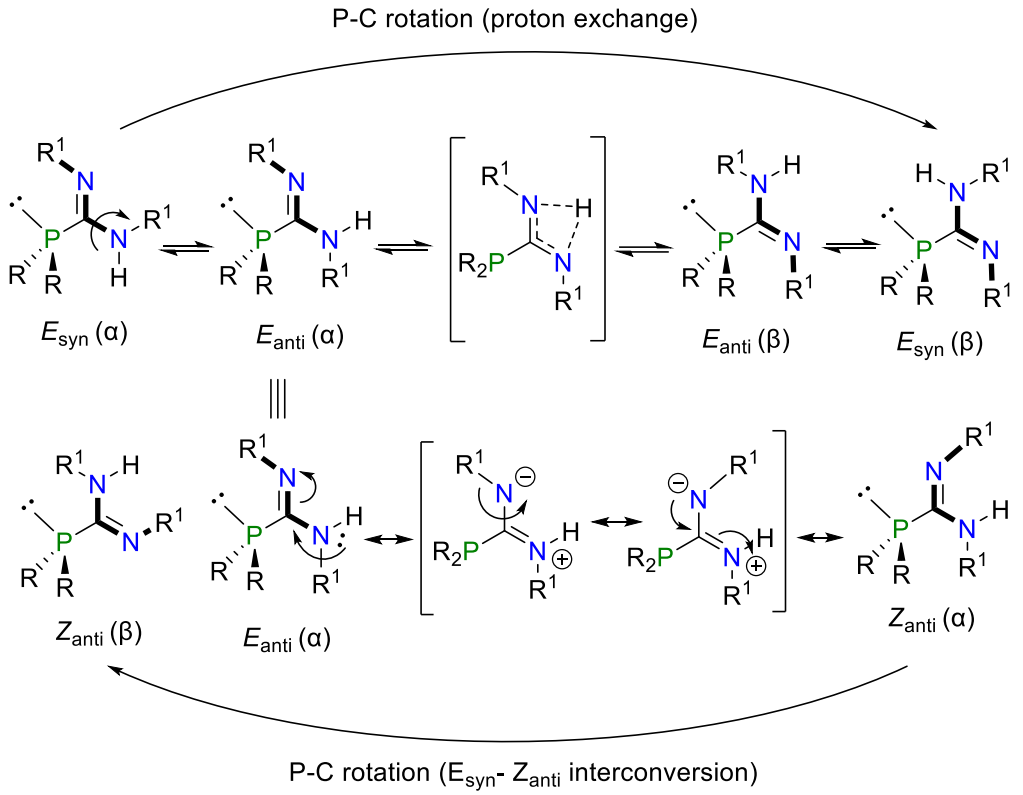


Scheme 62. *General scheme for the hydrophosphination of CyN=C=NCy with $FcPH_2$ by conditions of* ***Table 36****, entries 1-4.*

In addition to the major product resonance for **63a** (**Table 48**, entry 2) there is an additional *ca* 2% conversion to seven further resonances within the ^{31}P NMR spectrum, which may be due to different isomers of **63a** (^{31}P NMR resonances (in ppm) = –56.0, –52.4, –53.3, –51.1, –50.4, –49.7 and –47.7).

In single phosphaguanines (e.g., **60a**-**60d**) there are non-bonding interactions between the lone pair of the P(III) atom (or chalcogen if a P(V)-phosphaguanidine) and the amino N-H group, locking the restricting the amidine and rotation around the P-C bond. However, in turn this causes steric clashes between the imine and phosphorous substituents, with this conflict potentially causing C=N bond isomerisation to relieve unfavourable interactions and ultimately which of each phosphaguanidine isomer is present (**Scheme 63**).

It can be reasoned that for a double phosphaguanidine like **63a**, each individual phosphaguanidine motif will have this N-H non-bonding interaction *vs***.** imine and phosphorus substituent clash. However, there is a new possibility of internal N-H to imine hydrogen bonding occurring between each of the phosphaguanidine ligands. This further complicates matters as this interaction could free up the interaction between the phosphorus lone pair and imine now allowing for P-C bond rotation.



***Scheme 63**. Mechanisms of interconversion of phosphaguanidines.*[178]

Further computational analysis is needed, after geometry optimisation a convenient parameter to compare the planarity of these three-coordinate atoms (e.g. for the N-H non-bonding interaction to phosphorus lone pair) is the degree of pyramidisation, DP (where DP(%) = $\frac{360-\sum_{i=1}^{3}\alpha}{0.9}$) where α is the smallest bond angle of the particular atom. With the DP giving an estimation of the deviation of the three bond angles from the full angle ranging from 0% (planar) to 100% (for maximum pyramidisation, e.g., 3 mutually perpendicular 2pN orbitals). This library of computational DP(%) values then needs to be compared alongside crystal structures to iteratively assign probable isomers.

Overall, it is difficult to ascertain what possible isomers could exist and their likely relative stabilities. However excluding limitations by internal hydrogen bonding, based on previous work with single phosphaguanidines (8 isomers; E_{syn}-(α,β), E_{anti}-(α,β), Z_{syn}-(α,β), Z_{anti}-(α,β)) one could approximate that eight times the amount of isomers could exist for double hydrophosphination

products, *e.g.* 64; excluding possibilities of internal hydrogen bonding or molecule to molecule hydrogen bonding; which could reduce the amount of likely isomers. (**Figure 26** shows the 16 possible isomers for *EE'* structures; other isomers *EZ'*; *ZZ'* and *ZE'* will also each have 16 more possible isomers).

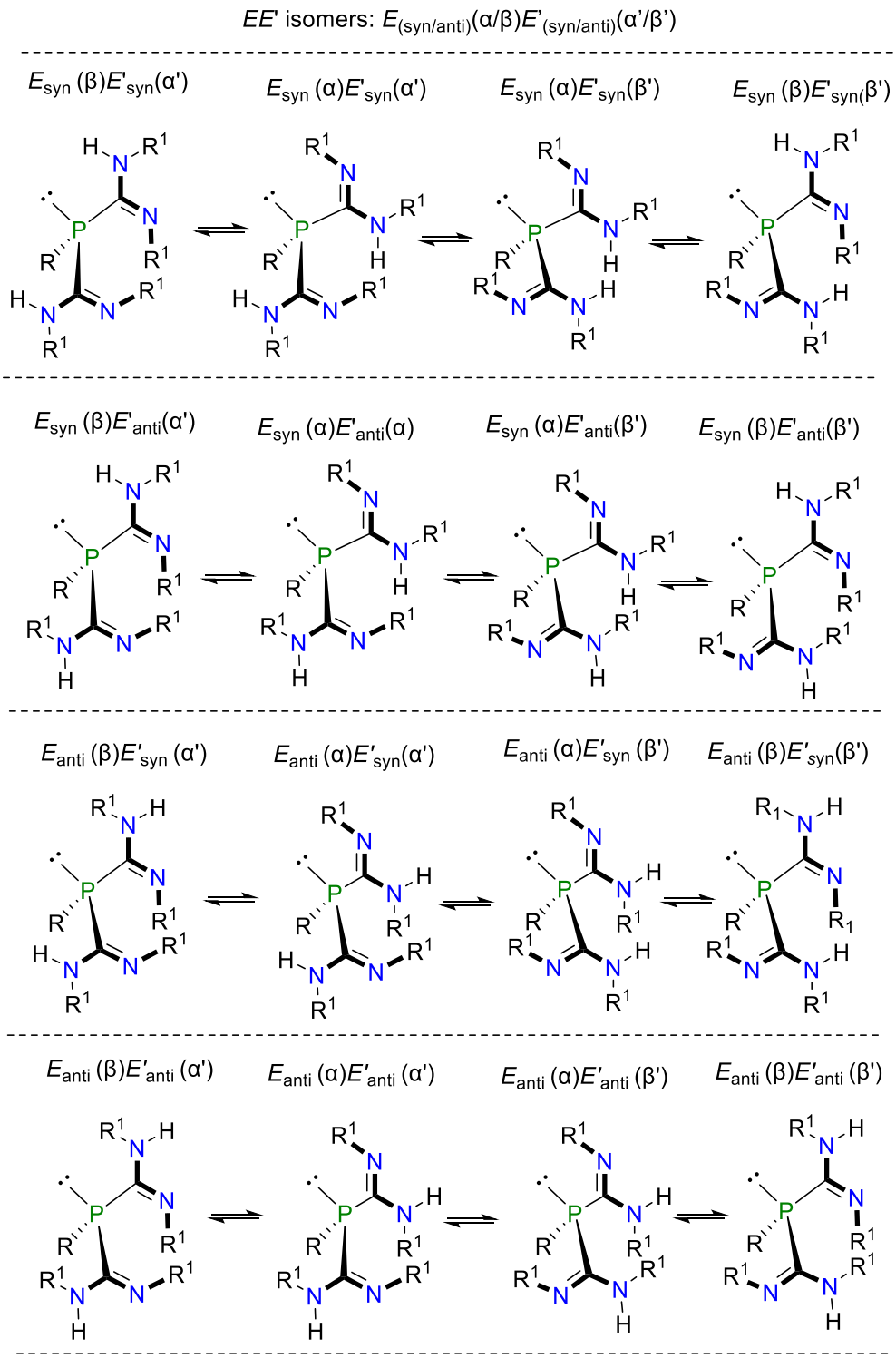


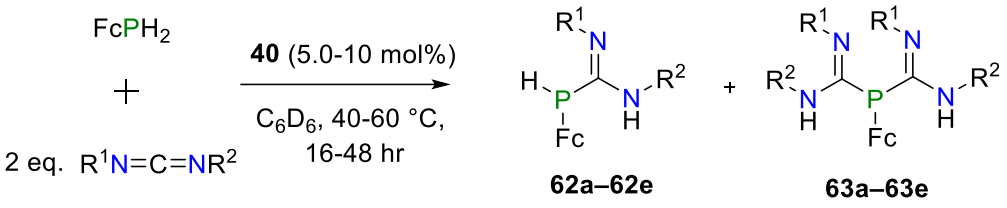
Figure 27. *Possible 16 EE': $E_{(syn/anti)}(\alpha/\beta)E'_{(syn/anti)}(\alpha'/\beta')$ isomers for double hydrophosphination of carbodiimides out of 64 possible isomers (a further 16 isomers each for EZ', ZZ' and ZE).'*

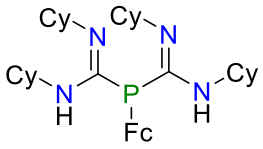
4.3.3.3 Double hydrophosphination of carbodiimides with $FcPH_2$

Following successful initial hydrophosphination reactions of CyN=C=NCy with $FcPH_2$, the carbodiimide substrate scope was expanded to ^{i}PrN=C=N^{i}Pr (**Table 49**) in which after 16 hours at 60 °C utilising 5.0 mol% of **40** gave a conversion (determined by ^{31}P NMR spectroscopy) of >99% from $FcPH_2$ to 94% of the double hydrophosphination product **63b** (^{31}P NMR = -54.9 ppm) and 1% of the single hydrophosphination product **62b.** The other 5% conversion corresponds to peaks at: –57.8 (s) ppm (1%), –51.0 (s) (3%) and –48.8(s) (1%), all of which are plausible values for minor isomers of the double hydrophosphination product, **63b**.

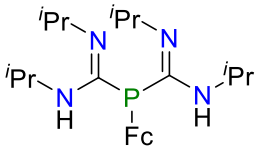
The use of bulkier carbodiimide, ^{t}BuN=C=NEt at 60 °C with 5.0 mol% of **40** for 16 hours gave a comparatively lower (23%) conversion (*cf.* >99% for CyN=C=NCy and ^{i}PrN=C=N^{i}Pr); with 22% being the double hydrophosphination product **63c** (δ_P = –51.3 ppm, singlet) and 1% the single hydrophosphination product **62c** (δ_P = –81.5 ppm, doublet ^{1}J(P,H) = 225 Hz, P–H). Heating of the reaction mixture for an additional 16 hours did not improve the conversion. Increasing the precatalyst loading of **40** to 10 mol% and increasing the reaction time to 32 hours gave a near-quantitative conversion from $FcPH_2$ to 87% of **63c** and 12% of **62c** (**Table 49**)**.** NMR spectroscopic analysis (using COSY, HSQC and HMBC), revealed regioselectivity for both “NCN” moieties with the N-H bond being formed on the nitrogen atom with the *tert*-butyl group attached (as was found previously with the single hydrophosphination of ^{t}BuN=C=NEt with $HPPh_2$).

Table 49. Catalytic single and double hydrophosphination of carbodiimides with $FcPH_2$[a,b,c]

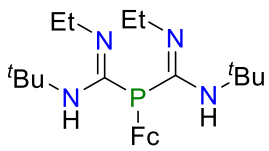




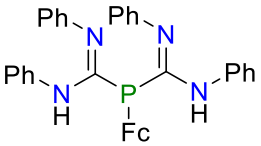
63a: 5.0 mol% **40**, 60 °C, 16 hr, 55%, (**62a**:**63a**, 1:96)



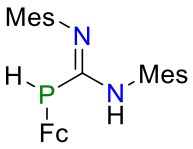
63b: 5.0 mol% **40**, 60 °C, 16 hr, (**62b**:**63b**, 1:94)



63c: 10 mol% **40**, 60 °C, 32 hr, (**62c**:**63c**, 12:87)



63d: 5.0 mol% **40**, 40 °C, 32 hr, (**62d**:**63d**, 7:53)



62e: 5.0 mol% **40**, 60 °C, 16 hr, (**62e**:**63e**, 71:16)

*[a] Reaction conditions for conversions: 1.0 eq. of $FcPH_2$ = 0.148 mmol and 2.0 eq. of $^1RN=C=NR^2$ (R^1 = R^2 = Cy, ^{i}Pr, Ph) = 0.292 mmol or 1.0 eq., of $FcPH_2$ = 0.0740 mmol and 2.0 eq. of MesN=C=NMes = 0.148 mmol and C_6D_6 (0.50 mL) for 16 hours under a nitrogen atmosphere unless otherwise stated.[b] Conversion determined by ^{31}P NMR spectroscopy by relative integration of ^{31}P NMR peaks.[c] Conversions to (**62**:**63**) given in brackets as ratios.*

The carbodiimide scope was further explored, changing from dialkyl carbodiimides to potentially more reactive diaryl carbodiimides. PhN=C=NPh was reacted at 60 °C with 5.0 mol% **40** demonstrating 100% conversion. Unfortunately, this reaction afforded a mixture of products as demonstrated by the formation of 18 new peaks in the ^{31}P NMR spectrum ranging from approximately –75 to 75 ppm (**Figure 28**).

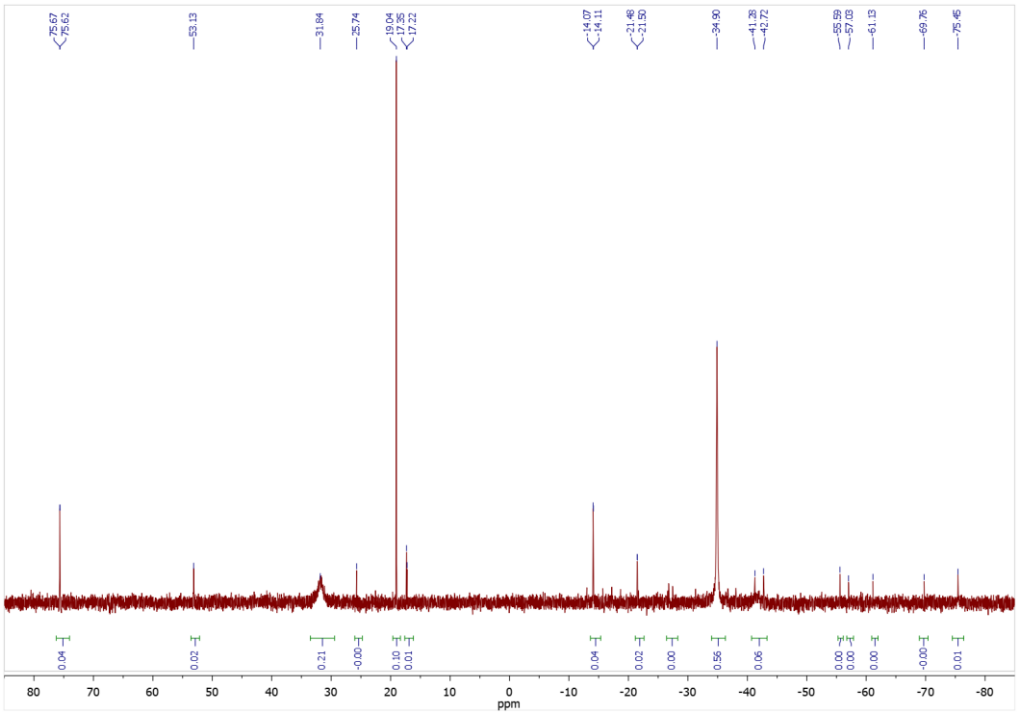


Figure 28. *^{31}P NMR spectra of the reaction of PhN=C=NPh, $FcPH_2$ and 5.0 mol% **40** at 60 °C after 16 hours.*

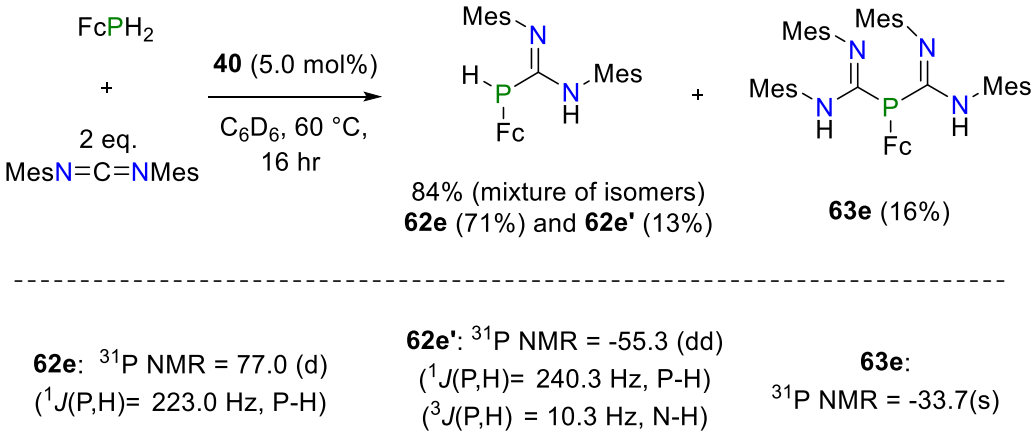
There are two major peaks at 56% (-34.9 ppm) and 21% (31.8 ppm) (**Figure 28**). These additional unexpected peaks may be due to polymerisation of the PhN=C=NPh as some insoluble precipitate was observed in the Young's NMR reaction tube. accompanied by hydrophosphination of the subsequent polymers. Or another possibility is that for R = Ph the formation of one specific hydrophosphination isomer is not as favoured to the same extent as compared to products from dialkyl carbodiimides.

Lowering the reaction temperature to 25 °C resulted in a much lower conversion of 2% to an unknown peak at δ_P = –74.0(s) ppm, and an additional 16 hours of reaction time did not increase the conversion. Utilising a moderate approach between the two temperatures at 40 °C after 16 hours gave a 42% conversion from $FcPH_2$ to 3% of single hydrophosphination product **62d** -75.5 (d, ^1J(P,H) = 233 Hz, P–H) and 26% of a peak at –34.9 (s) ppm which is tentatively assigned to the double hydrophosphination product, **63d**. This reaction also afforded an

additional mixture of unassigned peaks at 25.7 (s), 19.0 (s), –24.7 (s), –30.1 (s) ppm) in a 13% conversion**.** Further heating at 40 °C for 16 hours (total time = 32 hours) increased overall conversion to 77%; with 7% being **62d** and 53% for **63d** (**Table 49**). Other unknown peaks include 7% at –41.7 (s) ppm, 5% at 19.04 (s) ppm and 5% at 31.8 (s) ppm. Unfortunately, further heating of the reaction at 40 °C another 16 hours (48 hours in total), did not further increase conversions.

In an effort to achieve higher conversions with a diaryl carbodiimide substrate, the bulky carbodiimide MesN=C=Mes was chosen as a substrate; with the idea that increasing the steric demands of the R group would lead to the formation of fewer isomers of hydrophosphination products. Additionally, this substrate would exhibit improved stability against potential polymerisation at increased temperatures (compared to PhN=C=NPh).

Utilising 5.0 mol% of **40** with $FcPH_2$ and MesN=C=NMes at 60 °C for 16 hours resulted in a 100% conversion to only three species as determined by ^{31}P NMR spectroscopy (**Scheme 64**).



62e: ^{31}P NMR = 77.0 (d)
(^{1}J(P,H)= 223.0 Hz, P-H)

62e': ^{31}P NMR = -55.3 (dd)
(^{1}J(P,H)= 240.3 Hz, P-H)
(^{3}J(P,H) = 10.3 Hz, N-H)

63e:
^{31}P NMR = -33.7(s)

Scheme 64*. (Above) Hydrophosphination of MesN=C=NMes with $FcPH_2$ by precatalyst* ***40*** *and (Below) corresponding ^{31}P NMR values for* ***62e****/****62e'*** *and* ***63e****.*

Two of these compounds are single hydrophosphination products **62e** at 71% conversion (–77.0 ppm, d ^{1}J(P,H) =234 Hz) and **62e'** (–55.3 dd, ^{1}J(P,H) = 240 Hz and ^{3}J(P,H) = 10.3 Hz, N–H); **62e'** is labelled to differentiate from **62e** but the exact isomer is not known. Furthermore, there is a 16% conversion to the double hydrophosphination product **63e** (–33.7 ppm, br s, **Scheme 64**).

Further heating of the reaction at 60 °C (of MesN=C=NMes) for an additional 16 hours did not alter conversions. Of all carbodiimides tested MesN=C=NMes formed the highest ratio of single hydrophosphination (84% in total including both isomers) which is attributed to the high steric bulk of the Mes groups impeding a second addition for the free P–H bond of the single hydrophosphination product. This being said the use of bulky Mes group did limit the number of isomers formed from an aryl carbodiimide substrate compared to PhN=C=NPh.

4.4 Conclusions

Unlike hydrophosphination-type reactions of isocyanates (Chapter 3), attempted catalyst-free neat or in solution (C_6D_6) hydrophosphination reactions of carbodiimides were unsuccessful at either 25 °C or 60 °C after 16 hours ($HPPh_2$, HP^iPr_2 and $FcPH_2$ substrates).

Precatalyst **40** (5.0 mol%, at 60 °C for 16 hours) was found to be an excellent catalyst for the single hydrophosphination of carbodiimides, $R^1N=C=NR^2$ (R^1 = R^2 = Cy, ^{i}Pr, Ph or R^1 = Et; R^2 = ^{t}Bu) with $HPPh_2$. The expected single hydrophosphination products, **60a**-**60d** formed in excellent to quantitative conversions (91-99%; with minor conversions to $Ph_2P–PPh_2$ at 1-6%). Additionally, hydrophosphination of the asymmetric substrate ^{t}BuN=C=NEt was found to be regioselective with the N–H bond being formed adjacent to the bulkier *tert*-butyl group. In further success out of a possible eight isomers (by hindered rotation), all single hydrophosphination products **60a**-**60d** could be assigned to the E_{syn}(α) isomer; showing high selectivity by precatalyst **40**.

Less success was achieved with precatalyst **40** when the secondary phosphine scope was changed to dialkyl phosphines, utilising HP^iPr_2. Conversions were very low (1-19% with heating at 60 °C for 72 hours); this again highlights the known difficulty of dialkyl phosphines as HPR_2 substrates for the hydrophosphination of carbodiimides (and heterocumulenes in general).

The significantly less explored area of double hydrophosphination of carbodiimides with primary phosphines was investigated, again utilising precatalyst **40** (5.0 mol% at 60 °C). Dialkyl carbodiimides, $R^1N=C=NR^2$ (R^1 = R^2 = Cy, ^{i}Pr or R^1 = Et; R^2 = ^{t}Bu) underwent good to excellent conversions (87-96%) with $FcPH_2$ to the expected double hydrophosphination products **63a-63c** (with minor- low amounts of single hydrophosphination products being formed, **62a**-**62c**.)

Further heterocumulene scope expansion to utilising diaryl carbodiimide PhN=C=NPh proved more difficult, requiring a lower temperature of 40 °C (at 60 °C multiple unknown phosphorous containing signals form) undergoing a lower 53% conversion to the double hydrophosphination product **63d** after 32 hours. Use of bulky carbodiimide, MesN=C=NMes favoured the single hydrophosphination product, **62e** (71%; with minor 16% conversion to double hydrophosphination product, **63e**) likely due to the increased steric bulk of the mesityl groups hindering insertion into the available P–H bond.

Comparatively to products from single hydrophosphination (i.e., hydrophosphination with $HPPh_2$) the double hydrophosphination products (i.e., with $FcPH_2$) have a theoretical 64 total isomers with 16 isomers for each EE', EZ', ZE' or ZZ' pair. Without further computational analysis or X-ray crystal structures, the exact isomers cannot be determined. However, **63a**-**63c** appear to have similar ^{31}P NMR spectroscopic values at *ca* 53-55 ppm suggesting potentially they are the same isomer (or closely related isomer). **63d**-**63e** are likely different isomers given the difference in their ^{31}P NMR values (-41.3 ppm and -33.7 ppm).

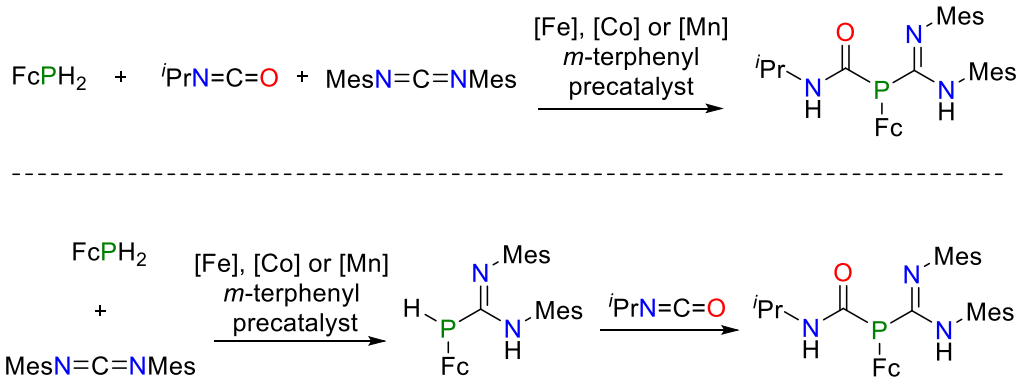
Overall, complex **40** has been shown to be an effective precatalyst for the single hydrophosphination of carbodiimides with $HPPh_2$ (forming only the E_{syn}(α) isomer) but a less successful precatalyst when the P–H scope is changed to HP^iPr_2. Double hydrophosphination (with $FcPH_2$) of dialkyl and diaryl carbodiimides has been explored to a greater extent for the first time, with precatalyst **40** favouring the formation of double hydrophosphination products except when bulky MesN=C=NMes is used (favours single hydrophosphination).

4.5 Future Work

For the single hydrophosphination of phosphines, there is still a distinct lack of examples with alkyl phosphines, potentially other *m*-terphenyl based catalysts (M = [Co] or [Mn]) could be investigated to study how changing the metal centre influences the reactivity with alkyl phosphines such as $HPiPr_2$ or $CyPH_2$.

As double hydrophosphination products are very novel further research needs to be done on their potential uses, particularly as ligands. Additionally with many potentially different isomers forming, computational analysis and crystal structures are necessary to confirm what isomers are forming.

Due to the demonstrated success of $FcPH_2$ with both carbodiimides and isocyanates (Chapter 3), it is plausible that a mixed species could form in a reaction with both substrates. This could either be by a one-pot mixture, or sequential formation of P-H bond species (**Scheme 65**). These mixed hard and soft donors could potentially be used as multi-dentate ligands with varying bonding modes.



Scheme 65. *Proposed one-pot (above) or (below) sequential mixed isocyanate-carbodiimide hydrophosphination by a metal m-terphenyl catalyst.*

4.6 Experimental Procedures

4.6.1 Hydrophosphination of carbodiimides with $HPPh_2$

4.6.1.1 initial catalyst-free control reaction in solution and neat

In an inert atmosphere glovebox, an oven dried Young's tap modified NMR tube was charged with $HPPh_2$ (1.0 eq., 12.8 µL, 0.0734 mmol) and $^{i}PrN=C=N^{i}Pr$ (1.0 eq., 11.4 µL, 0.0734 mmol) in C_6D_6 (0.6 mL) or neat. The sealed tube was left at 25 °C or heated to 60 °C for 16 hours. Both a ^{1}H and ^{31}P NMR spectrum were recorded, resulting in a 0% conversion from $HPPh_2$ by ^{31}P NMR spectroscopy.

4.6.1.2 Initial catalytic optimisation reactions hydrophosphination with $HPPh_2$

In an inert atmosphere glovebox, an oven dried Young's tap modified NMR tube was charged with $HPPh_2$ (1.0 eq., 12.8 µL, 0.0734 mmol), $^{i}PrN=C=N^{i}Pr$ (1.0 eq., 11.4 µL, 0.0734 mmol), **40** (5 mol%, 2.5 mg). The sealed tube was left at 25 °C or heated to 60 °C for 16 hours. A ^{31}P NMR spectrum was recorded and relative peaks compared. NMR spectroscopic yields (conv. to **60a**: conv to Ph_2P-PPh_2 %) = (12: 0%) and (98, 2%) respectively.

4.6.1.3 General procedure for the hydrophosphination of carbodiimides with $HPPh_2$ (NMR yields)

5.0 mol% of **40** (10.0 mg, 0.0147 mmol) was dissolved in C_6D_6 (0.6 mL) in a Young's NMR tube along with Ph_2PH (51 µL, 0.292 mmol), the corresponding carbodiimide (1:1, Ph_2PH: RN=C=NR) and PPh_3 (15.4 mg, 0.0585 mmol). The reaction was either carried out at room temperature or heated to 60 °C. The reaction was monitored by ^{1}H and ^{31}P NMR spectroscopy. Conversion was quantified by integration of ^{31}P NMR spectra with PPh_3 as an internal standard.

4.6.1.4 Scaled up reaction of CyN=C=NCy and $HPPh_2$

A Schlenk flask was charged with a stirrer bar, CyN=C=NCy (1.00 g, 4.85 mmol), Ph_2PH (0.84 mL, 4.9 mmol), **40** (165 mg, 0.24 mmol, 5.0 mol%), and toluene (10 mL), and heated to 60 °C for 24 h with stirring. The rest of the procedure was conducted under argon, using solvent that was degassed but not anhydrous. The reaction was cooled to room temperature, and degassed water (30 mL) and toluene (20 mL) were added. The organic layer was separated, and the aqueous layer washed with more toluene (2 × 10 mL). The combined organics were dried over anhydrous $MgSO_4$ and filtered to obtain a dark brown solution. Activated charcoal (*ca.* 100 mg) was added, the reaction heated to *ca.* 100 °C for 1 minute, then cooled to room temperature and filtered again to afford a yellow/orange solution. Volatiles were removed *in vacuo* to afford a light brown solid. The crude product was dissolved in a minimum volume of hot hexane and recrystallised at −30 °C to afford pure **2a** as an off-white crystalline solid (1.576 g, 4.01 mmol, 83%). Characterisation matched literature data.[90]

4.6.2 Hydrophosphination of carbodiimides with HP^iPr_2

4.6.2.1 initial catalyst-free control reaction

In an inert atmosphere glovebox, an oven dried Young's tap modified NMR tube was charged with HP^iPr_2 (1.0 eq., 10.8 µL, 0.0734 mmol) and $^iPrN=C=N^iPr$ (1.0 eq., 11.4 µL, 0.0734 mmol) in C_6D_6 (0.6 mL) or neat. The sealed tube was left at 25 °C or heated to 60 °C for 16 hours. Both a ^1H and ^{31}P NMR spectrum were recorded, resulting in a 0% conversion from $HPPh_2$ by ^{31}P NMR spectroscopy.

4.6.2.2 Initial catalytic hydrophosphination of ^{i}PrN=C=N^{i}Pr with HP^{i}Pr$_2$

40 (0.05 eq. = 2.5 mg, 0.00366 mmol or 0.1 eq., = 5.0 mg, 0.00732 mmol) was dissolved in C_6D_6 (0.6 mL) in a Young's NMR tube along with HP^{i}Pr$_2$ (1.0 eq., 21.6 µL, 0.00.147 mmol), and ^{i}PrN=C=N^{i}Pr (1.0 eq., 22.7 µL, 0.147 mmol). The reaction was either heated to 25 or 60 °C for 16 hours. The reaction was monitored by ^{1}H and ^{31}P NMR spectroscopy. Conversion was quantified by integration of ^{31}P NMR spectra by relative integration of the ^{31}P NMR peaks. Respective NMR spectroscopic yields (conv. to **61a**: conv to ^{i}Pr$_2$P-P^{i}Pr$_2$ %) = (0: 0%) and (1, 0%) respectively.

4.6.2.3 General procedure for the hydrophosphination of CyN=C=NCy and ^{t}BuN=C=NEt with HP^{i}Pr$_2$ (NMR yields)

40 (0.05 eq., 5.0 mg, 0.00734 mmol) was dissolved in C_6D_6 (0.6 mL) in a Young's NMR tube along with HP^{i}Pr$_2$ (1.0 eq., 21.6 µL, 0.147 mmol), the corresponding carbodiimide (1 eq., RN=C=NR, 0.147mmol) and heated to 60 °C for 72 hours. The reaction was monitored by ^{1}H and ^{31}P NMR spectroscopy. Conversion was quantified by integration of ^{31}P NMR spectra by relative ^{31}P NMR peaks. Respective NMR spectroscopic yields with conversion to **61b** = 10% and to **61c** = 18% respectively.

4.6.3 Hydrophosphination of carbodiimides with FcPH$_2$

4.6.3.1 initial catalyst-free control reaction

In an inert atmosphere glovebox, an oven dried Young's tap modified NMR tube was charged with HPPh$_2$ (1.0 eq., 12.8 µL, 0.0734 mmol) and ^{i}PrN=C=N^{i}Pr (1.0 eq., 11.4 µL, 0.0734 mmol) in C_6D_6 (0.6 mL) or neat. The sealed tube was left

at 25 °C or heated to 60 °C for 16 hours. Both ^{1}H and ^{31}P NMR spectra were recorded, resulting in a 0% conversion from $HPPh_2$ by ^{31}P NMR spectroscopy.

4.6.3.2 Initial catalytic hydrophosphination of CyN=C=NCy with $FcPH_2$

40 (0.01 eq., 0.025 eq. or 0.05 eq.) was dissolved in C_6D_6 (0.6 mL) in a Young's NMR tube along with $FcPH_2$ (1.0 eq., 31.9 mg, 0.146 mmol), and CyN=C=NCy (2.0 eq., 60.4 mg, 0.293 mmol). The reaction was either heated to 25 or 60 °C for 16 hours. The reaction was monitored by ^{1}H and ^{31}P NMR spectroscopy. Conversion was quantified by integration of ^{31}P NMR spectra by relative integration of the ^{31}P NMR peaks. NMR spectroscopic yields (conv. to **62a** : conv to **63a**) = (7: 14% from 5.0 mol% **40** at 25 °C), (1 : 96% from 5.0 mol% **40** at 60 °C), (1 : 58% from 2.5 mol% **40** at 60 °C) and (2:10% from 1.0 mol% **40** at 25 °C) respectively.

4.6.3.3 General procedure for the hydrophosphination of carbodiimides with $FcPH_2$ (NMR yields)

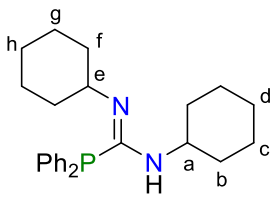
40 (0.05 eq., 5.0 mg, 0.00732 mmol (**63a**-**63b**, **63d** and **62e**) or 0.1 eq., 10.0 mg, 0.0146 mmol (**63c**)) was dissolved in C_6D_6 (0.6 mL) in a Young's NMR tube along with $FcPH_2$ (1.0 eq., 31.8 mg, 0.148 mmol), the corresponding carbodiimide, $^{1}RN=C=NR^{2}$ (2.0 eq., 0.292 mmol). The reaction was heated to 40 °C (**63d**) or 60 °C (**63a**-**63c** and **62e**) for 16 hours (**63a**-**63b** and **62e**) or 32 hours (**63c**-**63d**). The reaction was monitored by ^{1}H and ^{31}P NMR spectroscopy. Conversion was quantified by integration of ^{31}P NMR spectra by relative ^{31}P NMR peaks. Respective NMR spectroscopic yields (conv. to **62**: conv to **63**) (1:96%; $R^1 = R^2 = Cy$), (1:94 %; $R^1 = R^2 = {}^{i}Pr$), (12:87%; $R^1 = Et$; $R^2 = {}^{t}Bu$), (7:53%; $R^1 = R^2 = Ph$) and (71:16% ; $R^1 = R^2 = Mes$)

4.6.3.4 Scaled up hydrophosphination of cyclohexyl isocyanate with $FcPH_2$ (isolated yields)

In an inert atmosphere glovebox, a 25 mL oven dried Young's tap modified flask was charged with $Fe(C_6H_3\text{-}2,6\text{-}Mes_2)_2$, (0.05 eq., 30.0 mg, 0.044 mmol), $FcPH_2$ (1.0 eq., 191.2 mg, 0.879 mmol) and CyN=C=NCy (2.0 eq., 362.7 mg, 1.76 mmol) in toluene (4.0 mL) and the reaction stirred at 60 °C overnight. The remaining procedure was carried out under an inert atmosphere as the products are air-sensitive. Degassed H_2O (5.0 mL) was added to the reaction mixture for *ca* 5 minutes and then the two layers were allowed to separate. The upper organic layer was filtered into a Schlenk flask containing $MgSO_4$ (*ca* 10g) and the remaining aqueous layer was washed with toluene (4 × 5.0 mL) and the organic extracts combined into the flask containing $MgSO_4$. The organic-$MgSO_4$ mixture was stirred (*ca* 5.0 minutes) and filtered. Volatiles were removed *in vacuo* to afford the crude product as a dark orange-red. This was then washed in the minimum amount of cold hexane (3 × 5.0 mL). Dark brown-solid 302.1 mg (55%).

4.6.4 Yields and characterisation for **60a**-**60d**

4.6.4.1 $Ph_2PC(=NCy)NH(Cy)$ (**60a**)



Off-white crystalline solid 1.58g, 83% (99% NMR yield). **^{1}H NMR** (400 MHz, C_6D_6, 25 °C) δ = 7.57-7.49 (m, 4H, PPh_2^{m}), 7.11-7.00 (m, 6H, PPh_2^{o+p}), 4.28-4.05 (m, 2H, CH^{a+e}), 3.84 (d, ^3J(H,H) = 7.1 Hz, 1H, N*H*), 1.98-1.85 (m, 4H, CH_2^{f}), 1.82-1.66 (m, 4H, CH_2^{b}), 1.53-1.44 (m, 2H, CH_2^{h}), 1.40-1.13 (m, 6H, CH_2^{d+g}), 1.06-0.91 (m, 4H, CH_2^{c}) ppm.

^{13}C{^{1}H} NMR (101 MHz, C_6D_6, 25 °C) δ = 152.4 (d, ^1J(C,P) = 31.8 Hz, *C*=N), 135.8 (d, ^1J(C,P) = 14.4 Hz, PPh_2^{i}), 134.4 (d, ^3J(C,P) = 19.6 Hz, PPh_2^{m}), 129.8

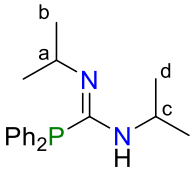
(PPh$_2$^{p}), 129.1 (d, ^{2}J(C,P) = 6.8 Hz, PPh$_2$^{o}), 60.4 (d, ^{4}J(C,P) = 34.0 Hz, *C*H^{e}), 49.3 (s, *C*H^{a}), 35.8 (s, *C*H$_2$^{b}), 32.7 (s, *C*H$_2$^{c}), 26.5 (s, *C*H$_2$^{g}), 26.3 (*C*H$_2$^{f}), 25.3 (*C*H$_2$^{h}), 24.7 (*C*H$_2$^{d}). ppm.

^{31}P{^{1}H} NMR (162 MHz, C_6D_6, 25 °C) δ = –18.3 ppm.

HRMS (ESI) expected: 393.2454, found: 393.2455 (err [ppm] = 0.30) $[M+H]^+$.

Characterisation matched literature data.[90]

4.6.4.2 Ph$_2$PC(=N^{i}Pr)NH(^{i}Pr) (**60b**)



Selected values from *in situ* reaction 99% (NMR yield).

^{1}H NMR (400 MHz, C_6D_6, 25 °C) δ = 7.46 (br s, 4H, Ph^{o}), 7.06 (br s, 6H, Ph^{m+p}), 4.41 (br s, 1H, C*H*^{a}), 4.33 (br s, 1H, C*H*^{c}), 1.24 (br s, 6H, C*H*$_3$^{b}), 0.96 (br s, 6H, C*H*$_3$^{d}) ppm.

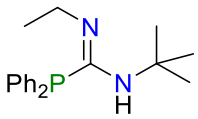
^{13}C{^{1}H} NMR (101 MHz, C_6D_6, 25 °C) δ = 152.4 (d, ^{1}J(C,P) = 32.1 Hz, *C*=N), 135.6 (d, ^{1}J(C,P) = 14.2 Hz, Ph^{i}), 134.3 (d, ^{2}J(C,P) = 19.7 Hz, Ph^{o}), 129.4 (Ph^{p}), 129.1 (d, ^{3}J(C,P) = 6.7 Hz, Ph^{m}), 52.2 (d, ^{4}J(C,P) = 35.2 Hz, *C*H^{a}), 42.9 (s, *C*H^{c}), 25.4 (s, *C*H$_3$^{b}), 22.5 (s, *C*H$_3$^{d}) ppm.

^{31}P{^{1}H} NMR (162 MHz, C_6D_6, 25 °C) δ = –18.5 ppm.

HRMS (ESI) expected: 313.1828, found: 313.1845 (err [ppm] = 5.40) $[M+H]^+$.

Characterisation matched literature data.[90]

4.6.4.3 Ph$_2$PC(=NEt)NH(^{t}Bu) (**60c**)



Selected values from *in situ* reaction. 99% (NMR yield).

^{1}H NMR (400 MHz, C_6D_6, 25 °C) δ = 7.51–7.40 (m, 4H, Ph^{m}), 7.10–7.01 (m, 6H, Ph^{o+p}), 3.78–3.70 (m, 3H, C*H*$_2$CH$_3$ + N*H*), 1.34 (s, 9H, CC*H*$_3$), 1.28 (t, ^{3}J(H,H) = 7.1 Hz, 3H, CH$_2$C*H*$_3$) ppm.

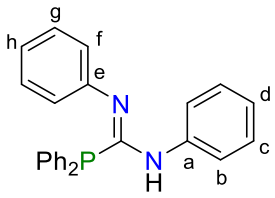
$^{13}C\{^1H\}$ NMR (101 MHz, C_6D_6, 25 °C) δ = 153.8 (d, ^1J(C,P) = 33.5 Hz *C*=N), 135.5 (d, ^1J(C,P) = 14.2 Hz Ph^i), 134.4 (d, ^3J(C,P) = 19.5 Hz, Ph^m), 129.3 (Ph^p), 129.1 (d, ^2J(C,P) = 6.8 Hz, Ph^o), 52.2 (*C*CH_3) 47.0 (d, ^4J(C,P) = 36.9 Hz *C*H_2CH_3), 28.8 (C*C*H_3), 17.8 (CH_2*C*H_3) ppm.

$^{31}P\{^1H\}$ NMR (162 MHz, C_6D_6, 25 °C) δ = –16.1 ppm.

HRMS (ESI) expected: 131.1828, found: 313.1829 (err [ppm] = 0.10) $[M+H]^+$.

Characterisation data matched literature data.[179]

4.6.4.4 $Ph_2PC(=NPh)NH(Ph)$ (**60d**)



Selected values from *in situ* reaction. 99% (NMR yield). **^1H NMR** (400 MHz, C_6D_6, 25 °C) δ = 7.68 (d, ^3J(H,H) = 8.0 Hz, 4H, Ph^{b+f}), 7.44-7.28 (m, 6H, PPh_2^{o+p}), 7.13-7.05 (m, 2H, Ph^{d+h}), 7.00 (m, 4H, PPh_2^m), 6.91-6.81 (m, 4H, Ph^{c+g}), 6.44 (s, 1H, N*H*) ppm.

$^{13}C\{^1H\}$ NMR (101 MHz, C_6D_6, 25 °C) δ = 155.3 (*C*=N, ^1J(C,P) = 41.0 Hz), 150.8 (PPh_2^i, ^1J(C,P) = 12.3 Hz), 141.9 (s, Ph^e), 141.0 (s, PPh_2^o), 139.4 (s, Ph^a), 134.4 (d, ^4J(C,P) = 20.2 Hz, PPh_2^p), 129.8 (s, Ph^b), 129.3 (d, ^4J(C,P) = 6.9 Hz, Ph^h), 129.2 (s, Ph^d), 123.2 (s, Ph^g), 122.9 (s, Ph^c), 122.8 (d, ^3J(C,P) = 2.3 Hz, PPh_2^m), 119.0 (s, Ph^f) ppm.

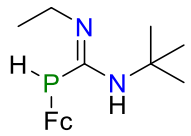
$^{31}P\{^1H\}$ NMR (162 MHz, C_6D_6, 25 °C) δ = –11.3 ppm.

HRMS (ESI) expected: 381.1515, found: 381.1534 (err [ppm] = 5.00) $[M+H]^+$.

Characterisation matched literature data.[173]

4.6.5 Yields and characterisation for **62c**-**62e**

4.6.5.1 FcPH(C(=NEt)NH(^{t}Bu) (**62c**)



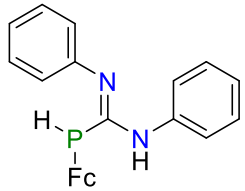
Selected values from *in situ* reaction. (12% NMR yield).

^{31}P NMR (162 MHz, C_6D_6, 25 °C) δ -81.6 (d, ^1J(P,H) = 225 Hz).

^{31}P{^{1}H} NMR (162 MHz, C_6D_6, 25 °C) δ -81.6 (s).

HRMS (ESI) expected: 345.1177, found: 345.1179 (err [ppm] = 0.40) $[M+H]^+$.

4.6.5.2 FcPH(C(=NPh)NH(Ph)) (**62d**)



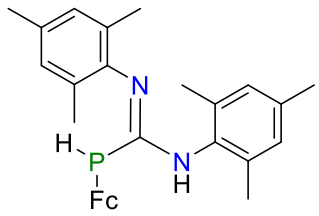
Selected values from *in situ* reaction. (7% NMR yield).

^{1}H NMR (400 MHz, C_6D_6, 25 °C) δ 4.83 (d, ^1J(H,P) = 232.6 Hz, P*H*).

^{31}P NMR (162 MHz, C_6D_6, 25 °C) δ - 75.5 (d, ^1J(P,H) = 233 Hz).

^{31}P{^{1}H} NMR (162 MHz, C_6D_6, 25 °C) δ -75.5 (s).

4.6.5.3 FcPH(C(=NMes)NH(Mes)) (**62e**/**62e**')



Selected values *in situ* reaction. Major Isomer, **62e**: (70% NMR yield).

^{1}H NMR (400 MHz, C_6D_6, 25 °C) δ 6.79 (m, Mes, 4H, Mes C*H*), 5.50 (s, NH^f, 1H) 4.68 (d, ^{1}J(H,P) = 233.8 Hz, 1H, PH^g).

^{13}C{^{1}H} NMR (101 MHz, C_6D_6, 25 °C) δ 157.4 (d, ^1J(C,P) = 30.2 Hz, P*C*).

^{31}P NMR (162 MHz, C_6D_6, 25 °C) δ -77.0 (d, ^1J(P,H) = 234 Hz).

^{31}P{^{1}H} NMR (162 MHz, C_6D_6, 25 °C) δ -77.0 (s).

Selected values from *in situ* reaction. Minor isomer, **62e'**: (13% NMR yield).

^{1}H NMR (400 MHz, C_6D_6, 25 °C) δ 5.41 (s, N*H*, 1H).

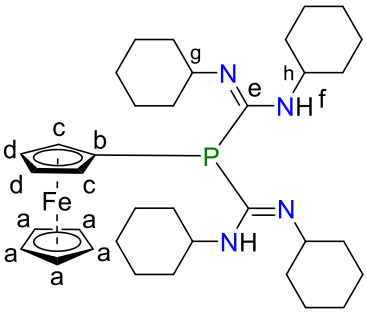
^{31}P NMR (162 MHz, C_6D_6, 25 °C) δ – 55.3 (dd, ^{1}J(P,H) = 240 Hz, ^{2}J(H,H) = 10.3 Hz).

^{31}P{^{1}H} NMR (162 MHz, C_6D_6, 25 °C) δ -55.3 (s).

HRMS (ESI) expected: 497.1803, found: 497.1805 (err [ppm] = 0.10) $[M+H]^+$.

4.6.6 Yields and characterisation for **63a**-**63e**

4.6.6.1 FcP(C(=NCy)NH(Cy))$_2$ (**63a**)



Selected values from *in situ* reaction. 96% (NMR yield).

^{1}H NMR (400 MHz, C_6D_6, 25 °C) δ 4.64 (d, J(H,H) = 6.7Hz, 2H H^g), 4.33-4.30 (m, 2H, H^f), 4.28-4.20 (m, 2H, H^k) 4.15 (s, 5H, H^a), 4.13 -4.11 (m, 2H, H^c), 4.11-4.05 (m, 2H, H^d), 1.92-1.79 (m, 8H, Cy *H*), 1.62-1.43 (m, 10H, Cy *H*), 1.41-1.29 (m, 8H, Cy *H*), 1.31-1.17 (m, 4H, Cy *H*), 1.16 – 0.98 (m, 10H, Cy *H*).

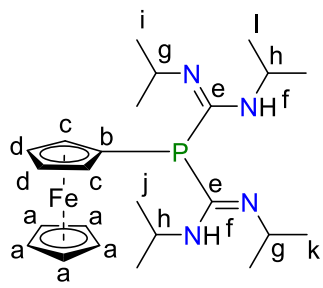
^{13}C{^{1}H} NMR (101 MHz, C_6D_6, 25 °C) δ 152.5 (d, ^{3}J(C,P) = 38.2 Hz), 73.6 (d, ^{1}J(C,P) = 18.4 Hz, Fc C^b) 72.8 (d, ^{2}J(C,P) = 11.2 Hz, C^c), 71.0 (d, ^{3}J(C,P) = 2.5 Hz, C^d), 70.0 (s, C^a), 60.7 (d, ^{4}J(C,P) = 35.3 Hz, C^g) 49.7 (s, C^h), 35.4 (s, Cy *C),* 33.0 (s, Cy *C)*, 26.6 (s, Cy *C)*, 26.4 (s, Cy *C)*, 25.5 (s, Cy *C)*, 24.9 (s, Cy *C)*.

^{31}P NMR (162 MHz, C_6D_6, 25 °C) δ -53.3 (t, ^{3}J(P,H) = 8.3 Hz, NH).

^{31}P{^{1}H} (162 MHz, C_6D_6, 25 °C) δ -53.3 (s).

HRMS (ESI) expected: 631.3586, found: 631.3604 (err [ppm] = 2.70) $[M+H]^+$.

4.6.6.2 FcP(C(=N^{i}Pr)NH(^{i}Pr))$_2$ (**63b**)



Selected values from *in situ* reaction. 94% (NMR yield).

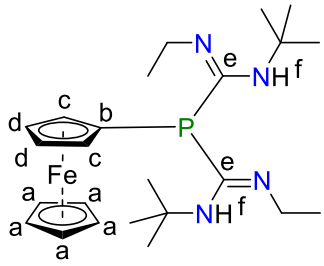
^{1}H NMR (400 MHz, C_6D_6, 25 °C) δ 4.59 (dp, *J*(H,H) = 9.0, 6.1 Hz, 2 x C*H*^{G}), 4.44 (d, ^{3}J(P,H) = 6.4 Hz, 2 x N*H*^{F}), 4.30-4.19 (m, 4H, 2 x Fc *H*^{C} + 2 x C*H*^{H}), 4.10 (s, 5 x Fc *H*^{A}), 4.07 (t, ^{3}J(H,H) = 1.8 Hz, 2 x Fc *H*^{D}), 1.45 (d, ^{3}J(H,H) = 6.1 Hz, 2 x CH_3^{I}), 1.39 (d, ^{3}J(H,H) = 6.1 Hz, 2 x CH_3^{J}), 1.07 (d, ^{3}J(H,H) = 6.4 Hz, 2 x CH_3^{K}), 1.03 (d, ^{3}J(H,H) = 5.3 Hz, 2 x CH_3^{L}).

^{13}C{^{1}H} NMR (101 MHz, C_6D_6, 25 °C) δ 152.4 (d, ^{1}J(C,P) = 37.3 Hz, P*C*^{E}), 72.9 (d, ^{1}J(C,P) = 18.0 Hz, Fc *C*^{B}), 72.7 (d, ^{2}J(C,P) = 11.8 Hz, Fc *C*^{C}), 71.0 (d, ^{3}J(C,P) = 2.6 Hz, Fc *C*^{D}), 69.9 (s, Fc *C*^{A}), 53.0 (d, ^{3}J(C,P) = 38.0 Hz, C=N*C*^{G}), 43.0, (s, C-N*C*^{H}), 26.1, (s, *C*^{I}), 25.3, (s, *C*^{J}), 22.6, (s, *C*^{K}), 22.6, (s, *C*^{L}).

^{31}P{^{1}H} NMR (162 MHz, C_6D_6, 25 °C) δ -54.9 (s).

HRMS (ESI) expected: 471.2334, found: 471.2330 (err [ppm] = 1.10) $[M+H]^+$.

4.6.6.3 FcP(C(=NEt)NH(^{t}Bu))$_2$ (**63c**)



Selected values from *in situ* reaction. 87% (NMR yield).

^{1}H NMR (400 MHz, C_6D_6, 25 °C) δ 4.45 (s, 2 x Fc *H*^{d}, 2H), 4.37-4.32 (m, 2 x Fc *H*^{c}, 2H), 4.09 (s, 5 x Fc *H*^{A}, 5H), 4.05-3.85 (m, N*H* + CH_2CH_3, 6H),1.41 (s, 18H, CC*H*$_3$), 0.99 (t, ^{3}J(H,H) = 7.2 Hz, 3H, CH_2CH_3).

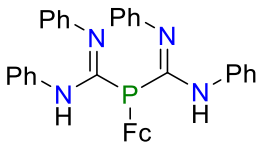
^{13}C{^{1}H} NMR (101 MHz, C_6D_6, 25 °C) δ 153.6 (d, ^{1}J(C,P) = 36.7 Hz, P*C*^{E}), 73.6 (d, ^{1}J(C,P) = 14.6 Hz, Fc *C*^{B}), 72.4 (d, ^{2}J(C,P) = 19.1 Hz, Fc *C*^{C}), 71.5 (d, ^{3}J(C,P) = 3.5 Hz, Fc *C*^{D}), 69.9 (s, Fc *C*^{A}), 52.3 (s, *C*CH_3), 47.9 (d, ^{4}J(C,P) = 40.4 Hz *C*H_2CH_3), 28.8 (s, C*C*H_3), 18.0 (s, CH_2*C*H_3) ppm.

^{31}P NMR (162 MHz, C_6D_6, 25 °C) δ -51.5 (br t, ^3J(P,H) = 5.4 Hz, NH).

^{31}P{^{1}H} NMR (162 MHz, C_6D_6, 25 °C) δ -54.9 (s).

HRMS (ESI) expected: 497.1803, found: 479.1805 (err [ppm] = 0.10) $[M+H]^+$.

4.6.6.4 FcP(C(=NPh)NH(Ph))$_2$ (**63d**)



Selected values from *in situ* reaction. Major isomer (54% (NMR yield).

^{1}H NMR (400 MHz, C_6D_6, 25 °C) δ 7.72 (s, N*H*).

^{31}P NMR (162 MHz, C_6D_6, 25 °C) δ – 34.9 (s).

^{31}P{^{1}H} NMR (162 MHz, C_6D_6, 25 °C) δ -34.9 (s).

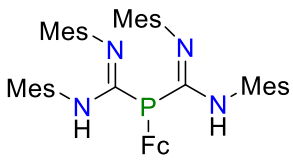
Minor isomer: 7% NMR conversion, selected values.

^{31}P NMR (162 MHz, C_6D_6, 25 °C) δ – 41.3 (s).

^{31}P{^{1}H} NMR (162 MHz, C_6D_6, 25 °C) -41.3 (s).

HRMS (ESI) expected: 471.2334, found: 471.2338 (err [ppm] = 0.70) $[M+H]^+$.

4.6.6.5 FcP(C(=NMes)NH(Mes))$_2$ (**63e**)



Selected values from an *in situ* reaction. (17% NMR yield).

^{31}P NMR (162 MHz, C_6D_6, 25 °C) δ -33.7 (s).

^{31}P{^{1}H} NMR (162 MHz, C_6D_6, 25 °C) δ -33.7 (s).

HRMS (ESI) expected: 775.3586, found: 775.3570 (err [ppm] = 2.30) $[M+H]^+$.

Chapter 5:

Concluding Remarks

The aim of this thesis was to expand the knowledge regarding the synthesis of heteroatom-rich organophosphorus analogues of ureas, thioureas and guanidines by the atom-efficient P-H unit (e.g., $HP(O)R_2$, $HP(O)(OR)_2$, HP(O)R(OR), HPR_2 and RPH_2) addition to heterocumulenes (e.g., RN=C=O, RN=C=S and RN=C=NR). The synthesis of these compounds has required overcoming selectivity challenges mainly: single *vs*. double hydrophosphination and monoinsertion *vs*. diinsertion selectivity. Overcoming these synthetic challenges has required catalytic approaches using low-coordinate *m*-terphenyl complex **40** and in other cases perhaps unexpectedly; a catalyst-free neat or highly concentrated approach.

The hydrophosphinylation ($HP(O)R_2$) of isocyanates was found to surprisingly proceed catalyst-free when either neat or as a concentrated solution despite previous literature suggestions, highlighting the importance of performing catalyst-free control reactions (and most significantly neat control reactions for hydrofunctionalisation reactions). In order to avoid common homogeneity problems with the use of solid substrates a 4 eq. of 2-MeTHF was used as solvent This allowed for a robust procedure allowing for the use of liquid and solid isocyanates and isothiocyanates in yields that matched or exceeded that of previous literature. However subsequent P-H scope expansion to closely related hydrophosphonylation could only be performed neat with aryl isocyanates at elevated temperatures of 60 °C, with isolation being problematic due to the difficult removal of excess unreacted $HP(O)(OR)_2$ starting material.

These subtle differences of neat versus highly concentrated dependence for closely related catalyst-free hydrophosphinylation and hydrophosphonylation reactions; highlight the importance of performing catalyst-free control reactions; even if the P-H (or more generally E-H) substrate scope is similar. In this regard for any catalytic hydrofunctionalisation of heterocumulenes reaction, four simple

and quick reactions should be required to establish the need for a catalyst; in solution (concentrated e.g., ~ 4.0 eq., of solvent) at 25 °C and 60 °C and neat at 25 and 60 °C all for ~16 hours. This is particularly important for electrophilic substrates such as heterocumulenes but given that some reactions have been shown to proceed catalyst-free neat with alkenes (e.g., hydrophosphination); it can also be argued to be applicable to all unsaturated substrates used in hydrofunctionalisation reactions.

The underexplored area of hydrophosphination of isocyanates with primary isocyanates was pursued ($FcPH_2$ and $AdPH_2$), initially starting with neat-catalyst control reactions with $FcPH_2$ to determine if a catalyst was needed. The reaction did show moderate conversion neat at 60 °C to multiple different products from single and double hydrophosphination to single hydrophosphination-diinsertion products. As one of the main aims in this thesis when using isocyanates and primary phosphines is to try and selectively obtain only one of the possible new products; further inquiries into the catalyst-free reaction were stopped.

Instead utilising precatalyst **40** demonstrated similar high reactivity to previously reported hydrophosphination of isocyanates with secondary phosphines; in this case, forming the desired double hydrophosphination products in high conversions (with $FcPH_2$). Attempts at using more forcing conditions (increased isocyanate concentration, temperature and catalyst loading) to synthesise the theoretically proposed novel double-diinsertion products were unsuccessful. Interestingly rare diinsertion-cyclisation products formed (two isocyanates inserted into one P-H bond; followed by the remaining P-H bond dehydrocoupling with the carboxamide N-H bond to form a 5-membered ring). Only once before have similar products been synthesised but not in a catalytic manner through an atom efficient hydrophosphination-type methodology.[153]

With more forcing conditions the diinsertion-cyclisation products, **52a**-**52d** could be selectivity synthesised in moderate to high conversions. Further requirements are the use of a non-coordinating solvent such as toluene or benzene as coordinating THF stops the formation of any diinsertion products and significantly slows the reaction. Only aryl isocyanates are the only tolerated heterocumulene substrate (possibly due to a combination of lower steric and higher electrophilicity compared to alky isocyanates).

Given there are so few examples of hydrophosphination of isocyanates with primary phosphines the P-H substrate scope was changed to $AdPH_2$. Which for moderate yields proved far more difficult to use than $FcPH_2$. Requiring more forcing conditions of 10 mol% of **40**, 60 °C for 32 hours versus 5.0 mol% of **40**, 25 °C at 16 hours for $FcPH_2$; potentially due to the large steric bulk of the adamantyl group hindering attack of the second P-H bond.

Surprisingly under the same conditions utilising functionalised aryl isocyanates (R = 4-OMe, 4-Me, 3-Cl) seemed to have a large, unexpected effect of selectivity with only the diinsertion-cyclisation products being formed in 72% conversion with no double hydrophosphination products. However, under the same conditions, alkyl isocyanates (R = Cy and ^{t}Bu) changed the selectivity back to double hydrophosphination in high conversions (81 and 71%). This suggests the electronics of the aryl group affect the selectivity more when $AdPH_2$ is used (vs $FcPH_2$), however, it should be noted for R = Cy a small amount (13%) of the diinsertion-cyclisation was present, contrary to findings for $FcPH_2$ and alkyl isocyanates.

Unlike hydrophosphination-type reactions of isocyanates (Chapter 3), attempted catalyst-free neat or solution (C_6D_6) hydrophosphination of carbodiimides was unsuccessful (0% yields in all cases) at either 25 °C or 60

°C after 16 hours ($HPPh_2$, HP^iPr_2 and $FcPH_2$; P–H substrates); proving a baseline and need for further catalytic research.

Precatalyst **40** (5.0 mol%, at 60 °C for 16 hours) was found to be an excellent catalyst for the single hydrophosphination of carbodiimides with $HPPh_2$. The expected single hydrophosphination products, **60a**-**60d** formed in excellent to quantitative conversions. Additionally for the asymmetric substrate ^{t}BuN=C=NEt was found to be regioselective for the isomer with the N–H bond forming on the nitrogen atom with the bulkier *tert*-butyl group. A further success is that out of a possible eight isomers (by hindered rotation), all single hydrophosphination products **60a**-**60d** could be assigned to the E_{syn}(α) isomer; showing high selectivity by precatalyst **40**. The identification and assignment of a single isomer is important as often for the hydrophosphination of carbodiimides; these selectivity challenges are overlooked or not discussed; except in a few cases in the literature.[162]

As expected, moving the P-H scope to primary phosphines required more forcing conditions of 60 °C and in some cases an increase in catalytic loading, but for most products excellent conversions were obtained. The use of aryl carbodiimides proved more difficult forming a mix of single (**62d-62e**) and double (**63d**-**63e**) hydrophosphination products for PhN=C=NPh and MesN=C=NMes, with the bulkier MesN=C=NMes favouring the formation of single hydrophosphination products. Additionally, for diaryl carbodiimides no diinsertion products are seen, contrary to findings with aryl isocyanates. As discussed previously for the single hydrophosphination of carbodiimides the isomer synthesised is important but underreported. The hydrophosphination of primary phosphines is still underdeveloped and computational analysis and crystal structures are needed for accurate isomer assignment. However based on the logic applied to single hydrophosphination isomers plausibly there could

be 64 possible isomers but: for many cases only one isomer forms (with minor isomers at conversions of <1-2% being apparent by ^{31}P NMR spectroscopy). Further work is needed to obtain crystal structures to propose which isomers are more likely to form and at what ^{31}P NMR peaks.

Overall, this work has shown that there is still novel research that can be performed on P-H bond addition reactions with heterocumulenes. Moving past repeated small improvements in reactions just focussed on single hydrofunctionalisation and monoinsertion. Being able to perform reactions forming novel products with single *vs.* double and mono *vs.* diinsertion selectively. Because of the novel nature of the reactions and this research improvements can be made in terms of catalytic conditions, with the formation of products from diinsertion-cyclisation of aryl isocyanates requiring more forcing conditions as well as the double hydrophosphination of carbodiimides.

To finish, there still are more selectivity challenges in the hydrophosphination of heterocumulenes to overcome such as the synthesis of one catalyst that can selectively yield either single or double hydrophosphination products as well as the corresponding mono or diinsertion of the same reaction. For example, utilising a primary phosphine ($FcPH_2$ or $AdPH_2$) with two equivalents of phenyl isocyanate to either selectively form the single hydrophosphination diinsertion product (e.g., **50a** or **53a**) or the double hydrophosphination mono insertion product (e.g., **49a** or **54a**); rather than a mixture of both possible combinations.

Chapter 6:

General Experimental

6.1 General Experimental

6.1.1 Manipulation of air sensitive compounds

All manipulations were performed in strict anaerobic and anhydrous conditions using standard Schlenk line and glovebox techniques under an atmosphere of nitrogen or argon stated otherwise.

6.1.2 Preparation of solvents

C_6D_6 was dried over potassium and degassed with three freeze/pump/thaw cycles prior to use. 2-methyltetrahydrofuran (2-MeTHF) was dried by distilling over molten potassium under nitrogen. Dichloromethane was dried by distilling over calcium hydride under nitrogen. Tetrahydrofuran (THF), toluene, diethyl ether and *iso*-hexane were dried by passing through a solvent drying tower of activated alumina. Both were degassed *in vacuo* and stored over activated 4 Å molecular sieves prior to use.

6.1.3 Preparation of reagents

6.1.3.1 P(O)-H and P-H reagents

All reagents were stored in an inert nitrogen glovebox before use.

Diphenylphosphine oxide, $HP(O)Ph_2$ was prepared following the procedures described in the literature.[180,181] Diisopropylphosphine oxide, $HP(O)^iPr_2$ was prepared according to section 2.5.8.1. Methyl phenylphosphinate, HP(O)Ph(OMe) was prepared with a minor modification of a literature procedure.[182] Diethyl phosphite, $HP(O)(OEt)_2$ and dimethyl phosphite, $HP(O)(OMe)_2$ were acquired commercially and purified by vacuum distillation. Ferrocenylphosphine, $FcPH_2$ was prepared with minor modification of a

literature procedure, with subsequent further purification by vacuum sublimation.[183] Adamantyl phosphine, $AdPH_2$ was prepared following a literature procedure.[183] Diphenyl phosphine, $HPPh_2$ was obtained commercially and used as received. $HP(^iPr)_2$ was prepared according to literature.

6.1.3.2 Heterocumulene reagents

All reagents were stored in an inert nitrogen glovebox before use.

Solid (at 25 °C) isocyanates, RN=C=O (R = 3,5-dimethoxyphenyl and 4-nitrophenyl), isothiocyanates, RN=C=S (R = 4-chlorophenyl, 4-nitrophenylphenyl and cyclohexyl) and carbodiimides, $R^1N=C=NR^2$ (R^1= R^2 = cyclohexyl) were acquired commercially and dried overnight under vacuum before use. Dimesitylcarbodiimide was prepared with minor modification of a literature procedure, with subsequent further purification by vacuum sublimation.[183]

Liquid (at 25 °C) isocyanates, RN=C=O (R = *p*-Tol, 4-bromophenyl, 2-fluorophenyl, 3-chlorophenyl, isopropyl, tert-butyl, ethyl, n-propyl, cyclohexyl and n-hexyl) isothiocyanates, RN=C=S (R = *p*-Tol, 4-methoxylphenyl, isopropyl and allyl) and carbodiimides, $R^1N=C=NR^2$ (R^1= R^2 = diisopropyl and R^1 = terty-butyl; R^2 = ethyl) were acquired commercially and stored over 4 Å molecular sieves at -30 °C. Phenyl isocyanate was acquired commercially, dried by stirring for 16 hours over Drierite^{Tm} ($CaSO_4$) ~10% w/w and purified vacuum distillation. Diphenylcarbodiimide was prepared with minor modification to the literature procedure, with further purification by vacuum distillation.[184] Additionally, for the reader's clarity Phenyl isocyanate, phenyl isothiocyanate and diphenyl carbodiimide were not stored over 4 Å molecular sieves, but were stored at -30 °C.

All other reagents and solvents were acquired commercially and used as received unless otherwise stated.

6.1.3.3 General use and handling considerations

Over time isocyanates, isothiocyanates and carbodiimides will tend to polymerise to dimers and cyclotrimers. This is more problematic for liquid heterocumulenes, in particular aryl isocyanates and unsubstituted aryl heterocumulenes (i.e., phenyl isocyanate, phenyl isothiocyanate and diphenyl carbodiimide). Whilst polymerisation can be slowed by storage at -30 °C depending on how frequently the samples are removed it may be advisable to further purify; either by distillation, filtration or by synthesising a new sample on a timescale of ~6 months. Polymerisation is visually evident when the sample becomes much more viscous and/or starts to form a precipitate.

Ferrocenylphopshine and adamantylphosphine are mildly pyrophoric and in small quantities (<30 mg) can be exposed to air with little to no issues (excluding the pungent smell). However, for ferrocenylphosphine at ~25-30 °C when it becomes a liquid, it is much more pyrophoric and needs to be disposed of with appropriate care.

6.2 Physical Measurements

6.2.1 NMR spectroscopy

All NMR spectra were acquired on a Bruker AV400, AV(III)400 or AV(III)400HD spectrometer. Chemical shifts are quoted in ppm relative to neat TMS (^{1}H, $^{13}C\{^{1}H\}$), $CFCl_3$ ($^{19}F\{^{1}H\}$) and 85% H_3PO_4 ($^{31}P\{^{1}H\}$).

6.2.2 Mass spectrometry

Mass spectra were recorded on a Bruker ESI-TOF MicroTOF II by the departmental service at the University of Nottingham.

6.2.3 Elemental analysis

Elemental analyses were performed at the University of Nottingham by Dr Tong Liu on a CE-440 Elemental Analyser, Exeter Analytical, INC. with samples combusted at temperatures of 975 °C before being measured.

6.2.4 Infrared spectroscopy

IR absorption spectra were recorded on a Bruker Alpha FTIR instrument with a 'Platinum' ATR attachment.

6.2.5 X-ray crystallography

Crystal mounting, solution and refinement were performed by Cameron Huke. With the exceptions of: **44m** which was refined by Dr Stephen Argent, **44n** which was refined with Dr Laurence Taylor, **49a** which was mounted by Dr Laurence Taylor and **51b** and **56** which were mounted by Dr Nathan Coles.

Single crystals were selected and mounted using Fomblin® (YR-1800 perfluoropolyether oil) on a polymer-tipped MiTeGen MicroMountTM and cooled rapidly to 120 K in a stream of cold N_2 using an Oxford Cryosystems open flow cryostat.[185]

Single crystal X-ray diffraction data were collected either on an Oxford Diffraction GV1000 (TitanS2 CCD area detector, mirror-monochromated Cu-Kα radiation source; λ = 1.54184 Å, ω scans), an Oxford Diffraction GV1000 (AtlasS2 CCD area detector, mirror-monochromated Cu-Kα radiation source; λ = 1.54184 Å, ω scans), an XtaLAB PRO MM007 (PILATUS3 R 200K Hybrid Pixel Array detector, mirror-monochromated Cu-Kα radiation source; λ = 1.54184 Å, ω scans) or an SuperNova Duo diffractometer (Atlas CCD area detector, mirror-monochromated Mo-Kα radiation source; λ = 0.71073 Å; ω scans).

Cell parameters were refined from the observed positions of all strong reflections in each data set and absorption corrections were applied using a Gaussian numerical method with beam profile correction (CrysAlisPro).[186] The structures were solved within Olex2[187] by dual space iterative methods (SHELXT)[188] and all non-hydrogen atoms refined by full-matrix least-squares on all unique F2 values with anisotropic displacement parameters (SHELXL).[189]

Hydrogen atoms were refined with constrained geometries and riding thermal parameters with the exception of amide hydrogen atoms whose positions were

refined to a target value of 0.88 Å (DFIX). The isotropic displacement parameters of amide hydrogen atoms were fixed at a value of 1.2 times U_{eq} of their parent nitrogen atoms. Distances for hydrogen bonds are represented as values for donor atom (D) minus acceptor atom (A); D-A and angles as donor atom-hydrogen atom-acceptor atom, D-H-A.

Hydrogen bonds are located, with a requirement of a minimum angle of 150° and a maximum bond length of 2.9 Å.

All anisotropic displacement parameters are set at 50% probability.

Structure **44i**: was a 2-component twin. The orientations of the two twin components were determined in CryAlisPro,[186] and integrated to provide a single component HKL file which was used for the initial solution, and a multi-component HKL file which was used for the final refinement of the structure.

Structure **44j** contains positional disorder and is modelled for the n-propyl moieties, C62A, C63A, C64A and C62B, C63B, C64B. The occupancies of the two sites were refined and constrained to sum to unity with values of 0.84(3) and 0.16(3) respectively. Rigid bond and similarity restraints were applied to the C-C bonds of two disordered n-propyl moieties (RIGU, SADI).

Structure **44m**: the benzyl moiety of the main residue is conformationally disordered over three positions. The occupancies of the three positions were restrained to sum to unity using a linear restraint (SUMP) resulting in values of 0.33(2), 0.17(1) and 0.50(2) for components A, B and C respectively. The geometries of the three components were restrained to be similar and have two-fold symmetry (SAME, SADI). The disordered phenyl rings and attached methylene carbon atoms were restrained to have planar geometries (FLAT). The toluene solvent residue is disordered across an inversion centre. All 1,2 and 1,3 distances of the toluene residue were restrained to have suitable target values taken from the Olex2 Fragment database (DFIX, DANG). The toluene

residue was restrained to have planar geometry (FLAT). Rigid bond restraints were applied to the anisotropic displacement parameters of all atoms in the structure (RIGU). Similarity restraints were applied to the anisotropic displacement parameters of all the disordered benzyl atoms (SIMU). The anisotropic displacement parameters of the three disordered benzyl methylene carbon atoms were constrained to be identical (EADP).

Structure **44n**: positional disorder is modelled for both furfuryl moieties, furfuryl moiety 1: C15, O3A, C16A-C18A and C15, O3B, C16B-C18B, and furfuryl moiety 2: C33, 06A, C34A-C34A and 06B, C34B-C34B. The occupancies of the two sites of furfuryl moiety 1 were refined and constrained to sum to unity with values of 0.86(8) and 0.14(8) respectively. The occupancies of the two sites of furfuryl moiety 2 were refined and constrained to sum to unity with values of 0.68(5) and 0.32(5) respectively. The geometries of all furfuryl ligands were restrained to be planar (FLAT). Rigid bond and similarity restraints were applied to the anisotropic displacement parameters of the disordered furfuryl ligands (SIMU, RIGU). Furfuryl moiety chemically equivalent C-O and C-C bonds were restrained to have similar distances (SADI).

Structures were checked with checkCIF.[190]

CCDC 2064932-2064941 contains the supplementary data for compounds: **44i**, **44j**, **44d**, **44e**, **44m**, **44n**, **45c**, **45d**, **45e** and **45h**. These data can be obtained free of charge from The Cambridge Crystallographic Data Centre via www.ccdc.cam.ac.uk/data_request/cif.

References

1 R. Sadigov, *Sci. World J.*, 2022, **2022**, 1–8.

2 D. E. Bloom, *Science* , 2011, **333**, 562–569.

3 OECD, *Material Resources, Productivity and the Environment; OECD Green Growth Studies*, OECD Publishing, Paris, 2015.

4 S. A. Bandh, S. Shafi, M. Peerzada, T. Rehman, S. Bashir, S. A. Wani and R. Dar, *Environ. Sci. Pollut. Res.*, 2021, **28**, 24872–24888.

5 UN 17 Sustainable Development Goals, https://sdgs.un.org/goals, (accessed Sep 2023).

6 J. H. Clark, *Green Chem.*, 1999, **1**, 1–8.

7 P. T. Anastas and J. C. Warner, *Green Chemistry: Theory and Practice*, Oxford University Press, New York, 1998.

8 C. R. McElroy, A. Constantinou, L. C. Jones, L. Summerton and J. H. Clark, *Green Chem.*, 2015, **17**, 3111–3121.

9 Ad-hoc Working group on defining critical raw materials, *Annexes To the Report on Critical Raw Materials for the Eu*, 2014.

10 A. J. Hunt, A. S. Matharu, A. H. King and J. H. Clark, *Elemental sustainability and the Importance of Scarce Element Recovery*, RSC, Cambridge, UK, 2013.

11 S. Failla, P. Finocchiaro and G. A. Consiglio, *Heteroat. Chem.*, 2000, **11**, 493–504.

12 W. X. Zhang, L. Xu and Z. Xi, *Chem. Commun.*, 2015, **51**, 254–265.

13 P. Ertl, E. Altmann and J. M. Mckenna, *J. Med. Chem.*, 2020, **63**, 8408–8418.

14 M. Eto, *Biosci. Biotechnol. Biochem.*, 1997, **61**, 1–11.

15 L. Bourget-Merle, M. F. Lappert and J. R. Severn, *Chem. Rev.*, 2002, **102**, 3031–3065.

16 B. Schlummer and U. Scholz, *Adv. Synth. Catal.*, 2004, **346**, 1599–1626.

17 X. Liu and J. R. Hamon, *Coord. Chem. Rev.*, 2019, **389**, 94–118.

18 J. E. Taylor, S. D. Bull and J. M. J. Williams, *Chem. Soc. Rev.*, 2012, **41**, 2109–2121.

19 P. Selig, *Synth.*, 2013, **45**, 703–718.

20 R. H. Beddoe, K. G. Andrews, V. Magné, J. D. Cuthbertson, J. Saska, A. L. Shannon-Little, S. E. Shanahan, H. F. Sneddon and R. M. Denton, *Science* , 2019, **365**, 910–914.

21 V. Rodriguez-Ruiz, R. Carlino, S. Bezzenine-Lafollée, R. Gil, D. Prim, E. Schulz and J. Hannedouche, *Dalton Trans.*, 2015, **44**, 12029–12059.

22 S. Bezzenine-Lafollée, R. Gil, D. Prim and J. Hannedouch, *Molecules*, 2017, **22**, 1901–1929.

23 J. V. Obligacion and P. J. Chirik, *Nat. Rev. Chem.*, 2018, **2**, 15–34.

24 R. A. Shenvi, J. L. M. Matos and S. A. Green, *Org. React.*, 2019, **100**, 383–470.

25 Y. Zhang, X. Xu and S. Zhu, *Nat. Commun.*, 2019, **10**, 1–9.

26 B. M. Trost and Z. T. Ball, *J. Am. Chem. Soc.*, 2005, **127**, 17644–17655.

27 M. Kamitani, M. Itazaki, C. Tamiya and H. Nakazawa, *J. Am. Chem. Soc.*, 2012, **134**, 11932–11935.

28 S. L. Shi and S. L. Buchwald, *Nat. Chem.*, 2015, **7**, 38–44.

29 K. Yamamoto, Y. Mohara, Y. Mutoh and S. Saito, *J. Am. Chem. Soc.*, 2019, **141**, 17042–17047.

30 Z. Cheng, J. Guo and Z. Lu, *Chem. Commun.*, 2020, **56**, 2229–2239.

31 C. Q. Zhao, L. B. Han and M. Tanaka, *Organometallics*, 2000, **19**, 4196–4198.

32 N. Krause and C. Winter, *Chem. Rev.*, 2011, **111**, 1994–2009.

33 M. S. Jung, W. S. Kim, Y. H. Shin, H. J. Jin, Y. S. Kim and E. J. Kang, *Org. Lett.*, 2012, **14**, 6262–6265.

34 P. Koschker and B. Breit, *Acc. Chem. Res.*, 2016, **49**, 1524–1536.

35 C. Wang, W. J. Teo and S. Ge, *Nat. Commun.*, 2017, **8**, 1–9.

36 G. Li, X. Huo, X. Jiang and W. Zhang, *Chem. Soc. Rev.*, 2020, **49**, 2060–2118.

37 S. Bagherzadeh and N. P. Mankad, *Chem. Commun.*, 2016, **52**, 3844–3846.

38 R. K. Sahoo, M. Mahato, A. Jana and S. Nembenna, *J. Org. Chem.*, 2020, **85**, 11200–11210.

39 J. Wang, F. Xu, T. Cai and Q. Shen, *Org. Lett.*, 2008, **10**, 445–448.

40 M. Ito, M. Itazaki and H. Nakazawa, *ChemCatChem*, 2016, **8**, 3323–3325.

41 A. D. Ibrahim, S. W. Entsminger and A. R. Fout, *ACS Catal.*, 2017, **7**, 3730–3734.

42 I. Banerjee, A. Harinath and T. K. Panda, *Eur. J. Inorg. Chem.*, 2019, **2019**, 2224–2230.

43 E. Ballinger, J. Mosior, T. Hartman, K. Burns-Huang, B. Gold, R. Morris, L. Goullieux, I. Blanc, J. Vaubourgeix, S. Lagrange, L. Fraisse, S. Sans, C. Couturier, E. Bacqué, K. Rhee, S. M. Scarry, J. Aubé, G. Yang, O. Ouerfelli, D. Schnappinger, T. R. Ioerger, C. A. Engelhart, J. A. McConnell, K. McAulay, A. Fay, C. Roubert, J. Sacchettini and C. Nathan, *Science* , 2019, **363**, 1–8.

44 I. H. Kim, H. J. Tsai, K. Nishi, T. Kasagami, C. Morisseau and B. D. Hammock, *J. Med. Chem.*, 2007, **50**, 5217–5226.

45 J. M. McCall, R. E. TenBrink and J. J. Ursprung, *J. Org. Chem.*, 1975, **40**, 3304–3306.

46 V. Froidevaux, C. Negrell, S. Caillol, J. P. Pascault and B. Boutevin, *Chem. Rev.*, 2016, **116**, 14181–14224.

47 N. E. Mansfield, M. P. Coles and P. B. Hitchcock, *Polyhedron*, 2012, **37**, 9–13.

48 M. B. Geeson, A. R. Jupp, J. E. Mcgrady and J. M. Goicoechea, *Chem Commun*, 2014, **50**, 12281–12284.

49 V. Sharova, E, I. Artyushin, O, V. Nelyubina, Y, A. Lyssenko, K, P. Passechnik, M and L. Odinets, I, *Russ. Chem. Bull.*, 2008, **57**, 1890–1896.

50 C. Boehme, G. Wipff, L. Msm, U. M. R. Cnrs, I. De Chimie and B. Pascal, *Inorg. Chem.*, 2002, **41**, 494–499.

51 C. D. Huke and D. L. Kays, *Adv. Organomet. Chem.*, 2021, **75**, 1–54.

52 H. Mayr, T. Bug, M. F. Gotta, N. Hering, B. Irrgang, B. Janker, B. Kempf, R. Loos, A. R. Ofial, G. Remennikov and H. Schimmel, *J. Am. Chem. Soc.*, 2001, **123**, 9500–9512.

53 R. Lucius, R. Loos and H. Mayr, *Angew. Chem., Int. Ed.*, 2002, **41**, 91–95.

54 H. Mayr, B. Kempf and A. R. Ofial, *Acc. Chem. Res.*, 2003, **36**, 66–77.

55 H. Mayr and A. R. Ofial, *SAR QSAR Environ. Res.*, 2015, **26**, 619–646.

56 Z. Li, R. J. Mayer, A. R. Ofial and H. Mayr, *J. Am. Chem. Soc.*, 2020, **142**, 8383–8402.

57 Q. Jia, T. Cai, M. Huang, H. Li, M. Xian, T. L. Poulos and P. G. Wang, *J. Med. Chem.*, 2003, **46**, 2271–2274.

58 T. C. McMorris, R. Chimmani, K. Alisala, M. D. Staake, G. Banda and M. J. Kelner, *J. Med. Chem.*, 2010, **53**, 1109–1116.

59 P. A. Yonova and G. M. Stoilkova, *J. Plant Growth Regul.*, 2004, **23**, 280–291.

60 E. Rodríguez-Fernández, J. L. Manzano, J. J. Benito, R. Hermosa, E. Monte and J. J. Criado, *J. Inorg. Biochem.*, 2005, **99**, 1558–1572.

61 J. Wu, Q. Shi, Z. Chen, M. He, L. Jin and D. Hu, *Molecules*, 2012, **17**, 5139–5150.

62 A. Guan, C. Liu, X. Yang and M. Dekeyser, *Chem. Rev.*, 2014, **114**, 7079–7107.

63 M. Kurien, N. M. Claramma and A. P. Kuriakose, *J. Appl. Polym. Sci.*, 2004, **93**, 2781–2789.

64 B. Lin and R. M. Waymouth, *J. Am. Chem. Soc.*, 2017, **139**, 1645–1652.

65 W. Liu, Y. Tang, Y. Guo, B. Sun, H. Zhu, Y. Xiao, D. Dong and C. Yang, *Appl. Organomet. Chem.*, 2012, **26**, 189–193.

66 A. Shakeel, *J. Drug Des. Med. Chem.*, 2016, **2**, 10–20.

67 S. Dawn, S. R. Salpage, B. A. Koscher, A. Bick, A. C. Wibowo, P. J. Pellechia and L. S. Shimizu, *J. Phys. Chem. A*, 2014, **118**, 10563–10574.

68 I. Gumus, U. Solmaz, G. Binzet, E. Keskin, B. Arslan and H. Arslan, *Res. Chem. Intermed.*, 2019, **45**, 169–198.

69 F. Paul, J. Fischer, P. Ochsenbein and J. A. Osborn, *Organometallics*, 1998, **17**, 2199–2206.

70 J. Zhao, Z. Li, S. Yan, S. Xu, M. A. Wang, B. Fu and Z. Zhang, *Org. Lett.*,

2016, **18**, 1736–1739.

71 V. Krishnakumar, B. Chatterjee and C. Gunanathan, *Inorg. Chem.*, 2017, **56**, 7278–7284.

72 E. V. Vinogradova, B. P. Fors and S. L. Buchwald, *J. Am. Chem. Soc.*, 2012, **134**, 11132–11135.

73 A. Yagodkin, K. Löschcke, J. Weisell and A. Azhayev, *Tetrahedron*, 2010, **66**, 2210–2221.

74 A. R. Katritzky, S. Ledoux, R. M. Witek and S. K. Nair, *J. Org. Chem.*, 2004, **69**, 2976–2982.

75 S. Sharma, *Synthesis* , 1978, **1978**, 803–820.

76 A. Staab, H, *Angew. Chem., Int. Ed.*, 1967, **1**, 351–367.

77 J. Bernstein, H. L. Yale, K. Losee, M. Holsing, J. Martins and W. A. Lott, *J. Am. Chem. Soc.*, 1951, **73**, 906–912.

78 J. G. Erickson, *J. Org. Chem.*, 1956, **21**, 483–484.

79 J. Liu, Academic Press, Elsevier, 2010, pp. 1725–1731.

80 Y. Yamaoka, H. Miyabe and Y. Takemoto, *J. Am. Chem. Soc.*, 2007, **129**, 6686–6687.

81 H. J. Petersen, C. K. Nielsen and E. Arrigoni-Martelli, *J. Med. Chem.*, 1978, **21**, 773–781.

82 T. G. Ong, G. P. A. Yap and D. S. Richeson, *J. Am. Chem. Soc.*, 2003, **125**, 8100–8101.

83 X. Zhu, Z. Du, F. Xu and Q. Shen, *J. Org. Chem.*, 2009, **74**, 6347–6349.

84 A. Hernán-Gómez, T. D. Bradley, A. R. Kennedy, Z. Livingstone, S. D. Robertson and E. Hevia, *Chem. Commun.*, 2013, **49**, 8659–8661.

85 K. Bano, S. Anga, A. Jain, H. P. Nayek and T. K. Panda, *New J. Chem.*, 2020, **44**, 9419–9428.

86 K. Naktode, S. Das, J. Bhattacharjee, H. P. Nayek and T. K. Panda, *Inorg. Chem.*, 2016, **55**, 1142–1153.

87 W. Thewissen, D, H, M and M. Ambrosius, H, P, M, *Recl Trav Chim Pay-Bas*, 1980, **99**, 344–350.

88 M. Ambrosius, H, P, M, M. Van Der Linden, A, H, I and J. J. Steggerda, *J. Organomet. Chem.*, 1981, **204**, 211–220.

89 K. Issleib, H. Schmidt and H. Meyer, *J. Organomet. Chem.*, 1980, **192**, 33–39.

90 W. X. Zhang, M. Nishiura and Z. Hou, *Chem. Commun.*, 2006, **0**, 3812–3814.

91 M. R. Crimmin, A. G. M. Barrett, M. S. Hill, P. B. Hitchcock and P. A. Procopiou, *Organometallics*, 2008, **27**, 497–499.

92 A. C. Behrle and J. A. R. Schmidt, *Organometallics*, 2013, **32**, 1141–1149.

93 X. Gu, L. Zhang, X. Zhu, S. Wang, S. Zhou, Y. Wei, G. Zhang, X. Mu, Z.

Huang, D. Hong and F. Zhang, *Organometallics*, 2015, **34**, 4553–4559.

94 D. Mukherjee, S. Shirase, T. P. Spaniol, K. Mashima and J. Okuda, *Chem. Commun.*, 2016, **52**, 13155–13158.

95 C. Weetman, M. S. Hill and M. F. Mahon, *Chem. - Eur. J.*, 2016, **22**, 7158–7162.

96 M. D. Anker, M. Arrowsmith, R. L. Arrowsmith, M. S. Hill and M. F. Mahon, *Inorg. Chem.*, 2017, **56**, 5976–5983.

97 H. Liu, K. Kulbitski, M. Tamm and M. S. Eisen, *Chem. - Eur. J.*, 2018, **24**, 5738–5742.

98 Q. Shen, X. Ma, W. Li, W. Liu, Y. Ding, Z. Yang and H. W. Roesky, *Chem. - Eur. J.*, 2019, **25**, 11918–11923.

99 Y. Ding, X. Ma, Y. Liu, W. Liu, Z. Yang and H. W. Roesky, *Organometallics*, 2019, **38**, 3092–3097.

100 Y. Yang, M. D. Anker, J. Fang, M. F. Mahon, L. Maron, C. Weetman and M. S. Hill, *Chem. Sci.*, 2017, **8**, 3529–3537.

101 I. Ojima and S. ichi Inaba, *J. Organomet. Chem.*, 1977, **140**, 97–111.

102 A. J. Huckaba, T. K. Hollis and S. W. Reilly, *Organometallics*, 2013, **32**, 6248–6256.

103 A. Farkas and G. A. Mills, *Adv. Catal.*, 1962, **13**, 393–446.

104 A. Baishya, T. Peddarao, M. K. Barman and S. Nembenna, *New J. Chem.*, 2015, **39**, 7503–7510.

105 X. Zhu, M. Xu, J. Sun, D. Guo, Y. Zhang, S. Zhou and S. Wang, *Eur. J. Org. Chem*, 2021, **2021**, 5213–5218.

106 M. A. Dureen, D. W. Stephan and C. Ms, *J. Am. Chem. Soc*, 2010, **132**, 13559–13568.

107 A. C. Mcquilken, Q. M. Dao, A. J. P. Cardenas, J. A. Bertke, S. Grimme and T. H. Warren, *Angew. Chem., Int. Ed.*, 2016, **55**, 14335–14339.

108 M. Fischer and M. Schmidtmann, *Chem. Commun.*, 2020, **56**, 6205–6208.

109 R. Boese, R. Koster and M. Yalpanib, *Z. Naturforsch., B J. Chem. Sci.*, 1994, **49**, 1453–1458.

110 A. Ramos, A. Antiñolo, F. Carrillo-Hermosilla, R. Fernández-Galán, A. Rodríguez-Diéguez and D. García-Vivó, *Chem. Commun.*, 2018, **54**, 4700–4703.

111 M. Itazaki, T. Matsutani, T. Nochida, T. Moriuchi and H. Nakazawa, *Chem. Commun.*, 2020, **56**, 443–445.

112 L. L. Schafer, P. Mountford and W. E. Piers, *Dalton. Trans.*, 2015, **44**, 12027–12028.

113 P. Chirik and R. Morris, *Acc. Chem. Res.*, 2015, **48**, 2495.

114 P. P. Power, *Chem. Rev.*, 2012, **112**, 3482–3507.

115 H. R. Sharpe, A. M. Geer, W. Lewis, A. J. Blake and D. L. Kays, *Angew. Chem., Int. Ed.*, 2017, **56**, 4845–4848.

116 R. Sharpe, H, M. Geer, A, L. Williams, H, E, J. Blundell, T, W. Lewis and D. L. Kays, *Chem Commun*, 2017, **53**, 937–940.

117 A. J. South, A. M. Geer, L. J. Taylor, H. R. Sharpe, W. Lewis, A. J. Blake and D. L. Kays, *Organometallics*, 2019, **38**, 4115–4120.

118 H. R. Sharpe, A. M. Geer, H. E. L. Williams, T. J. Blundell, W. Lewis, A. J. Blake and D. L. Kays, *Chem. Commun.*, 2017, **53**, 937–940.

119 A. M. Aguiar, J. Giacin and H. J. Greenberg, *J. Org. Chem.*, 1963, **28**, 3545–3547.

120 K. Issleib and G. Harzfeld, *Angew. Chem., Int. Ed.*, 1965, **77**, 917–918.

121 O. Iwao, A. Kin-ya and I. Naoki, *Bull. Chem. Soc. Jpn.*, 1969, **42**, 2975–2981.

122 S. Härling, J. Greiser, T. M. A. Al-Shboul, H. Görls, S. Krieck and M. Westerhausen, *Aust. J. Chem.*, 2013, **66**, 1264–1273.

123 S. M. Härling, H. Görls, S. Krieck and M. Westerhausen, *Inorg. Chem.*, 2016, **55**, 10741–10750.

124 J. Bhattacharjee, A. Harinath, I. Banerjee, H. P. Nayek and T. K. Panda, *Inorg. Chem.*, 2018, **57**, 12610–12623.

125 M. Westerhausen, S. Krieck, J. Langer, T. M. A. Al-Shboul and H. Görls, *Coord. Chem. Rev.*, 2013, **257**, 1049–1066.

126 R. B. Fox and D. L. Venezky, *J. Am. Chem. Soc.*, 1956, **78**, 1661–1663.

127 Z. Tashma, *J. Org. Chem.*, 1982, **47**, 3012–3015.

128 P. Nylen, *Ber. Dtsch. Chem. Ges.*, 1924, **57**, 1023–1038.

129 T. Reetz, D. H. Chadwick, E. E. Hardy and S. Kaufman, *J. Am. Chem. Soc.*, 1955, **77**, 3813–3816.

130 B. Kaboudin and H. Zahedi, *Heteroat. Chem.*, 2009, **20**, 250–253.

131 A. Publication, *Org. Synth.*, 1936, **16**, 77.

132 G. W. Huber, S. Iborra and A. Corma, *Chem. Rev.*, 2006, **106**, 4044–4098.

133 F. Parodi, in *Comprehensive Polymer Science and Supplements Volume 5*, Elsevier, Amsterdam, Netherlands, vol. 5., 1989, pp. 387–412.

134 Y. Moglie, M. J. González-Soria, I. Martín-García, G. Radivoy and F. Alonso, *Green Chem.*, 2016, **18**, 4896–4907.

135 F. Alonso, Y. Moglie, G. Radivoy and M. Yus, *Green Chem.*, 2012, **14**, 2699–2702.

136 L. R. Wen, Y. X. Sun, J. W. Zhang, W. S. Guo and M. Li, *Green Chem.*, 2018, **20**, 125–129.

137 S. M. Härling, S. Krieck, H. Görls and M. Westerhausen, *Inorg. Chem.*, 2017, **56**, 9255–9263.

138 O. Baslé and C. J. Li, *Chem. Commun.*, 2009, **0**, 4124–4126.

139 W. Han, P. Mayer and A. R. Ofial, *Adv. Synth. Catal.*, 2010, **352**, 1667–1676.

140 J. Xie, H. Li, Q. Xue, Y. Cheng and C. Zhu, *Adv. Synth. Catal.*, 2012, **354**, 1646–1650.

141 S. Ortial, H. C. Fisher and J. L. Montchamp, *J. Org. Chem.*, 2013, **78**, 6599–6608.

142 F. Hudson, R and G. Searle, R, J, *J. Chem. Soc. B*, 1968, **0**, 1349–1353.

143 F. Jäkle, M. Mattner, T. Priermeier and M. Wagner, *J. Organomet. Chem.*, 1995, **502**, 123–130.

144 T. W. Campbell, J. J. Monagle and V. S. Foldi, *J. Am. Chem. Soc.*, 1962, **84**, 3673–3677.

145 J. J. Monagle and J. V. Mengenhauser, *J. Org. Chem.*, 1966, **31**, 2321–2324.

146 G. Aksnes and P. Froyen, *Acta Chem. Scand.*, 1969, **23**, 2697–2703.

147 G. R. Fulmer, A. J. M. Miller, N. H. Sherden, H. E. Gottlieb, A. Nudelman, B. M. Stoltz, J. E. Bercaw and K. I. Goldberg, *Organometallics*, 2010, **29**, 2176–2179.

148 A. Łupicka-Słowik, M. Psurski, R. Grzywa, M. Cuprych, J. Ciekot, W. Goldeman, E. Wojaczyńska, J. Wojaczyński, J. Oleksyszyn and M. Sieńczyk, *Invest. New Drugs*, 2020, **38**, 1350–1364.

149 C. B. Provis-Evans, E. A. C. Emanuelsson and R. L. Webster, *Adv. Synth. Catal.*, 2018, **360**, 3999–4004.

150 S. Urinda, D. Kundu and A. Majee, *Heteroat. Chem.*, 2009, **20**, 232–234.

151 S. Buckler and M. Epstein, US3052719A, 1962.

152 T. M. Horsley Downie, M. F. Mahon, J. P. Lowe, R. M. Bailey and D. J. Liptrot, *ACS Catal.*, 2022, **12**, 8214–8219.

153 F. U. Richter, *Chem. - Eur. J.*, 2009, **15**, 5200–5202.

154 J. A. Widegren and R. G. Finke, *J. Mol. Catal. A Chem.*, 2003, **198**, 317–341.

155 R. H. Crabtree, *Chem. Rev.*, 2012, **112**, 1536–1554.

156 A. M. Träff, M. Janjetovic, L. Ta and G. Hilmersson, *Angew. Chem., Int. Ed.*, 2013, **52**, 12073–12076.

157 Y. Li, S. Yu, X. Wu, J. Xiao, W. Shen, Z. Dong and J. Gao, *J. Am. Chem. Soc.*, 2014, **136**, 4031–4039.

158 B. J. Hornstein, J. D. Aiken and R. G. Finke, *Inorg. Chem.*, 2002, **41**, 1625–1638.

159 J. F. Sonnenberg and R. H. Morris, *Catal. Sci. Technol.*, 2014, **4**, 3426–3438.

160 K. J. Gallagher and R. L. Webster, *Chem. Commun.*, 2014, **50**, 12109–12111.

161 W. X. Zhang, M. Nishiura, T. Mashiko and Z. Hou, *Chem. - Eur. J.*, 2008, **14**, 2167–2179.

162 W. Ma, L. Xu, W. X. Zhang and Z. Xi, *New J. Chem.*, 2015, **39**, 7649–7655.

163 R. J. Batrice and M. S. Eisen, *Chem. Sci.*, 2016, **7**, 939–944.

164 T. M. Horsley Downie, J. W. Hall, T. P. Collier Finn, D. J. Liptrot, J. P. Lowe, M. F. Mahon, C. L. McMullin and M. K. Whittlesey, *Chem. Commun.*, 2020, **56**, 13359–13362.

165 R. J. Schwamm and M. P. Coles, *Eur. J. Inorg. Chem.*, 2022, **2022**, 1–6.

166 I. S. R. Karmel, M. Tamm and M. S. Eisen, *Angew. Chem., Int. Ed.*, 2015, **54**, 12422–12425.

167 A. Di Giuseppe, R. De Luca, R. Castarlenas, J. J. Pérez-Torrente, M. Crucianelli and L. A. Oro, *Chem. Commun.*, 2016, **52**, 5554–5557.

168 M. D. Greenhalgh, A. S. Jones and S. P. Thomas, *ChemCatChem*, 2015, **7**, 190–222.

169 F. Paul, S. Moulin, O. Piechaczyk, P. Le Floch and J. A. Osborn, *J. Am. Chem. Soc.*, 2007, **129**, 7294–7304.

170 D. Liu, D. Zhou, H. Yang, J. Li and C. Cui, *Chem. Commun.*, 2019, **55**, 12324–12327.

171 C. Li, W. Zhao, J. He and Y. Zhang, *Chem. Commun.*, 2019, **55**, 12563–12566.

172 T. M. A. Al-Shboul, G. Volland, H. Görls and M. Wusterhausen, *Z. Anorg. Allg. Chem.*, 2009, **635**, 1568–1572.

173 Y. Zhang, L. Qu, Y. Wang, D. Yuan, Y. Yao and Q. Shen, *Inorg. Chem.*, 2018, **57**, 139–149.

174 N. E. Mansfield, M. P. Coles and P. B. Hitchcock, *Dalton. Trans.*, 2005, 2833–2841.

175 N. E. Mansfield, M. P. Coles and P. B. Hitchcock, *J. Chem. Soc. Dalton. Trans.*, 2006, **44**, 2052–2054.

176 G. Jin, C. Jones, P. C. Junk, K. A. Lippert, R. P. Rose and A. Stasch, *New J. Chem.*, 2009, **33**, 64–75.

177 J. Grundy, M. P. Coles and P. B. Hitchcock, *Dalton. Trans.*, 2003, **4**, 2573–2577.

178 N. E. Mansfield, J. Grundy, M. P. Coles, A. G. Avent and P. B. Hitchcock, 2006, **128**, 13879–13893.

179 A. G. M. Barrett, M. R. Crimmin, M. S. Hill, P. B. Hitchcock, S. L. Lomas, M. F. Mahon and P. A. Procopiou, *Dalton. Trans.*, 2010, **39**, 7393–7400.

180 M. M. Kabat, L. M. Garofalo, A. R. Daniewski, S. D. Hutchings, W. Liu, M. Okabe, R. Radinov and Y. Zhou, *J. Org. Chem.*, 2001, **66**, 6141–6150.

181 L. D. Quin and R. E. Montgomery, *J. Org. Chem.*, 1963, **28**, 3315–3320.

182 K. E. DeBruin, C.-L. W. Tang, D. M. Johnson and R. L. Wilde, *J. Am. Chem. Soc.*, 1989, **111**, 5871–5879.

183 B. A. Surgenor, L. J. Taylor, A. Nordheider, A. M. Z. Slawin, K. S. Athukorala Arachchige, J. D. Woollins and P. Kilian, *RSC Adv.*, 2016, **6**, 5973–5976.

184 C. Jiang, P. J. Young, C. B. Durr, T. F. Spilker and M. H. Chisholm, *Inorg. Chem.*, 2016, **55**, 5836–5844.

185 J. Cosier and A. M. Glazer, *J. Appl. Crystallogr.*, 1986, **19**, 105–107.

186 *Rigaku Oxford Diffraction, (2018), CrysAlisPro Software system, version 1.171.40.45a, Rigaku Corporation, Oxford, UK.*, Rigaku Corporation, Oxford, UK.

187 O. V. Dolomanov, L. J. Bourhis, R. J. Gildea, J. A. K. Howard and H. Puschmann, *J. Appl. Crystallogr.*, 2009, **42**, 339–341.

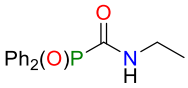
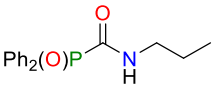
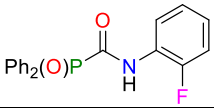
188 G. M. Sheldrick, *Acta Crystallogr. A*, 2015, **71**, 3–8.

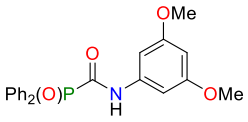
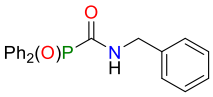
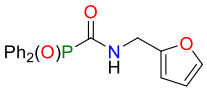
189 G. M. Sheldrick, *Acta Crystallogr. C*, 2015, **71**, 3–8.

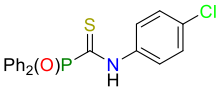
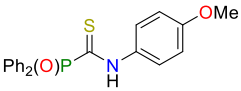
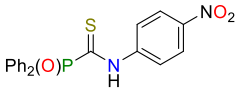
190 “CheckCIF” can be found under, http://checkcif.iucr.org.

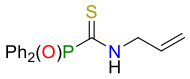
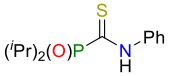
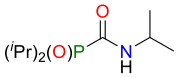
Appendices

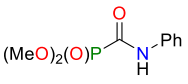
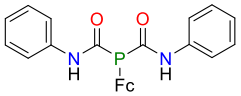
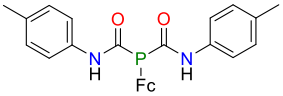
8.1 Crystallographic Data

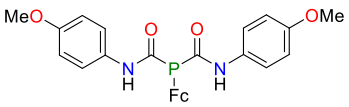
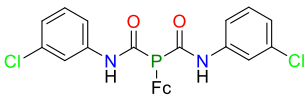
Compound	44i	44j	44d
			
Identification code	OCHDKB	OCHDKC	OCHDKL
Empirical formula	$C_{15}H_{16}NO_2P$	$C_{16}H_{18}NO_2P$	$C_{19}H_{15}FNO_2P$
Formula weight	273.26	287.28	339.29
Temperature/K	120(2)	120(2)	120(2)
Crystal system	triclinic	triclinic	triclinic
Space group	$P\bar{1}$	$P\bar{1}$	$P\bar{1}$
a/Å	8.7838(4)	13.2516(2)	8.6254(3)
b/Å	8.7951(4)	14.6070(2)	8.9016(3)
c/Å	20.4442(8)	17.4270(3)	10.8499(3)
α/°	90.450(3)	108.1640(10)	80.225(3)
β/°	93.891(3)	109.2100(10)	85.954(3)
γ/°	117.301(4)	94.7470(10)	77.248(3)
Volume/Å^3	1398.88(11)	2961.44(8)	800.24(5)
Z	4	8	2
R_1 [I>=2σ (I)]	R_1 = 0.0356, wR_2 = 0.1038	R_1 = 0.0280, wR_2 = 0.0763	R_1 = 0.0277, wR_2 = 0.0699

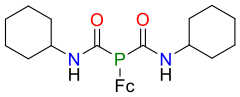
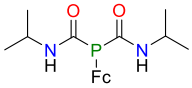
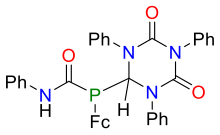
Compound	44e	44m	44n
			
Identification code	OCHDKF	OCHDKJ	OCHDKI
Empirical formula	$C_{21}H_{20}NO_4P$	$C_{23.5}H_{22}NO_2P$	$C_{18}H_{16}NO_3P$
Formula weight	381.35	381.39	325.29
Temperature/K	120(2)	120(2)	120(2)
Crystal system	triclinic	triclinic	triclinic
Space group	$P\bar{1}$	$P\bar{1}$	$P\bar{1}$
a/Å	11.1796(4)	8.7408(2)	8.4872(3)
b/Å	12.4375(6)	10.3990(3)	11.6741(5)
c/Å	14.5087(7)	11.2630(3)	16.8354(6)
α/°	102.974(4)	82.043(2)	108.405(4)
β/°	93.417(4)	85.124(2)	96.291(3)
γ/°	104.758(4)	82.282(2)	90.405(3)
Volume/Å^3	1886.37(15)	1002.41(5)	1571.67(11)
Z	4	2	4
R_1 [I>=2σ (I)]	R_1 = 0.0318, wR_2 = 0.0798	R_1 = 0.0369, wR_2 = 0.0926	R_1 = 0.0388, wR_2 = 0.0852

Compound	45c	45d	45e
			
Identification code	OCHDKE	OCHDKD	OCHDKA
Empirical formula	$C_{19}H_{15}NOPSCl$	$C_{20}H_{18}NO_2PS$	$C_{19}H_{15}N_2O_3PS$
Formula weight	371.80	367.38	382.36
Temperature/K	120(2)	120(2)	120(2)
Crystal system	monoclinic	monoclinic	monoclinic
Space group	*P2₁/n*	*P2₁/n*	*C2/c*
a/Å	12.19340(10)	12.19830(10)	18.86710(10)
b/Å	10.76950(10)	10.78100(10)	11.72690(10)
c/Å	13.88080(10)	13.91420(10)	16.05540(10)
α/°	90	90	90
β/°	105.7350(10)	104.7200(10)	95.5790(10)
γ/°	90	90	90
Volume/Å^3	1754.48(3)	1769.80(3)	3535.47(4)
Z	4	4	8
R_1 [I>=2σ (I)]	R_1 = 0.0278, wR_2 = 0.0725	R_1 = 0.0254, wR_2 = 0.0664	R_1 = 0.0269, wR_2 = 0.0736

Compound	45h	46b	46c
			
Identification code	OCHDKH	OCHDKM	OCHDKN
Empirical formula	$C_{16}H_{16}NOPS$	$C_{13}H_{20}NOPS$	$C_{10}H_{22}NO_2P$
Formula weight	301.33	269.33	219.25
Temperature/K	120(2)	120(2)	120(2)
Crystal system	monoclinic	triclinic	triclinic
Space group	*P2₁/c*	$P\bar{1}$	$P\bar{1}$
a/Å	9.07790(10)	7.7651(3)	7.6704(5)
b/Å	16.1069(2)	8.8001(4)	9.6106(6)
c/Å	10.53440(10)	11.2150(5)	10.3912(6)
α/°	90	95.604(4)	66.020(6)
β/°	102.0600(10)	109.376(4)	72.989(6)
γ/°	90	93.345(3)	75.881(5)
Volume/Å^3	1506.31(3)	716.13(6)	662.38(8)
Z	4	2	2
R_1 [I>=2σ (I)]	R_1 = 0.0246, wR_2 = 0.0638	R_1 = 0.0306, wR_2 = 0.0853	R_1 = 0.0272, wR_2 = 0.0705

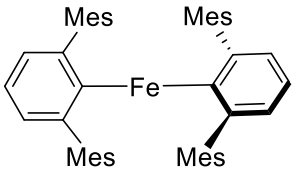
Compound	47b	49a	49b
			
Identification code	OCHDKQ	FELJTA	FECHLD
Empirical formula	$C_9H_{12}NO_4P$	$C_{24}H_{21}N_2O_2PFe$	$C_{26}H_{25}FeN_2O_2P$
Formula weight	229.17	456.25	484.3
Temperature/K	120(2)	120(2)	120(2)
Crystal system	triclinic	monoclinic	monoclinic
Space group	$P\bar{1}$	$P2_1/n$	$P2_1/n$
a/Å	7.2681(4)	11.1136(2)	13.8847(3)
b/Å	8.6775(5)	9.8908(2)	9.6793(2)
c/Å	9.4652(5)	18.5424(2)	17.0929(4)
α/°	105.959(5)	90	90
β/°	92.531(4)	92.3440(10)	104.878(3)
γ/°	114.084(5)	90	90
Volume/Å^3	515.61(5)	2036.52(6)	2220.17(9)
Z	2	4	4
R_1 [I>=2σ (I)]	R_1 = 0.0271, wR_2 = 0.0675	R_1 = 0.0261, wR_2 = 0.0705	R_1 = 0.0317, wR_2 = 0.0813

Compound	49c	49d
		
Identification code	FECHLE	FECHLH
Empirical formula	$C_{26}H_{25}FeN_2O_4P$	$C_{24}H_{19}Cl_2FeN_2O_2P$
Formula weight	516.3	525.13
Temperature/K	120(2)	120(2)
Crystal system	monoclinic	monoclinic
Space group	$P2_1/n$	$I2/a$
a/Å	14.2004(2)	23.0786(5)
b/Å	9.6001(2)	10.6303(2)
c/Å	16.9062(3)	20.6874(4)
α/°	90	90
β/°	96.163(2)	121.453(3)
γ/°	90	90
Volume/Å^3	2291.42(7)	4329.57(19)
Z	4	8
R_1 [I>=2σ (I)]	R_1 = 0.0329, wR_2 = 0.0818	R_1 = 0.0244, wR_2 = 0.0664

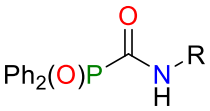
Compound	51a	51b	56
			
Identification code	FECHLI	FECHLJ4	FECHLK
Empirical formula	$C_{24}H_{33}N_2O_2PFe$	$C_{18}H_{25}N_2O_2PFe$	$C_{39}H_{32}Cl_3N_4O_3PFe$
Formula weight	468.34	388.22	797.85
Temperature/K	120(2)	119.97(10)	120(2)
Crystal system	monoclinic	monoclinic	triclinic
Space group	$P2_1/c$	$P2_1/n$	$P\bar{1}$
a/Å	14.3466(7)	11.12100(10)	11.8937(4)
b/Å	14.4167(5)	9.90120(10)	13.4612(4)
c/Å	12.0295(5)	16.9793(2)	13.9240(3)
α/°	90	90	104.145(2)
β/°	114.390(6)	95.8870(10)	111.147(3)
γ/°	90	90	108.182(3)
Volume/Å^3	2266.02(19)	1859.75(3)	1807.98(10)
Z	4	4	2
R_1 [I>=2σ (I)]	R_1 = 0.0460, wR_2 = 0.1061	R_1 = 0.0281, wR_2 = 0.0759	R1 = 0.0405, wR2 = 0.1052

8.2 List of Compounds

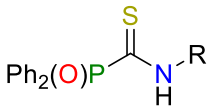
Chapter 2



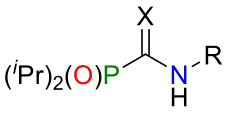
40



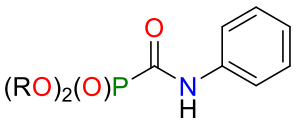
44a-44h



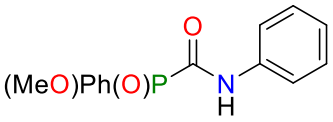
45a-45h



46a-46c

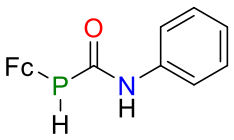


47a-47b

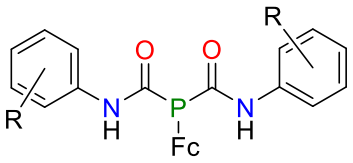


47c

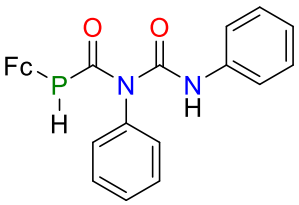
Chapter 3



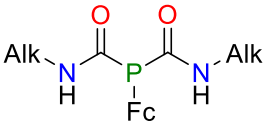
48a



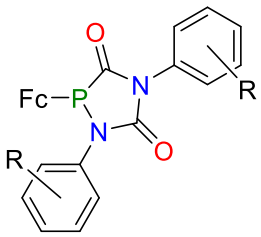
49a-49d



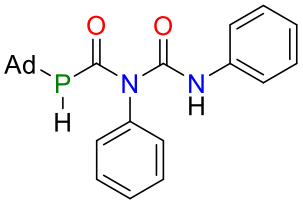
50a



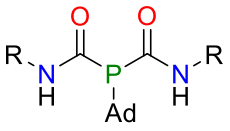
51a-51c



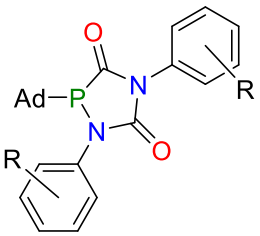
52a-52d



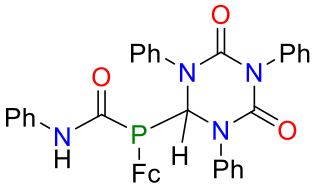
53a



54a-54c

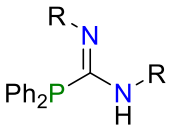


55a-55d

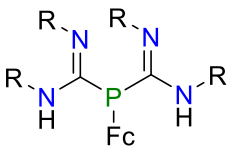


56

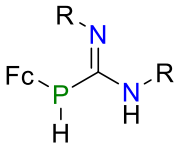
Chapter 4



60a-60d



62a-62e



63a-63e